ENERGY CONSERVATION

ORNL/Sub/82-17485/1

Development and Demonstration of a Stirling/Rankine Heat Activated Heat Pump

Final Report

Phase IIIB—Engine Technology Development Testing

Report Prepared by

GENERAL ELECTRIC COMPANY
Advanced Energy Programs Department
P.O. Box 527
King of Prussia, Pennsylvania 19406

under
Subcontract 86X-17485C

for

OAK RIDGE NATIONAL LABORATORY
operated by
MARTIN MARIETTA ENERGY SYSTEMS, INC.
for the

U.S. DEPARTMENT OF ENERGY

OFFICE OF BUILDINGS ENERGY
RESEARCH AND DEVELOPMENT

Printed in the United States of America. Available from
National Technical Information Service
U.S. Department of Commerce
5285 Port Royal Road, Springfield, Virginia 22161
NTIS price codes—Printed Copy: A10 Microfiche A01

This report was prepared as an account of work sponsored by an agency of the United States Government. Neither the United States Government nor any agency thereof, nor any of their employees, makes any warranty, express or implied, or assumes any legal liability or responsibility for the accuracy, completeness, or usefulness of any information, apparatus, product, or process disclosed, or represents that its use would not infringe privately owned rights. Reference herein to any specific commercial product, process, or service by trade name, trademark, manufacturer, or otherwise, does not necessarily constitute or imply its endorsement, recommendation, or favoring by the United States Government or any agency thereof. The views and opinions of authors expressed herein do not necessarily state or reflect those of the United States Government or any agency thereof.

ORNL/Sub/82-17485/1
Dist. Category UC-95d

DEVELOPMENT AND DEMONSTRATION OF A STIRLING/RANKINE HEAT ACTIVATED HEAT PUMP

FINAL REPORT

PHASE IIIB - ENGINE TECHNOLOGY DEVELOPMENT TESTING

Date Published - November 1984

Report Prepared by

General Electric Company
Advanced Energy Programs Department
P.O. Box 527
King of Prussia, PA 19406

under

Subcontract 86X-17485C

for

Oak Ridge National Laboratory
Oak Ridge, Tennessee 37831
operated by
MARTIN MARIETTA ENERGY SYSTEMS, INC.
for the
U.S. DEPARTMENT OF ENERGY
Under Contract No. DE-AC05-84OR21400

DOE DISCLAIMER

This book was prepared as an account of work sponsored by an agency of the United States Government. Neither the United States Government nor any agency thereof, nor any of their employees, makes any warranty, express or implied, or assumes any legal liability or responsibility for the accuracy, completeness, or usefulness of any information, apparatus, product, or process disclosed, or represents that its use would not infringe privately owned rights. Reference herein to any specific commercial product, process, or service by trademark, manufacturer, or otherwise, does not necessarily constitute or imply its endorsement, recommendation, or favoring by the United States Government or any agency thereof. The views and opinions of authors expressed herein do not necessarily state or reflect those of the United States Government or any agency thereof.

ABSTRACT

This report presents the results of the Phase II and Phase IIIB Stirling/Rankine Heat Activated Heat Pump product development program. In the Phase II program, a complete gas fired heat activated prototype residential heat pump system was developed and tested. Results of the product system development are presented in Volume I of this report, emphasizing the key components of the system: the free piston Stirling engine prime mover and the free piston linear inertia compressor. Detailed test data from the Phase II program are presented in Volume II of this report.

Results of the Phase II program indicated deficiencies in the performance of the free-piston Stirling engine and mismatching of the dynamic characteristics of the engine and the compressor. These deficiencies were further investigated during in-depth diagnostic testing of the engine/compressor unit in the Phase IIIB program. Results of these tests identified the engine design deficiencies and indicated appropriate engine/compressor matching criteria. The Phase IIIB results are presented in Volume III of this report.

Results of the Phase IIIA program were previously published under GE Document No. 82 AEP-004. The Phase IIIA program concentrated on an evaluation of alternative engine/compressor concepts to determine if there were alternative configurations with better technical and cost characteristics than the configuration developed in the Phase II program.

TABLE OF CONTENTS

Section Page

1 INTRODUCTION....1-1

1.1 Program History....1-1
1.2 Phase II Accomplishments....1-4
1.3 Phase III Results....1-7
1.3.1 Compressor Performance Verification....1-7
1.3.2 Engine/Compressor Matching....1-7
1.3.3 Engine Performance....1-7
1.3.4 Engine Heat Exchanger Losses....1-8

2 DEVELOPMENT OF PHASE IIIB TEST REQUIREMENTS....2-1

2.1 Phase II Results and Conclusions....2-1
2.1.1 Phase II Test Description....2-1
2.1.2 Engine Performance Deficiencies....2-4
2.1.3 Compressor Operation Uncertainties....2-7
2.1.4 Matching Engine and Compressor Characteristics.2-7
2.1.5 Simulation Model Discrepancies....2-8
2.1.6 Phase III Program Plan....2-8
2.2 Instrumentation Analysis....2-11
2.2.1 Regenerator Effectiveness....2-11
2.2.2 Flow Work....2-18
2.3 Matching and Control Analysis....2-22
2.3.1 Matching Requirements....2-22
2.3.2 Control Options....2-23
2.3.3 Matching Analysis....2-24
2.3.4 Control System Validation....2-33

3 TEST SYSTEM DESIGN....3-1

3.1 Instrumentation Selection....3-1
3.1.1 Existing Phase II Instrumentation....3-1
3.1.2 Additional Instrumentation Options....3-1
3.1.3 Selection....3-3
3.2 Data Acquisition System (DAS) Selection....3-7
3.2.1 Existing Phase II DAS....3-7
3.2.2 DAS Options....3-11
3.2.3 DAS Selection....3-13
3.3 Engine/Compressor Modifications....3-13
3.3.1 Engine Heater Head Modifications....3-16
3.3.2 Compressor Modifications....3-16
3.3.3 Combustor Modifications....3-19

4 TEST SYSTEM FABRICATION AND INSTALLATION....4-1

4.1 Test Hardware Fabrication....4-1
4.1.1 Engine/Compressor Fabrication and Instrumentation Installation....4-1
4.1.2 Delta-P Transducer Phase Shift Tests....4-2
4.2 DAS Installation....4-9
4.2.1 Hardware Installation....4-9

TABLE OF CONTENTS
(Continued)

Section Page

4.2.2 Software Developed....4-9
4.2.3 Sample DAS Output....4-16
4.3 Check Out Tests....4-32
4.3.1 Functional Performance....4-32
4.3.2 DAS Error Analysis....4-33

5 TEST PROGRAM....5-1

5.1 Test Plan....5-1
5.1.1 Test Objectives....5-1
5.1.2 Test Matrix....5-2
5.2 Test Data and Major Results....5-12
5.3 Compressor Verification....5-21
5.3.1 Compressor Test Data....5-21
5.3.2 Comparison of Test Results to Predictions & Compressor Component Tests....5-22
5.3.3 Interpretation and Evaluation....5-29
5.4 FPSE Performance Tests....5-32
5.4.1 Engine Test Data....5-32
5.4.2 Comparison to Phase II Data....5-33
5.4.3 Interpretation and Evaluation....5-36
5.5 Matching Analysis Verification....5-44
5.5.1 Engine/Compressor Matching Test Data....5-44
5.5.2 Matching Flexibility and HAHP Control....5-46
5.5.3 Evaluation of Matching and Control Technique...5-49
5.6 Heat Exchanger Losses....5-51
5.6.1 Measured Loss Data....5-51
5.6.2 Comparison to Predictions....5-53
5.6.3 Interpretation of Results....5-53

6 CONCLUSIONS AND RECOMMENDATIONS....6-1

6.1 Results and Conclusions....6-1
6.1.1 FPSE Indicated Power....6-1
6.1.2 Engine Indicated Efficiency....6-1
6.1.3 Engine Heat Exchanger Flow Friction Losses....6-5
6.1.4 Other Power Losses....6-5
6.1.5 Compressor Performance....6-6
6.1.6 Engine/Compressor Matching and Control....6-6
6.1.7 Predictive Design Tools....6-8
6.2 Performance Potential....6-8
6.3 Recommendations....6-13
6.3.1 General Recommendations....6-13
6.3.2 Short Term Program Recommendation....6-14

References....R-1

Appendix A Nomenclature and Abbreviations....A-1

Appendix B Phase IIIB Test Data....B-1

LIST OF ILLUSTRATIONS

Figure		Page
1-1	HAHP Product Development Schedule	1-2
1-2	Stirling/Rankine HAHP Concept	1-4
2-1	Proto 2 Combustor/Engine/Compressor Assembly	2-2
2-2	Proto 2 Combustor/Engine/Compressor Integrated Test	2-5
2-3	Regenerator Temperature Histories	2-13
2-4	Heater, Regenerator, and Cooler Configuration for Stirling Engine	2-19
2-5	Load Matching Technique	2-25
2-6	Computation Procedure for Load Matching Analysis	2-26
2-7	Compressor Power Map at 95°F Ambient Day	2-27
2-8	Compressor Map Over Operating Ambient Temperature Range	2-28
2-9	Engine Operating Frequency as a Function of Heater Head Temperature and Compressor Natural Frequency	2-30
2-10	Engine Power Map	2-31
2-11	Compressor Characteristics	2-32
2-12	Compressor Power Map at 80°F Ambient Temperature	2-34
2-13	Operating Lines for Compressor at 80°F Ambient Day Conditions	2-35
2-14	Operating Lines for Compressor at 95°F Ambient Day Conditions	2-36
2-15	Operating Lines for Compressor at 95°F Ambient Day Conditions	2-37
2-16	FPSE Power Map with Compressor Match Points	2-39
3-1	Proto 2 FPSE Additional Instrumentation	3-4
3-2	Phase III DAS Configuration	3-15
3-3	Proto 2 Engine Housing Modifications	3-17
3-4	Compressor LVDT Assembly/Installation	3-18
3-5	Combustor Modified for Additional Instrumentation	3-20
4-1	Pressure Transducer Phase Shift Test Rig Schematic	4-3
4-2(a)	Differential Pressure Transducer Phase Shift for $T_1=T_2=80°F$	4-6
4-2(b)	Differential Pressure Transducer Phase Shift for $T_1=T_2=1220°F$	4-7
4-3	Pressure Transducer Error Versus Tube Temperature	4-8
4-4	Phase III DAS Components in Test Stand	4-10
4-5	Phase III DAS Components and Existing DAS Equipment in Test Stand	4-11
4-6	Existing DAS Equipment in Test Stand	4-12
4-7	Operating Code Flowchart	4-14
4-8	Second Gas Spring Pressure/Stroke History and P-V Diagram	4-23
4-9	Engine Compression Space Pressure-Stroke History & P-V Diagram	4-24
4-10	Engine Displacer Gas Spring Pressure-Stroke History & P-V Diagram	4-25
4-11	Compressor Upper Cylinder Pressure-Stroke History and P-V Diagram	4-26
4-12	Compressor Lower Cylinder Pressure-Stroke History and P-V Diagram	4-27
4-13	Compressor Upper Gas Spring Pressure-Stroke History and P-V Diagram	4-28
4-14	Compressor Lower Gas Spring Pressure-Stroke History and P-V Diagram	4-29
4-15	Engine and Compressor Dynamic Component Motion Histories	4-30
4-16	Pressure Histories in Engine Components	4-31

LIST OF ILLUSTRATIONS

Figure		Page
4-17	Compression Space and Displacer Gas Spring Variations with Signal Phase Angle	4-34
4-18	Second Gas Spring Power Vs. Sensitivity to Signal Phase Angle	4-36
5-1	Compressor Code Predictions of Compressor Operating Characteristics	5-3
5-2	Engine-Compressor Matching Characteristics	5-6
5-3	Engine-Compressor Matching with Constant Firing Rate	5-10
5-4	Compressor Test Data - No Regulator and 80 psia Regulator	5-23
5-5	Compressor Test Data - Regulator at 96 psia	5-24
5-6	Compressor Test Data for Various Suction/Discharge Conditions	5-25
5-7	Compressor Code/Component Test Correlation	5-26
5-8	Predicted Compressor Performance	5-27
5-9	Influence of Friction on Predicted Compressor Operating Conditions	5-28
5-10	Cylinder Power Balance in Compressor	5-30
5-11	FPSE Performance Map	5-34
5-12	Power/Efficiency Relation for Proto 2 Engine	5-35
5-13	Second Gas Spring Dissipation (Test)	5-37
5-14	Second Gas Spring Work Dissipation	5-38
5-15	Comparison of Phase II and Phase IIIB Second Gas Spring Work Dissipation	5-40
5-16	FPSE Test Performance Versus Prediction	5-42
5-17	2nd Order Code Correlation with Phase II Test Data	5-43
5-18	FPSE/Compressor Performance Map (Test)	5-45
5-19	FPSE/Compressor Match - No Compressor Gas Spring Regulator	5-47
5-20	FPSE/Compressor Match - Compressor Gas Spring Regulator at 95 psia	5-48
5-21	Gas Spring Control of Engine/Compressor Match Point	5-50
5-22	Heat Exchangers and Regenerator Friction Loss	5-52
6-1	FPSE Indicated Power Trend	6-2
6-2	Effect of Phase Angle and Swept Volume Ratio on Engine Power	6-3
6-3	Effect of Piston Stroke and Frequency on Engine Efficiency	6-4
6-4	Engine/Compressor Matching and Control Map	6-7
6-5	Effect of Regenerator Effectiveness and Total Engine Flow Losses on Engine Efficiency	6-12
6-6	Phase IIIC Program Candidate Tasks	6-15
6-7	Candidate Task Schedule	6-16

LIST OF TABLES

Table		Page
2-1	Operating Test Point Matrix	2-6
2-2	Thermal Response of Thermocouples	2-17
2-3	Matched Engine/Compressor Operating Points	2-38
3-1	Phase II Integrated Test Facility Instrumentation	3-2
3-2	Additional Instrumentation Requirements	3-5
3-3	Phase II Steady State Instrumentation	3-8
3-4	Phase II Dynamic Instrumentation Data	3-10
3-5	DAS Components and Costs	3-14
4-1	Effect of Tube Length on Pressure Transducer Phase Shift	4-5
4-2	Oscilloscope Integration Constants	4-15
4-3	Free-Piston Stirling Engine Performance Summary	4-17
4-4	Free-Piston Stirling Engine Data Summary - Combustor and Compressor	4-18
4-5	Free-Piston Stirling Engine Data Summary - Engine	4-19
4-6	Free-Piston Stirling Engine Fluke Datalogger	4-20
4-7	Sensitivity of Power Calculation to Waveform Parameters	4-39
5-1	Configuration of Build 1-64	5-4
5-2	Test Points for Compressor Performance Verification	5-5
5-3	Engine/Compressor Matching Test Points	5-8
5-4	Constant Firing Rate Engine/Compressor Matching Test Points	5-9
5-5	Maximum Engine Power Test	5-11
5-6	Test Measurements and Data Reduction Models	5-13
5-7	Phase IIIB Test History	5-16
5-8	Test Results Summary	5-17
5-9	Nomenclature for Table 5-8	5-20
5-10	Principal Differences Between Compressor Component Tests and Engine/Compressor Integrated Tests	5-31
5-11	Comparison of Measured Versus Predicted Heat Exchanger Flow Losses	5-54
6-1	Comparison of Measured Versus Predicted Heat Exchanger Flow Losses	6-9
6-2	Power and Loss Breakdown for Phase IIIB Test and Potential Engine Performance	6-10

SECTION 1
INTRODUCTION

SECTION 1
INTRODUCTION

This report presents the results and conclusions of the Phase III program for the development and demonstration of a Stirling/Rankine Heat Activated Heat Pump (HAHP). The objective of the Phase III program was to continue development of the HAHP, concentrating on the engine/compressor technology issues that were encountered in the Phase II program. A brief background of the preceding Phase I and Phase II programs is presented in this section, along with the accomplishments, conclusions and recommendations of the Phase III program.

1.1 PROGRAM HISTORY

In January 1975, General Electric and the American Gas Association (AGA) initiated a multi-phase program for the development of a Heat Activated Heat Pump (HAHP). The Department of Energy (DOE) joined General Electric and the AGA in the program in 1976, and the Gas Research Institute assumed responsibility for the program from the AGA in 1977. The Oak Ridge National Laboratories (ORNL) was assigned technical responsibility for the DOE in 1978.

The program schedule is shown in Figure 1-1. Phase I, Product Selection, was initiated and completed in 1975. The primary objective of the Phase I program was to evaluate, through an analytical effort, if a gas heat pump product could evolve into a viable business venture. A comparison of the possible heat activated heat pump concepts showed that the Stirling/Rankine and the absorption cycle were the most promising from the standpoint of performance (potential operating savings) region of application, and market application (residential and/or commercial).

Further refinement of the design, cost and performance estimates for the two candidate systems and a definition of a product introduction scenario and pricing strategies were then used to perform a business evaluation of the two concepts. As a result of this Phase I effort, the Stirling/Rankine concept was selected as the most promising approach, and a decision was made to proceed with Phase II.

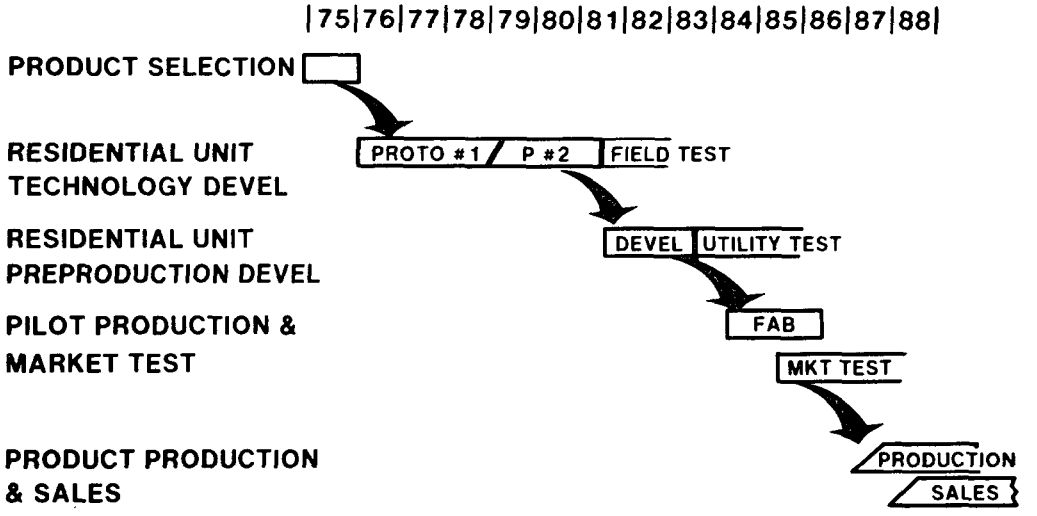

Figure 1-1. HAHP Product Development Schedule

The objective of the Phase II program, Residential Unit Technology Development, was to demonstrate that the performance estimates generated during Phase I could be realized and that product cost goals were realistic. The Phase II program was initiated in 1976 and completed in 1981. The final report for this program is presented in Reference 1.

Two generations of prototype hardware were developed during the Phase II program. Prototype I was the first attempt to test a complete Stirling/Rankine HAHP system with heat pump configured hardware. This system was comprised of hardware of a primarily developmental nature. The Prototype 2 system consisted of more mature hardware, incorporating the results of the Prototype 1 development effort and designed toward the eventual product.

Design, fabrication and testing of each of the Prototype 1 components and subsystems were completed, and the Prototype 1 system (indoor and outdoor units) was tested in an environmental simulation facility. Design, fabrication and testing of the Prototype 2 components and subsystems were completed, but the Prototype 2 system tests in the simulation facility and the planned field tests were deferred due to engine performance deficiencies. These deficiencies, and the status of the system technology at the end of Phase II, are described in Reference 1.

Originally, Phase III of the program, Residential Unit Preproduction Development and Utility Field Test, was targeted for the development of a preproduction prototype, followed by the fabrication of 10-20 field test units for installation at gas utility test sites throughout the nation. Due to the need for additional engine technology development, the Phase III program was preceeded by the Phase IIIA and Phase IIIB programs, Engine Technology Development. The Phase IIIA program initated in May of 1981, included the evaluation of alternative HAHP concepts and technologies to verify the technical and economic potential of the Stirling/Rankine configuration. The evaluation presented in Reference 2, reconfirmed that the concept under development has the best potential for a residential size heat activated heat pump. An independent assessment of the HAHP technology was conducted by the NASA Lewis Research Center in January of 1982. NASA LeRC concluded that the HAHP concept was technically reasonable and capable of successful development.

Based on these results, it was decided to proceed with the engine/compressor technology development plan developed in Phase IIIA. This effort, initiated in March of 1982 under the Phase IIIA program, was initially conducted under the sponsorship of DOE/ORNL and GRI. The Phase IIIA program was reformulated into the Phase IIIB program sponsored by DOE/ORNL, when GRI withdrew from the program, effective June 1982. GRI determined that its objectives and resources prevented it from being involved in a program with the technology development requirements of the HAHP. The completion of the engine/compressor test effort was accomplished under the Phase IIIB program. The effort of the Phase IIIA and Phase IIIB programs for the engine/compressor technology development is the subject of this report.

1.2 PHASE II ACCOMPLISHMENTS

The Phase I and Phase II programs led to the successful development of most of the Stirling/Rankine HAHP components and subsystems, demonstrated the feasibility of the product concept, and verified the product's market potential. The prior accomplishments of the Phase I and Phase II programs, their results and conclusions and the recommendations leading to formulation of the Phase III program, are detailed in Reference 1. A brief summary of these results is presented below.

The Stirling/Rankine Heat Activated Heat Pump (HAHP) concept is schematically illustrated in Figure 1-2. The heart of the system is the combustor/Stirling engine/linear compressor assembly which replaces the conventional motor/compressor unit employed in electric heat pumps. Heat input from a gas combustor provides thermal energy to the Stirling engine working fluid, helium. The engine displacer and the engine power piston operate with a prescribed phase and displacement relationship to create the highly efficient Stirling thermodynamic cycle.

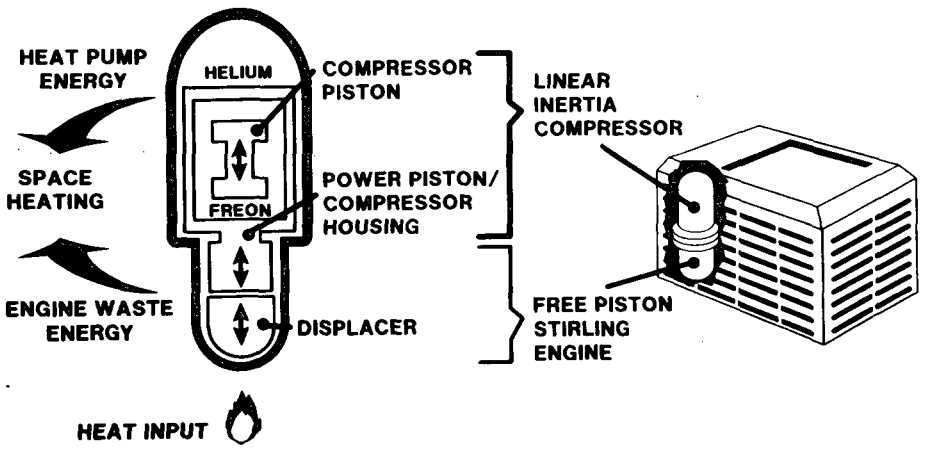

Figure 1-2. STIRLING/RANKINE HAHP CONCEPT

Power delivered by the power piston is transferred to the heat pump refrigerant through a linear inertia compressor. The power piston is directly connected to the compressor housing, with the refrigerant being compressed by a free piston reciprocating within the housing - also with a prescribed phase and displacement relationship. The unit's operation is

determined by the rate of the heat input, the phase and displacement between the displacer, the power piston, and the compressor piston, and by the external conditions imposed on the refrigerant coils by the load (building) and the outdoor ambient air temperature.

Performance projections for both the Stirling/Rankine HAHP and a gas furnace/electric air conditioner system show substantial operating cost savings potential for the HAHP as gas and electricity prices escalate. The penetration of the HAHP into the HVAC market will be a function of the performance of the HAHP and competing products (gas and electricity savings), the regional prices of gas and electricity (operating cost savings), the size of the new construction and replacement markets, the pricing strategy used, the advertising and sales promotion program, and many other factors. Based on the sales histories of other HVAC products and the relative operating cost savings of the HAHP (and similar gas heat pump products), sales projections for the gas heat pump industry indicated that the HAHP could be an attractive product offering for heat pump manufacturers.

The hardware development approach was to develop two cycles of prototype hardware. The first cycle was an engineering prototype, designated Prototype 1. Development of the engineering prototype began in 1976. The combustor, operating on natural gas, provided the heat input for the helium working fluid. The compact combustor operated with 15% excess air, yielding a CO emission level of less than 0.04% at the combustor exhaust. Testing verified the 82 to 83% efficiency goal for the combustor, operating with an 800°F air preheat level. The free piston linear inertia compressor configuration used in the first prototype to demonstrate and characterize its performance achieved a 76% efficiency (isentropic) exceeding its initial design goal. The first prototype unit free piston engine, including the engine housing, regenerators, heater head subassembly, and the dynamic components (displacer and power piston) operated with a maximum helium temperature of approximately 1250°F and had a 3 kilowatt power output. Because of high thermal losses and a low operating frequency (26 Hz), engine testing yielded only 20-26% operating efficiency as opposed to the 30% efficiency goal. However, testing of the Prototype 1 combustor/engine/compressor assembly outdoor fan/coil unit and its matching indoor unit demonstrated the technical feasibility of the Stirling/Rankine HAHP and paved the road for the development of the Prototype 2 unit.

The Prototype 2 unit was designed and tested through the same process. The engine/compressor design was improved to reduce thermal losses and to simulate a production configuration to the extent practical. In addition, a gas spring was added to the engine power piston/compressor housing assembly to increase engine operating frequency. Testing of the combustor, compressor, indoor and outdoor fan/coil units, and the control system verified that the component performance goals (similar to those of the first prototype) were all met. However, testing of the combustor/engine/compressor unit yielded an engine indicated power range from 2.2 kw to 2.7 kw, versus a 3.2 kw goal. Engine indicated efficiency achieved in test was from 22% to 27%, versus a 32% goal. And, although the gas spring increased the operating frequency to the 30 Hz goal, the design has high venting and leakage losses.

Results of these tests were used to revise the engine analytical design tools and redesign the engine. Prototype 2 engine heater head and cooler designs were modified to increase heat transfer effectiveness and decrease flow losses. Engine regenerator effectiveness was also increased. Testing of the modified Prototype 2 engine confirmed the increase heat transfer effectiveness of the modified engine components, but showed no increase in engine power or efficiency due to too large an increase in void volume.

As the Phase II program drew to a close, in-depth diagnostic testing and investigative analyses were conducted on the Prototype 2 baseline and modified engines. The major conclusions of these evaluations were:

- Changes to the engine components are required to achieve the design performance goals.
  - Engine regenerator effectiveness must be increased substantially, even at the expense of higher flow losses.
  - Engine heater head flow losses must be reduced.
  - Engine hot side swept volume must be reduced.
  - The engine displacer gas spring should be reduced in size and the second gas spring should be eliminated.

- Better engine/compressor matching is required to maintain engine performance at off-design conditions.

- Improved analytical tools are required to confidently design the next generation of Stirling/Rankine heat pump hardware.

1.3 PHASE III RESULTS

The Phase III test program presented in this report concentrated on:

- Verifying compressor performance
- Verifying engine/compressor matching techniques
- Maximizing engine performance
- Developing detailed performance data on the engine heater head, regenerator and cooler designs.

1.3.1 COMPRESSOR PERFORMANCE VERIFICATION

The compressor had met its performance goals in Phase II when tested independently on its own test stand. When tested with the engine, however, it was suspected that it was not operating properly, thereby acting as a power governor on the engine under some test conditions. In Phase III, this was verified by adding an LVDT to the compressor assembly to directly measure the motion of the compressor free piston. The piston motion is lower than that measured in independent compressor tests. Several potential explanations were evaluated but further analysis and diagnostic testing will be required to determine the reason for the difference between compressor piston motion measured in independent tests and that measured when the compressor is driven by the engine.

1.3.2 ENGINE/COMPRESSOR MATCHING

The engine/compressor unit's operation is significantly affected by the matching of engine operating characteristics and compressor operating characteristics. A technique for matching engine/compressor operation over a broad range of conditions was developed in the Phase IIIA program and verified by test in the Phase IIIB program. The verified technique confirmed the HAHP control system concept and demonstrates the ability to control the unit operation over its design operating conditions.

1.3.3 ENGINE PERFORMANCE

Testing of the engine in Phase IIIB achieved an indicated power of over 3 kw, as compared to a maximum of 2.7-2.8 kw achieved in Phase II tests.

However, the maximum indicated efficiency achieved was 25 percent as compared to 27 percent in Phase II. These differences are primarily due to the improved instrumentation and data acquisition system used in Phase III. Thus, the Phase III tests are considered to be more representative of actual performance.

The improved data acquisition system also revealed that the engine second gas spring losses are lower than previously measured in Phase II. However, the second gas spring losses are still too high, resulting in a maximum engine brake efficiency of 21%.

1.3.4 ENGINE HEAT EXCHANGER LOSSES

In Phase III, additional instrumentation and the improved data acquisition system permitted measurements of flow losses in the engine heat exchanger components. The measurements confirmed that overall heat exchanger flow losses are too high, but that regenerator losses are relatively low, confirming the Phase II recommendation to increase regenerator effectiveness and accept the small increase in regenerator flow loss. It was also found that cooler losses are very high, equal to the heater and regenerator losses combined. This is probably due to the use of spiral spring inserts in the cooler tubes.

The Phase III test results indicated where improvements in the heat exchangers can be made to improve performance. The measurements also emphasized the limited accuracy of the simulation models available in industry for designing Stirling components. Although the test results can be used directly to improve the engine heat exchanger designs, it is recommended that the currently available hardware be used for further diagnostic and engine component testing. In the Phase III tests, only one of three different engine designs was tested. Testing of the other engine designs could significantly add to the data base of engine performance/ engine exchanger losses, leading to improved simulation models and higher confidence in a redesign of the engine.

SECTION 2

DEVELOPMENT OF PHASE IIIB TEST REQUIREMENTS

SECTION 2
DEVELOPMENT OF PHASE IIIB TEST REQUIREMENTS

The development of the test requirements for the Phase IIIB tests is described in this section. A brief description of the Phase II test program and the hardware and facility that were modified for the Phase IIIB tests is included. A more detailed description of the Phase II tests and equipment can be found in Reference 1. This section also contains the analyses used to derive the instrumentation requirements and to define the test plan.

2.1 PHASE II RESULTS AND CONCLUSIONS

2.1.1 PHASE II TEST DESCRIPTION

Test Objectives

The Phase II test effort focused on testing the Proto 2 combustor/engine/compressor in the Integrated Test Facility. The purposes of the integrated tests were to provide:

- Proof of design concept
- Performance of the Proto 2 FPSE, compressor and combustor in the assembled/integrated configuration
- Optimization of the engine gas spring and related mass characteristics.

Proto 2 Combustor/Engine/Compressor Description

The Proto 2 combustor/engine/compressor assembly consists of a gas-fired combustor supplying heat input to a free-piston Stirling engine (FPSE) that is coupled to a free-piston linear compressor. Figure 2-1 is a design layout of the assembly. The three major subassemblies have the following design features:

- Combustor - The natural gas-fired combustor is composed of two basic components - a radiation cooled transpiration burner and an air preheater. Air enters the combustor at ambient conditions, passes through the preheater, mixes with the fuel and flows inside the cylindrical burner element. The fuel/air mixture next passes radially through the burner element and ignites, forming a laminar flame several millimeters in height on the outer surface of the burner. The combustion products then pass through the finned tube heat exchanger

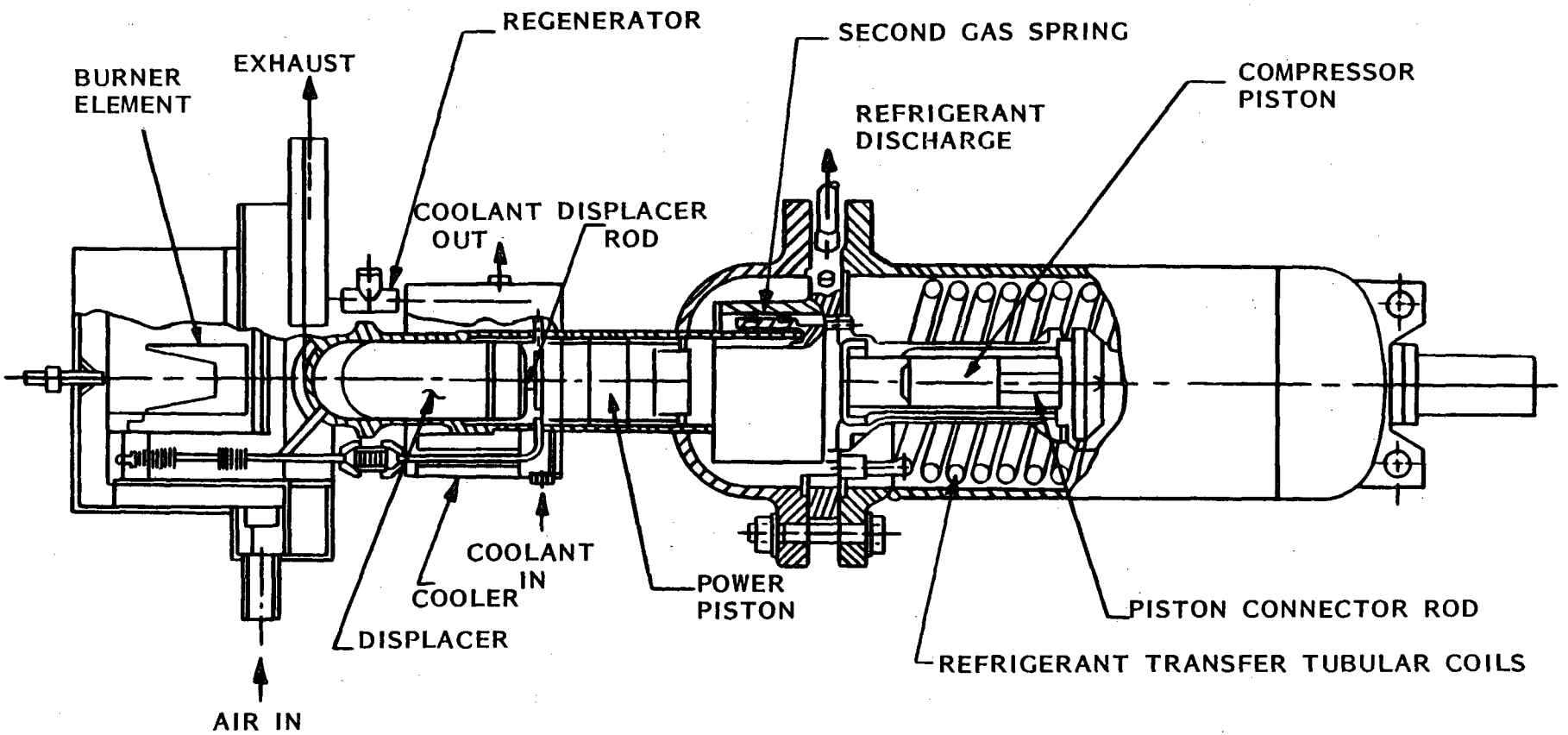

Figure 2-1. Proto 2 Combustor/Engine/Compressor Assembly

assembly (part of the engine housing assembly), after which they flow through adjacent alternate sections of the air preheater and out the exhaust port. Other components include a flame detector, an electronic spark igniter, and a view port which permits visual inspection of the flame.

- Free piston Stirling engine - The Proto 2 FPSE is a single cylinder engine, thermally driven oscillator operating on a Stirling cycle. Its housing assembly is the pressure vessel member and contains the heater head, regenerators and cooler subassemblies. Additional engine subassemblies include a working fluid displacer and a power piston. The linear compressor housing is an integral part of the engine power piston, and, as such, results in an engine/compressor assembly having three freely moving masses: the fluid displacer, the engine power piston, and the compressor piston. Relative motion of the three free bodies are constrained only by the working fluid pressures, and are dependent on load and operating parameters. The oscillating motion of the engine displacer shuttles the working fluid back and forth through the heat exchangers, thereby phasing the rates at which heat is absorbed and rejected from the engine working fluid (helium for the Proto 2 engine). This motion is affected by a gas spring action between the power piston and the displacer rod.
- Compressor - The Proto 2 compressor is a free piston inertia compressor. Power input is through the oscillating cylinder housing which is an integral part of the engine power piston. The inertia of the compressor free piston provides the refrigerant gas compression forces. The piston assembly is fastened by a connecting rod which is pinned to each piston. A floating seal is incorporated in the midsection housing to divide the two cylinder sections, thereby isolating the two cylinders. Suction and discharge valve assemblies are provided at each end of the compressor housing. Tubular spring coils are used for transferring the suction and discharge refrigerant gases to and from the oscillating compressor housing, providing for hermetic sealing of both the engine working fluid (helium) and the refrigerant (Freon).

Test Facility Description

The Integrated Test Facility is a simulated heat pump installation utilizing water side heat exchlangers for the refrigerant loop. This provides more test flexibility than testing with the indoor and outdoor unit air side heat exchangers, thus permitting characterizing the engine/compressor assembly independent of the air handlers. Figure 2-2 shows a Proto 2 FPSE assembly installed in the Integrated Test Facility.

Test Description

Integrated testing of the Proto 2 engine/compressor assembly was conducted in three phases - initial baseline Proto 2 engine tests, final Proto 2 baseline engine tests and modified Proto 2 engine tests. During the first phase the test fixture was checked out, dynamic tuning of the engine was undertaken and initial estimates of engine power level and efficiency were obtained. During the second phase, dynamic tuning of the engine was continued, changes were made to the second gas spring, and additional data reduction techniques were investigated. As a result of this testing, changes were made to the engine heater, regenerator, and cooler components in an effort to increase engine efficiency. The redesign was designated the modified Proto 2 engine. An extensive series of tests was conducted in which test conditions were set and data taken to determine the resulting performance characteristics at various engine charge pressures, combustor firing levels, and compressor ratios. Table 2-1 presents a matrix of the major portion of the test conditions evaluated. Results of these tests and the conclusions reached are given in subsequent sections.

2.1.2 ENGINE PERFORMANCE DEFICIENCIES

The Proto 2 engine performed below both power and efficiency goals during Phase II testing. The baseline Proto 2 engine indicated power limit was approximately 2.75 kw and maximum indicated efficiencies were 25-26%, versus goals of 3.2kw and 32% respectively. The modified Proto 2 engine power limit was approximately 2kw with a maximum indicated efficiency of 28%. Both engines were tuned to increase or decrease indicated power over a limited range with an associated decrease or increase in indicated efficiency. Diagnostic testing and investigative analyses conducted at the close of Phase II indicated that these performance deficiencies were mainly due to low regenerator effectiveness, high heater head flow losses and

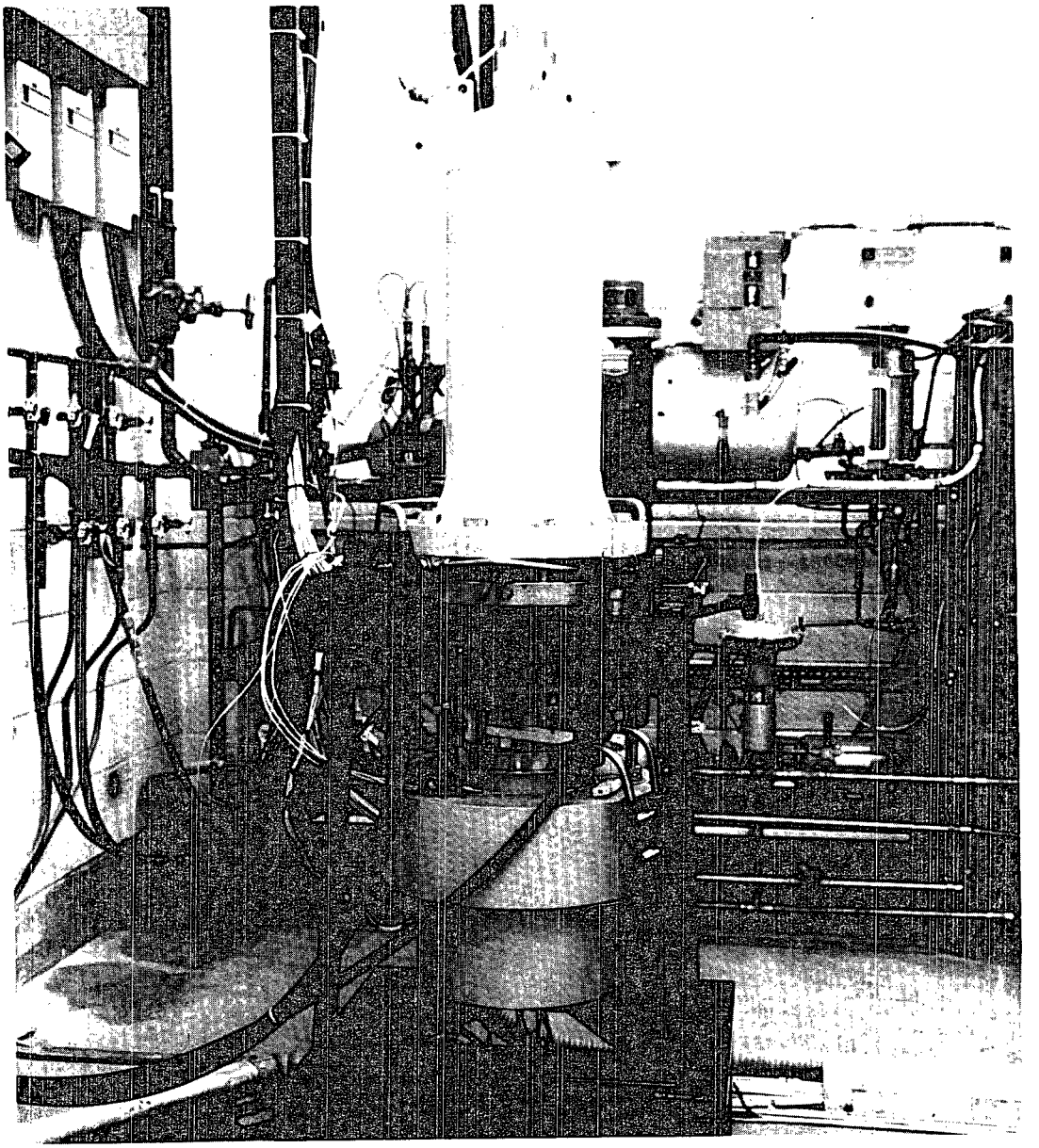

Figure 2-2. Proto 2 Combustor/Engine/Compressor Integrated Test

Table 2-1. Operating Test Point Matrix

Firing Rate (Btu/hr)		24,400			41,000	
Fuel Flowrate (SCFM)		0.44			0.73	
Air Flowrate (SCFM) (Allowance = ± 3%) (% Excess)		4.25 0	4.89 15	5.52 30	7.09 0	8.15 15	9.22 30
Helium Charge Pressure (psia)		870 ± 25			870 ± 25	
Coolant Flowrate (GPM)		2.0 ± 0.05			2.0 ± 0.05	
Evaporator R-22 Discharge Pressure/ Temperature (psia/°F		Degree Day			Degree Day	
	Cooling Mode	80	95		95	105
	Pressure Temperature	100 57	105 59		94 52	99 56
	Heating Mode	47	62		32	17
	Pressure Temperature	71 37	93 52		49 18	38 5
Condenser R-22 Inlet Pressure (psia)	Cooling Mode	80	95		95	105
	Pressure	193	235		271	301
	Heating Mode	47	62		32	17
	Pressure	206	211		233	222

excessive hot side swept volume. (Reference 1 provides a more detailed discussion of the performance results and interpretations.) Thus, the need to determine the thermal performance and flow losses of the individual engine heat exchangers was identified as a prime requirement of future testing.

2.1.3 COMPRESSOR OPERATION UNCERTAINTIES

During the Phase II program the Proto 2 compressor was tested on its own component test stand to verify its performance. After some minor hardware modifications, the compressor met its performance goals (output flow and efficiency) and was mated with the Proto 2 FPSE for integrated testing. Throughout the Proto 2 integrated engine/compressor testing, the compressor flow output was below that measured on its own test stand for the same test conditions. A number of diagnostic tests and analyses were conducted to determine the reason(s). Excessive suction superheating, compressor gas spring regulator malfunctions, non-sinusoidal motion and several other potential explanations were evaluated and ruled out. Reference 1 provides a detailed description of the compressor development effort.

The principal instrumentation deficiency in the Phase II integrated testing was the lack of a measurement of the location (stroke and phase angle) of the compressor piston. Instrumentation difficulties and the objectives of the Phase II testing had led to the decision to not include this instrumentation in the test. (An LVDT had been used in the compressor component tests to confirm compressor piston motion.) When it became apparent that Phase II performance goals could not be met, the testing became more diagnostic. Under this philosophy, the location of the compressor piston became more important as it can be used to verify analytical understanding of the compressor processes as well as empirically correlate compressor performance. It, therefore, was identified as a prime requirement for subsequent testing.

2.1.4 MATCHING ENGINE AND COMPRESSOR CHARACTERISTICS

During the end of Phase II testing an engine/compressor matching technique was developed to better understand scatter in observed operating points. This technique is described in Section 2.3. The technique is also required to design the heat pump control system. While the technique predicted

reasonable results, the data points to test it against were mostly run before it was available. In addition, during Phase II, several techniques were used to measure engine power, thereby limiting the number of consistant data points. Therefore, at the close of Phase II, the need to both refine the engine/compressor matching technique and confirm its validity through test were identified.

2.1.5 SIMULATION MODEL DISCREPANCIES

Throughout the Phase II program, the analytical tools used to design the hardware and predict test results were upgraded as new tests were conducted. During testing of the first ("Baseline") Proto 2 engine, these tools were correlated with test data and used to design modifications to the "Baseline" engine, leading to the "Modified" Proto 2 engine design described in Reference 1. As detailed in Reference 1, the analyses successfully predicted increased efficiency but failed to predict the magnitude of the associated power output decrease. Additionaly, predictive checks by another Stirling contractor, Sunpower, Inc. confirmed the need for substantial improvements in the engine models.

As discussed in Section 2.1.2, it was determined early in Proto 2 testing in the Phase II program that heat exchanger design deficiencies were limiting engine performance, but the necessary tools for improving the designs of the individual components were not available. Therefore, an additional goal was established for further testing: to develop sufficient performance data on typical FPSE engine heat exchangers to permit improvements in the design tools needed to redesign the engine.

2.1.6 PHASE III PROGRAM PLAN

The basic test needs identified at the conclusion of Phase II, as discussed above, were to:

1) verify compressor performance when operated with the engine.
2) develop performance data on individual engine heat exchanger components to permit upgrading of the engine design tools.
3) verify the engine/compressor matching analysis technique and confirm the HAHP control system approach.

These needs related directly to the continued development of the basic FPSE/linear compressor concept for the HAHP. The broader DOE/ORNL requirements for HAHP development required an examination of alternative configurations for a residential Stirling heat pump. Combined with the identified Proto 2 tests and analyses, these requirements lead to the Phase IIIA program.

Phase IIIA Program

The Phase IIIA program was initiated in May of 1981. Its objectives were to:

1) Evaluate alternative Stirling engine driven residential heat pumps and compare their performance, cost, development risks and product potential to that of the Proto 2 concept.
2) Develop the requirements and prepare a design of an oscillating flow test rig which could be used to test FPSE type engine heat exchangers under simulated engine operating conditions. The data from such tests were to be used to improve the engine design tools.
3) Refine the engine/compressor matching analysis and verify the Proto 2 control concept.
4) Develop the test plan for Phase III.

Results of the evaluation of alternative Stirling HAHP concepts, and the design of the oscillating flow test rig are presented in Reference 2. The alternative concepts evaluation indicated that the most attractive concepts for a residential size (3 ton) heat pump are a slightly modified version of the current free piston Stirling engine/linear compressor configuration (Proto 2) and a kinematic Stirling engine/rotary drive compressor configuration. It was also determined that a free piston Stirling engine/linear alternator/electric motor-compressor concept could also be competitive if the high efficiency and low cost goals for the alternator can be achieved. However, the Proto 2 configuration was determined to have the lowest production cost potential and, hence, the greatest product potential. This result confirmed the recommendation to continue development of the concept.

To obtain an independent evaluation of the technical merits of the Proto 2 concept, General Electric requested the NASA Lewis Research Center to conduct an independent review of the Stirling/Rankine system technology in January, 1982. Detailed results of the review are given in Reference 1.

The NASA Lewis conclusions confirmed that the free piston Stirling engine/linear compressor concept is technically feasible and capable of successful development. The technical deficiencies of the current hardware were also confirmed, and GE's engine technology development plan was deemed reasonable with one major exception: NASA Lewis recommended obtaining individual engine heat exchanger performance data from the existing engine, rather than through the use of an oscillating test rig, since the engine itself was the best test rig simulator available and already existed.

The conclusions of the alternative concepts evaluation and the NASA Lewis technology review led to the decision to perform tests on the Proto 2 unit with additional instrumentation on the engine heat exchangers and to improve the data acquisition system. The requirements for the intrumentation were developed as reported in Section 2.2. The matching and control analyses were also refined to establish the expected results and help define the test plan. These analyses are presented in Section 2.3 Because of the general value to the Stirling technology community of an oscillating flow test rig, this effort was transferred to the Argonne National Laboratories for implementation.

Phase IIIB Program

The test hardware fabrication and testing was executed under the Phase IIIB program, sponsored by DOE/ORNL. During the Phase IIIA program, GRI re-evaluated its participation in the Stirling/Rankine project and determined that its objectives and resources prevented it from being involved in the technology development required. GRI's sponsored research is oriented toward applied research and development directed toward development of a commercial product, and its involvement in technology development programs is limited. Therefore, the program was reformulated under sole DOE/ORNL sponsorship with the following priorities:

1) To verify compressor performance
2) To verify engine/compressor matching
3) To tune engine/compressor dynamics to achieve maximum engine performance
4) To obtain component level test data on the regenerators, heater head, cooler, displacer gas spring, and combustor.

The activities and results of the Phase IIIB program are presented in Sections 3, 4 and 5.

2.2 INSTRUMENTATION ANALYSIS

Based on both theoretical calculations and Proto 2 test data, it was determined that engine performance was limited by the heat exchanger designs. Proto 2 engine component thermal performance is low and the total flow losses in the heat exchangers is high. To assess these conclusions, dynamic pressure and temperature instrumentation were to be installed on the engine for direct measurement of component performance. This section discusses elements of the theory behind these conclusions as they relate to the choice of instrumentation. The selection of the appropriate instrumentation and the test data reduction techniques are described in Section 4 and Section 5.

2.2.1 REGENERATOR EFFECTIVENESS

The ideal Stirling cycle can be represented as:

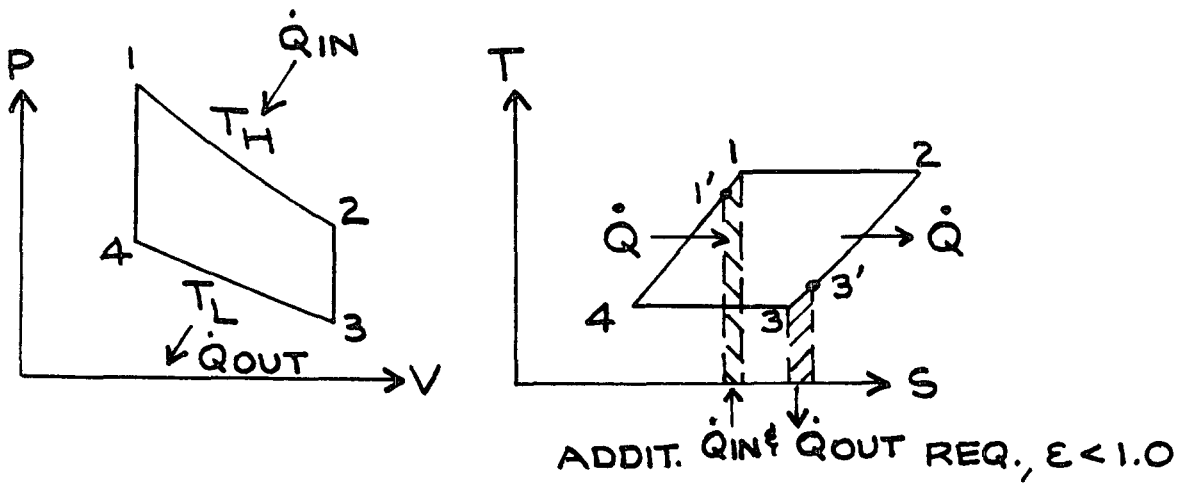

During the process 2-3, heat is stored in, and during 4-1, it is released from the regenerator. For an ideal regenerator (i.e., with effectiveness, ε, equal to 1.0) $T_1 = T_2$. For a non-ideal regenerator, the gas will exit the regenerator at some temperature lower than T_1. Therefore, additional heat must be added at the heater to bring the gas temperature to T_1. The effectiveness thus can be calculated (assuming an ideal gas) as:

$$\varepsilon = \frac{T_1' - T_3}{T_2 - T_3} = \frac{\dot{Q}_{ACTUAL}}{\dot{Q}_{MAX}} \qquad (1)$$

The real Stirling cycle, as represented by the FPSE, requires a more complex formulation. Non-ideal processes, with their attendant pressure, temperature, and density differences, must be incorporated into an accurate calculation of ε. This is presented below.

Energy Balance

The transient flow energy balance on the regenerator is:

$$\dot{Q} + \dot{W}_{NET} + (h + \frac{\dot{x}^2}{2} + zg)\,\dot{m}_{IN} - (h + \frac{\dot{x}^2}{2} + zg)\,\dot{m}_{OUT} = \dot{U} \tag{2}$$

There being no work performed, and with kinetic and potential energy terms approximately 0, this reduces to:

$$\dot{Q} + h\dot{m}_{IN} - h\dot{m}_{OUT} = \dot{U} \tag{3}$$

Over half a cycle (π radians; refer to Figure 2-3):

$$Q = \int_0^{\pi} h(\frac{dm}{dt})dt_{OUT} - \int_0^{\pi} h\,(\frac{dm}{dt})dt_{IN} + \int_0^{\pi} (\frac{dU}{dt})dt \tag{4}$$

Using the ideal gas relation of $\Delta U = \int C_v dT$ and integrating,

$$Q = (mh)_{OUT} - (mh)_{IN} + (mC_v\,\Delta T)_{C.V.} \tag{5}$$

With the assumption that $m_{OUT} \approx m_{IN}$

$$Q = m\Delta h + (mC_v\,\Delta T)_{C.V.} \tag{6}$$

Again, using the ideal gas relation of $\Delta h = \int C_p dt$,

$$Q = mC_p\,(T_{OUT} - T_{IN}) + (mC_v\Delta T)_{C.V.} \tag{7}$$

Figure 2-3. Regenerator Temperature Histories

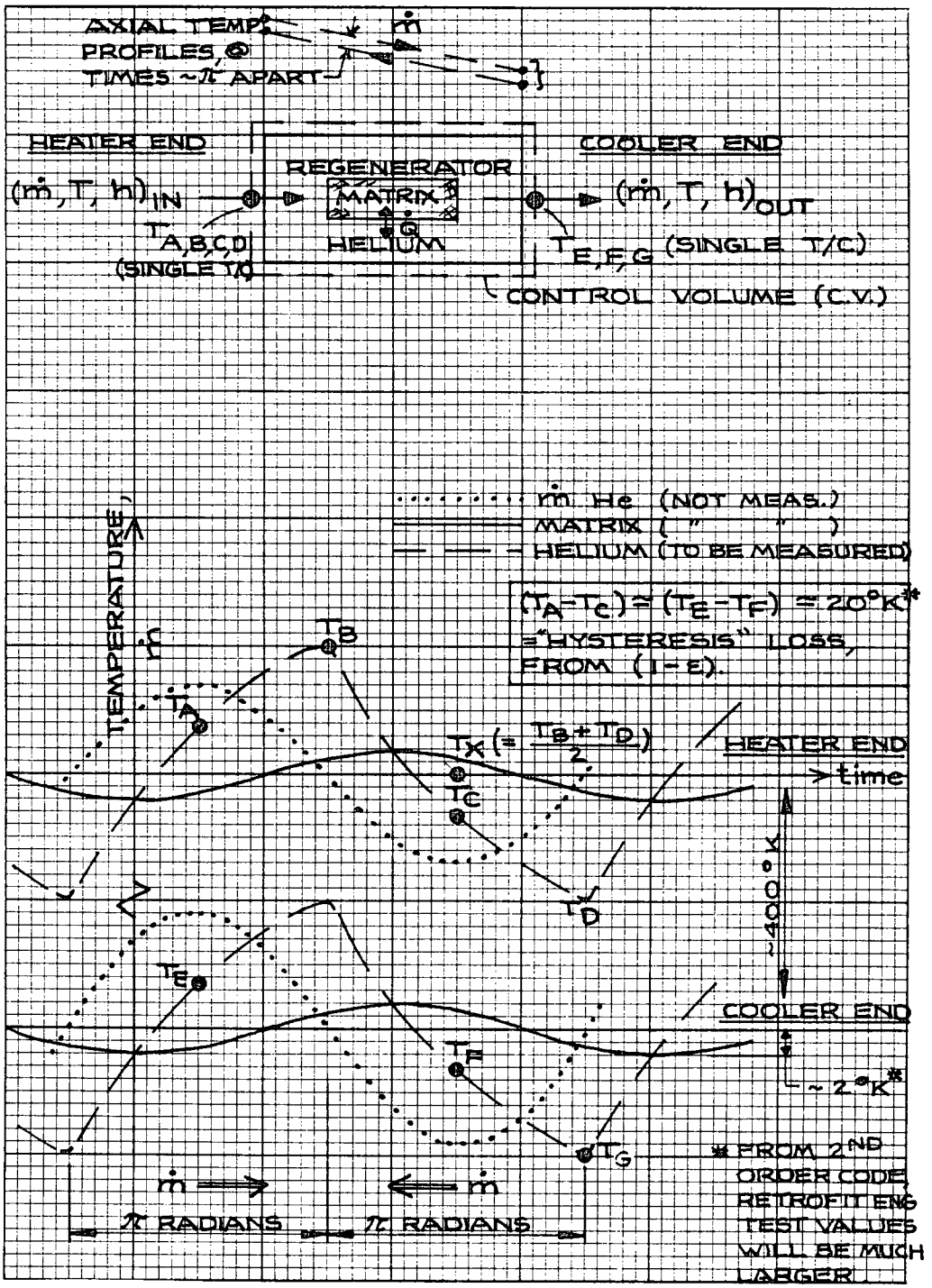

Now placing this on a (average) rate basis, by dividing each term by Δt,

$$\dot{Q} \simeq \frac{Q}{\Delta t} \simeq \frac{m}{\Delta t} C_p (T_{OUT} - T_{IN}) + \frac{1}{\Delta t} (mC_V \Delta T)_{C.V.} \tag{8}$$

On examining Figure 2-3, the second term on the right hand side of the equation is quite small ($<$ 2% of the first term, since $T_B - T_D \ll T_B - T_G$), and can be ignored with little error. Now the effectiveness equation can be properly formulated.

Reheat Loss

The reheat loss, which is due to the regenerator ineffectiveness (i.e., $1 - \varepsilon$), can be computed from the temperature "hysteresis". Referring to Figure 2-3, the reheat loss equals $\bar{\dot{m}}_1 C_p (T_A - T_C)$. Therefore, with $\varepsilon = \dot{Q}_{ACTUAL}/\dot{Q}_{MAX}$, and employing the results from the energy balance discussion,

$$1 - \varepsilon = 1 - \frac{\bar{\dot{m}}_1 C_p (T_A - T_C)}{\bar{\dot{m}} C_p (T_B - T_G)} \tag{9}$$

Although, this means of calculating ε is the simplest to visualize, a number of practical deterrents to its use exist:

a. It is not clear when T_A and T_C occur in the cycle. In a temperature - time profile as in Figure 2-3, T_A and T_C would occur at the mid-points of the half-cycle. A larger inaccuracy is associated with measuring these temperatures (on the slope of the curve) than with measuring the maximum/minimum.

b. If T_A and T_C are selected as outlined above, a properly averaged $\dot{m}$ must be determined from:

$$\bar{\dot{m}}_1 \simeq \frac{\Sigma (\dot{m}) (T) (\Delta t)}{\Sigma (T) (\Delta t)} \tag{10}$$

and will probably differ significantly from a simple time-averated m, associated with the ideal temperatures T_B and T_G. ($\dot{m}$ was not measured in the tests due to hardware limitations.)

Direct Computation

The effectiveness can be computed directly, using the definition and the results from the energy balance discussion presented earlier. Thus:

$$\varepsilon \equiv \frac{\dot{Q}_{ACTUAL}}{\dot{Q}_{MAX}} \simeq \frac{\bar{\dot{m}}_H C_p T_X - \bar{\dot{m}}_C C_p T_G}{\bar{\dot{m}}_H C_p T_B - \bar{\dot{m}}_C C_p T_G} \tag{11}$$

where the time averaged helium mass flow rates at the hot and cold ends of the regenerator, respectively, are $\bar{\dot{m}}_H$ and $\bar{\dot{m}}_C$. In equation (11):

a. $C_p = f(T)$, and drops out of the equation.

b. The time-averaged $\dot{m}$ are used correctly. The ideal regenerator, operating between T_B and T_G, exhibits no time-varying temperature profiles, and therefore, a strictly time-based average $\dot{m}$ can be associated with these. For a time-averaged temperature T_X, a similar rationale applies.

c. Only one time-averaged temperature (T_X) is used in the numerator.

d. An approximation can be made that $\bar{\dot{m}}_C = 1.25\ \bar{\dot{m}}_H$. Using this ratio and comparing the resulting ε to one calculated for $\bar{\dot{m}}_C = \bar{\dot{m}}_H$, a small error is evident. For the temperatures anticipated ($T_B \approx 925^oK$, $T_D \approx 900^oK$, $T_G \approx 460^oK$) the results differ by about 1-1/2 percentage points. Since $\dot{m}$ will not be measured, the actual difference applicable will remain unknown. The computed effectiveness will be somewhat high.

e. Thermodynamic temperature effects (i.e., due to compression and expansion of the gas) have been ignored. Because of the strong thermal coupling between the gas and the regenerator matrix, heat transfer mechanisms dominate, so that pressure changes introduce

only a small perturbation on top of the cyclical temperature variation causes by heat transfer. Negligible error is introduced by ignoring this perturbation.

The formulation for ε for use with the test data then becomes:

$$\varepsilon \simeq \frac{T_X - T_G}{T_B - T_G} \tag{12}$$

It was planned that, after the first few tests, the temperature profiles be examined. If these exhibited significant departures from symmetry, some additional averaging (of T_X) might be necessary.

Instrumentation Response

As indicated in Figure 2-3, the temperatures on either side of the regenerator are time dependent and will vary with a frequency of approximately 30 HZ. Thus the transient response of the thermal instrumentation must be considered as well as its steady state accuracy. Measurements in Heat Transfer, by Eckert and Goldstein, analyzes the effects of transient convection on thermocouple response. The equation relating the wall temperature of the thermocouple to the fluid stream temperature is:

$$T_W = \bar{T}_f + \frac{\Delta T_f}{\sqrt{1+\omega^2\theta^2}} \times [\sin(\omega t - \tan^{-1}\omega\theta)] \tag{13}$$

where:

T_W is the thermocouple wall temperature.
$\bar{T}_f$ is the average fluid temperature.
ΔT_f is the amplitude of the temperature excursion.
ω is the frequency of the fluid temperature excursion.
θ is the time constant of the thermocouple
t is time

The above equation can be written as:

$$\frac{(T_W - \bar{T}_f)}{(T_f - \bar{T}_f)} = \frac{\sin(\omega t - \tan^{-1}\omega\theta)}{\sqrt{1+\omega^2\theta^2}} \qquad (14)$$

The numerator of the left hand side is the temperature excursion registered by thermocouple, ΔT_W, while the denominator is the actual temperature excursion, ΔT_f. Table 2-2 presents the ratio $\Delta T_W / \Delta T_f$, and the per cent error as a function of the phase lag, $\alpha = \tan^{-1}\omega\theta$.

Table 2-2. THERMAL RESPONSE OF THERMOCOUPLES

α (deg)	α (RAD)	$\frac{\Delta T_W}{\Delta T_f}$	% Error
1	.01745	0.99139	-0.86
2	.03491	0.98298	-1.702
3	.05236	0.97478	-2.522
4	.06981	0.96677	-3.323
5	.08727	0.95893	-4.107
10	.17453	0.90220	-7.8

Currently, thermocouple vendors advertise fast response devices with time constants between 0.1 and 1.0 milliseconds. This range results in phase angles between 1° and 10° and errors between 1% and 8% (see Table 2-2). To assess the severity of these errors, equation (12) is rewritten as:

$$\epsilon = \frac{T_{MH} - T_{MC} - \Delta T_{MC}}{T_{MH} + \Delta T_H - T_{MC} - \Delta T_{MC}} \qquad (15)$$

where T_{MC} and T_{MH} are the mean cold and hot temperatures respectively and ΔT_{MC} and ΔT_{MH} are their respective excursions.

The sensitivity of ϵ was tested using $T_{MH} = 800^oK$, $T_{MC} = 400^oK$, $\Delta T_{MH} = \Delta T_{MC} = 20^oK$. If a dynamic uncertainty of 10% exists in ΔT_{MH} and ΔT_{MC} (0 = 1.0 millisec per above), equation (15) has a dynamic uncertainty of 1.0%. Thus, a 1.0 millisecond response time was specified as the maximum allowable. Steady state accuracies of 1.0^oK are standard for calibrated thermocouples and were judged adequate for the evaluation of equation (15).

2.2.2 FLOW WORK

The frictional work performed during each cycle of operation of the Stirling engine is important for estimating overall efficiency. The evaluation of this term is particularly difficult since the flow is unsteady and oscillatory in nature. A study was undertaken to solve for the friction work term by performing an order of magnitude analysis on the momentum equation. In this manner, higher order terms were eliminated and a simplified friction expression was obtained. The relationships between the kinetic and internal energies were also investigated.

Consider the combination of displacer, piston, heater, regenerator and cooler as illustrated in Figure 2-4. Typical temperature levels are also presented. The following one-dimensional momentum equation is applicable for this situation:

$$\frac{\partial u}{\partial t} + u \frac{\partial u}{\partial x} = - \frac{1}{\rho} \frac{dp}{dx} + X_b + F \tag{16}$$

where u is the gas velocity

x is the displacer displacement

p is the gas pressure

ρ is the gas density

X_b is the body force

and F is the friction force

This equation was applied to the heater, regenerator and cooler and the importance of each term was evaluated. The rms pressure drops in each component were considered at 5 psi, 2 psi, and 3 psi respectively based upon steady state calculations. Body forces were assumed negligible and the frequency, ω , of the displacer piston was taken to be 30 Hz. Each component of equation 16 was then evaluated. The pressure gradients in the components are given by:

$$\left(\frac{dp}{dx}\right)_{Regen} \approx \frac{2 \text{ psi}}{1.5 \text{ In}} = 1.33 \text{ lb/in}^3$$

$$\left(\frac{dp}{dx}\right)_{Heater} \approx \frac{5 \text{ psi}}{15.8 \text{ In}} = .32 \text{ lb/in}^3$$

$$\left(\frac{dp}{dx}\right)_{Cooler} \approx \frac{3 \text{ psi}}{6.378 \text{ In}} = .47 \text{ lb/in}^3$$

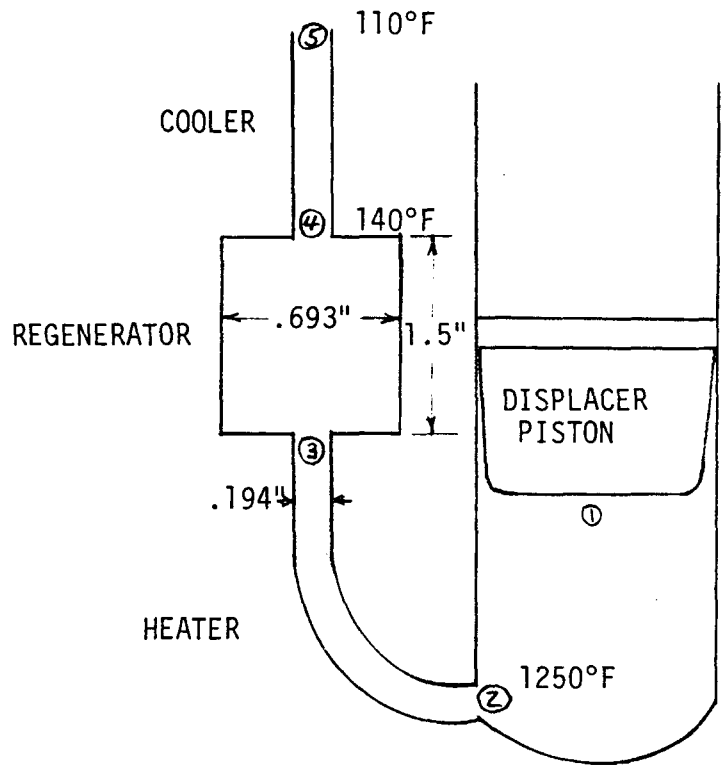

Figure 2-4. Heater, Regenerator, and Cooler Configuration for Stirling Engine

The displacer piston traverses a total distance of 1.7" so that the amplitude of displacement is 0.85". The motion of the displacer is given by $\dot{X}_D = \frac{.85}{12} \omega \cos \omega = 2.13 \cos \omega$. Conditions at station 2 were approximated using the steady flow continuity equation and assuming constant density in the displacer region for a particular time. There are 12 heater tubes so the mass flow in any one tube is 1/12 the displacer flow:

$$\frac{1}{12} \rho_1 V_1 A_1 = \rho_1 V_2 \frac{\pi}{4} \left(\frac{.194}{12}\right)^2$$

$$\therefore V_2 = 39.03 \cos \omega \quad \text{ft/sec}$$

The density of helium at 528^0R, 2114 lb/ft^2 is .01043 lb/ft^3. The average pressure in the heater tube was estimated to be 885 psia based upon Proto 2 tests. Using the ideal gas relation,

$$\frac{P_2}{P_{ref}} = \frac{\rho_2 T_2}{\rho_{ref} T_{ref}}$$

the density at station 2 becomes:

$$\rho_2 = \frac{885 \times 144}{2114} \times \frac{1}{95.9} \times \frac{528}{1710} = .1941 \text{ lb/ft}^3$$

Similarly, at station 3,

$$\rho_3 = \frac{890}{885} \times .1941 \times \frac{1710}{1680} = .1987 \text{ lb/ft}^3$$

From continuity, $V_3 = \frac{\rho_2}{\rho_3} V_2 = 38.12 \cos \omega$ ft/sec

Also, $\rho_4 = \frac{892}{890} \times \frac{.1987 \times 1680}{600} = .5576$ lb/ft^3

and $\rho_5 = \frac{895}{892} \times .5576 \frac{600}{570} = .5890$ lb/ft^3

The velocity at station 4 was estimated to be $V_4 = \frac{\rho_3}{\rho_4} = 13.58 \cos \omega$ ft/sec

In a similar manner, $V_5 = \frac{\rho_4}{\rho_5} V_4 = 12.86 \cos \omega$ ft/sec

Each term in Equation (16) was estimated for the regenerator in order to establish the dominant expressions.

The period for one complete cycle is $T = \frac{2\pi}{\omega}$ and if $t = \frac{\pi}{2\omega}$, the $\cos \omega$ expression varies from 1 to 0. The first term in Equation (16) can be estimated as:

$$\frac{\partial u}{\partial t} \approx \frac{\Delta u}{\Delta t} = \frac{38.12(-1)}{\pi/2\omega} = 728 \text{ ft/sec}^2$$

The second term is:

$$u \frac{\partial u}{\partial x} = \left(\frac{13.58 + 38.12}{2}\right) \frac{(38.12 - 13.58)}{1.5/12} = 5075 \text{ ft/sec}^2$$

The pressure gradient term is of the following order:

$$-\frac{1}{\rho} \frac{dp}{dx} = \frac{-1}{(.1987 + .5576)/2} \frac{2 \times 144}{1.5/12} \frac{\text{ft}^3}{\text{lbm}} \times 32.2 \frac{\text{lbm - ft}}{\text{lbf - sec}^2} = 196189 \text{ ft/sec}^2$$

It can clearly be observed that the pressure gradient term dominates such that the left side of Equation 16 can be neglected. The frictional term is the only expression which can balance the equation, and, therefore, it must be of the same order. Similar results are obtained for the heater and cooler.

The friction loss can be estimated by integrating the following approximate form of equation (16):

$$0 \approx -\int \dot{m}_{avg} \frac{1}{\rho} \frac{dp}{dx} dx + \int \dot{m}_{avg} F \, dx$$

The frictional power loss is then estimated by:

$$\int \dot{m}_{avg} F \, dx \simeq \frac{\dot{m}_{avg}}{\rho} (\Delta p)_{rms} \tag{17}$$

For sinusoidal pressure variations, $\Delta P_{rms} = \Delta P_{max}/\sqrt{2}$. State of the art dynamic pressure tranducers have over 2 orders of magnitude greater frequency response than that required to measure pressure variations in the 30 hertz FPSE. Thus, dynamic accuracy is not a major concern. Pressure transducer diaphrams were specified by the expected ΔP_{max} to be monitored. The possibility of dynamic affects in the tubing connecting the pressure transducers to the engine was, however, considered. Section 5.1 of this report describes the test plan which was implemented to insure that this error is minimized.

2.3 MATCHING AND CONTROL ANALYSIS

2.3.1 MATCHING REQUIREMENTS

One of the important technical issues facing the FPSE/linear compressor concept is the matching of the engine output to the compressor requirements over the operating range of the HAHP. The requirements for dynamic and load matching of the engine to the compressor have been addressed since the beginning of the Phase II hardware development program (Reference 1) and the Proto 2 control system was developed to provide adequate system control with minimum complexity. However, during testing of the Proto 2 engine/compressor, it was apparent that engine operation was limited under some conditions due to mismatching of engine operating frequency and power output to compressor operating frequency and power requirements.

In the initial stages of the Phase IIIA program, it was concluded that the current control system required modifications to provide adequate engine/compressor matching over the full range of HAHP operating conditions. The "adequate" is stressed because the prime criteria for engine/compressor matching and control in the HAHP is not maximum performance but minimum ownership and operating cost. Therefore, the re-examination of engine/compressor controls was predicated on minimizing additions to the current controls while achieving acceptable engine/compressor matching.

2.3.2 CONTROL OPTIONS

The current HAHP operating control system consists of two active component controls; a gas combustor firing rate control and a compressor gas spring pressure regulator. The high firing rate is used for very high and very low ambient temperature conditions where maximum engine power is required to meet high cooling and heating loads. The low firing rate is used at moderate temperatures to reduce output and thereby improve the refrigeration system COP. An additional benefit is to reduce cycling losses by better matching of output to load. Part of this benefit is, of course, offset by the increase in parasitic power required to operate longer periods. The two-step firing rate concept was selected as an optimum combination of manufacturing and operating costs during the Phase II program (see Reference 1 for results of the study).

The need for a pressure regulator for the compressor gas springs was determined in the Phase II program (Reference 1). At low ambient temperature conditions, refrigerant density decreases, causing the free piston of the compressor to operate at longer strokes. This characteristic of the free piston compressor results in a slower drop off in compressor capacity with ambient temperature than that of conventional fixed stroke compressors. However, at very low temperatures, overstroke of the piston can occur. Therefore, a pressure regulator, feeding the compressor piston gas springs, is used to limit the tendency to overstroke. In the Proto 2 hardware, it was determined that a constant pressure feed from the regulator would be adequate to control piston motion.

Subsequent tests and analyses of the Proto 2 engine/compressor revealed the need for additional control of the engine/compressor dynamic characteristics. This can be accomplished in several ways:

1) Combustor firing rate can be modulated
2) Engine charge pressure can be modulated
3) Compressor gas spring pressure can be modulated
4) Combinations of the above can be utilized

In operation, engine/compressor operating frequency varies over a narrow range, with little effect on engine ouptut power. Compressor capacity is, however, very sensitive to operating frequency and the most logical method

to achieve engine/compressor matching is to modulate compressor characteristics through control of its gas springs. This could be accomplished by modifying the existing compressor regulator. Therefore, this approach was investigated in detail to determine if it could meet the matching requirements of the engine and compressor and what other changes might be necessary to the control system.

2.3.3 MATCHING ANALYSIS

Several test data correlated codes were used for the matching analysis. The codes are described in Reference 1. The technique for the analyses is described in detail in References 1 and 2 and summarized in Figures 2-5 and 2-6.

The codes generate data from which three "maps" can be drawn. A compressor map, an engine map, and the dynamic interaction between the engine and the compressor as a function of ambient temperature were developed. A fourth code models the Freon heat exchanger loop and yielded information on compressor conditions for a given firing rate and ambient temperature. By overlaying the compressor and FPSE maps, the matching power points can be determined.

Preliminary Evaluation

The first iteration in the matching analysis was simplified for ease of estimation. The compressor was designed to absorb approximately 3kW at both the 95°F and 2°F outdoor conditions, and approximately 1.5 kW at 47°F. When the compressor map was cross-plotted against an analogous engine map, it appeared that a three-firing rate control method might satisfy these three ambient day conditions.

A second iteration was then undertaken to determine system operation at other ambient temperature conditions. More detailed engine and compressor maps were generated and used in this second iteration. These maps were bounded by the freqnencies, strokes, temperatures, etc. which the first iteration produced. Figure 2-7 shows the compressor power map for 95°F ambient conditions. Note the dependence on operating frequency. Similar maps were calculated for other conditions. A composite compressor map, showing all the operating curves, is shown in Figure 2-8. The operating

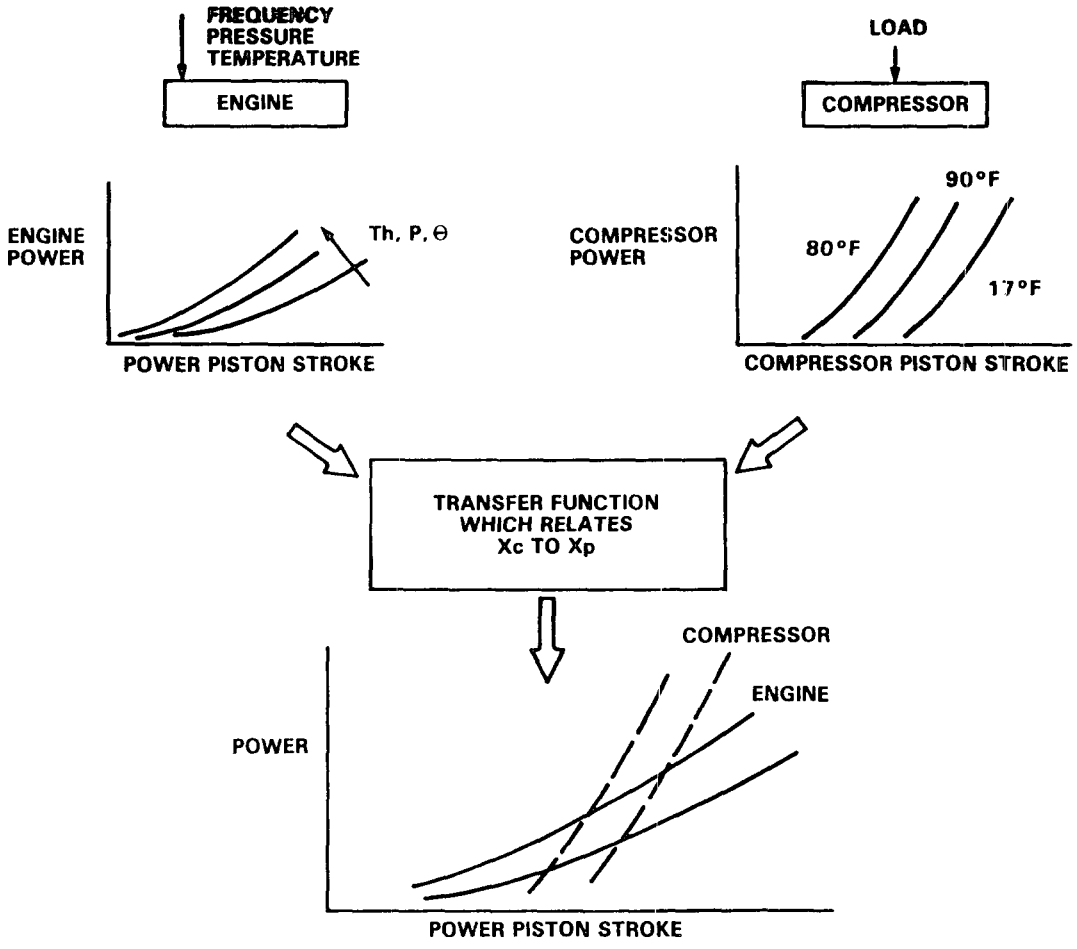

Figure 2-5. Load Matching Technique

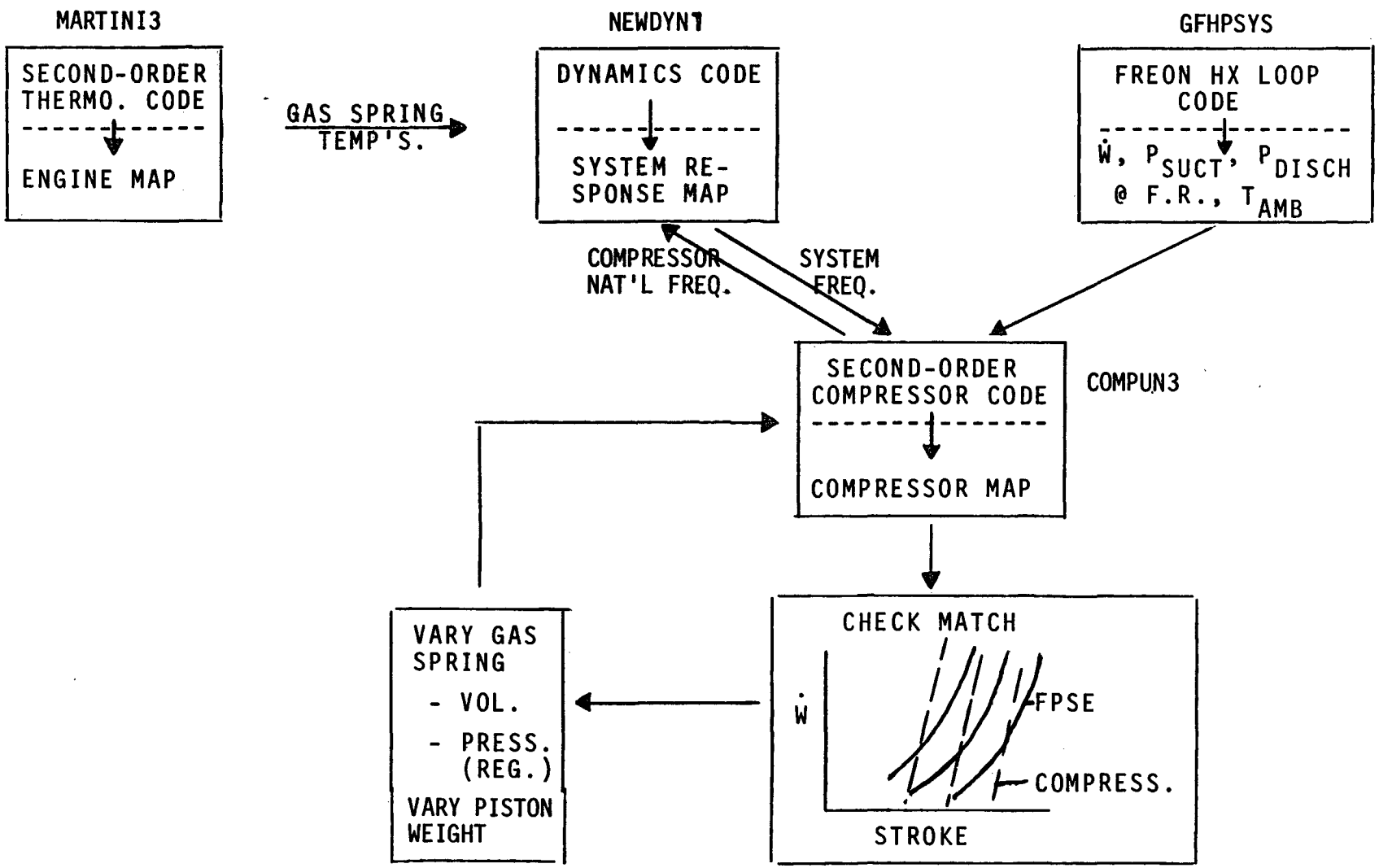

Figure 2-6. Computation Procedure for Load Matching Analysis

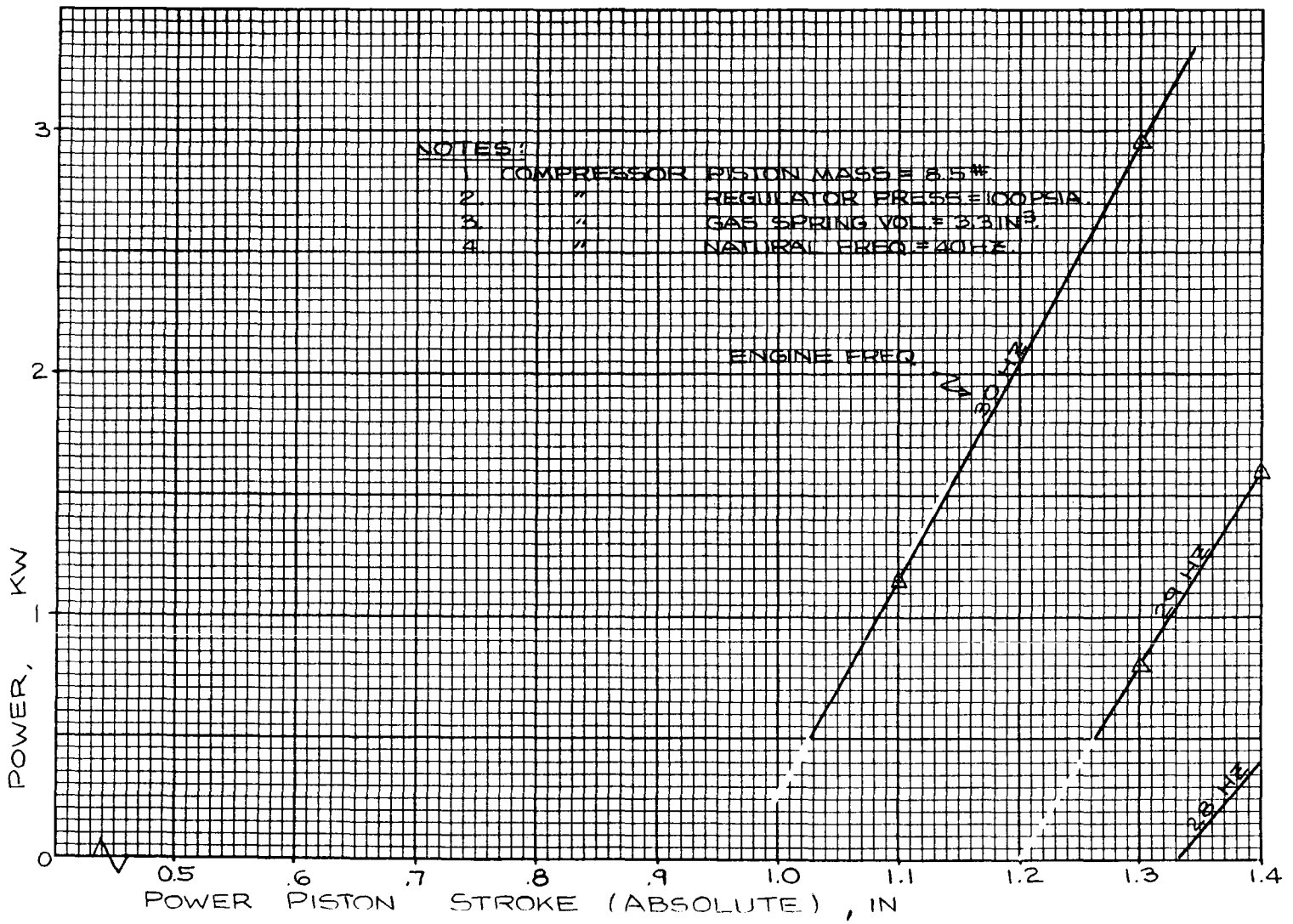

Figure 2-7. Compressor Power Map at 95°F Ambient Day

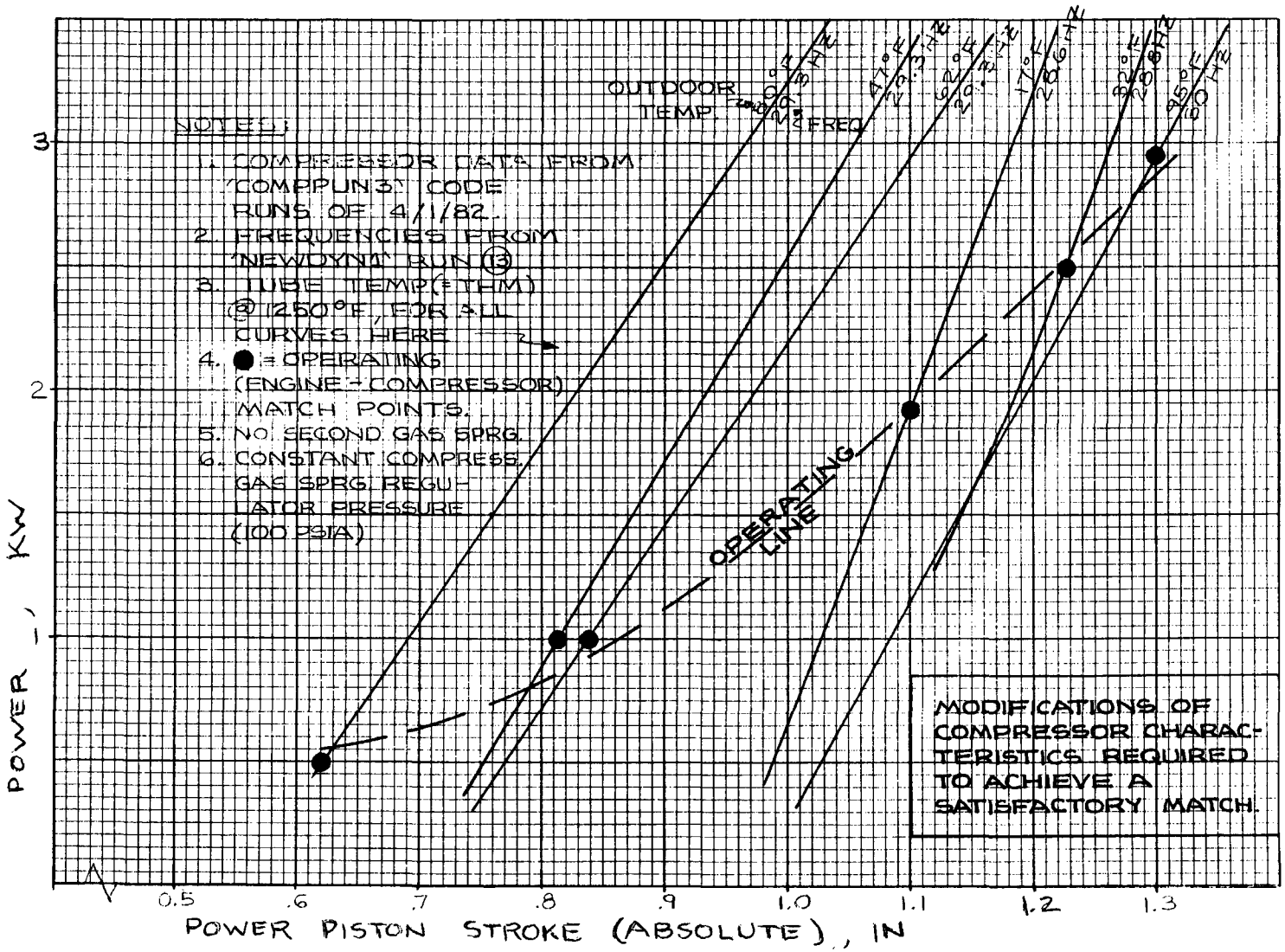

Figure 2-8. Compressor Map Over Operating Ambient Temperature Range

frequencies were determined from Figure 2-9, which plots operating frequency as a function of compressor natural frequency (predicted by the three body dynamics code).

When the compressor map of Figure 2-8 is superimposed on the engine map of Figure 2-10, the system operating points (i.e., points where compressor power and frequency match those of the engine) are determined. These are displayed as heavy circles on Figure 2-8.

It is evident that this particular match is inadequate: unsatisfactory power levels are available at all times except at the 32°F and 95°F conditions. This suggests that firing rate (heater head temperature) control alone does not suffice. Some form of control on the compressor is required to bring the operating lines (particularly at 80°F and 47°F) closer together, and permit the engine to run at longer strokes and higher power. This approach was explored further.

Selected Approach

Initial determinations of compressor power had been based on a constant compressor pressure ratio at a given ambient temperature (Figure 2-11(a)). A better representation of compressor performance takes into account the variation in pressure ratio with power. The Freon system code was employed to calculate the compressor suction and discharge pressures at a given ambient temperature amd at two power levels. The more accurate representation of compressor power is shown by the dashed line in Figure 2-11 (b). Other ambient temperature points were similarly calculated (Figure 2-11 (c)). Improved matching resulted from a compressor map where power required lines are nearly parallel with engine power available lines. But the spread among the different ambient temperature operating lines remained (Figure 2-11 (c)). Additional control was, therefore, necessary to reduce this spread and provide acceptable matching. The most feasible control method was varying the compressor gas spring pressure using a pressure regulator (Figure 2-11 (d)). In the ideal case, a single operating line would result.

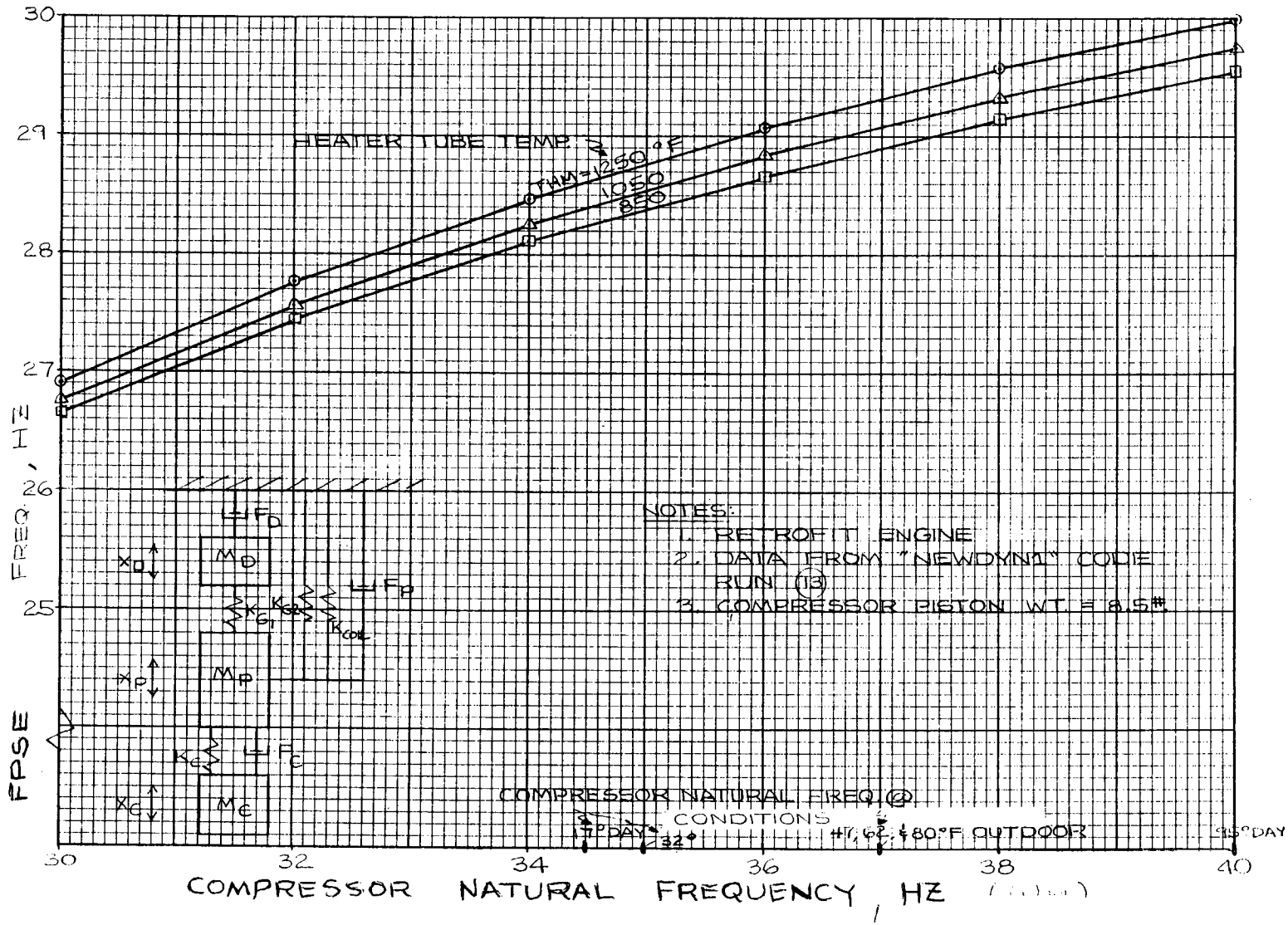

Figure 2-9. Engine Operating Frequency as a Function of Heater Head Temperature and Compressor Natural Frequency

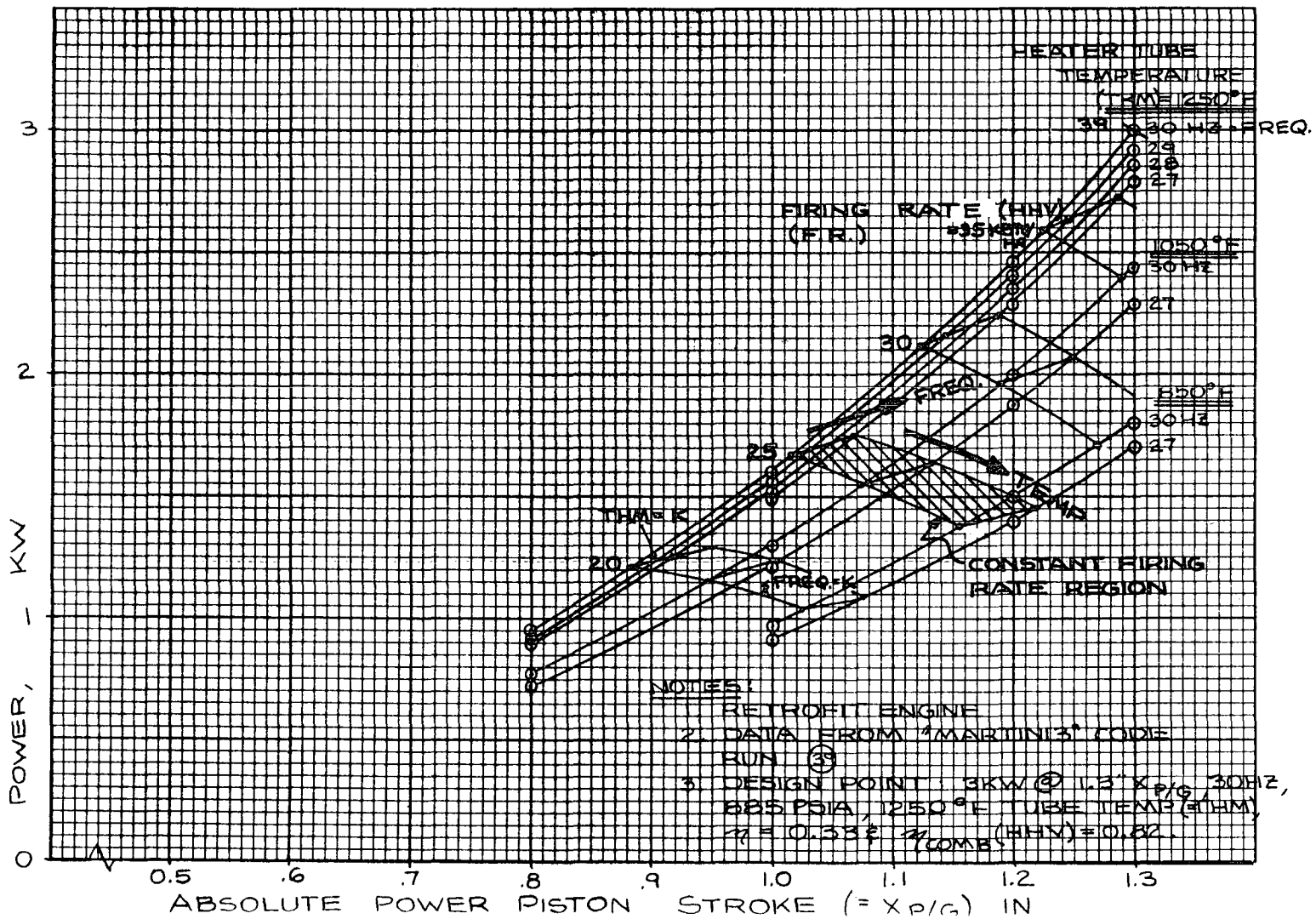

Figure 2-10. Engine Power Map

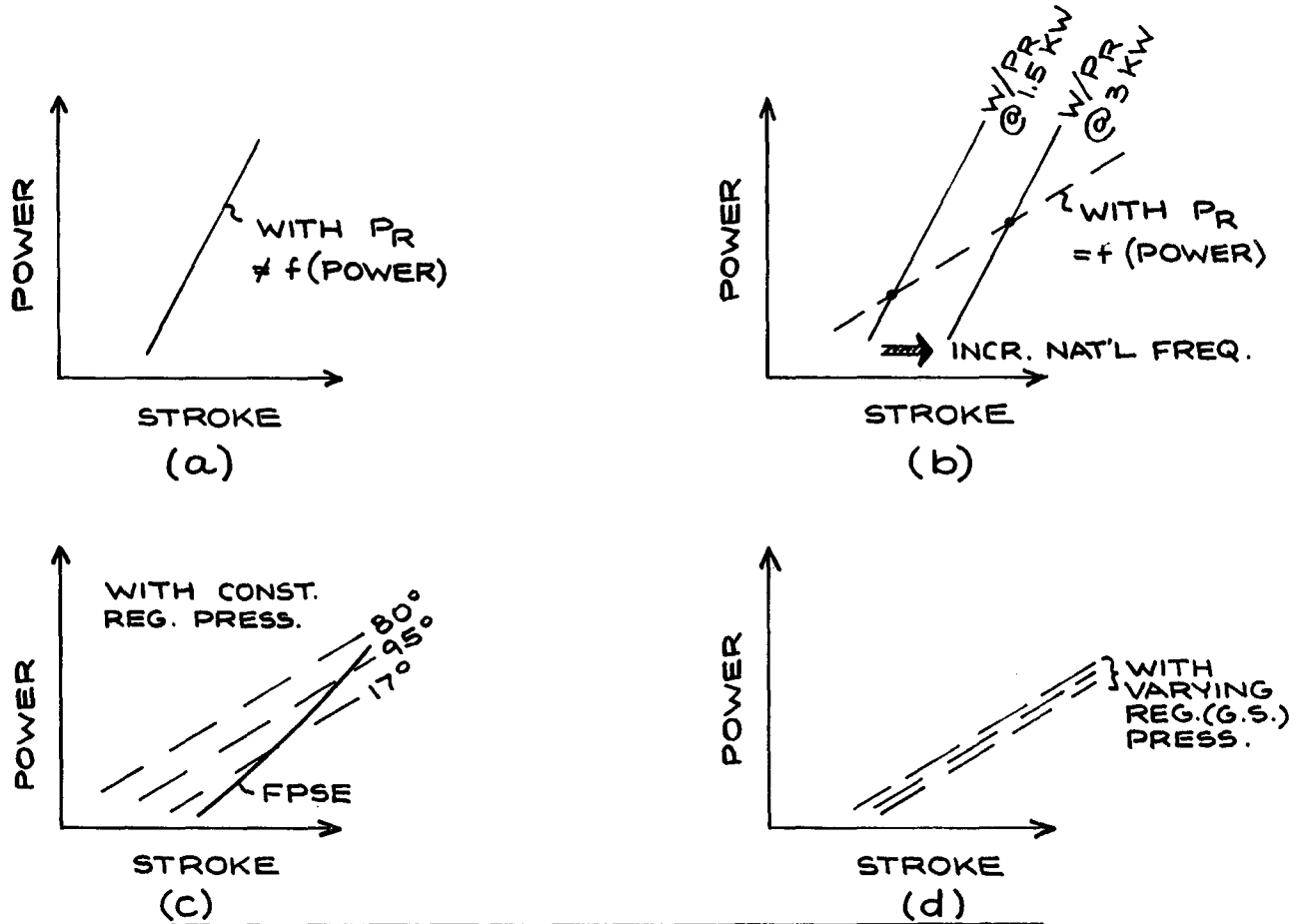

- PRESSURE RATIO (P_R) VARIATION WITH POWER HAS A SIGNIFICANT EFFECT.
- VARIATION OF COMPRESSOR GAS SPRING REGULATOR PRESSURE NEEDED TO LOCATE CURVES FOR SATISFACTORY MATCH POINTS.

Figure 2-11. Compressor Characteristics

For an 80°F ambient day, Figure 2-12 illustrates some of the results of this analysis from a number of compressor code runs. Varied were frequency, compressor pressure ratio (i.e., power), and gas spring pressure. The operating lines at the appropriate system frequency are given in Figure 2-13. Figures 2-14 and 2-15 provide summary information for the other ambient temperature conditions. When the entire compressor map is superimposed on the engine map of Figure 2-10, the system operating points given in Table 2-3 and Figure 2-16 are determined. The compressor natural frequencies in the final analysis differed from those identified on Figure 2-9. New system frequencies were determined with the aid of that figure. The appropriate frequencies are noted on Figure 2-13, 2-14, and 2-15.

A valuable feature of the proposed control concept is the flexibility in matching points that can be achieved. Because gas spring control and firing rate control shift the compressor and engine operating points along different axes, a wide range of control over the engine map (Figure 2-10) is possible.

2.3.4 CONTROL SYSTEM VALIDATION

As noted above, earlier studies in Phase II had indicated that the optimal combustor firing rate control consisted of two firing rates. This analysis confirmed that approach, with high fire/power and low fire/power corresponding to high and low load conditions, respectively. Precise engine/compressor matching control appeared to be achieveable using a variable compressor gas spring pressure regulator. A regulator range from about 75 to 175 psia was judged adequate for most locations in the continental U.S. No feedback control would be required. Based on ambient temperature (or compressor pressure ratio), the regulator would set the gas spring pressure on a pre-determined schedule. Also, this control technique appeared forgiving enough to work well when faced with manufacturing tolerance stack-up, individual heat pump installation peculiarities, and performance degradation with time. The analysis also indicated that with this control approach, compressor efficiencies changed only slightly over the engine operating range when compared to operation with the original control system. Thus, COP and capacity estimates were as originally estimated, as well as operating costs. A small extra equipment cost would be incurred by the regulator modification, but should be negligible.

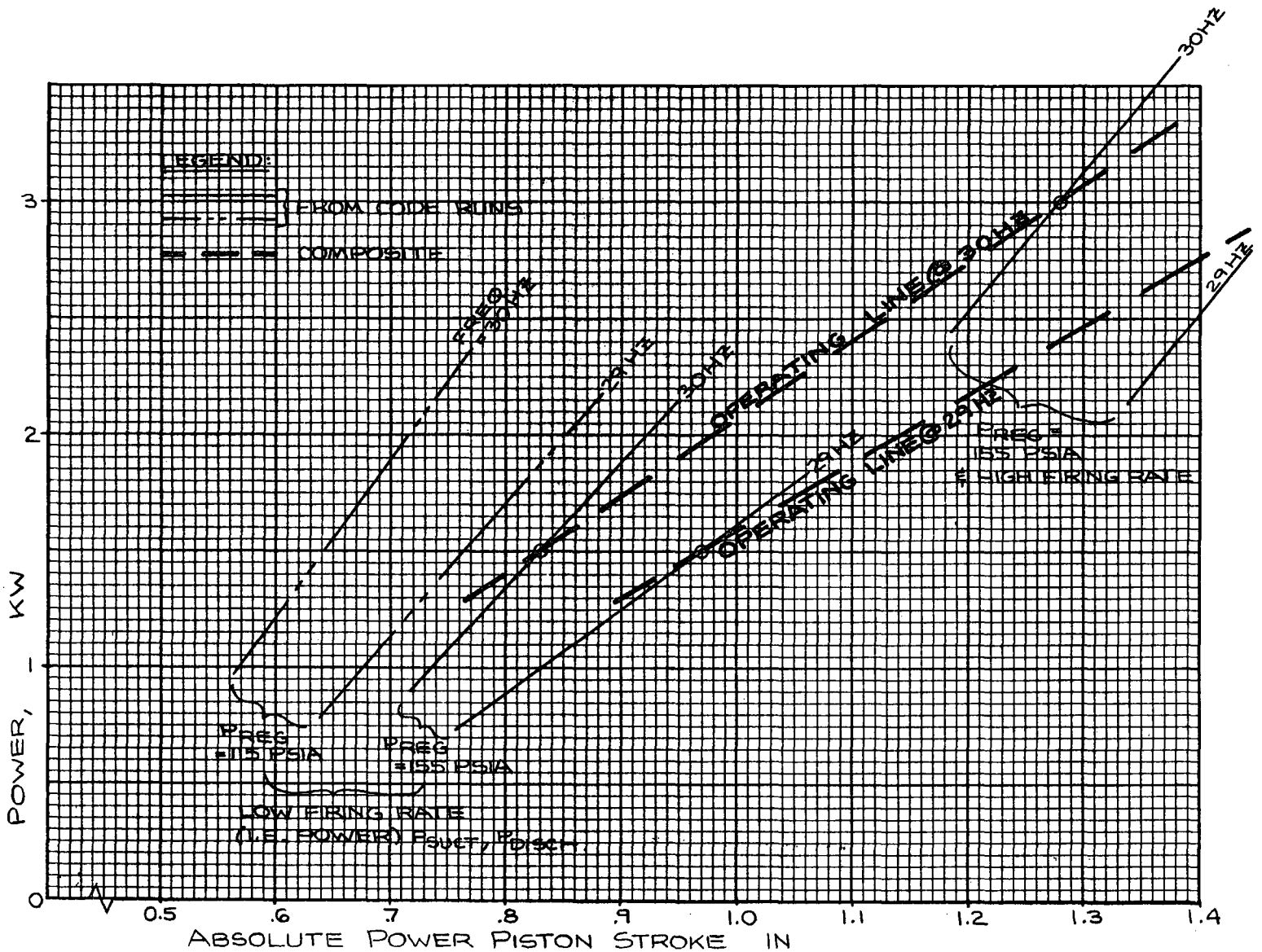

Figure 2-12. Compressor Power Map at 80°F Ambient Temperature

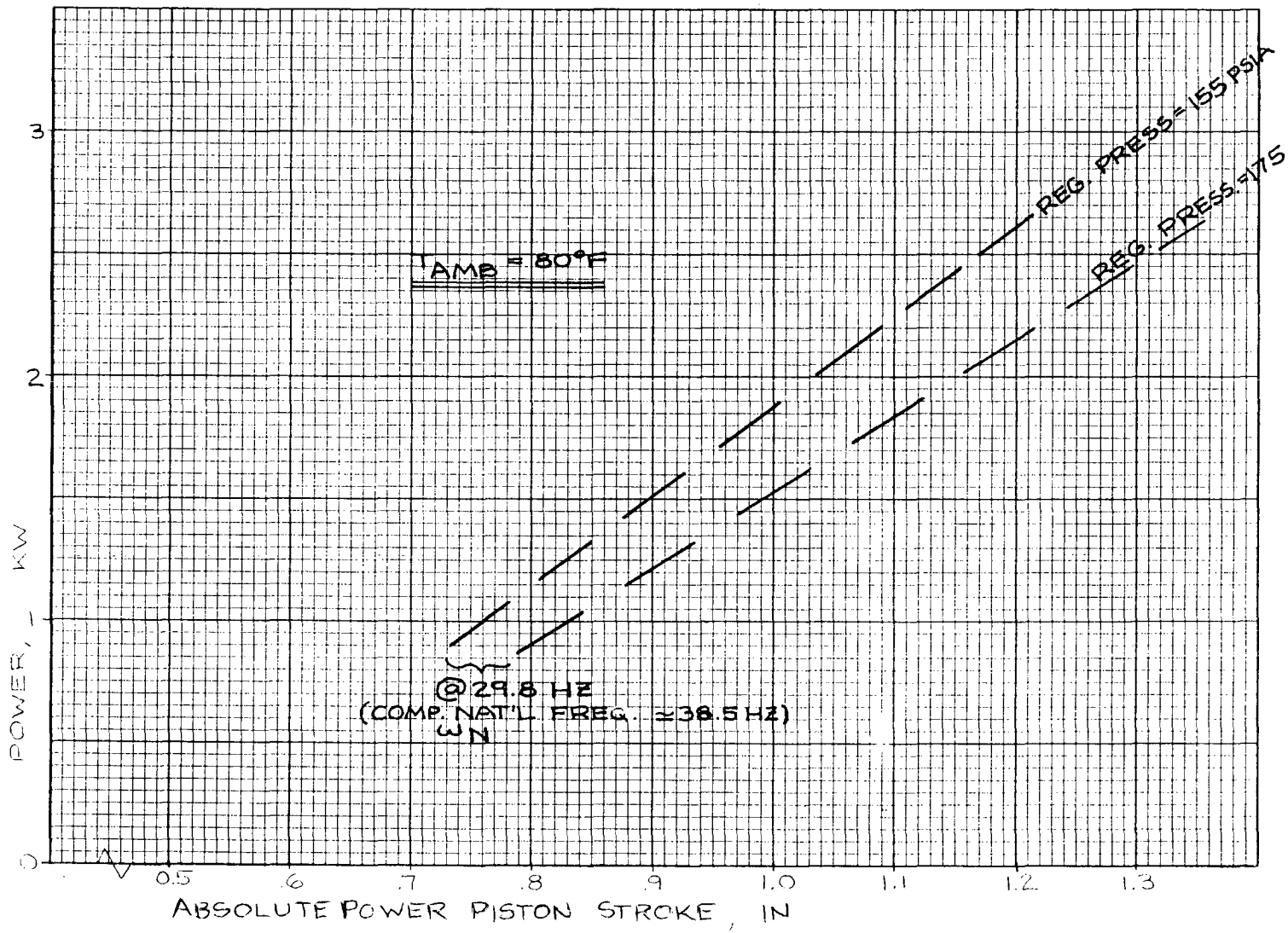

Figure 2-13. Operating Lines for Compressor at 80°F Ambient Day Conditions

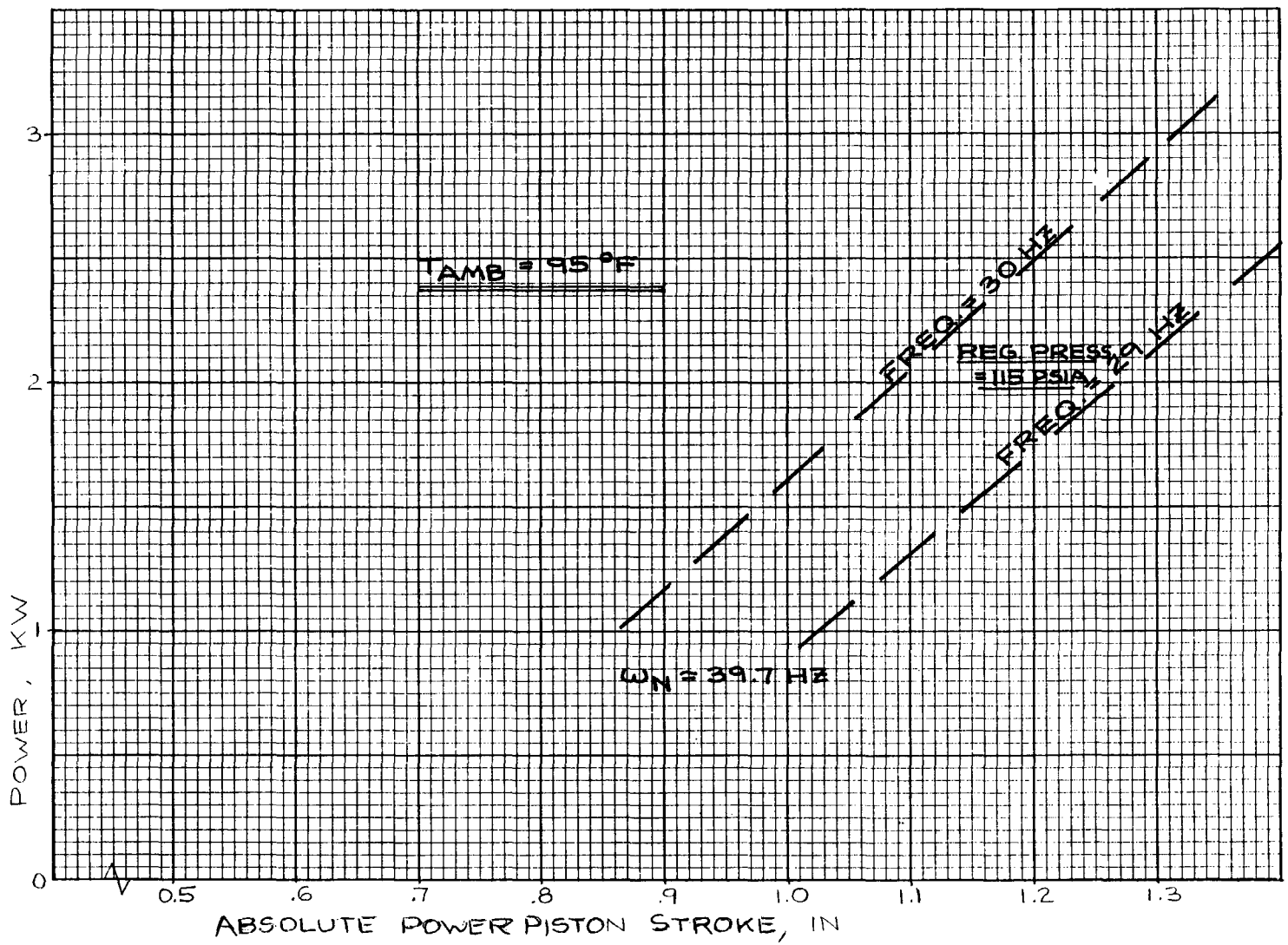

Figure 2-14. Operating Lines for Compressor at 95°F Ambient Day Conditions

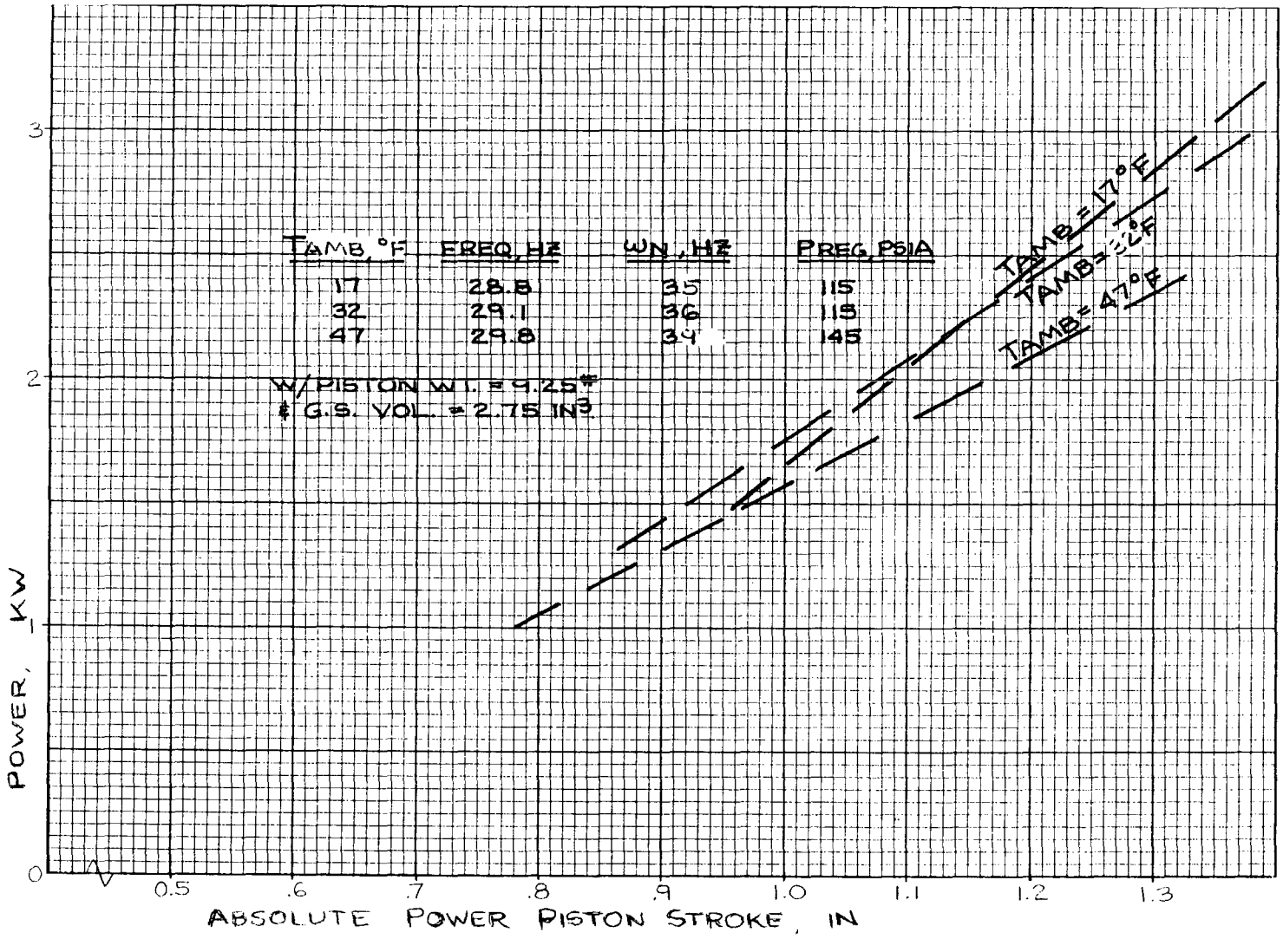

Figure 2-15. Operating Lines for Compressor at 17°F, 32°F and 47°F Ambient Day Conditions

TABLE 2-3

MATCHED ENGINE/COMPRESSOR OPERATING POINTS

$T_{AMBIENT}$, °F	REQUIRED[a] POWER, KW	ACTUAL COMPRESSOR POWER, KW	@ REGULATOR PRESSURE, PSIA	ACTUAL COMPRESSOR POWER, KW	@ REGULATOR PRESSURE, PSIA
95	3	3	100	3	115
80	1.5	0.5		1.5	175
62	1.5	1.0		NOT RUN	-
47	1.5	1.0		1.5	145
32	3	2.5[b]		2.95	115
17	3	1.8	100	2.9[b]	115

(a) APPROXIMATE POWER SUFFICIENT TO MEET LOAD, USING 2 FIRING RATES

(b) PROBABLY ADEQUATE

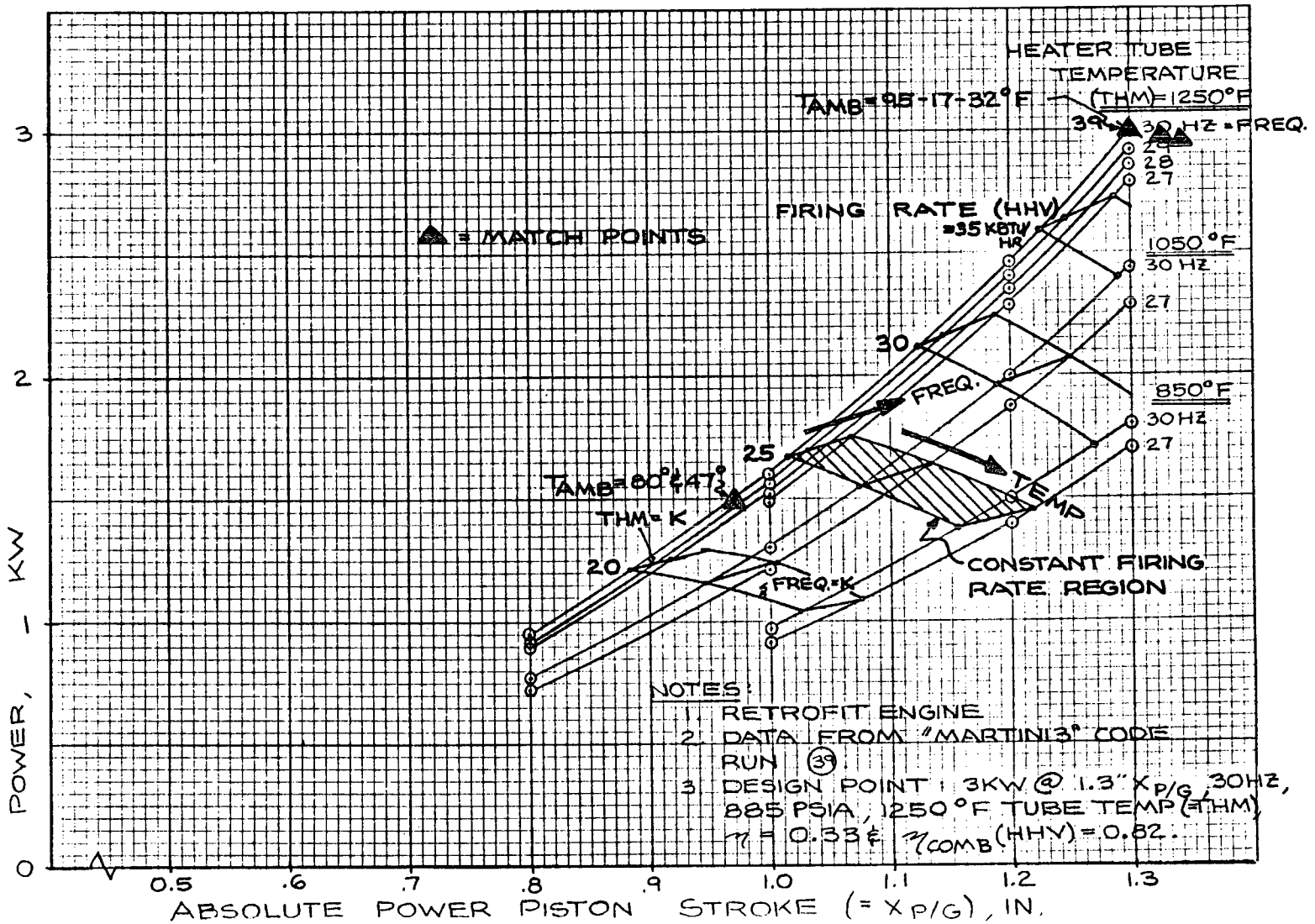

Figure 2-16. FPSE Power Map with Compressor Match Points

Confirmation of the matching analysis model and verification of the recommended control system modification was planned to be achieved through the series of engine/compressor tests planned in the Phase IIIB program. The test requirements to provide the confirming data are discussed in Section 5.1.

SECTION 3
TEST SYSTEM DESIGN

SECTION 3
TEST SYSTEM DESIGN

This section presents a description of the instrumentation and data acquisition system selections made to meet the test requirements and objectives described in Section 2. A summary of the changes to the Proto 2 design to install the instrumentation is also presented. Implementation of the design is described in Section 4.

3.1 INSTRUMENTATION SELECTION

3.1.1 EXISTING PHASE II INSTRUMENTATION

The instrumentation provided for Phase II testing was selected for the proof-of-design concept evaluation and combustor/engine/compressor assembly performance evaluation. Reference is made to Table 3-1 for a listing of the Phase II Integrated Test Facility instrumentation. A review of this instrumentation list shows that, while extensive in providing combustor, engine, and compressor assembly performance data, in-depth diagnostic data were not available for the engine heat exchangers/regenerators at the component level, or the compressor piston motion.

3.1.2 ADDITIONAL INSTRUMENTATION OPTIONS

Component level instrumentation options to provide in-depth diagnostic data were identified and were reviewed for potential implementation. These options included:

Combustor

- Ambient heat loss measurement to provide an accurate quantification of the heat input to the engine.

Engine

- Heater head, regenerator, and cooler subassembly pressure drops to provide gas flow pressure losses.
- Heater head, regenerator, and cooler subassembly dynamic gas temperature measurement for evaluating heat exchanger effectiveness.
- Heat exchanger gas mass flow rate measurement for accurate calculation of gas flow power losses and heat exchanger effectiveness.

Table 3-1

PHASE II INTEGRATED TEST FACILITY INSTRUMENTATION

Temperatures
Engine
• Heater head fins and tubes
• Cylinder head and walls
• Regenerator walls (hot, midpoint, cold)
• Coolant in and out
• Bounce space helium
• Second gas spring housing and helium
• Compression space helium
• Housing dome
• Cooler walls
• Pressure vessel
Combustor
• Pre-heater exit air
• Air and natural gas in
• Exhaust gas out
• Exhaust seal flange
• Pre-heater O.D.
Compressor
• Housing wall
• Cylinder heads
• Suction and discharge manifolds
• Refrigerant system (refrigerant and coolant)
Pressures
• Gas and air supply
• Engine charge
• Refrigerant loop
• Compressor cylinder
• Compressor gas springs
• Displacer gas spring
• 2nd gas spring
• Compression space
Flows
• Gas and air
• Coolant
• Refrigerant
Displacements
• Displacer to power piston
• Power piston to housing
• Housing to ground

- Displacer gas spring wall temperature and heat flux measurement to determine heat transfer from/to the gas spring.
- Pressure vessel heat flux measurement to improve heat balance calculations.

Compressor

- Compressor piston motion measurement to improve system dynamic analyses.
- Engine power piston to compressor housing force transducer to measure working force input to the compressor from the engine.

3.1.3 SELECTION

The selection of additional instrumentation was made primarily on the basis of installation feasibility. Instrumentation which was judged not feasible is discussed at the end of this section.

The additional diagnostic instrumentation selected for reinstrumenting the Proto 2 combustor/engine/compressor assembly at the component level consisted of the following:

- Additional pressure and temperature measurement systems on the engine heater head, regenerator, and cooler subassemblies.
- The addition of a displacement transducer on the compressor piston.
- The addition of a heat flux transducer to the back wall of the displacer gas spring, plus a temperature measurement at the same location.
- The installation of a cooling air shroud/heat loss measurement system around the combustor.
- The installation of heat flux transducers around the pressure vessel for heat loss measurement.

Figure 3-1 presents a cross-sectional drawing of the combustor/engine/compressor assembly with the additional instrumentation and location denoted.

Table 3-2 presents the requirements of the additional instrumentation, along with the selected vendors/models, and their respective ranges and specification limits.

The two instrumentation options that were not implemented were deleted for the following reasons:

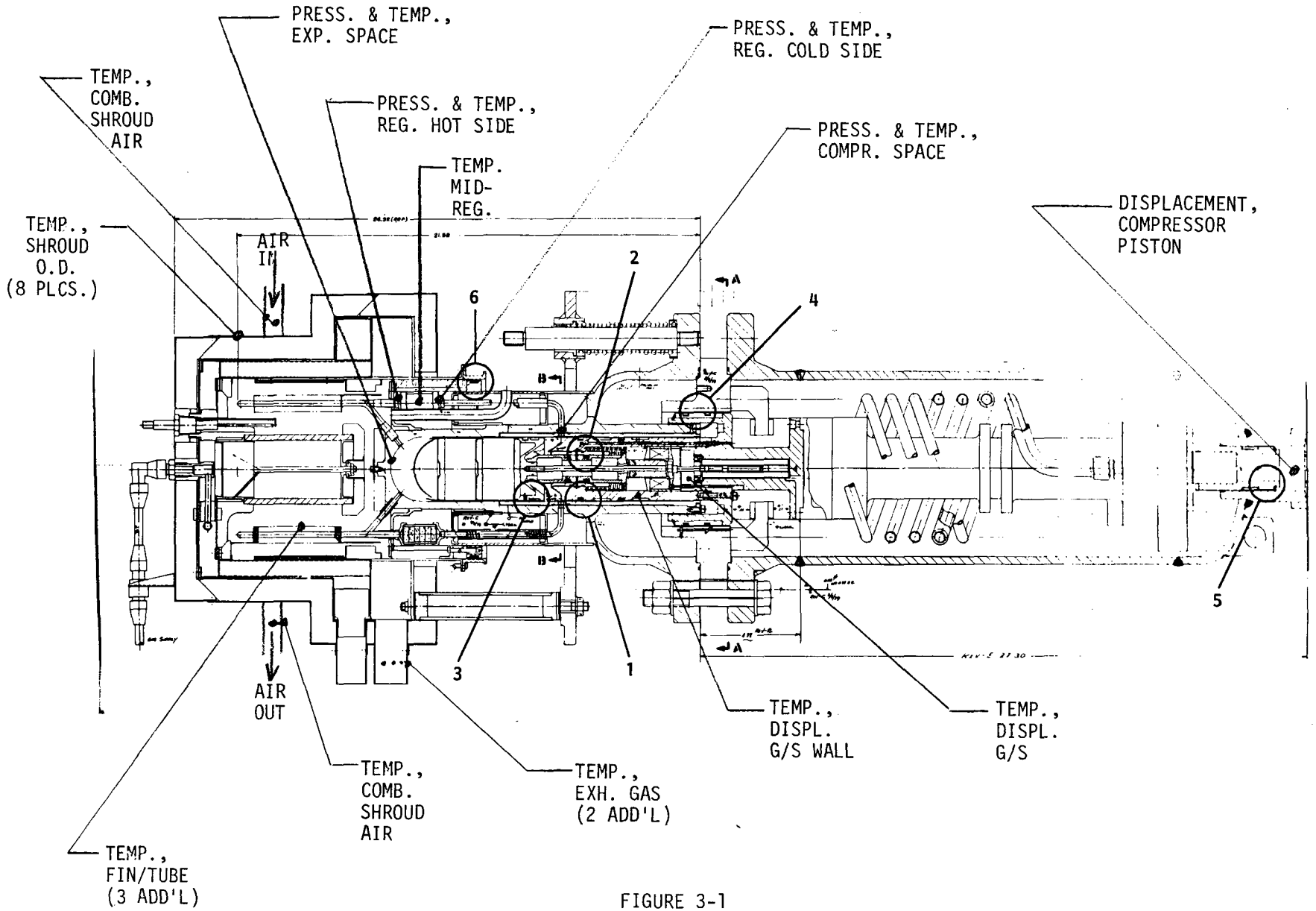

FIGURE 3-1

PROTO 2 FPSE

ADDITIONAL INSTRUMENTATION

TABLE 3-2

ADDITIONAL INSTRUMENTATION REQUIREMENTS

A. DYNAMIC PRESSURE TRANSDUCERS

SPECIFICATIONS	REQUIRED	AVAILABLE
		VALIDYNE, MODEL DP-15
PRESSURE RANGE	±10 PSID ±150 PSID	±1, 2, 5, 10, 15 PSID ±250 PSID
LINEARITY	±1.% F.S.	±1/2% F.S.
HYSTERESIS	1/2% PRESSURE EXCURSION	1/2% PRESSURE EXCURSION
THERM. SENSIT. SHIFT	ZERO	0.02%/°F*

*HEAT SINKED TO MAINTAIN CONSTANT TEMP.

		SENSOTEC, TYPE-S
PRESSURE RANGE	0-400 PSIA ±150 PSID	0-500 PSIA ±500 PSID
LINEARITY	±1% F.S.	±0.5% F.S.
HYSTERESIS	1/2% PRESSURE EXCURSION	1/2% PRESSURE EXCURSION
THERM. SENSIT. SHIFT	ZERO	0.02%/°F**

**TRANSDUCER WILL BE CALIBR. AT TEMP.

CONDITIONING EQUIPMENT

ACCURACY	0.1%	0.05%
STABILITY	±1.%	±1.%

TABLE 3-2 (Cont.)

B. DYNAMIC TEMPERATURE SENSORS (GAS)

SPECIFICATIONS	REQUIRED	AVAILABLE
		MEDTHERM CORP. FAST RESP. MODEL
ACCURACY	±1. °F	±1.°F*
HYSTERESIS	±0.4 °F	TBD (BY CALIBRATION)
TIME CONSTANT	<1. ms	10. MICRO-SEC

*ATTAINED BY CALIBRATION

SIGNAL CONDITIONING EQUIP.

ACCURACY	±0.5%	±0.5%
DRIFT	ZERO	ZERO

C. DISPLACEMENT TRANSDUCERS (LVDT'S)

SPECIFICATIONS	REQUIRED	AVAILABLE
		ROBINSON-HALPERN (MODEL NO'S. K-220-032/033)
LINEARITY	±1.0% F.S.	±2% F.S.*
0° PHASE SHIFT @ 30 Hz	ZERO	ZERO**
DYN. FREQ. RANGE	20 TO 30 Hz	

*BEST KNOWN/AVAILABLE
**±2% @ 20 AND 40 Hz

SHAVITZ (MODEL NO. H-200)

SAME AS ABOVE ON SPECS.

- Engine heat exchanger gas mass flow rate - a hot wire anemometer was evaluated for this measurement, and it was found that inadequate space was available within the envelope of the Proto 2 FPSE for installing the necessary probes/hardware.
- Engine power piston to compressor housing force transducer - a vendor/literature search was unsuccessful in identifying a force transducer/load cell that would measure axial forces (as required) while also being subjected to radial loads. The radial load capability is necessary since the power piston/compressor assembly support bearings are at the outboard ends of the assembly, and the force transducer would have to be installed at a mating flange/joint between the power piston and compressor cylinder head. Inadequate space and orientation limitations did not allow the installation of separate radial bearings to circumvent this limitation.

3.2 DATA ACQUISITION SYSTEM (DAS) SELECTION

3.2.1 EXISTING PHASE II DAS

The existing Phase II data acquisition system was selected for compatibility with the Phase II instrumentation. The purpose of this instrumentation was to provide data for proof-of-design concept evaluation and combustor/engine/compressor assembly performance evaluation. Acquisition of steady state and dynamic data was as follows.

Steady state data

The Phase II steady state instrumentation and DAS (along with range and accuracy) is presented in Table 3-3. Manual readout/recording was required for all pressure gauges and liquid and gas flow rates; all temperatures were recorded by data loggers. This system was found to be inadequate for:

- accurately determining heat transfer within and to the ambient for the combustor/engine/compressor assembly.
- accurately determining the heat input to the engine.
- measuring displacer gas spring heat losses/gains.

Table 3-3

PHASE II STEADY STATE INSTRUMENTATION

DESCRIPTION	MODEL #	RANGE TOTAL	ACCURACY/ RESOLUTION % F.S.
FIN & TUBE TEMPERATURE RECORDER SYSTEM (ESTERLINE ANGUS)	E-1124E	0-2000°F TYPE K	4°F/20°F
PRESSURE TRANSDUCER SYSTEM (MOORE)	10600-8	0-1500 PSI	±0.5%/±10
DIGITAL T/C INDICATOR (IRCON)	7-K250F-0	-30 to 2500°F	±1°F
T/C TYPE K	STANDARD	32-532°F 532-2500°F	±4°F MAX. ±3/4% MAX.
TEMPERATURE/RECORDER/ DATA LOGGER (DORIC)	220		
ETHYLENE GLYCOL/H_2O FLOWMETER (BROOKS)	1110-R-9M-25-2/9-RS-33	0.3-3.2 GPM	2%/0.06 GPM
GAS FLOWMETER (ROCKWELL)	175S	0-175 CFH	.005 FT^3
AIR FLOWMETER (ANNUBAR)	71-1" 316SS	0-20 CFM	±1.55%
SLANT GAUGE (DWYER)	102.5	0.2--0-20"	±5%/0.01"
R-22 FLOWMETER (COX)	AN8-4	0.25-2.5 GPM	±0.5%
ETHYLENE GLYCOL/H_2O FLOWMETER (BROOKS)	1110-24-R-10M-3-10-RS-138	1.05-10.95 GPM	1%FS/0.05 GPM
PRESSURE GAGE (US GAGE)	132019	0-100 PSIG	1/2%/1 PSI
PRESSURE GAGE (US GAGE)	132023	0-400 PSIG	1/2%/5 PSI
ΔP GUAGE (MIDWEST)	110	30-0-30 PSI	1/2%/0.25 PSI

Dynamic data

The Phase II dynamic instrumentation/DAS system is presented in Table 3-4. Dynamic pressure signals acquired included:

- Engine
  - Compression space to bounce space delta-P
  - Displacer gas spring to bounce space delta-P
  - Second gas spring to bounce space delta-P
  - Bounce space absolute pressure
- Compressor absolute pressures
  - Upper cylinder
  - Upper gas spring
  - Lower cylinder
  - Lower gas spring

Displacement measurements included:

- Displacer to power piston
- Power piston to engine housing
- Engine housing to ground

Table 3-4

PHASE II DYNAMIC INSTRUMENTATION DATA

	DESCRIPTION	MODEL NO.	TOTAL RANGE	ACCURACY
A.	PRESSURE TRANSDUCERS DIFFERENTIAL (SENSOTEC) ABSOLUTE (SENSOTEC) SENSOTEC SPECS: • LINEARITY • HYSTERESIS • THERM. SENSIT. SHIFT	 TYPE-S(10-32) TYPE-S(10-32)	 ±500 PSI 0-500 PSIA	 ± 0.5% F.S. T/2% PRESS. EXCUR. 0.02%/°F*
	*CALIBRATED AT TEMP TO REDUCE THIS ERROR			
	DIFFERENTIAL (KULITE) ABSOLUTE (KULITE) KULITE SPECS: • LINEARITY • HYSTERESIS • THERM. SENSIT. SHIFT	 HKM-375±5000 HKM-375-2000A	 ±500 PSI 0-2000 PSIA	 ± 0.5% F.S. T/2% PRESS. EXC. 0.02%/°F
	*CALIBRATED AT TEMP. TO REDUCE THIS ERROR			
	CONDITIONING EQUIPMENT • ACCURACY • STABILITY			 0.05% ±1.0%
B.	DISPLACEMENT TRANSDUCER LVDT (ROBINSON-HALPERN) LVDT (ROBINSON-HALPERN) LVDT (SHAVITZ)	 K220-033 K220-032 H-200	 ± 3/4" ± 2" ± 1/2"	 ± 2.0%/F.S. ± 3.0% F.S. ± 2.0% F.S.
C.	TAPE RECORDER (HEWLETT PACKARD) • LINEARITY	3968A	1V to 30V (P-P)	 ± 0.3% (P-P)
D.	STRIP CHART RECORDER (HEWLETT PACKARD) • LINEARITY	7700	--	 ± 0.3% (P-P)
E.	OSCILLOSCOPE (TEKTRONIX)	5103N	--	± 2.0%

Eight of these parameters were recorded on magnetic tape as well as being displayed on a strip chart for real time monitoring. Generally the parameters recorded consisted of all of the engine pressures, all of the displacement signals, and the compressor upper cylinder pressure. An occasional change was made if other parameter monitoring was desired.

In addition to the aforementioned recordings, various parameters were displayed on dual beam oscilloscopes, permitting real time displaying of selected parameters. Engine data displayed were displacer to power piston displacement, displacer gas spring pressure, and second gas spring pressure versus power piston to housing displacement. These displays provided displacer to power piston phasing and P x V diagrams for the displacer gas spring and second gas spring. The P x V diagrams were photographed and subsequently integrated to determine the work associated with these gas volumes.

Compressor cylinder and gas spring pressures were also displayed versus compressor housing (power piston) displacement, giving P x V diagrams for these gas volumes. Photographs were also taken of these displays. Integration of these diagrams determined the work being absorbed in the compressor cylinder and gas spring volumes.

The Phase II dynamic instrumentation/DAS system was found to be inadequate for the following measurements:

- accurate compressor to engine matching and compressor performance, due to the lack of compressor piston displacement measurements.
- accurate engine indicated power
- engine component level performance including heater, regenerator and cooler pressure drops, efficiencies and/or effectiveness.

3.2.2 DAS OPTIONS

For the Phase III tests, it was necessary to upgrade the DAS for two reasons:

1) to overcome the deficiencies of the existing DAS used in the Phase II tests, and
2) to accomodate the additional measurement requirements of the Phase III tests.

Recently developed digital oscilliscope systems appeared to offer the features and computing power necessary for the Phase III DAS and, hence, this became one of the major subsystems of the Phase III test facility.

As a minimum, the DAS must accomplish the following:

1) Acquire 24 channels of dynamic data, at a frequency of about 30 HZ.
2) Display data on a CRT.
3) Calculate parameters of interest (e.g., power, which equals $\int FdS$) in near-real-time.
4) Transfer, store, and print out data and calculations.
5) Have sufficient logic for automating the above, as well as monitoring instrument and HAHP status.
6) Acquire, format and print the steady state data.

A number of DAS options were examined, two of them in detail (including demonstrations of the equipment). The main features of each system are described below.

NORLAND

1) Stand-alone programmable digital oscilloscope.
2) Large memory for data storage (to 128K byte/channel x 4 channels).
3) 250 line programmability.
4) Limited graphics (printer/plotter control).
5) Talker/listener functions only (no equipment control beyond #4)
6) Difficulty in segregating waveforms in memory.
7) Limited software availability.
8) Additional equipment (e.g., multiplexer) must be provied by others.

TEKTRONIX

1) Stand-alone programmable (2000 lines) digital oscilloscope, easily interfaced with a microcomputer.
2) Small memory (scope has 5K byte, but computer contains 64K bytes).
3) Segregation of stored waveforms (up to 40).
4) Extensive graphics capability.
5) Microcomputer can act as controller of other devices.
6) Fair amount of available software (including math pacs, in ROM modules).
7) Large selection of compatible peripheral equipment

FLUKE

1) Power controller: runs FORTRAN; large RAM available (256K).
2) Few other relevant items available (e.g., oscilloscope).

HEWLETT PACKARD

1) 1980 A/B oscilloscope measurement system with limited control functions and other capabilities.
2) 3054A automatic DAS very powerful, built up of basic units. Relatively complex; would be costly and time-consuming to assembly.
3) Judged excellent for a totally new DAS; ;not as good at interfacing with the existing DAS.

The Norland and TEK equipment appeared to be the most promising and were configured for the Phase III requirements. Component details and costs are given in Table 3-5. These data were then used to select the DAS.

3.2.3 DAS SELECTION

The best match, at a reasonable investment in time and cost, was the Tektronix DAS. All of the desired equipment except a printer was available from TEK, easing concerns about potential interface problems. In addition, the programming flexibility was greater for the TEK system than for the Norland. Furthermore, the equipment was readily available on a rental basis, making it more attractive for the relatively short (about 6 months) period of testing envisioned. It was, therefore, elected to rent a Tektronix DAS, and to purchase a compatible bus for the Fluke datalogger, in order to transfer steady state data to the TEK system.

The selected Tektronix DAS consisted of the items listed on Table 3-5. Although the HP-2631G printer had a dot-addressable graphics capability, this was found to be tedious to use for any complicated plots. A TEK 4662 plotter was available at GE/AEPD and was later interfaced with the rest of the DAS. The final DAS configuration is shown on Figure 3-2.

3.3 ENGINE/COMPRESSOR MODIFICATIONS

The engine/compressor component tests were conducted on a reinstrumented Baseline Proto 2 FPSE. To assure that the additional pressure, temperature and displacement sensors/transducers met their required ranges, accuracies,

Table 3-5. DAS Components and Costs

	NORLAND			TEKTRONIX		
COMPONENT	DESCRIPTION	PURCH COST 10^3\$	RENTAL COST 10^3\$/MO	DESCRIPTION	PURCH COST 10^3\$	RENTAL COST 10^3\$/MO
Digital Oscilloscope	MOD. 3001	6.9		MOD. 7854 OPT 2D (4K Memory Exp.)	14	1.2
Monitor	3106R	1.2		-Built into Scope-		
Amplifiers	(2)-3215C, 12-bit, 10ns/point	3.8		(1)-7A22, 10 µV/div (1)-7A18, 5 µV/div	1.5 1.2	
Thermocouple Amps.	(9) - Omega	(2.2)[a]		---		~0.5
Memory Expansion	(2)-DMX-16; 16K byte	3.3		Option 24; 64K bytes computer memory	0.9	
Time Bases	---			(2)-7B50A, 5 µS/div	1.8	
Multiplexer	(2)-TEK SI5010	(3.7)		(2)-SI5010 RF Scanners	(3.7)	-
Multiplexer Power Supply	(1)-TEK TM5006	(1.0)		(1)-TM5006 Mainframe	(1.0)	-
Printer/ Plotter	(1)-3711R, 80 Col.	2.0		(1)-HP2631G (or equiv)	4.5	0.4
Storage Device	Dual 5-1/4" Disks	3.7		-Built into Micro-		
Microcomputer	---			(1)-4052A[c] w/Opt. 03	9.9	1.0
Software/ Interfaces	AD02 Graphics	0.7		(1) WP1310 Set	~2	0.2
Miscellaneous	Cables, etc.	(1)	-	Cables, etc.	(1)	-
Total Cost, 10^3\$;10^3\$/Month		29.5	2.2[d]		41.5	3.3[b]

NOTES:

a.) Items will probably have to be purchased ( ).
b.) Not discounted; discounted costs much lower.
c.) New model. May have to rent directly from Tektronix
d.) Norland rental @ 10% purchase price.

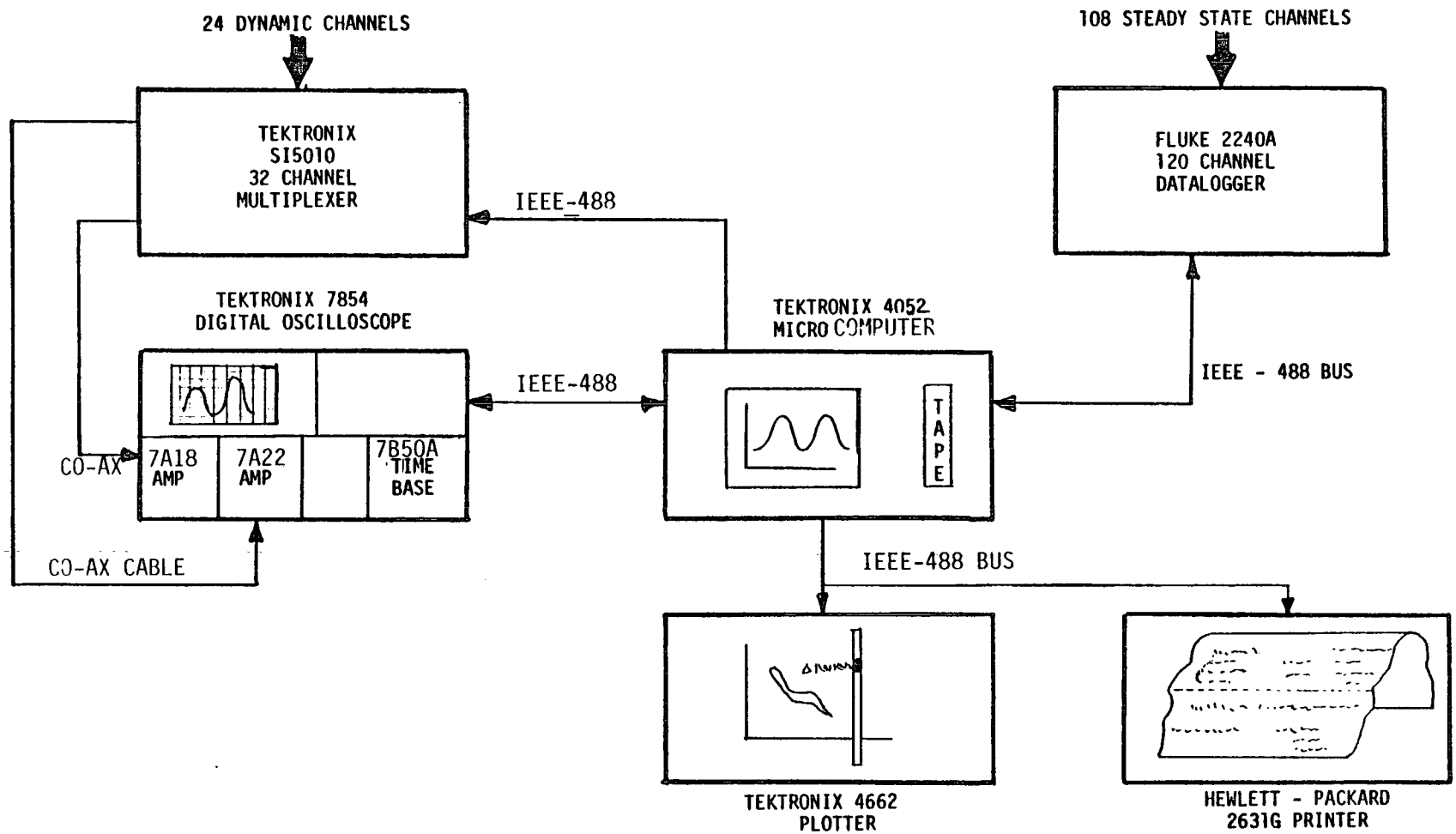

Figure 3-2. PHASE III DAS CONFIGURATION

and dynamic responses, NASA-LeRC was visited to review the proposed new instrumentation and installation in the Proto 2 FPSE assembly. The major emphasis of the review was on the pressure transducer connecting tubes, since improperly sized tubes can result in excessive errors due to pressure signal phase shift. Approaches taken by NASA on their Stirling engine programs were reviewed, and several worthwhile concepts were identified. NASA has had limited experience in fast response (micro-second time constant range) thermocouples, but noted that they would be very interested in our results. The modificiations to the Proto 2 components to accept the additional instrumentation are described below.

3.3.1 ENGINE HEATER HEAD MODIFICATIONS

Figure 3-3 shows the design modifications to a baseline engine housing assembly to incorporate component level pressure taps and working fluid (helium) temperatures. Pressure taps were installed to measure pressures at the expansion space and the hot and cold sides of one regenerator subassembly. Pressure taps were already available for the compression and bounce spaces. With these pressure taps, dynamic pressure drops could be measured across the fin/tube, regenerator, and cooler subassemblies, measuring the gas shuttling/pumping losses. The pressure differences between the compression and bounce spaces provide an input for determining the indicated engine power. All of the pressure sensing tubes were brazed into the engine housing assembly.

Gas temperature measurements were incorporated at the expansion space, compression space and the regenerator hot end, mid-point, and cold end (180° apart). Installation was accomplished by brazing Swagelok fittings at each of these port locations, and installing replaceable thermocouple probes compatible with these fittings.

3.3.2 COMPRESSOR MODIFICATIONS

Figure 3-4 shows the compressor piston displacement transducer installation. This transducer is a linear variable differential transformer (LVDT), and installation was accomplished by redesigning the original power piston LVDT housing assembly to accept both the power piston and compressor piston LVDT assemblies. The compressor upper cylinder head was also modified to permit attachment of the LVDT core assembly tie-rod to the compressor piston.

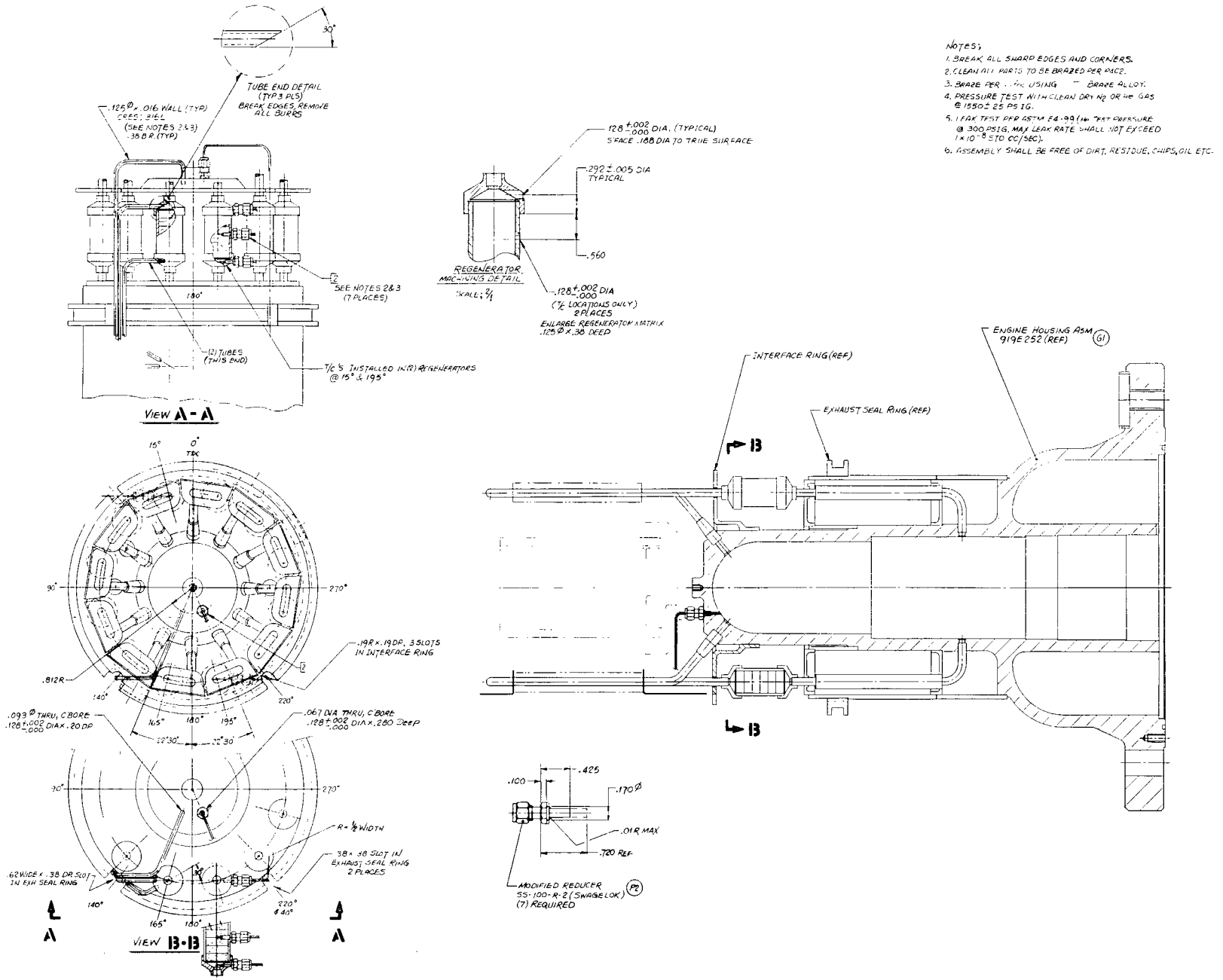

Figure 3-3. PROTO 2 ENGINE HOUSING MODIFICATIONS

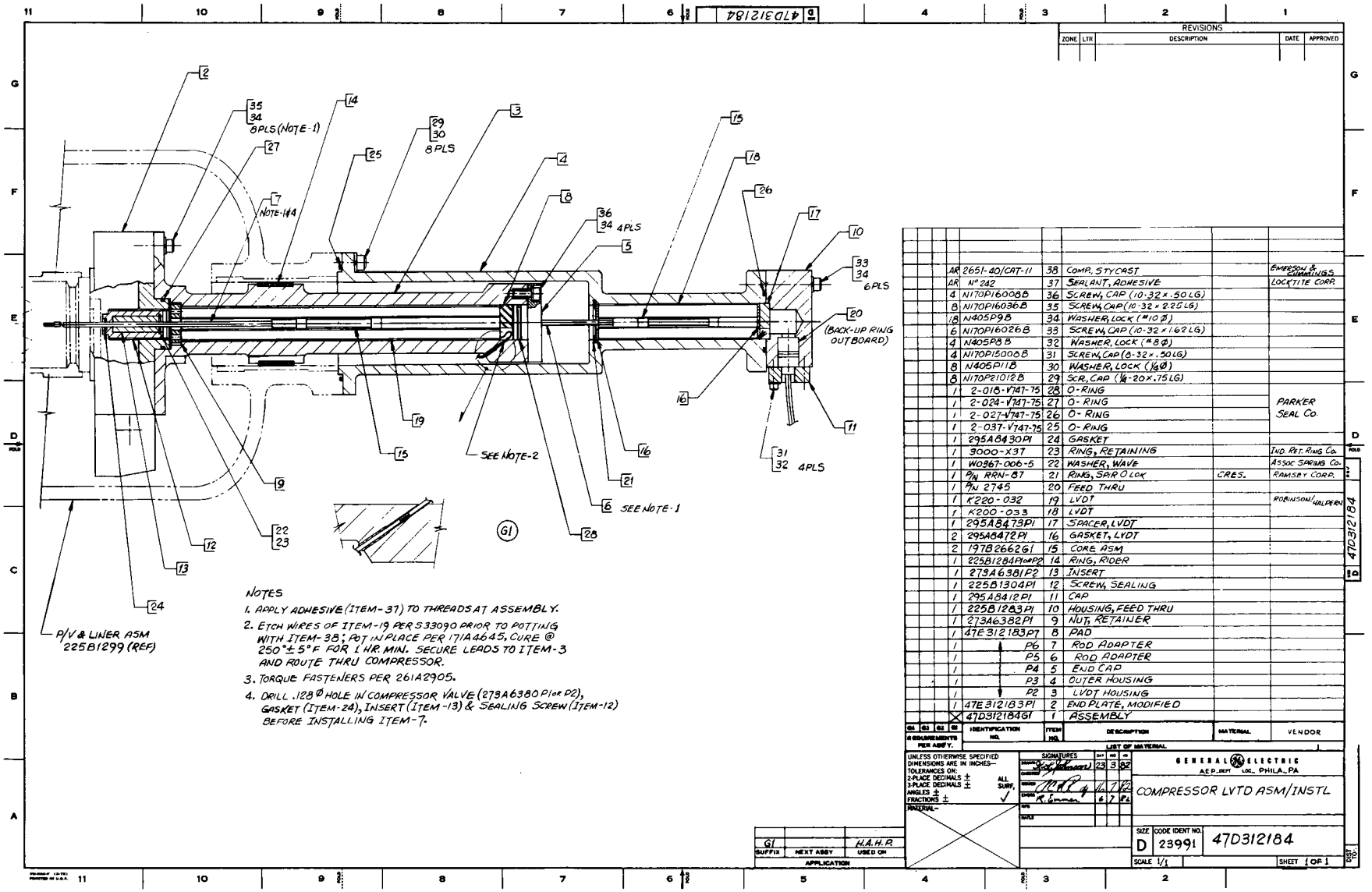

Figure 3-4. COMPRESSOR LVDT ASSEMBLY/INSTALLATION

Provision was made for a close fitting bearing assembly through which the tie-rod could pass unobstructed and thread into the end of the piston. Compressor piston to engine power piston relative motion measurement was thus provided.

3.3.3 COMBUSTOR MODIFICATIONS

Figure 3-5 shows the combustor modifications for a cooling air shroud/heat loss measurement system. A thin aluminum shroud encloses the preheater section of the combustor, providing an annular passage circumferentially around the assembly. Inlet and outlet ducts are provided (180^{0} apart), along with a splitter vane in the inlet to evenly distribute the flow around the assembly. Two thermocouple installation fittings are provided on both inlet and outlet, permitting measurement of the cooling air temperature rise as it passes through the shroud. A metered air supply is delivered to the assembly, thereby giving an accurate means of measuring the heat loss from the combustor. When combined with the exhaust heat loss, the heat delivered to the engine can be accurately determined.

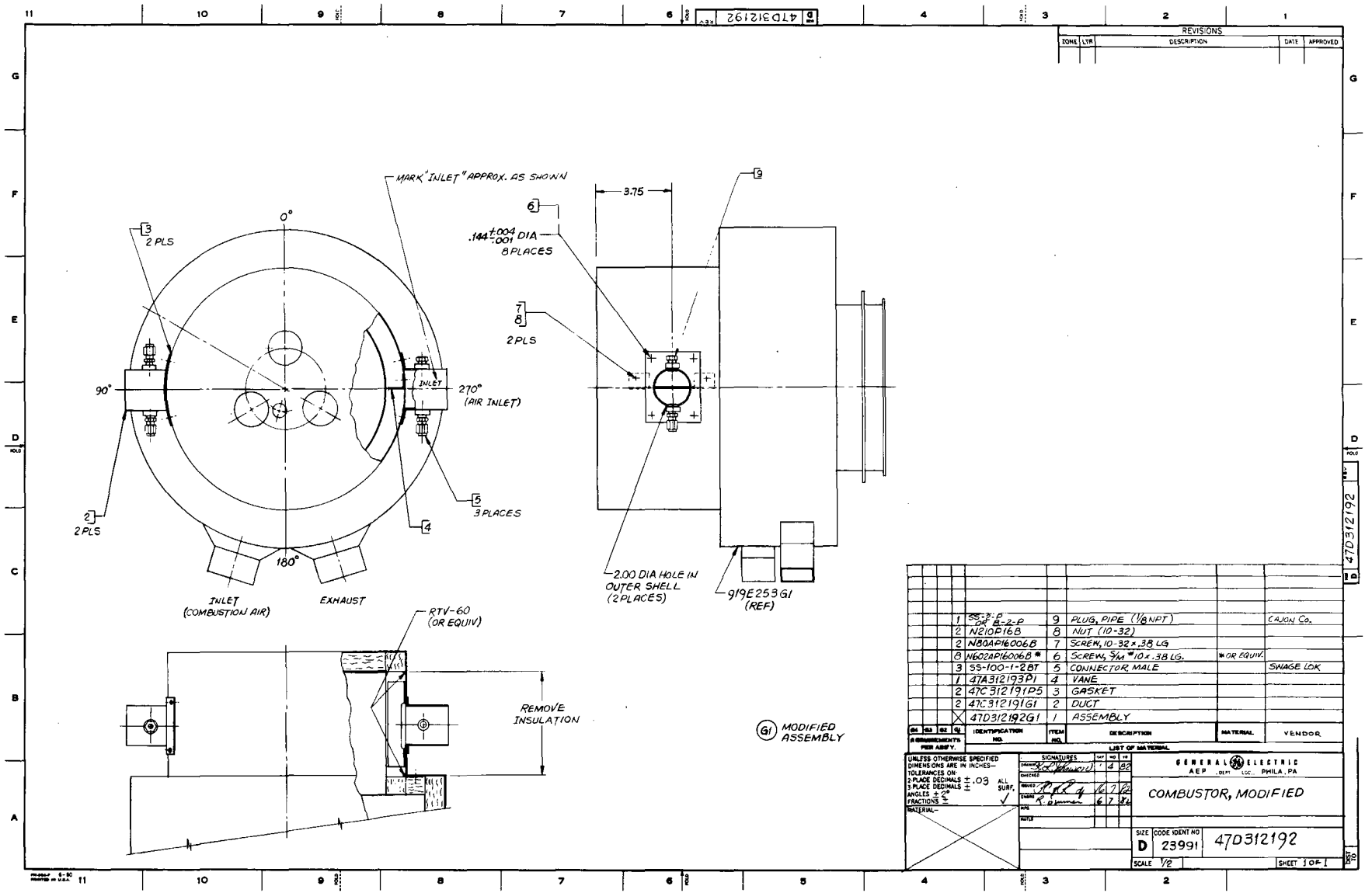

Figure 3-5. COMBUSTOR MODIFIED FOR ADDITIONAL INSTRUMENTATION

SECTION 4

TEST SYSTEM FABRICATION AND INSTALLATION

SECTION 4
TEST SYSTEM FABRICATION AND INSTALLATION

The fabrication and installation of the test hardware and data acquisition system in the engine/compressor test facility is described in this section. Descriptions of the pressure transducer installation configuration and the DAS software developed are included. The checkout and calibration tests performed to prepare the system for the planned tests are also described.

4.1 TEST HARDWARE FABRICATION

4.1.1 ENGINE/COMPRESSOR FABRICATION AND INSTRUMENTATION INSTALLATION

Engine Housing Assembly

Rework of the engine housing assembly to incorporate the pressure taps and thermocouple fittings entailed the drilling of the access/through holes at the specified locations, modifying the Swagelok fittings for brazing, pre-forming the pressure sensing tube runs, pre-assembling these parts to the engine housing, and processing the assembly through the furnace braze cycle. These tasks were accomplished without difficulty and the selected instrumentation was installed, except for the fast response thermocouples.

Fast Response Thermocouples

Fast response thermocouples having time constants of 1 millisecond or less were ordered for installation at the locations shown in Figure 3-3. These thermocouples were a sealed probe type having a constant probe diameter of 1/16", as required to fit a 1/16" Swagelok fitting. Unfortunately, the vendor misread the procurement specification and incorporated a 1/8" diameter x 1/2" long section at the sensing tip of the thermocouple. The units were, therefore, unusable. Standard (relatively slow response) thermocouples had been ordered as back-ups, however, and no delay was experienced in the test program. Only steady-state gas temperatures were recorded, however. The vendor attempted to rework the thermocouples but was not able to deliver satisfactory units until the testing was nearly over. A few tests were run with the fast response thermocouples but the output could not be interpreted without further calibration and checkout tests. Future testing on the engine/compressor assembly will include proof testing of the fast-response thermocouples to determine if their output characteristics meet the test requirments.

Compressor Assembly

To install the compressor piston displacement instrumentation required the fabrication of new LVDT housings, the installation of the LVDT armature and potting of the lead wires to prevent leakage, and modification of the compressor upper cylinder head and valve assembly to accept penetration of the compressor piston LVDT core tie-rod. Previously in the Phase II program, the dual LVDT installation (for the power piston and the compressor piston) were avoided due to leakage concerns between the helium and Freon systems. The dual LVDT assembly used on the compressor when it was tested on the compressor component test stand was reviewed and the improved design described in Section 3.3 selected.

Fabrication of the modified parts was straightforward. Several backup parts for the LVDT rod and related connector parts were fabricated due to the possibility of mechanical failure (described in Section 4.3.1).

4.1.2 DELTA-P TRANSDUCER PHASE SHIFT TESTS

Potential Installation Effects

High response differential pressure transducers were procured for measuring the engine heat exchanger component dynamic pressure drops. Identical natural frequencies in the pressure sensing tubing of a differential pressure transducer are necessary to prevent phase shift errors in the measurement. Tube designs were matched to account for tubing temperature and length differences in the Proto 2 engine test assembly. Phase shift tests were conducted to confirm the design or identify corrections needed.

Test Set-Up

The test facility for conducting the phase shift tests consisted of an adaptation of an existing pressure pulse generator used for starting the Proto 2 FPSE. The pressure pulse generator assembly consists of a variable speed DC motor driving the piston of a pneumatic cylinder assembly through a variable stroke crank mechanism. As shown in the schematic diagram of Figure 4-1, the cylinder outlet tubing is connected to a cross fitting, providing a common system pressure pulse to any combination of three different inter-connect tubes attached to two differential pressure transducers. A high pressure helium supply pressurizes the system to typical

Figure 4-1
PRESSURE TRANSDUCER PHASE SHIFT TEST RIG SCHEMATIC

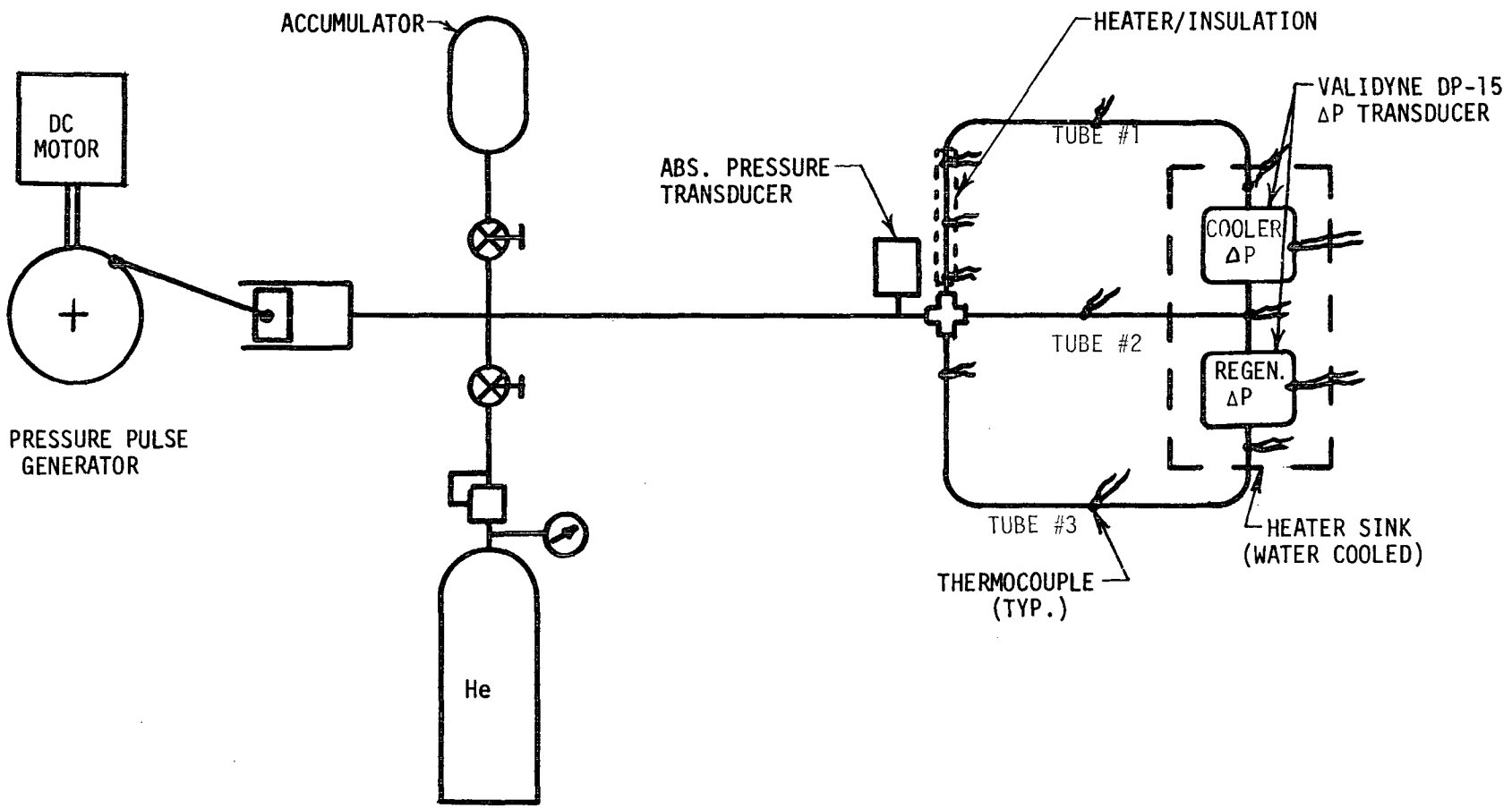

engine operating pressure (60 bars). Different tubing length and bend configurations could be installed and a heater was provided on one tubing run to simulate heater head temperatures.

The instrumentation required for the differential pressure transducer phase shift test consisted of the following:

a) Absolute Pressure Transducer: Kulite Model HKM-375-2000, range zero to 2000 psia. Purpose - to measure the nominal system pressure and the pressure pulse peak-to-peak excursions. The pulse frequency was also indicated.

b) Stroboscope. To establish the pressure pulse frequency.

c) Thermocouples: Standard Type K. Purpose - to measure the local/sectional connecting tube temperatures for subsequently establishing transducer phase shift as a function of variation in the tube temperatures.

d) Data Logger: Esterline Angus Model PD-2064. Purpose - to record the temperature measurements from the thermocouples.

e) Strip Chart Recorder: Hewlett Packard Model 7700. Purpose - to provide a permanent record of the pressure signals from the absolute transducers.

f) Oscilloscope: Tektronix Model 5103N. Purpose - to provide real time visual observation of resulting phase shifts.

G) Differential Pressure Transducers: Validyne Model DP-15, the prime test transducers.

Test results

Tests were conducted to establish the effects of temperature differences from room temperature to 1220^{0}F, tubing lengths of approximately 11 in. through 31 in. and three extra 90^0 bends in one tubing run. Test conditions were:

- System mean pressure = 870 psia
- Test fluid = helium
- Generated pulse pressure = 60 psi
- Pulse frequency = 29 HZ
- Tube No. 1 = Tube No. 2 = 21 in.
- Tube No. 3 and regenerator ΔP transducer removed and remaining fittings capped.

Tests were conducted to determine the effects of heating a six inch section of sensing tube No. 1 while maintaining tube No. 2 at room temperature. Figure 4-2,(a) shows photographs of the oscillograph traces of the generated/system pulse pressures and the related differential pressure transducer delta-P with both sensing tubes at 80°F. Perfectly matched sensing tubes (i.e., both having the same natural frequencies) would theoretically have a zero percent ratio of delta P to generated pulse pressure. As shown in Figure 4-2,(a) the configuration tested resulted in a ratio of 1.8%. The results of heating a 6 inch length of sensing tube No. 1 to 1220°F are shown by similar oscilloscope photographs in Figure 4-2(b). A delta P to generated pulse pressure ratio of 7% was obtained at the higher temperature. The results of these and other intermediate temperatures are shown in Figure 4-3. As seen from these data, a pressure difference error of approximately 7% would result at engine heater head temperatures of 1200° to 1250°F if no tube length/natural frequency corrections were made.

Similar comparative test runs were made to evaluate the effects of different sensing tube lengths and variations in bend configurations. The results are summarized in Table 4-1.

Table 4-1. Effect of Tube Length on Pressure Transducer Phase Shift

TRANSDUCER (REF. FIG. 4-1	SENSING TUBE LENGTHS (IN.) NO. 1	NO. 2	NO. 3	MAX Δ P/P %
COOLER ΔP	11.5	31.5	27.0	13.0
REGEN ΔP	11.5	31.5	27.0	16.0
COOLER ΔP	31.5	31.5	31.5	5.3
REGEN ΔP	31.5	31.5	31.5	6.7
COOLER ΔP	31.5	31.5*	31.5	5.7

*TUBE NO. 2 MODIFIED TO ADD 3 90° BENDS

As expected, equal sensing tube lengths resulted in considerably less error in delta-P measurement (by a factor of 2.5:1) than the configured unequal lengths. For the 31.5 inch tubes tested, errors of 5 to 7 percent remained with equal lengths. The interaction of crosses, tees and transducer volumes are believed to have introduced these residual errors. It is also noted that, as theory predicts, negligible differences were obtained by adding several 90° bends in one of the tubing runs.

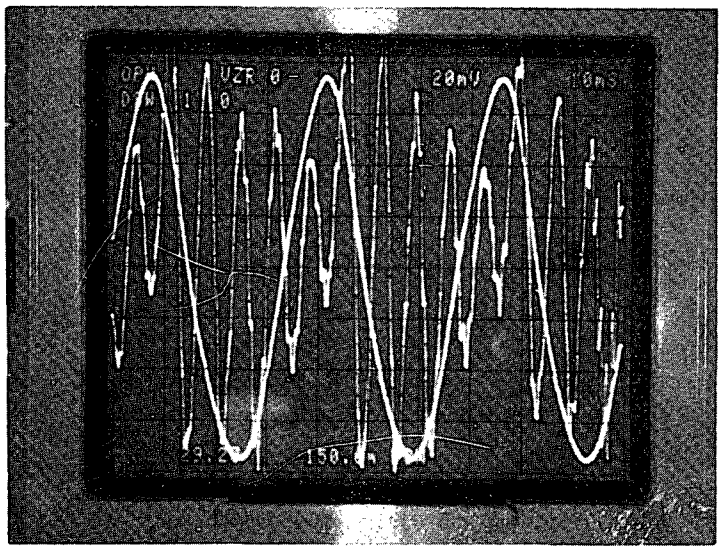

(1)

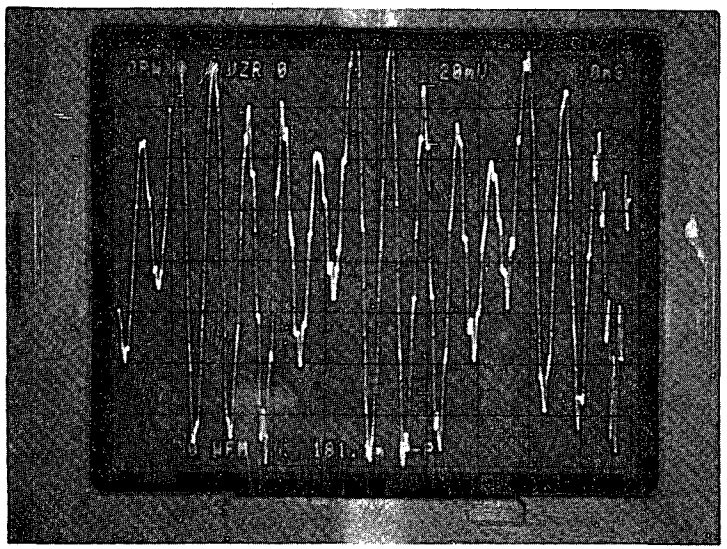

(2)

1) Input pressure pulse superimposed on transducer delta-P

2) Transducer delta-P

$P_{SYST.}$ (Peak to Peak) = 0.4 $\frac{PSI}{Mv}$ x 150 mv = 60 PSI; Max. Δ P = 0.006 $\frac{PSI}{Mv}$ x 181.1 mv = 1.087 PSI

$$\frac{MAX\ \Delta P}{P_{SYST.}} = 1.8\%$$

Figure 4-2(a). DIFFERENTIAL PRESSURE TRANSDUCER PHASE SHIFT FOR T_1=T_2=80°F

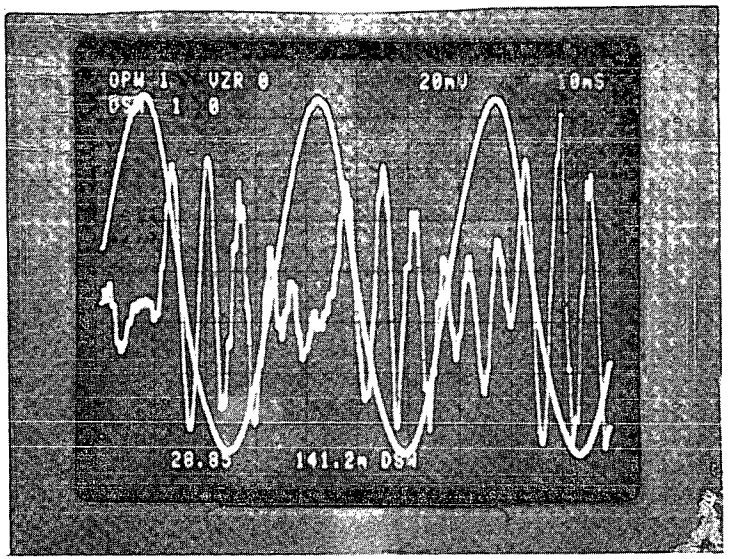

(1)

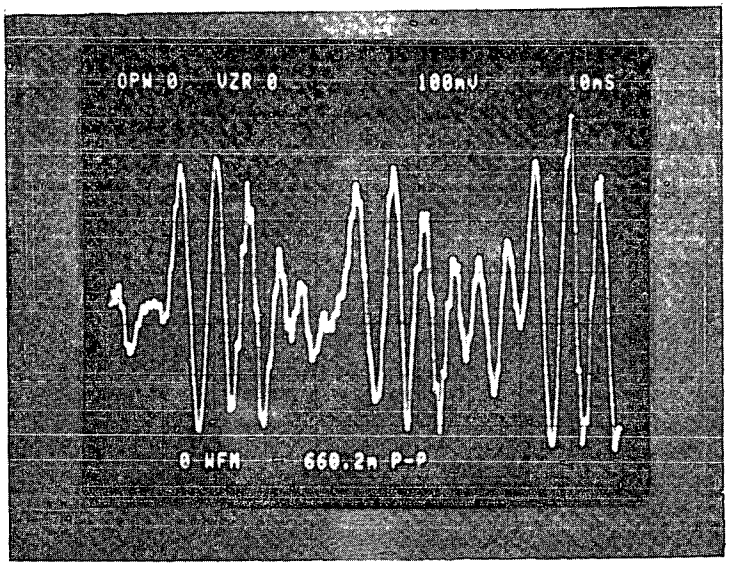

(2)

1) Input pressure pulse superimposed on transducer delta-P

2) Transducer delta-P

$P_{SYST.}$ (Peak to Peak) = 0.4 $\frac{PSI}{Mv}$ x 141.2 mv = 56.5 PSI; Max ΔP = 0.006 $\frac{PSI}{Mv}$ x 660.2 mv = 3.96 PSI

$$\frac{MAX\ \Delta P}{P_{SYST.}} \times 100 = 7.0\%$$

Figure 4-2(b). DIFFERENTIAL PRESSURE TRANSDUCER PHASE SHIFT FOR T_1=80°F, T_2=1220°F

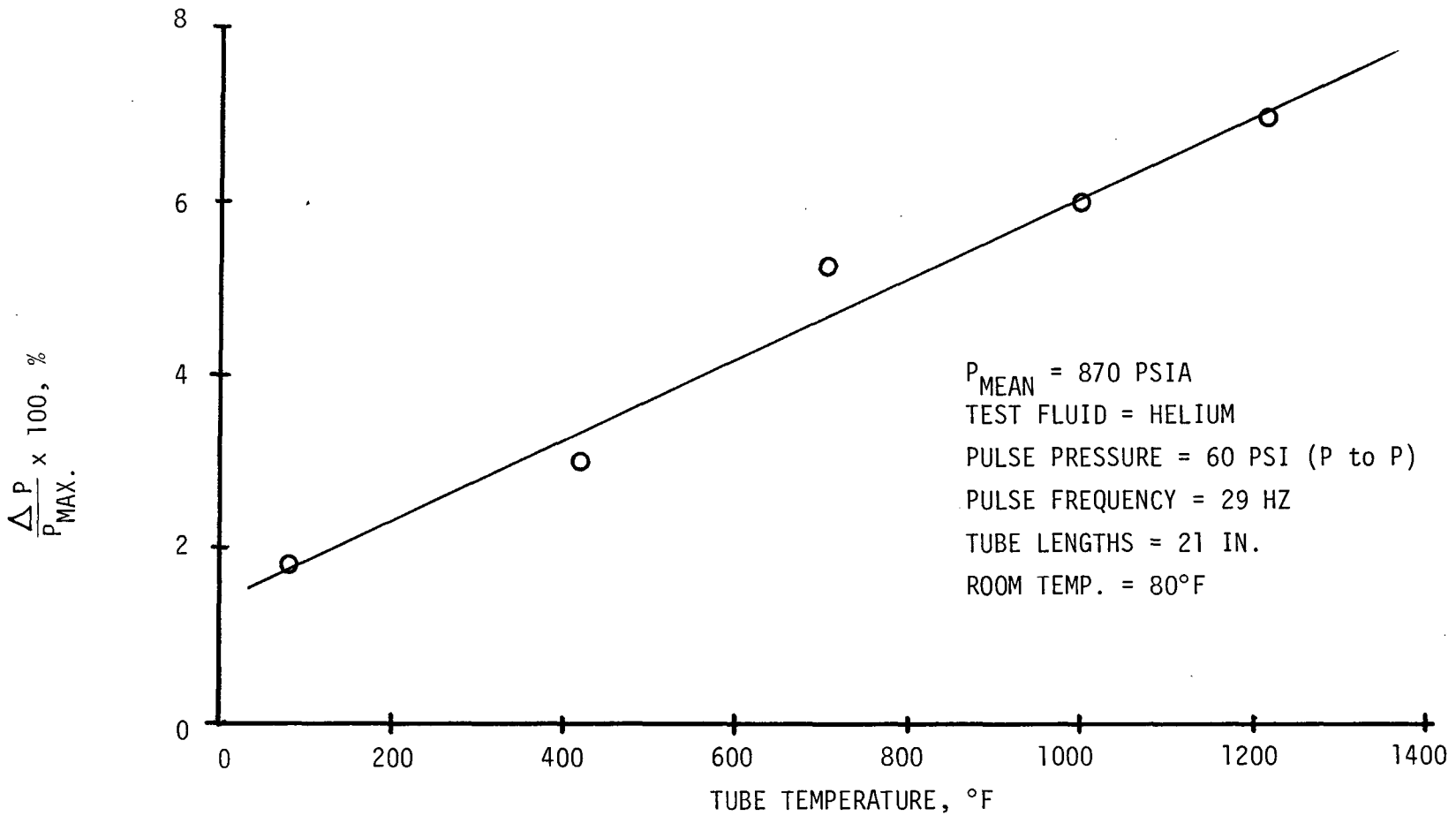

Figure 4-3. PRESSURE TRANSDUCER ERROR VERSUS TUBE TEMPERATURE

On the basis of the aforementioned test results, sensing tube lengths were installed to provide estimated delta-P measurement errors of 7% or less for the heater head fin/tube, regenerator, and cooler components.

4.2 DAS INSTALLATION

4.2.1 HARDWARE INSTALLATION

Installation of the DAS hardware was straightforward, with most attention devoted to the unit interfaces. Since the 7854 digital oscilloscope can sample only a single datastream at a time (chop mode permits rapidly alternating the data sampling between two datastreams) a multiplexer was required. The amps and time base plug-ins chosen for the scope had specifications which allowed accurate sampling and display of the data (waveforms). While some compensations could be performed by the scope, others would be performed by the 4052 microcomputer. This latter unit also controlled the multiplexer, acquisition of data by the scope and the Fluke datalogger and data transfer between devices (especially output, to the printer and/or plotter). The flexibility of the IEEE-488 bus is such that equipment interconnection can be in any desired pattern (linear, star, etc.) as long as cable lengths are not exceeded.

Figure 4-4 shows the Phase III DAS equipment as installed in the DAS section of the engine/compressor test stand. The engine/compressor test area shown in Figure 2-2 is in the adjacent cell to the right of Figure 4-4. The existing DAS strip chart recorder and tape recorder units are shown adjacent to the new equipment in Figure 4-5. Opposite to the setup shown in Figure 4-5 is the rest of the existing DAS equipment, as shown in Figure 4-6.

4.2.2 SOFTWARE DEVELOPED

No software was available which would accomplish all the tasks required for the Phase III testing. Some software for data transfer between the scope and microcomputer and CRT screen graphing was acquired from Tektronix. After evaluation, this software was found to be of limited utility in this application. Therefore, a new code had to be developed for the DAS, in order to fully exploit its power and capabilities to meet the test requirements. This software is described below.

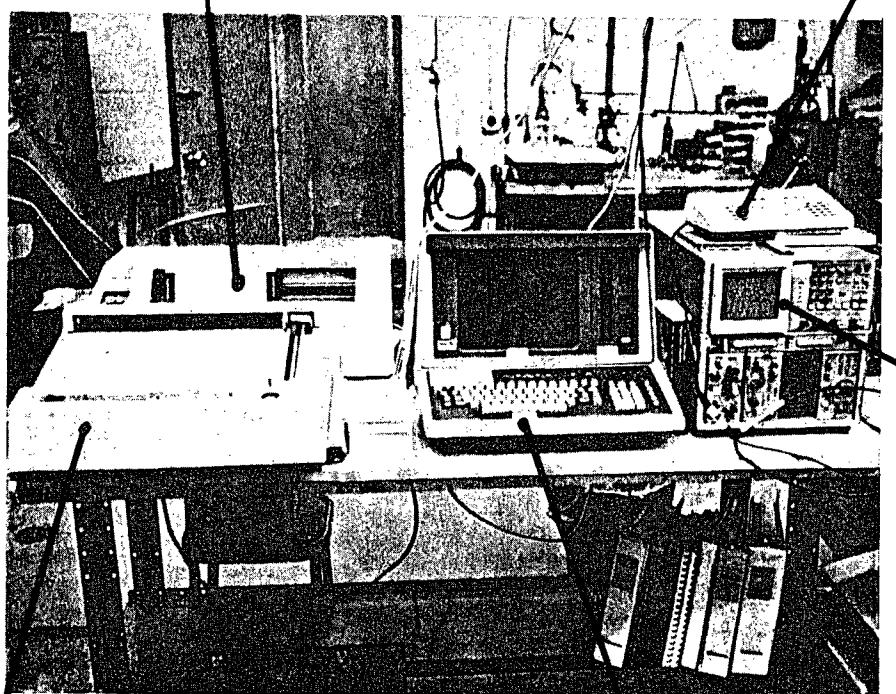

Figure 4-4. PHASE III DAS COMPONENTS IN TEST STAND

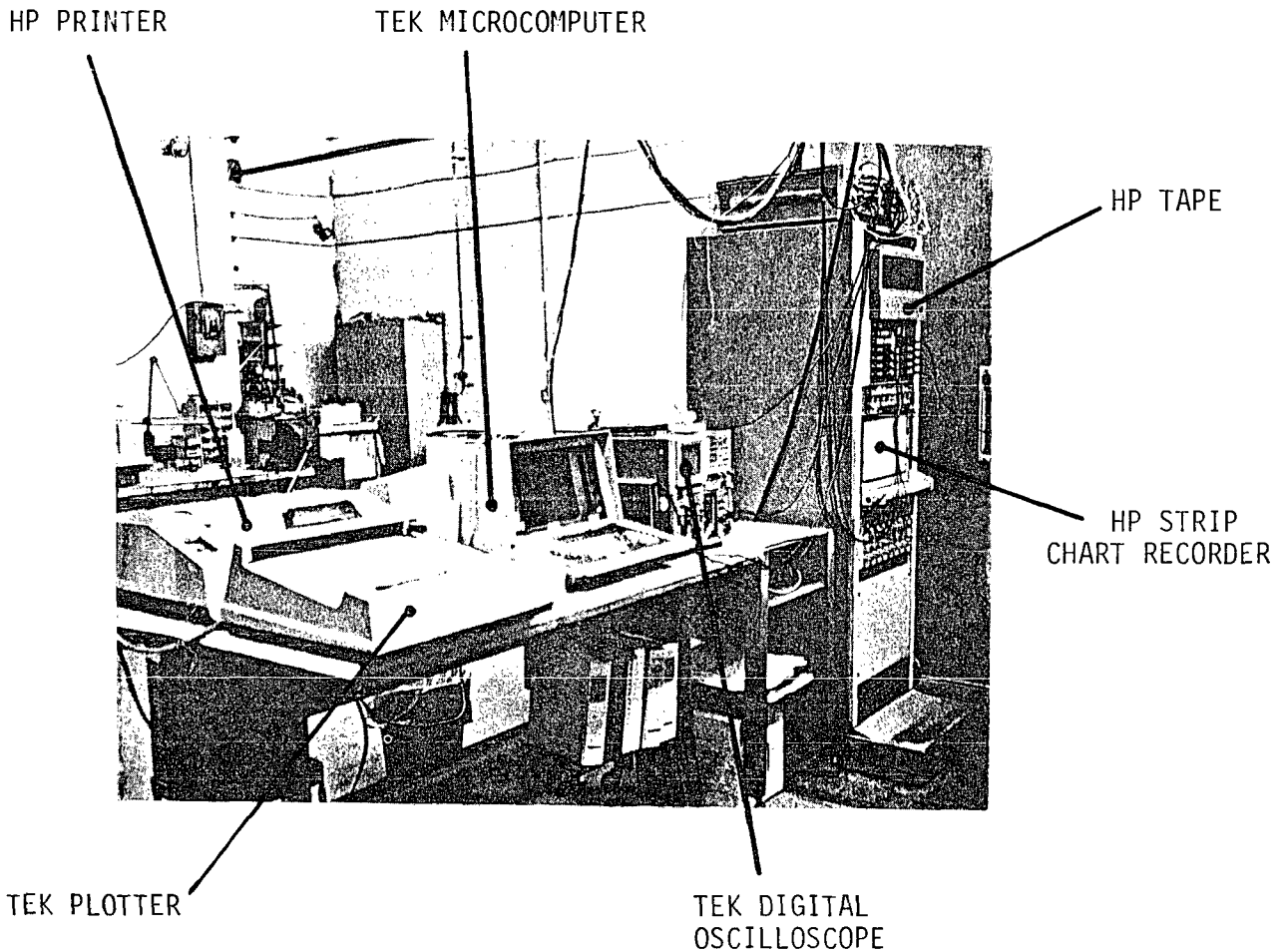

Figure 4-5. PHASE III DAS COMPONENTS AND EXISTING DAS EQUIPMENT IN TEST STAND

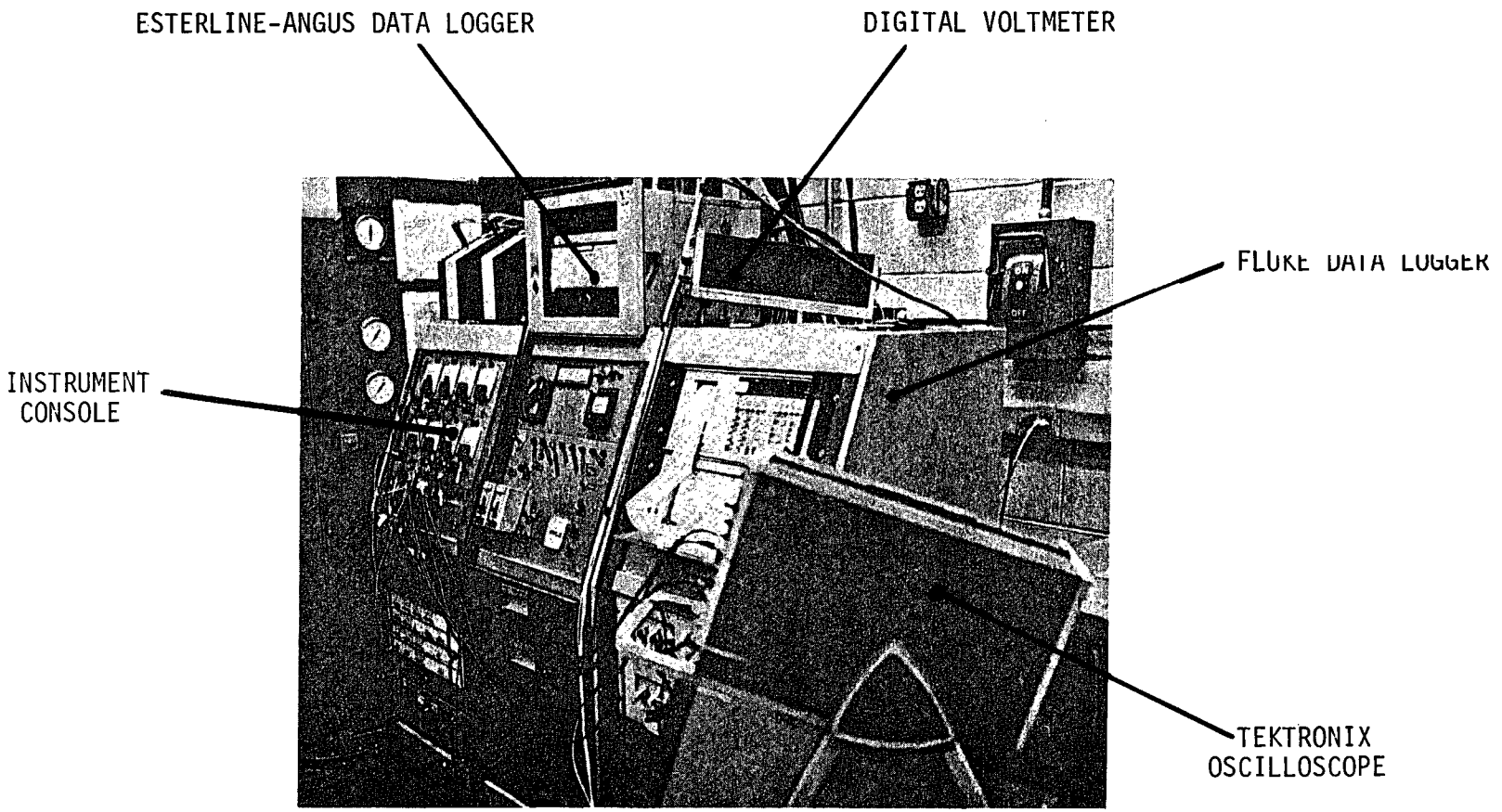

Figure 4-6. EXISTING DAS EQUIPMENT IN TEST STAND

4052 Microcomputer Software

The main system operating code controls the triggering, sequencing, and acquisition of the various data streams. This code includes subroutines which are transferred to the digital oscilloscope processor for integration of the appropriate PdV traces. The code also formats data printout and plots. The operating code flow chart is shown in Figure 4-7.

The DAS code (written in about 1200 lines of BASIC) instructs the 4052 microcomputer/controller to do the following:

1) Multiplex dynamic data channels in a chosen sequence.
2) Command the 7854 oscilloscope to acquire and store the incoming dynamic signals (24 channels) in the correct mode (chop mode was used for signals where phase shift errors could not be tolerated).
3) Trigger the Fluke Data Logger to acquire and store the steady state data (108 channels) at the proper time.
4) After all data acquisition is complete, transfer data to the microcomputer for subsequent display (screen and/or plotter) and printout.
5) While the microcomputer is engaged in output activities, have the oscilloscope simultaneously integrate PdV curves, transferring the result when requested by the microcomputer.
6) Request keyboard inputs for the few readings still taken manually.
7) Print and plot all data and results in the desired format.

Input activities (items 1-3, above) require less than 20 seconds. This includes switching amplifier settings several times in order to correctly acquire the data. Since the engine is operating at steady-state during this period, the acquisition can be considered real-time.

Output functions take considerably longer and are determined by the speed of the mechanism peripheral devices. Printout requires several minutes and each plot requires about 2-3 minutes. Storage of the dynamic waveform data on tape takes about 5 minutes. In all, about 45 minutes are required for the processing of each data point. Usually about 30-60 minutes is used between data points to assure stable operation at the selected conditions. Therefore, the DAS output time was a minor constraint on the test plan.

Figure 4-7. OPERATING CODE FLOWCHART

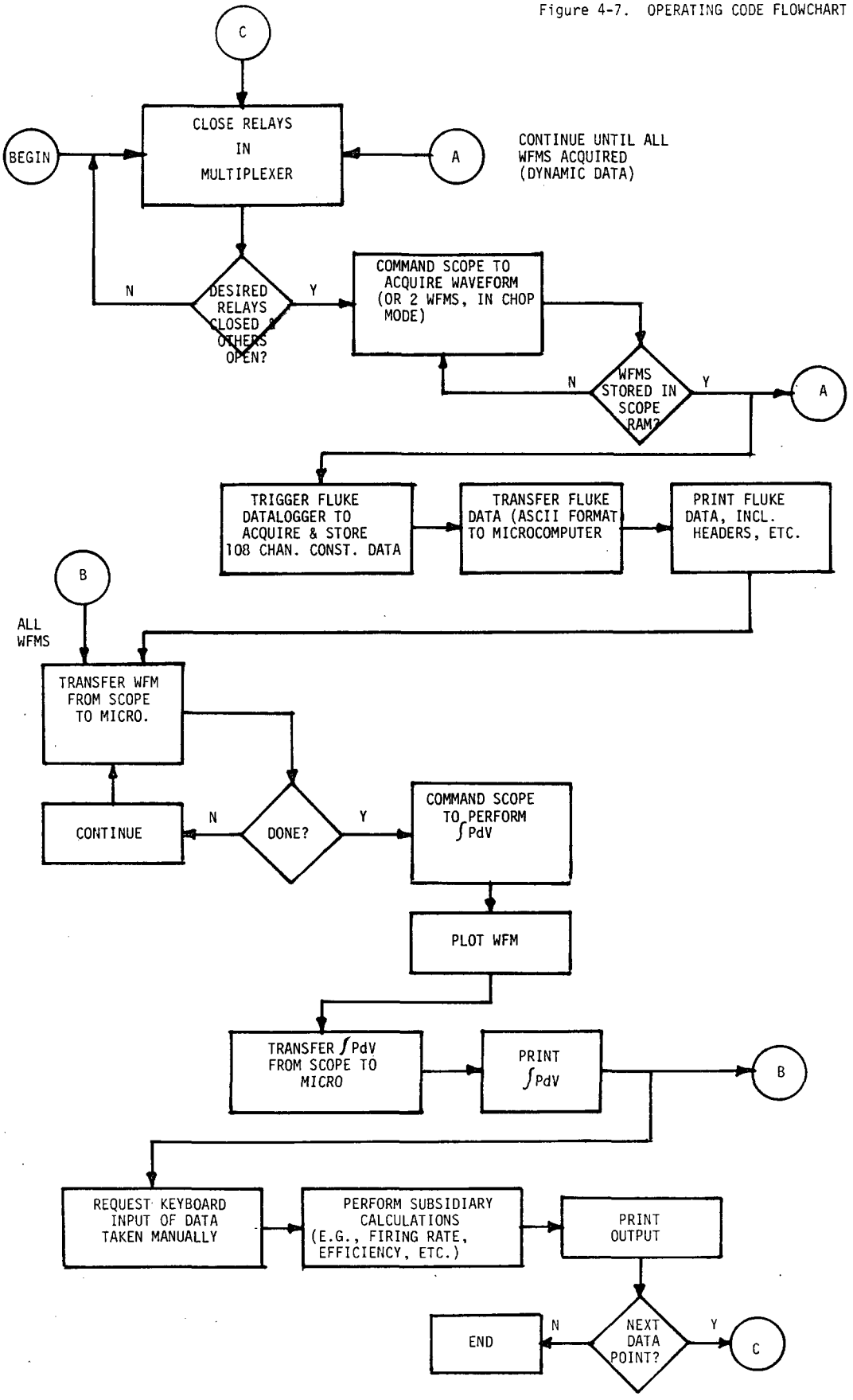

The BASIC language operating code also included a number of performance computations. Most of these were straightforward calculations of heat inputs and losses (e.g., combustor), as well as summaries.

7584 Oscilloscope Software

The oscilloscope processor employs a calculator-type language with RPN logic. A short program was written which performs the required $\int PdV$ or FdX calculations for determining FPSE and compressor power.

The scope cannot directly calculate the area of a closed curve (e.g., PV diagram). However, it can treat the separate waveforms making up the closed curve and thereby arrive at the area. The algorithm is as follows:

$$\text{Area} = \int_{V_1}^{V_2} PdV = \int_{t_1}^{t_2} P(dV/dt)dt$$

where $\frac{dV}{dt}$ is the differentiated volume (or stroke) waveform. In computing the area, the scope multiplies the discrete points making up the pressure waveform times the relevant slope, essentially performing a numerical integration by quadrature. The same algorithm (in a subroutine) is used for all the power calculations, but the constant multiplier corresponds to the volume being considered. These constants are given in Table 4-2. For accuracy, three cycles of each waveform are required and used in the algorithm.

Table 4-2

7854 Oscilloscope Integration Constraints

(for $\int PdV$)

	PRESSURE SCALE FACTOR, PSI/V	STROKE SCALE FACTOR, IN/V	CYLINDER AREA IN.^{2}	CONSTANT*
2ND GAS SPRING	100	0.2	11.6	2.622×10^{-2}
COMPRESSION SPACE	100	0.2	5.01	1.132×10^{-2}
DISPLACER GAS SPRING	100	0.2	1.58	3.571×10^{-3}
COMPRESSOR CYLINDER	100	0.4	3.545	1.602×10^{-2}
COMPRESSOR GAS SPRING	100	0.4	3.174	1.435×10^{-2}

*CONSTANT = (P SCALE FACTOR)(STORAGE SCALE FACTOR)(AREA)(0.113×10^{-3} $\frac{\text{KW-SEC}}{\text{LBF-IN}}$)

4.2.3 SAMPLE DAS OUTPUT

A sample data output for a single test point is presented in Table 4-3 through Table 4-6 and in Figures 4-8 through 4-16. Table 4-3 presents an overall summary of the major performance parameters and operating conditions of the Proto 2 combustor/engine/compressor assembly. Table 4-4 presents more detailed data on the combustor and compressor and Table 4-5 presents more detailed data on the engine. Table 4-6 gives the temperatures measured on the 108 locations in the test cell and test unit. (7777.7^{o}F indicates an open circuit).

Figure 4-8 shows the pressure and stroke histories and P-V diagram for the engine second gas spring. The scale labels indicate the value of each division of the scale. The pressure and stroke history diagram gives the operating frequency of the unit, the piston stroke (relative to the housing), the peak-to-peak pressure variation and the phase angle between the stroke and pressure curves. The integrated value of the P-V diagram (power consumed) by the second gas spring is given on the P-V diagram as well. Figures 4-9 and 4-10 present similar data for the engine compression space and displacer gas spring respectively. Figures 4-11 through 4-14 present similar data for the compressor upper cylinder, lower cylinder, upper gas spring, and lower gas spring respectively.

The engine displacer to power piston motions and compressor piston to compressor housing (power piston) motions are shown in Figure 4-15. The upper figure shows the engine and displacer motions (displacer relative to piston and piston relative to housing) with their relative phase angle and maximum (peak to peak)strokes. The lower figure shows the compressor piston and compressor housing motions (both relative to the engine housing). The compressor housing motion is the same as the engine power piston. Also shown are the phase angle between the compressor piston and its housing (engine power piston) and the maximum peak-to-peak strokes.

The measured pressure variations in the engine components are shown in Figure 4-16. The upper figure shows the variations in the engine compression space and bounce space, and the peak-to-peak values of those variations. The lower figure shows the pressure variations across the engine heater head tubes (expansion space to regenerator), the regenerators (in and out), and the cooler (regenerator to compression space).

Table 4-3

FREE-PISTON STIRLING ENGINE PERFORMANCE SUMMARY

TEST DATE 12/14/82 TEST TIME 14:24:16

ENGINE BUILD #1-65

FIRING RATE (HHV), KBTU/H	76.12
AVERAGE HEATER TUBE TEMPERATURE, DEG. F	1213.43
COMBUSTOR EFFICIENCY (HHV), %	56.56
COMPRESSOR SUCTION PRESSURE, PSIA	95.00
COMPRESSOR DISCHARGE PRESSURE, PSIA	281.00
COMPRESSOR DISCHARGE TEMPERATURE, DEG. F	209.20
SUPERHEAT AT COMPRESSOR DISCHARGE, DEG. F	88.00
COMPRESSOR PISTON STROKE, REL. TO POWER PISTON, IN	1.42
TOTAL COMPRESSOR POWER, KW	1.75
EXPANSION SPACE AVERAGE TEMPERATURE, DEG. F	1196.50
COMPRESSION SPACE AVERAGE TEMPERATURE, DEG. F	276.20
POWER PISTON STROKE, ABSOLUTE, IN	0.98
DISPLACER PISTON STROKE, REL. TO HOUSING, IN	1.66
DISPLACER TO POWER PISTON PHASE ANGLE, DEG	63.86
OPERATING FREQUENCY, HZ	30.21
SECOND GAS SPRING POWER, KW	0.28
INDICATED POWER, KW	3.03
INDICATED EFFICIENCY, %	23.99
ENGINE/COMPRESSOR SHAFT EFFICIENCY, %	16.11

Table 4-4

FREE-PISTON STIRLING ENGINE DATA SUMMARY
COMBUSTOR AND COMPRESSOR

TEST DATE 12/14/82 TEST TIME 14:24:16

ENGINE BUILD #1-65

COMBUSTOR (HHV.=1.025KBTU/FT3)

FIRING RATE, KBTU/H	76.12
EXHAUST HEAT LOSS RATE, KBTU/H	19.64
SHROUD HEAT LOSS RATE, KBTU/H	13.43
RATE OF HEAT INPUT INTO ENGINE, KBTU/H	43.06
COMBUSTOR EFFICIENCY, %	56.56

COMPRESSOR

SUCTION PRESSURE, PSIA	95.00
SUCTION TEMPERATURE, DEG. F	58.40
DISCHARGE PRESSURE, PSIA	281.00
DISCHARGE TEMPERATURE, DEG. F	209.20
COMPRESSOR PRESSURE RATIO	2.96
COMPRESSOR PISTON STROKE, REL. TO POWER PIST., IN	1.42
R-22 REFRIGERANT FLOW RATE, LBM/H	238.80
COMPRESSOR CYLINDER POWER, KW	1.43
COMPRESSOR GAS SPRING POWER, KW	0.32
TOTAL COMPRESSOR POWER, KW	1.75
EVAPORATOR R-22 REFRIGERANT HEAT LOAD, KBTU/H	0.02
EVAPORATOR COOLANT HEAT LOAD, KBTU/H	15.10
CONDENSER R-22 REFRIGERANT HEAT LOAD, KBTU/H	4.66
CONDENSER COOLANT HEAT LOAD, KBTU/H	-32.64
AVERAGE COOLANT TEMPERATURE, DEG. F	94.40

Table 4-5

FREE-PISTON STIRLING ENGINE DATA SUMMARY - ENGINE

TEST DATE 12/14/82 TEST TIME 14:24:16

ENGINE BUILD #1-65

ENGINE

RATE OF HEAT REJECTION TO COOLER, KBTU/H	35.28
THERMAL POWER, KW	12.62
AVERAGE HEATER TUBE TEMPERATURE, DEG. F	1213.43
HEATER TUBE PRESSURE DROP, PSI	21.27
REGENERATOR PRESSURE DROP, PSI	26.42
COOLER PRESSURE DROP, PSI	42.95
COMPRESSION SPACE PRESSURE VARIATION, PSI	452.10
ENGINE PRESSURE RATIO	1.46
SECOND GAS SPRING PRESSURE VARIATION, PSI	228.50
DISPLACER GAS SPRING PRESSURE VARIATION, PSI	306.20
ENGINE CHARGE PRESSURE, PSIA	1185.00
ENGINE HOUSING MOTION, IN	0.20
POWER PISTON STROKE, REL. TO HOUSING, IN	1.16
DISPLACER PISTON STROKE, REL. TO HOUSING, IN	1.66
COMPRESSOR PISTON STROKE, REL. TO HOUSING, IN	2.45
POWER PISTON STROKE, ABSOLUTE, IN	0.98
DISPLACER TO POWER PISTON PHASE ANGLE, DEG	63.86
COMPRESSOR TO POWER PISTON PHASE ANGLE, DEG	17.86
OPERATING FREQUENCY, HZ	30.21
COMPRESSION SPACE POWER, KW	1.96
DISPLACER GAS SPRING POWER, KW	1.07
SECOND GAS SPRING POWER, KW	0.28
INDICATED POWER, KW	3.03
HEATER TUBE PUMPING POWER, KW	0.35
REGENERATOR PUMPING POWER, KW	0.44
COOLER PUMPING POWER, KW	0.71
INDICATED EFFICIENCY, %	23.99
ENGINE/COMPRESSOR SHAFT EFFICIENCY, %	16.11
DISPLACER GAS SPRING HEAT FLUX, KBTU/H	0.00
PRESSURE VESSEL HEAT FLUX, KBTU/H	1.58

Table 4-6 Sheet 1 of 3

FREE-PISTON STIRLING ENGINE FLUKE DATALOGGER

TEST DATE 12/14/82 TEST TIME 14:24:16

ENGINE BUILD #1-65

T/C NO.	DESCRIPTION	DEG. F
1	HEATER HEAD FIN, LOCATION C, 0 DEG	7777.7
2	HEATER HEAD FIN, LOC. D, 0 DEG	1829.9
3	REGENERATOR WALL, MID, 0 DEG	706.8
4	HEATER HEAD FIN, LOC. C, 90 DEG	1472.6
5	HEATER HEAD FIN, LOC. C, OUTSIDE, 90 DEG	1263.8
6	HEATER HEAD TUBE, LOC. E, 120 DEG	1285.9
7	HEATER HEAD FIN, LOC. C, 180 DEG	7777.7
8	REGENERATOR WALL, MID, 180 DEG	601.1
9	HEATER HEAD FIN, LOC. D, 270 DEG	1761.9
10	HEATER HEAD TUBE, LOC. A, 0 DEG	1211.6
11	REGENERATOR WALL, HOT SIDE, 0 DEG	1146.4
12	REGENERATOR WALL, COLD SIDE, 0 DEG	312.4
13	HEATER HEAD FIN, LOC. B, 120 DEG	1432.2
14	HEATER HEAD TUBE, LOC. A, 120 DEG	1199.1
15	REGENERATOR WALL, HOT SIDE, 180 DEG	1070.7
16	REGENERATOR WALL, COLD SIDE, 180 DEG	292.5
17	HEATER HEAD FIN, LOC. B, 240 DEG	7777.7
18	HEATER HEAD TUBE, LOC. A, 240 DEG	1229.6
19	HEATER HEAD FIN, LOC. D, OUTSIDE, 270 DEG	1381.4
20	ENGINE CYLINDER HEAD, LOC. D, 0 DEG	1220.9
21	ENGINE CYL. WALL, 0.50 IN. FROM CLR., 0 DEG	899.0
22	ENGINE CYL. HEAD, LOC. A, 180 DEG	1226.2
23	ENGINE CYL. WALL, 0.50 IN. FROM CLR., 180 DEG	994.1
24	BURNER SUPPORT ROD	928.8
25	DISPLACER GAS SPRING, SIDE WALL	238.7
26	DISPLACER GAS SPRING, REAR WALL	191.8
27	COMBUSTOR FLANGE, EXHAUST SEAL	148.3
28	PREHEATER AIR, EXIT	7777.7
29	PREHEATER AIR, EXIT	1057.8
30	PREHEATER AIR, EXIT	744.6
31	PREHEATER AIR, EXIT	737.4
32	HEATER HEAD AIR, EXIT	1577.8
33	HEATER HEAD AIR, EXIT	1526.5
34	COMBUSTOR EXHAUST	774.4
35	COMBUSTOR EXHAUST	783.1
36	COMBUSTOR EXHAUST	792.7
37	PREHEATER SURFACE O.D	644.4
38	AMBIENT AIR	86.9
39	COMBUSTOR AIR, INLET	97.8
40	NATURAL GAS, INLET	79.0

Table 4-6 (Continued) Sheet 2 of 3

FREE-PISTON STIRLING ENGINE FLUKE DATALOGGER

TEST DATE 12/14/82 TEST TIME 14:24:16

ENGINE BUILD #1-65

T/C NO.	DESCRIPTION	DEG. F
41	ENGINE COOLANT, INLET	76.5
42	ENGINE COOLANT, OUTLET	112.3
43	ENGINE COOLANT, HX OUTLET	76.2
44	BOUNCE SPACE, HELIUM	224.2
45	PRESSURE VESSEL, TOP	212.1
46	PRESSURE VESSEL WALL, MID	211.5
47	PRESSURE VESSEL, FLANGE	194.1
48	ENGINE HOUSING, FLANGE	182.1
49	ENGINE HOUSING DOME, TOP	197.8
50	ENGINE HOUSING DOME, BOTTOM	189.5
51	2ND GAS SPRING, HOUSING I.D	7777.7
52	2ND GAS SPRING, HOUSING O.D	173.7
53	2ND GAS SPRING, HELIUM	195.6
54	ENGINE CYLINDER, WALL	207.8
55	ENGINE COOLER, MID	88.1
56	COMPRESSOR SUCTION, BEFORE FLEX HOSE	58.4
57	COMPRESSOR DISCHARGE, AFTER FLEX HOSE	209.2
58	COMPRESSOR SUCTION, INTERFACE RING	67.3
59	COMPRESSOR SUCTION, UPPER MANIFOLD	152.0
60	COMPRESSOR SUCTION, LOWER MANIFOLD	205.7
61	COMPRESSOR DISCHARGE, UPPER MANIFOLD	255.9
62	COMPRESSOR DISCHARGE, INTERFACE RING	244.4
63	COMPRESSOR DISCHARGE, UPPER HEAD	214.4
64	COMPRESSOR WALL, UPPER CYLINDER	215.7
65	COMP. UPPER GAS SPRING EXTERNAL VOL	185.6
66	R-22 FLOW *GPMx1000*	456.8
67	OPERATING FREQUENCY *HZ*	30.3
68	COMPRESSOR SUCTION, LOWER MANIFOLD	0.0
69	COMPRESSOR DISCHARGE, LOWER HEAD	221.2
70	SUCTION COIL TUBE, SKIN	178.2
71	DISCHARGE COIL TUBE, SKIN	239.3
72	COMBUSTOR SHROUD AIR, INLET	91.2
73	COMBUSTOR SHROUD AIR, INLET	91.7
74	COMBUSTOR SHROUD AIR, OUTLET	215.8
75	COMBUSTOR SHROUD AIR, OUTLET	259.5
76	COMBUSTOR O.D., TOP, 0 DEG	189.5
77	COMBUSTOR O.D., TOP, 90 DEG	182.0
78	COMBUSTOR O.D., TOP, 180 DEG	179.6
79	COMBUSTOR O.D., TOP, 270 DEG	146.7
80	COMBUSTOR O.D., BOTTOM, 0 DEG	161.2

Table 4-6 (Continued) Sheet 3 of 3

FREE-PISTON STIRLING ENGINE FLUKE DATALOGGER

TEST DATE 12/14/82 TEST TIME 14:24:16

ENGINE BUILD #1-65

T/C NO.	DESCRIPTION	DEG. F
81	COMBUSTOR O.D., BOTTOM, 90 DEG	7777.7
82	COMBUSTOR O.D., BOTTOM, 180 DEG	7777.7
83	COMBUSTOR O.D., BOTTOM, 270 DEG	7777.7
84	COMBUSTOR SHROUD, BOTTOM CENTER	74.0
85	REGENERATOR HELIUM, HOT SIDE, 0 DEG	1110.1
86	REGENERATOR HELIUM, MID, 0 DEG	715.2
87	REGENERATOR HELIUM, COLD SIDE, 0 DEG	315.2
88	REGENERATOR HELIUM, HOT SIDE, 180 DEG	1063.9
89	REGENERATOR HELIUM, MID, 180 DEG	601.4
90	REGENERATOR HELIUM, COLD SIDE, 180 DEG	288.3
91	EXPANSION SPACE	1196.5
92	COMPRESSION SPACE	276.2
93	HEAT FLUX, DISPLACER GAS SPRING *mV*	0.0
94	HEAT FLUX, PRESS. VESSEL WALL @2 IN/0 DEG. *mV*	22.1
95	HEAT FLUX, PRESS. VESSEL WALL @9 IN/0 DEG. *mV*	21.9
96	HEAT FLUX, PRESS. VESSEL WALL @16 IN/0 DEG. *mV*	25.4
97	HEAT FLUX, PRESS. VESSEL WALL @23 IN/0 DEG. *mV*	23.6
98	HEAT FLUX, PRESS. VESSEL WALL @9 IN/180 DEG. *mV*	18.9
99	HEAT FLUX, PRESS. VESSEL WALL @16 IN/180 DEG. *mV*	18.0
100	CONDENSER UNIT, R-22 INLET	203.6
101	CONDENSER UNIT, R-22 OUTLET	113.1
102	CONDENSER UNIT, COOLANT INLET	110.0
103	CONDENSER UNIT, COOLANT OUTLET	102.1
104	R-22 FLOWMETER, INLET	100.5
105	EVAPORATOR UNIT, R-22 INLET	49.2
106	EVAPORATOR UNIT, R-22 OUTLET	47.4
107	EVAPORATOR UNIT, COOLANT INLET	60.0
108	EVAPORATOR UNIT, COOLANT OUTLET	51.0

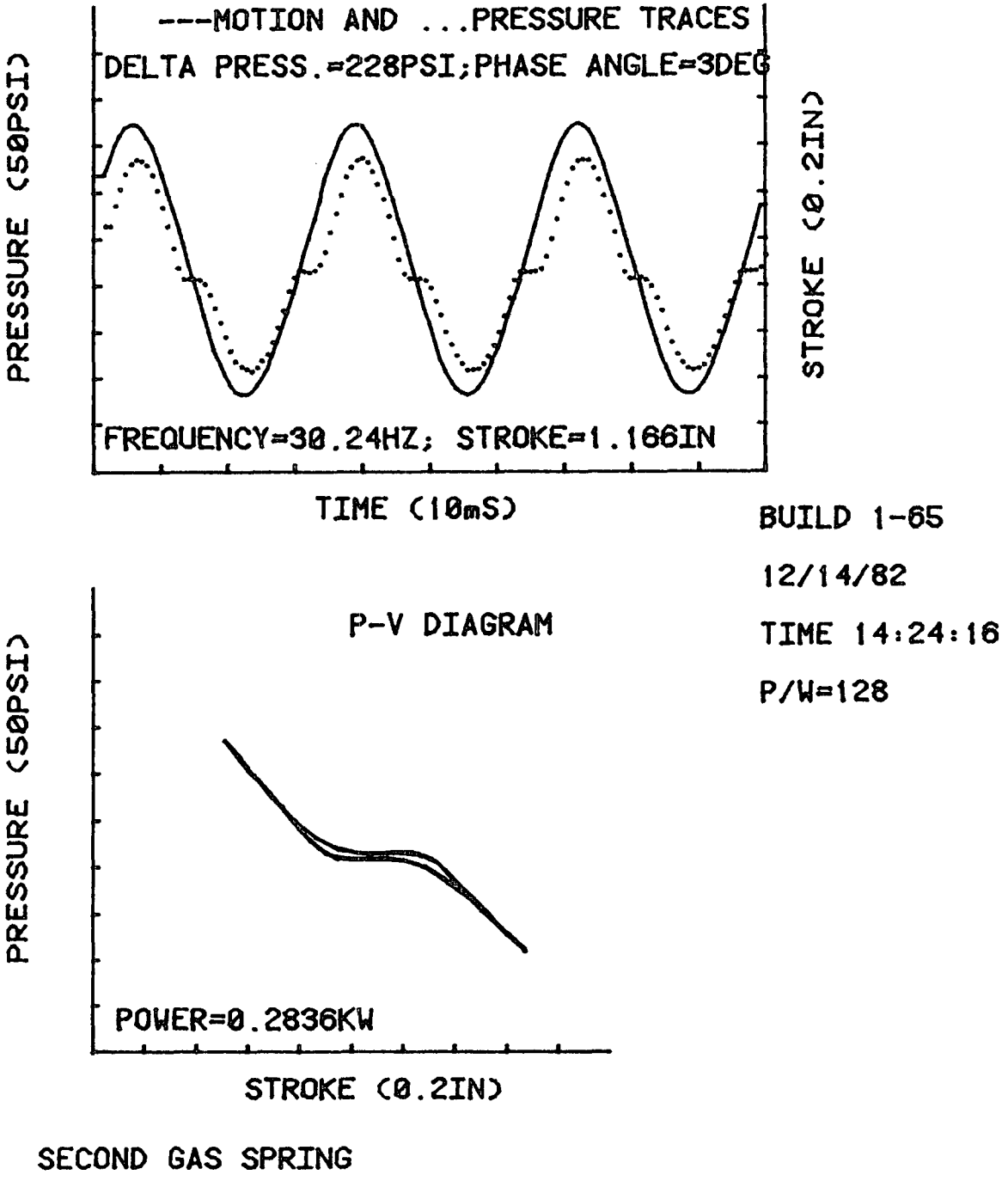

SECOND GAS SPRING

Figure 4-8. SECOND GAS SPRING PRESSURE/STROKE HISTORY AND P-V DIAGRAM

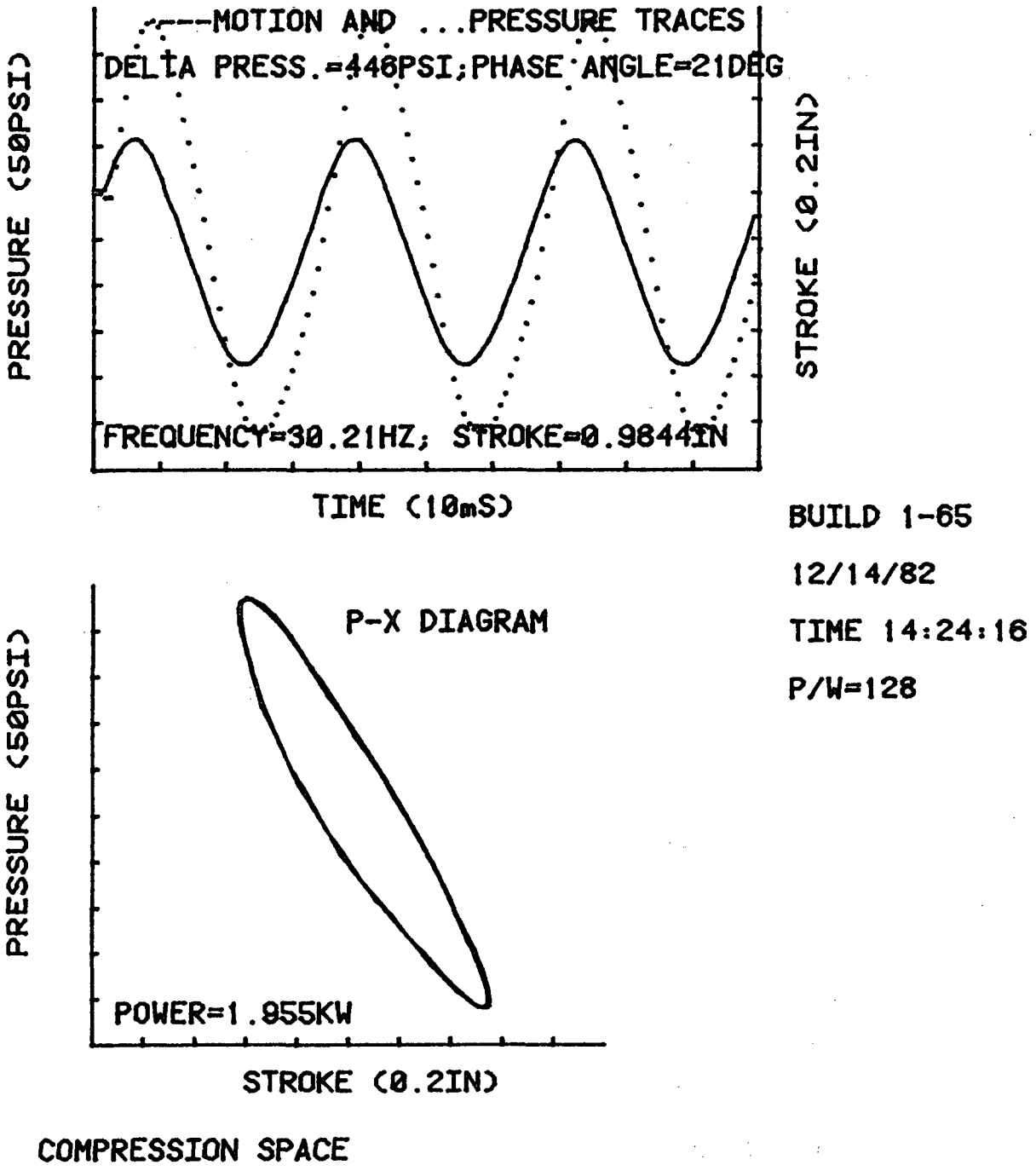

Figure 4-9. ENGINE COMPRESSION SPACE PRESSURE-STROKE HISTORY AND P-V DIAGRAM

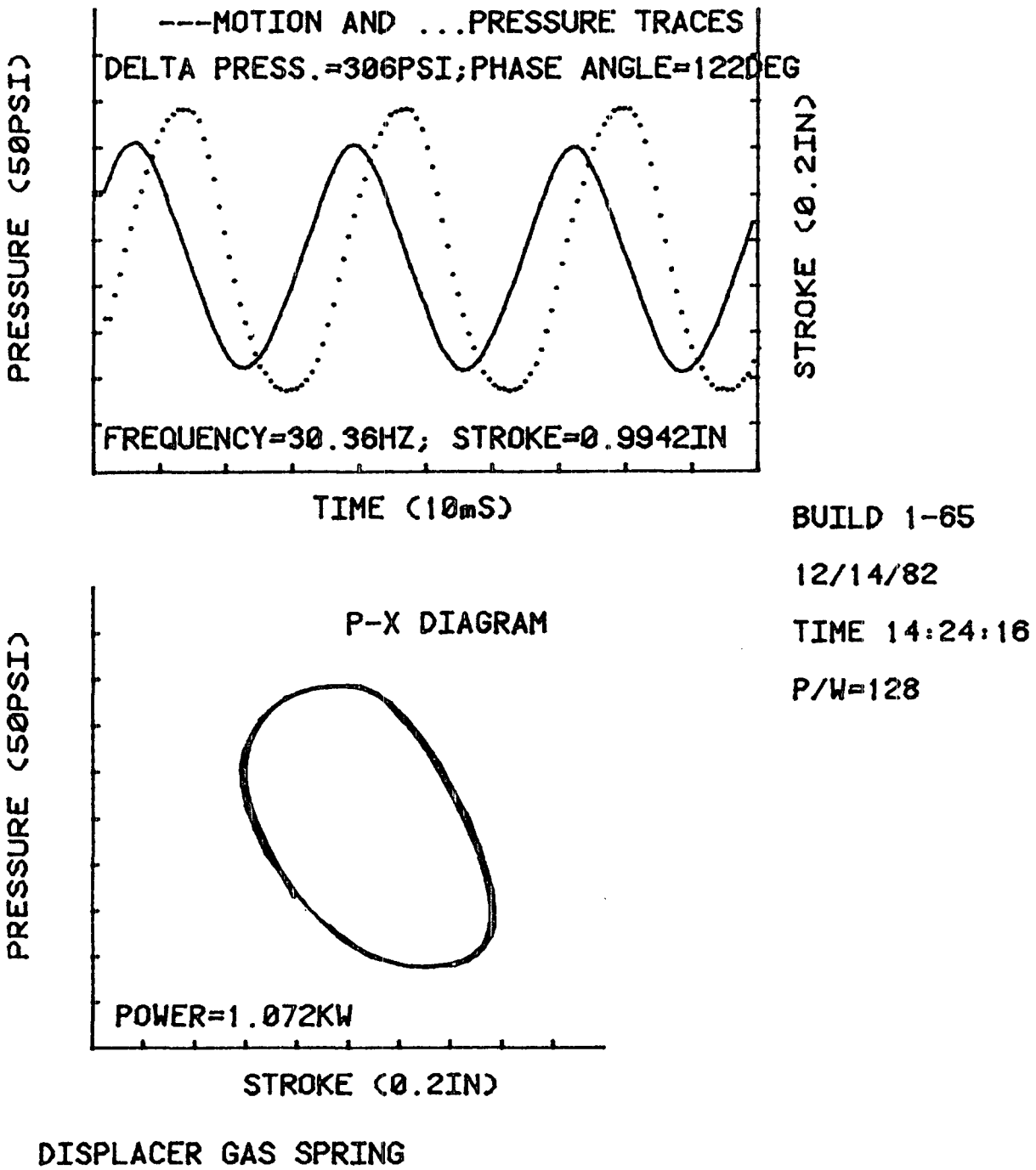

DISPLACER GAS SPRING

Figure 4-10. ENGINE DISPLACER GAS SPRING PRESSURE-STROKE HISTORY AND P-V DIAGRAM

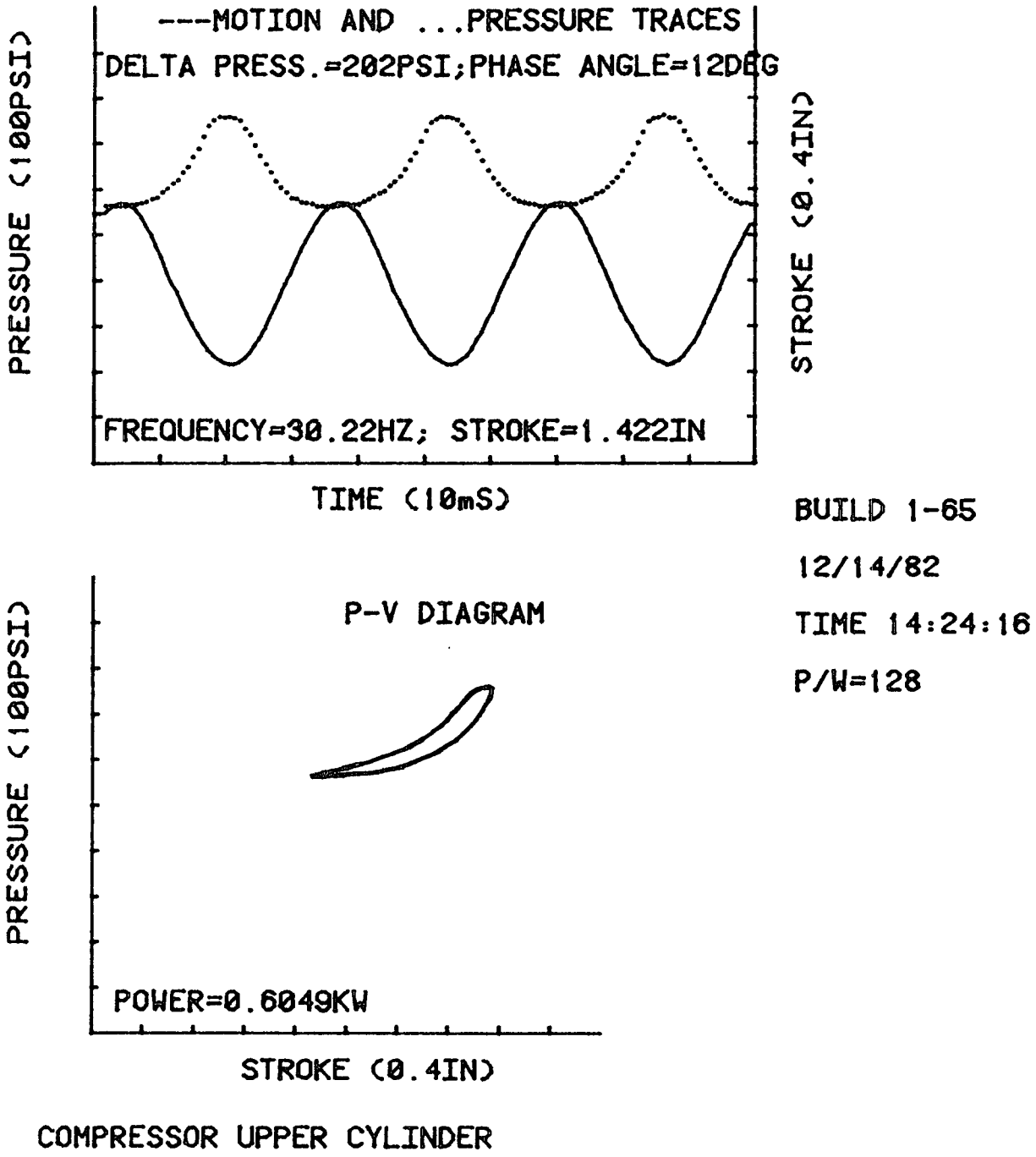

Figure 4-11. COMPRESSOR UPPER CYLINDER PRESSURE-STROKE HISTORY AND P-V DIAGRAM

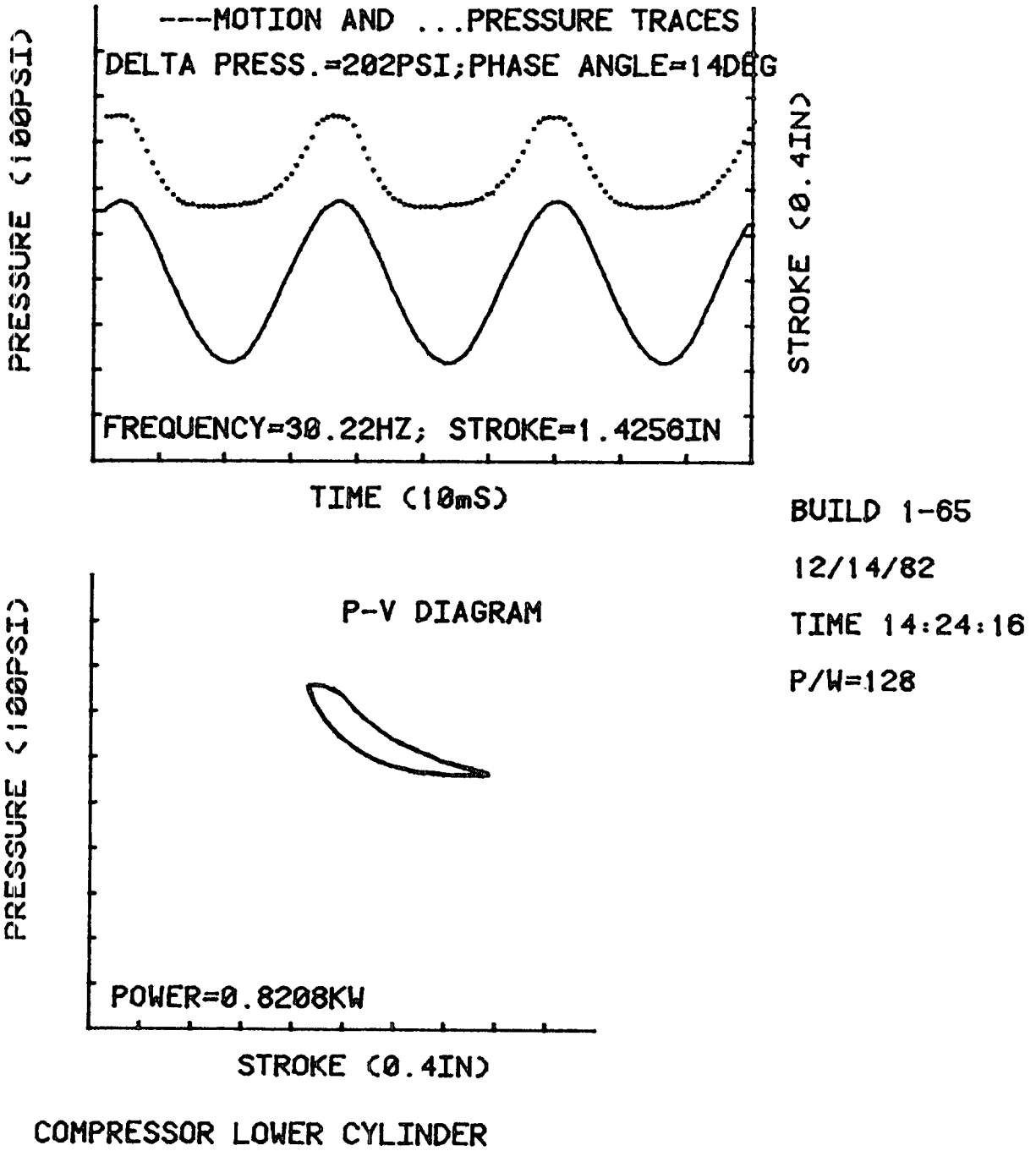

Figure 4-12. COMPRESSOR LOWER CYLINDER PRESSURE-STROKE HISTORY AND P-V DIAGRAM

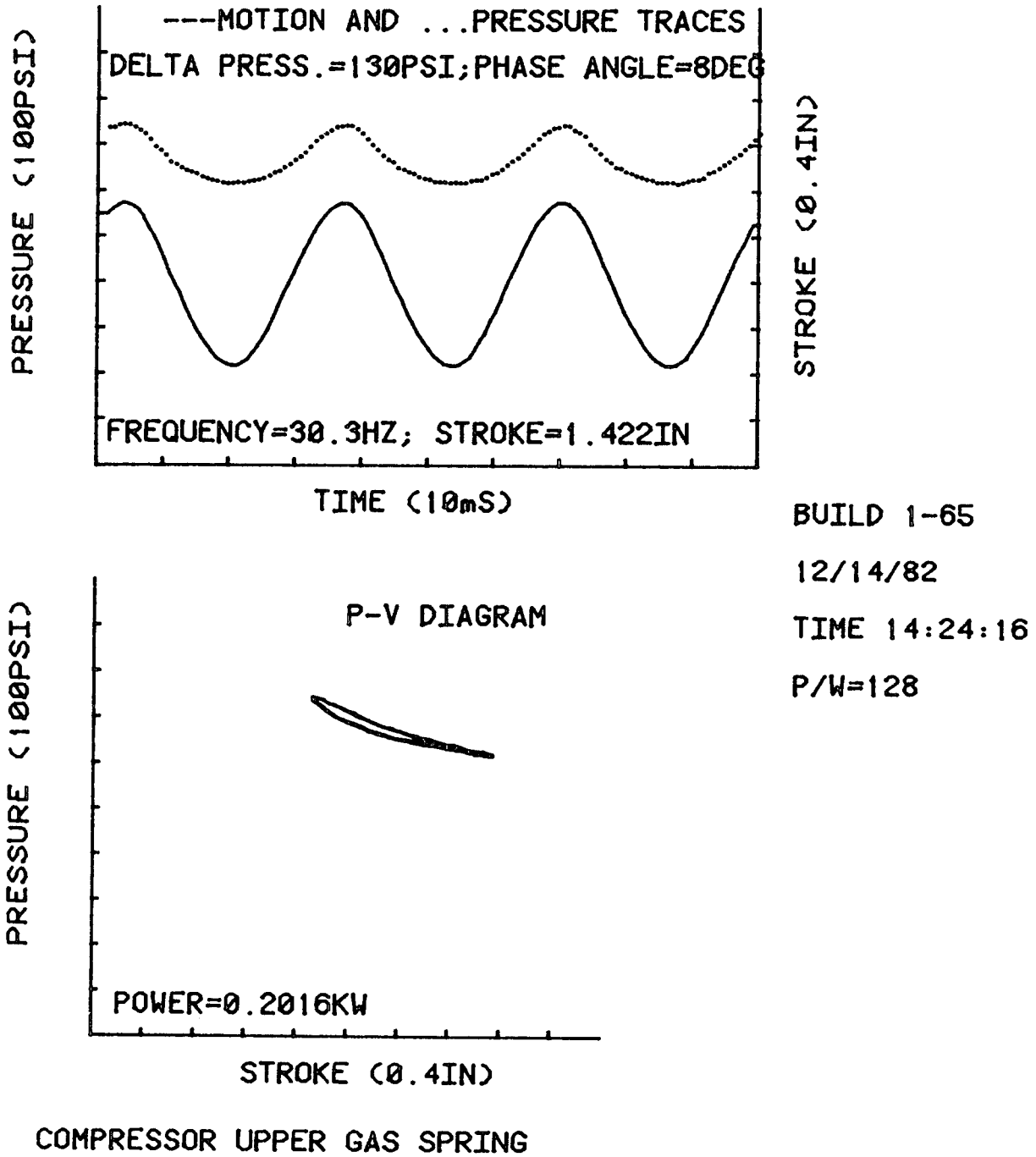

COMPRESSOR UPPER GAS SPRING

Figure 4-13. COMPRESSOR UPPER GAS SPRING PRESSURE-STROKE HISTORY AND P-V DIAGRAM

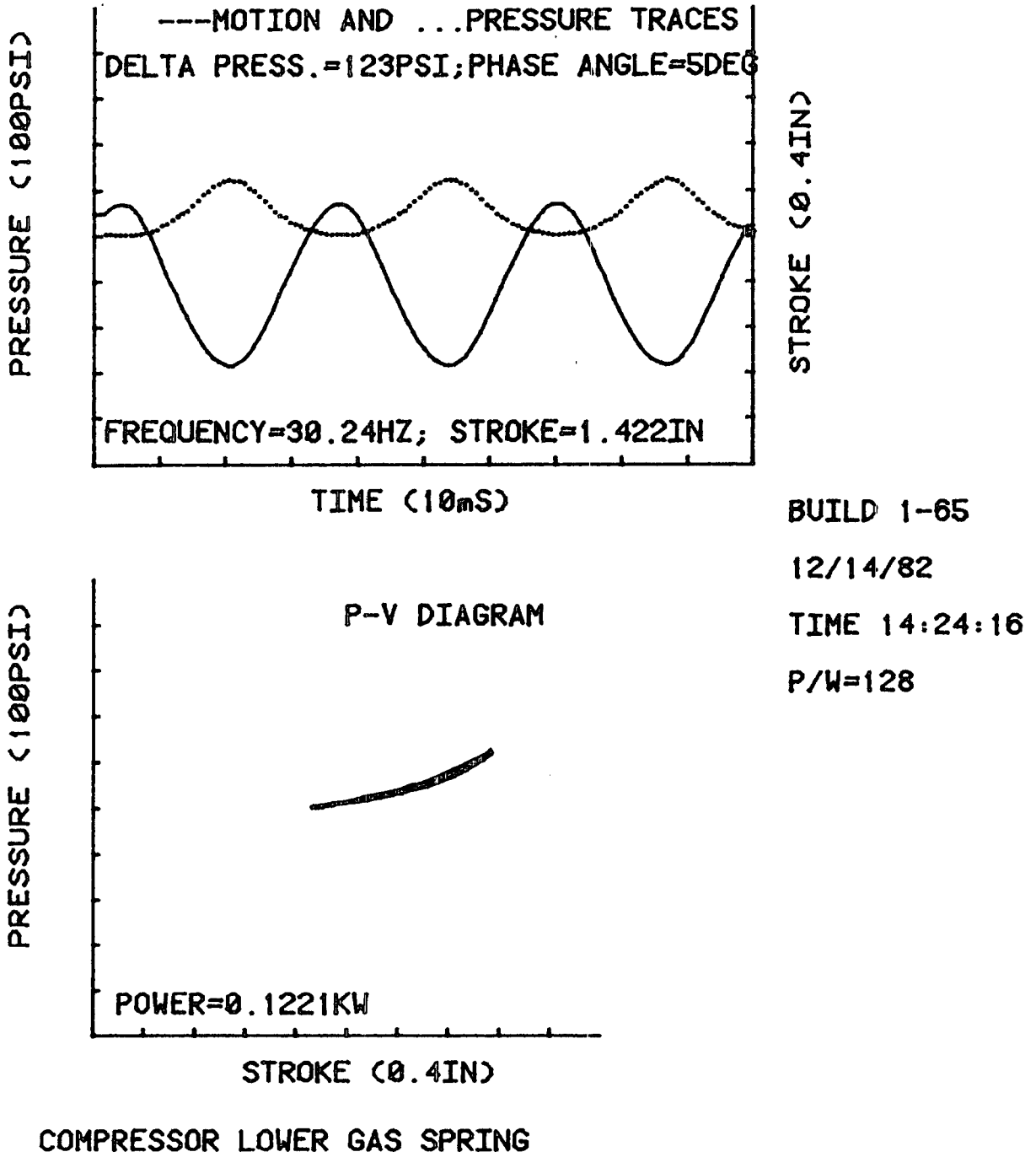

COMPRESSOR LOWER GAS SPRING

Figure 4-14. COMPRESSOR LOWER GAS SPRING PRESSURE-STROKE HISTORY AND P-V DIAGRAM

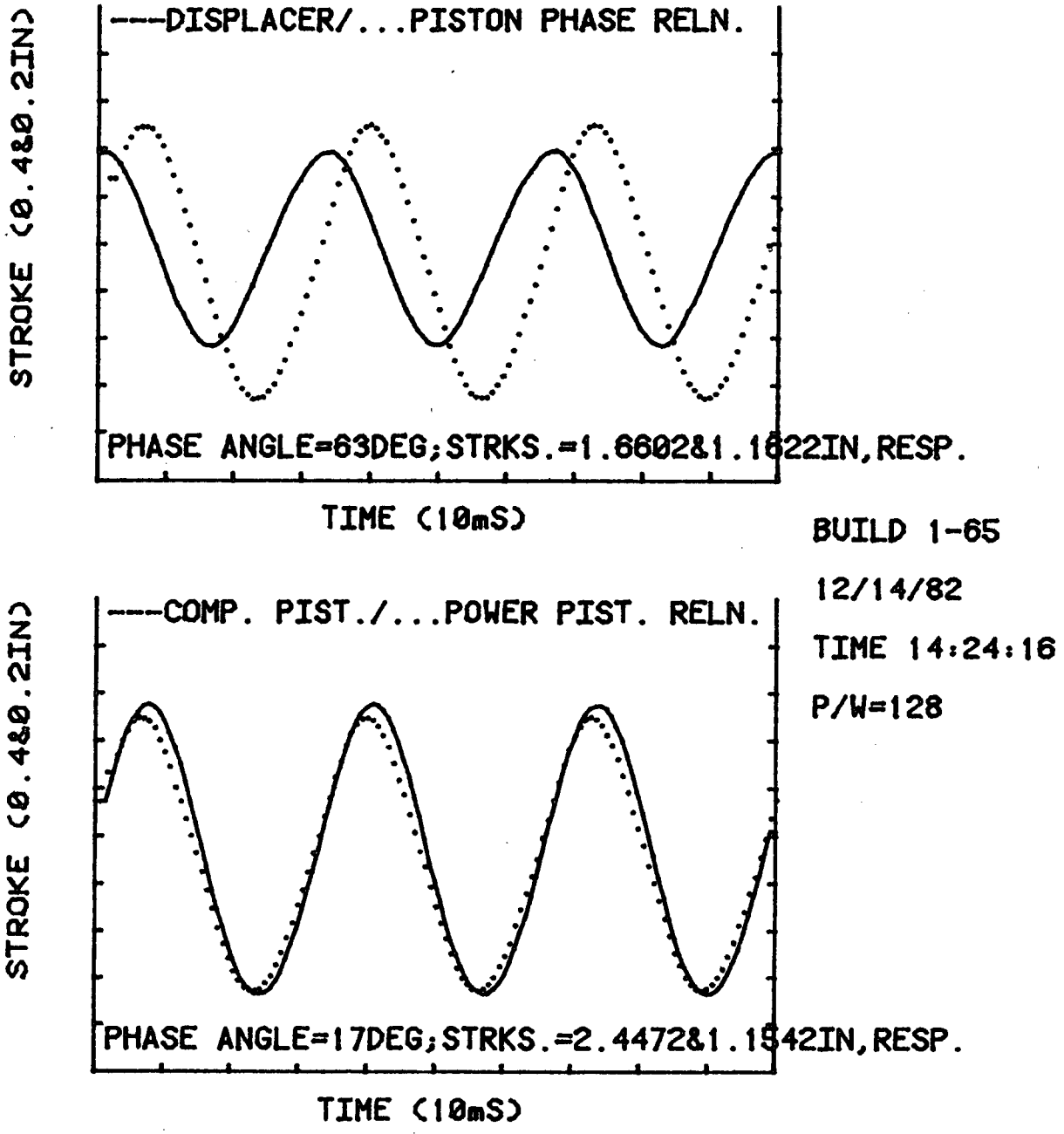

PISTON MOTIONS REL. TO HOUSING

Figure 4-15. ENGINE AND COMPRESSOR DYNAMIC COMPONENT MOTION HISTORIES

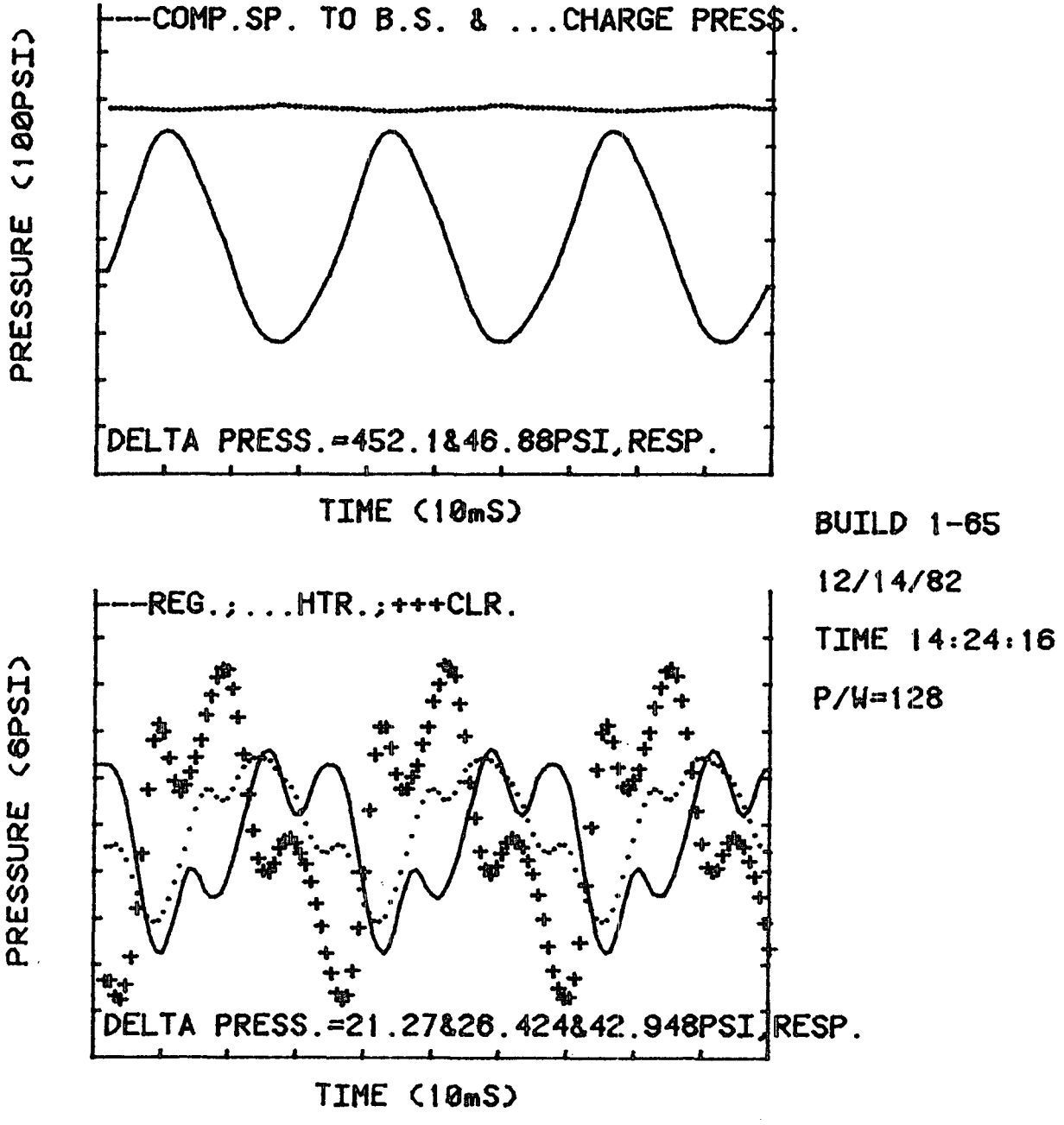

HELIUM PRESSURE TRACES

Figure 4-16. PRESSURE HISTORIES IN ENGINE COMPONENTS

The sample output shown for one test (Build 1-65 on 12/14/82 at 14:24 hours) illustrates the capability of the DAS to acquire, process and display the test results from a given run in a useful and consise format. This capability was a substantial improvement over the previous Phase II system and significantly aided in the performance verification and diagnostic analyses of the tests. (Use of these data and their interpretation are covered in Section 5.)

4.3 CHECK OUT TESTS

4.3.1 FUNCTIONAL PERFORMANCE

New Instrumentation Check-Out

Pre test functional check-outs were conducted to assure satisfactory operation of the combustor/engine/compressor assembly after being re-instrumented and re-assembled, and to verify that the new instrumentation and data acquisition system were functioning properly. Two hardware problems were experienced during check-out, the first a "third" gas spring effect and the second an LVDT tie-rod breakage.

- Third gas spring - an oversight in the design of the new compressor piston LVDT housing assembly resulted in a trapped volume between the outer housing and the LVDT housing. As previously shown in Figure 3-4, the LVDT housing is mounted directly to the compressor housing and as such is an integral part of the power piston assembly. Not only does the LVDT housing oscillate with the power piston relative to the outer housing, it also provides the linear bearing/rider ring support for the power piston upper bearing assembly. The rider ring, while not an efficient seal ring, was effective enough to seal the trapped volume and provide a sufficient gas spring effect to significantly restrict the power piston stroke. The problem was resolved by providing appropriate vent passage under the rider ring.

- LVDT tie-rod breakage - the LVDT tie-rod, connecting the LVDT core to the compressor piston, broke after a relatively short period of operation. The fracture occurred at the root of a thread where the rod was threaded into the end of the compressor piston. The problem was resolved by the procurement of new, straighter, ground-finish rods, and increasing the thread size.

Aside from these two initial difficulties, the functional checkout of the test hardware and instrumentation proceeded smoothly and no further difficulties were experienced throughtout the tests.

4.3.2 DAS ERROR ANALYSIS

During check out tests of the DAS, a number of anomalies were uncovered and resolved. The measured second gas spring power was significantly lower than in previous Phase II tests and exhibited substantial scatter from test to test. Indicated engine power was less than the sum of compressor power plus second gas spring power. In addition, the DAS computed compressor cylinder power differed from planimeter integrations of the P-V diagrams. These observations led to several check-out tests of both the instrumentation/ conditioning equipment and the DAS to resolve the problems. These activities are described below.

Phase Shift Error Analysis

A check of the power piston LVDT and pressure traces during early tests disclosed a differential phase angle between the signals. The LVDT conditioning equipment introduced a 11.5^{o} phase lag, while the pressure transducer signal conditioning equipment added only a 4.5^{o} lag. An error analysis was performed as follows:

1. The test run signals had been stored on a digital tape; these were then read by the microcomputer.
2. A PdV integration was performed numerically on the microcomputer. The value agreed with what had been calculated by digital oscilloscope during the tests.
3. A phase shift error was artificially introduced into the data (by displacing the digitized points representing one trace relative to the other) and the PdV integrated again. The sensitivity to this error is appreciable as the trend in the upper curve of Figure 4-17 shows.

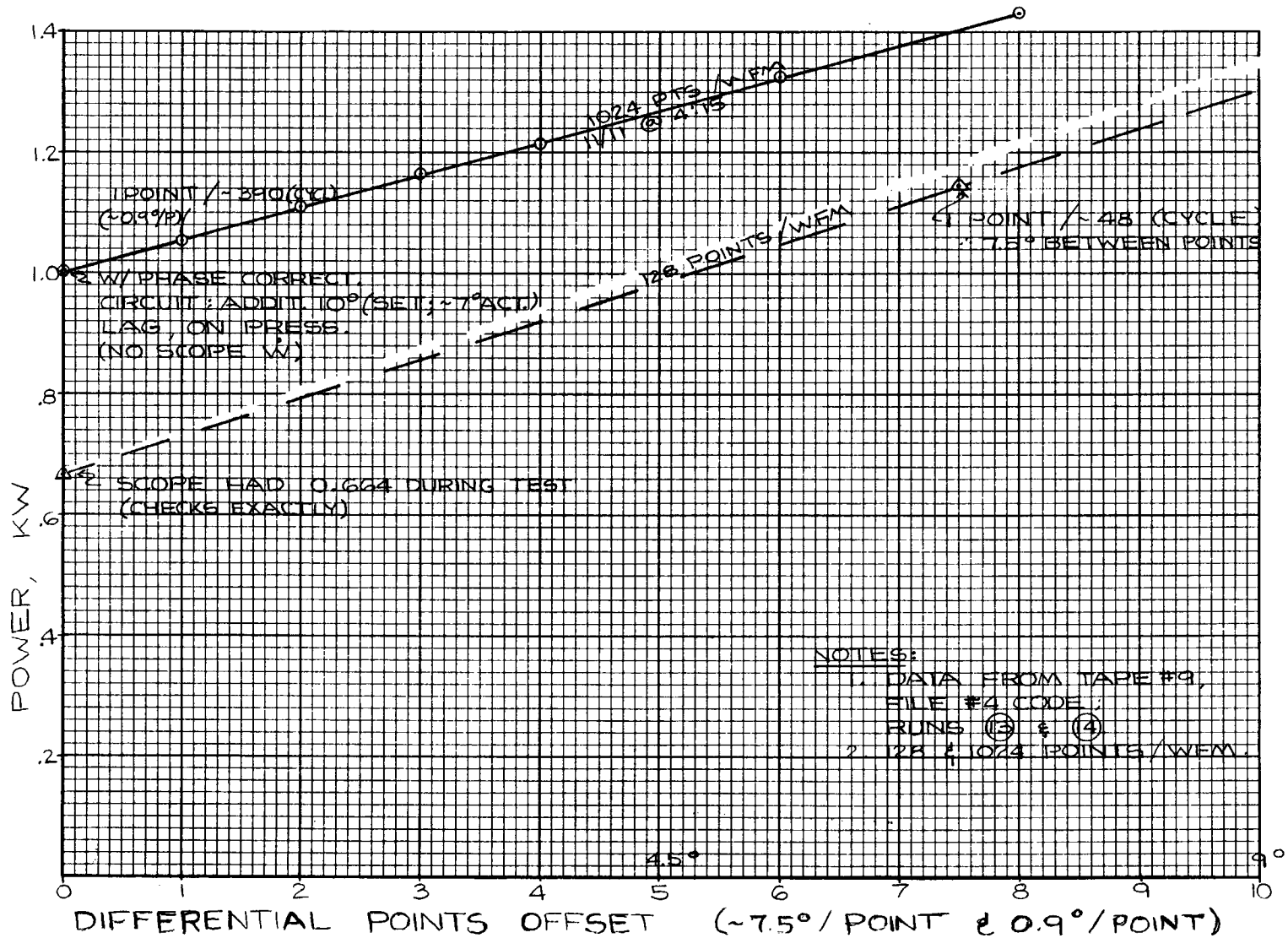

Figure 4-17. COMPRESSION SPACE AND DISPLACER GAS SPRING POWER VARIATIONS WITH SIGNAL PHASE ANGLE

A phase shift correction (a time delay device) was then added to the compression space pressure transducer circuit. This device was set to provide an additional 7° phase shift to the pressure signal, such that its phase lag was 11.5^{o}, (no differential phase angle between pressure and piston motion signals). It was observed in subsequent tests that the compression space power was now higher than before. The compression space signals were stored on digital tape, at 1024 points per waveform. The phase shift error analysis on this data was repeated and the results are shown as the upper curve (solid line) of Figure 4-17. Controlling the phase shift error to within one degree results in an error of less than 10% in power.

Displacer Gas Spring

The phase shifts on both pressure and motion traces for the displacer gas spring were 11.5^{o}, so no adjustments were required. Since the displacer gas spring power is about one-half of the compression space power, its sensitivity to a phase difference is approximated by the lower (dashed) curve on Figure 4-17.

Second Gas Spring

The anomalies and scatter in second gas spring power measurements led to a check of the signal conditioning equipment. Drifting of the pressure zero was observed, and the transducer was re-calibrated. This only partly corrected the problem. Further checking uncovered a malfunctioning switch on the signal conditioning filter. The entire conditioning circuit was replaced, and the signals re-calibrated. An examination of the phase shift error showed both pressure and motion traces had an 11.5^{o} lag, requiring no correction.

An error analysis similar to the one for the compression space was performed to ascertain the sensitivity of the second gas spring power to a phase shift. The results are given in Figure 4-18. The absolute value of the error is about 0.07 kw/degree of phase shift, about the same as for the compression space. However, the second gas spring power is much lower, so the relative (%) error is considerable: about 50%/degree. Second gas spring power was, therefore, carefully interpreted in the reduction and interpretation of test results.

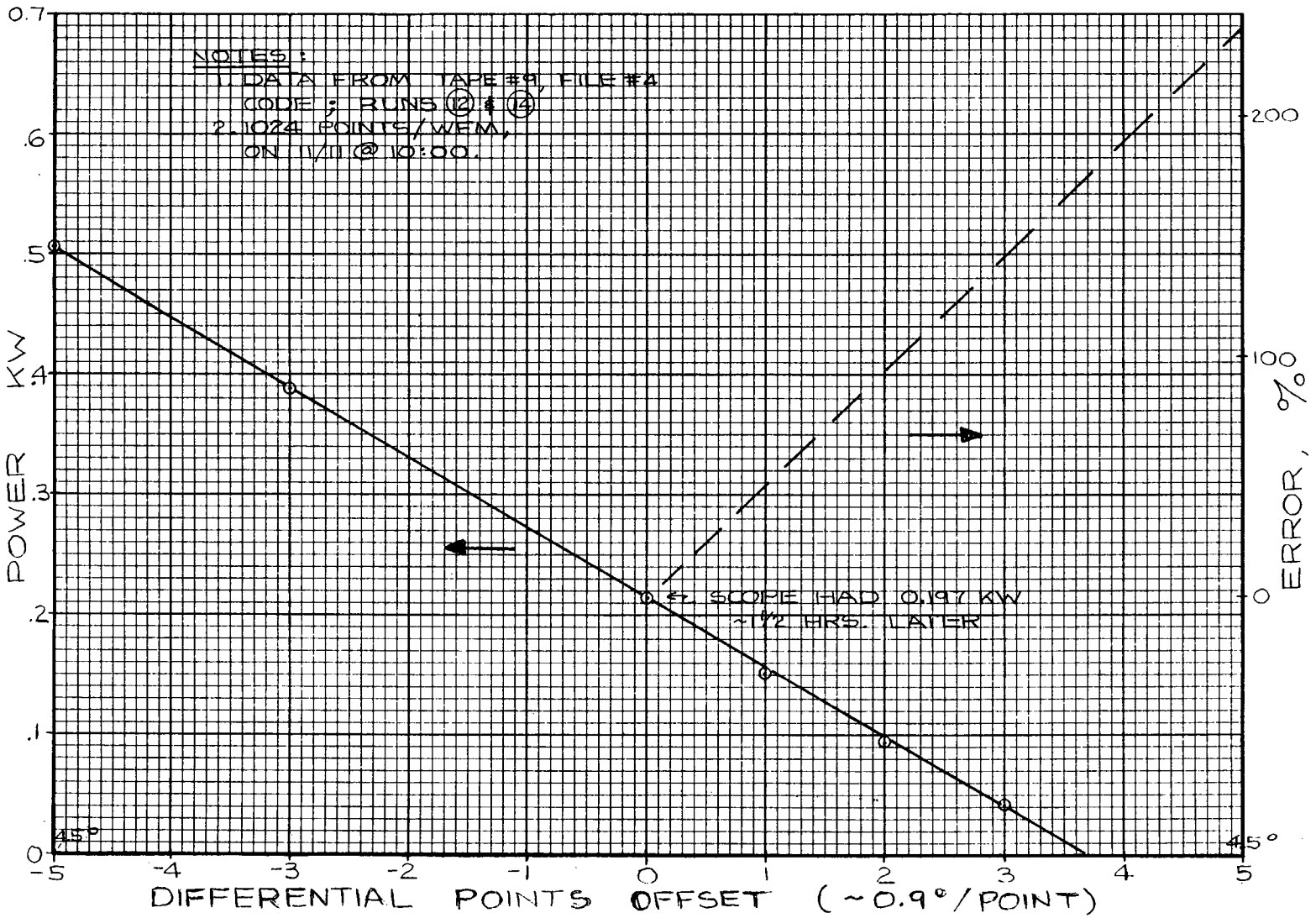

Figure 4-18. SECOND GAS SPRING POWER VS. SENSITIVITY TO SIGNAL PHASE ANGLE

Compressor

The compressor sensors and signal conditioning equipment are all from one manufacturer (the same as the second and displacer gas springs, which did not show phase shift mismatches). Error trends were, therefore, estimated to be similar to those discussed above (i.e., $\sim$ 0.07 kw/degree).

Compressor Power Algorithm

The observed anomalies in the compressor power calculations noted earlier were found to be caused by the particular integration algorithm used. The pressures within the compressor were measured as absolute pressures (all others used in PdV integrations were pressure differences), and entered the algorithm in the following manner:

$$\int_{t_1}^{t_2} [P(t)+\bar{P}]\ (dV/dt)dt,$$

where $\bar{P}$ = the mean pressure. This was verified by splitting the integration into its two components:

$$\int [P(t)]\ (dV/dt)\ dt + \int \bar{P}\ (dV/dt)\ dt$$

Separate integrations were performed on the oscilloscope for the complete equation and of each component. As expected, the individual component power values added up to the power calculated by the initial equation. This confirmed the approach to modify the algorithm.

The mean pressure of each trace was subtracted/added to the original values and the resulting trace was then used in subsequent P(dV/dt) dt integrations.
Checks on this technique showed consistent results, which agreed with planimeter integrations of PdV traces.

Additional Error Analyses

The digital oscilloscope provides many features and options in acquiring and storing waveforms: the number of points per waveform; waveform averaging over a number of cycles; and waveform smoothing. The sensitivity of the

power calculations to these parameters was examined, and is presented in Table 4-7. As shown, the differences between options was small. 128 points/waveform acquisition, with no additional waveform processing, was chosen for all test runs. This minimized the data acquisition and processing time, while maximizing memory use (i.e., 40 waveforms can be held in RAM at this resolution).

The effect of engine housing motion on second gas spring power was also evaluated. The results show that about half the power dissipated in the second gas spring is contributed by housing motion. This effect was not evaluated further for its design implications, but warrants further investigation.

Error Summary

During the DAS checkout phase, the principal sources of errors and inaccuracies were investigated and corrected. Instrument error was minimized by calibrating all LVDTs and pressure transducers. Errors on these instruments are approximately ± 2% and ± 0.5% respectively. Signal conditioning equipment drift was minimal as it is never turned off. The DAS introduces some additional error (± 2%, on the amplifiers), including the somewhat coarse quantization of 128 points/waveform used.

In general, the total error between power measured/calculated appears well within ± 5%. A review of the test data (Section 5) bears this out; comparison of the two high power points (tests #30 and 33) shows very consistent results and trends. However, the second gas spring power does vary significantly: observation of the P-V diagram on the oscilloscope during testing showed an unsteady P-V diagram. Since the total power consumption of the second gas spring is relatively small, the overall effect on total system power is small. However, when interpreting small changes in engine/compressor operation, the variability of second gas spring power must be taken into account. A further discussion of this effect is presented in Section 5.

Table 4-7. Sensitivity of Power Calculation to Waveform Parameters

CASE NO.	POINTS/WAVEFORM	AVERAGING OF WFM OVER 10 CYCLES	SMOOTHED WAVEFORM	NORMALIZED POWER
1	128	NO	NO	1.0
	512	NO	NO	1.022
	128	YES	NO	0.997
	128	NO	YES	0.971
2	128	NO	NO	1.0
	512	NO	NO	0.989
	128	YES	NO	1.017
	128	NO	YES	0.986

*Represents an average of 10 computations, performed at slightly different times around the data point (analog tape used for signals)

SECTION 5
TEST PROGRAM

SECTION 5
TEST PROGRAM

The results of the Phase IIIB test program and interpretation of those results are presented in this section. Much of the interpretation is based on previous Phase II results and analyses which are only briefly capsuled here for completeness. Reference 1 presents the detailed results of the Phase II program.

5.1 TEST PLAN

The Phase IIIB test plan established the procedure and test matrix to be followed in conducting the Phase IIIB integrated tests of the Proto 2 FPSE/Linear Compressor Unit.

5.1.1 TEST OBJECTIVES

The objectives of Phase IIIB testing, listed in order of their priority were:

1) To verify compressor performance as previously established on the compressor test stand. Compressor performance was to be determined by measurements of compressor power, compressor piston stroke, and compressor piston phase angle.

2) To verify engine/compressor matching. Matching was to be determined by recording frequency, stroke, and power level as a function of compressor conditions and heater head temperature.

3) To tune engine/compressor dynamics to achieve maximum engine performance. Engine power was to be measured as the sum of second gas spring power plus total compressor power absorbed. Engine efficiency was to be measured as power delivered divided by heat into the heater head.

4) To obtain component level test data on the regenerators, heater head, cooler, displacer gas spring, and combustor.

5.1.2 TEST MATRIX

The test points required to fulfill the purposes outlined above are discussed in this section. Test points were established for each area of priority. However, to make the most use of test time and resources, the data from individual test points were used in satisfying more than one test objective.

Compressor Performance

The linear inertial compressor had been operated on a component test stand in Phase II which excited the compressor housing at specified strokes and frequencies. Compressor power and compressor piston stroke and phase angle were measured. Stroke was held constant while frequency was increased. Such maps were compared to theoretical predictions of compressor performance determined from the compressor code. The code was calibrated in this fashion. Typical code predictions for compressor performance are shown on Figure 5-1. In integrated testing (with the engine), compressor housing strokes and frequency cannot be independently held constant. In Phase II integrated testing, the compressor piston motion was not measured. In the testing planned for Phase IIIB, this motion was to be measured.

To verify compressor performance, the engine was to be operated over a range of strokes and frequencies and the code run for the conditions of each test point. Code predictions of useful power, gas spring power consumption, piston stroke, and phase angle, were then to be compared with test measurements, and the compressor performance so verified. The engine/compressor configuration during this testing was to be that of Build 1-64, as shown in Table 5-1. This would allow comparison with previous integrated tests and component test results. The test points to be run to generate this data are shown in Table 5-2.

Engine/Compressor Matching

The understanding of engine/compressor matching prior to the tests is shown in Figure 5-2. For a given heater head temperature and frequency, the free piston engine delivers power along a single power versus stroke curve.

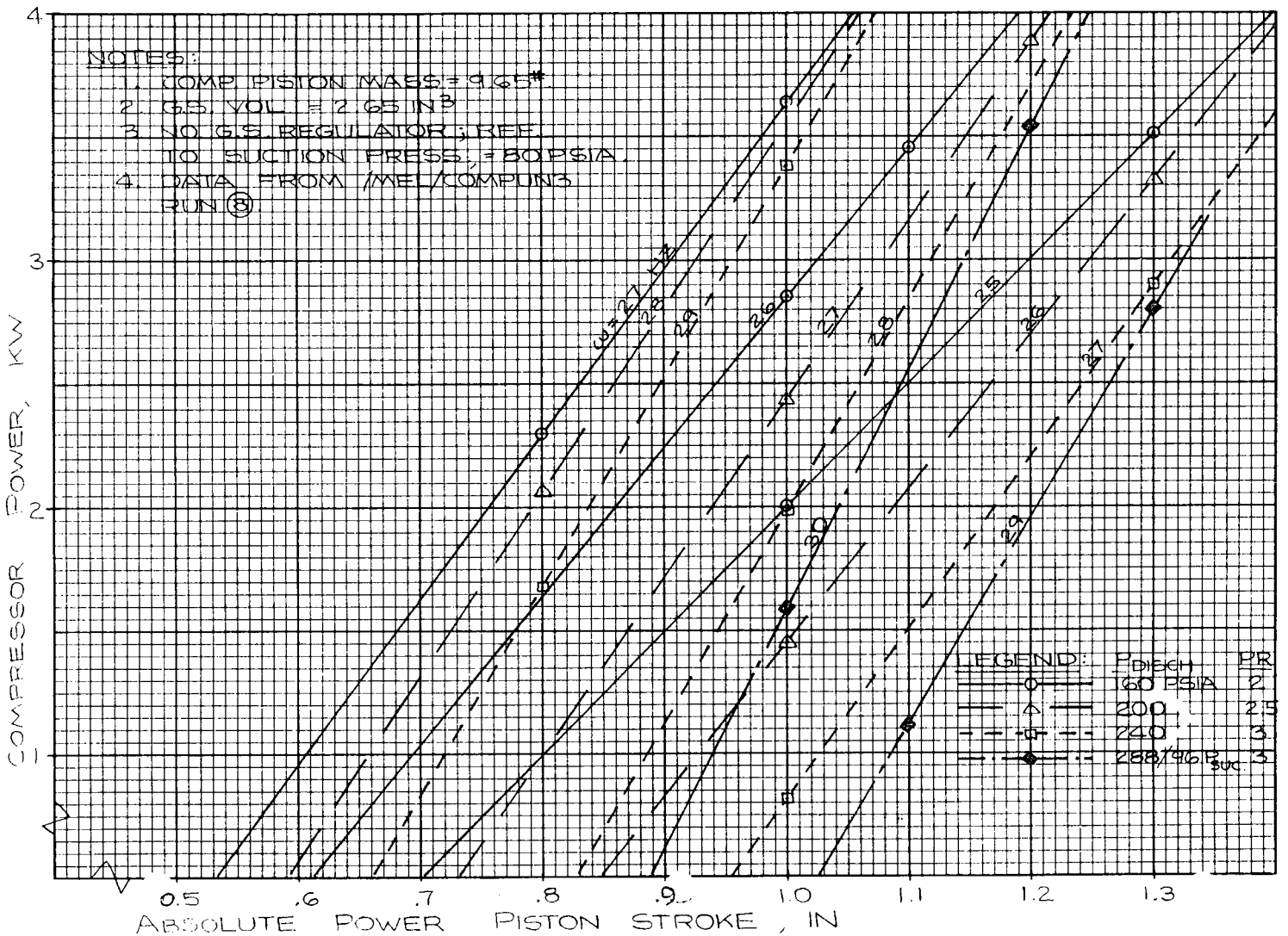

Figure 5-1. COMPRESSOR CODE PREDICTIONS OF COMPRESSOR OPERATING CHARACTERISTICS

TABLE 5-1

CONFIGURATION OF BUILD 1-64

ENGINE TYPE	PROTO 2 BASELINE
DISPLACER ROD DIAMETER	1.416 IN.
DISPLACER GAS SPRING VOLUME	12.57 IN^3
SECOND GAS SPRING AREA	11.6 IN^2
SECOND GAS SPRING VOLUME	81 IN^3
REGENERATOR MATRIX POROSITY	80%
COMPRESSOR PISTON WEIGHT	9.65 LBS.

TABLE 5-2

TEST POINTS FOR COMPRESSOR PERFORMANCE VERIFICATION

BUILD CONFIGURATION	HEATER HEAD TEMPERATURE	SUCTION PRESSURE	DISCHARGE PRESSURE	REGULATOR PRESSURE
1-64	1250°F	80 PSIA	160 PSIA	NONE
1-64	1250°F	80 "	200 "	NONE
1-64	1250°F	80 "	240 "	NONE
1-64	1250°F	96 "	288 "	NONE
1-64	1250°F	96 "	200 "	NONE

FIRING RATE AS REQUIRED

COOLANT TEMPERATURE - 70°F

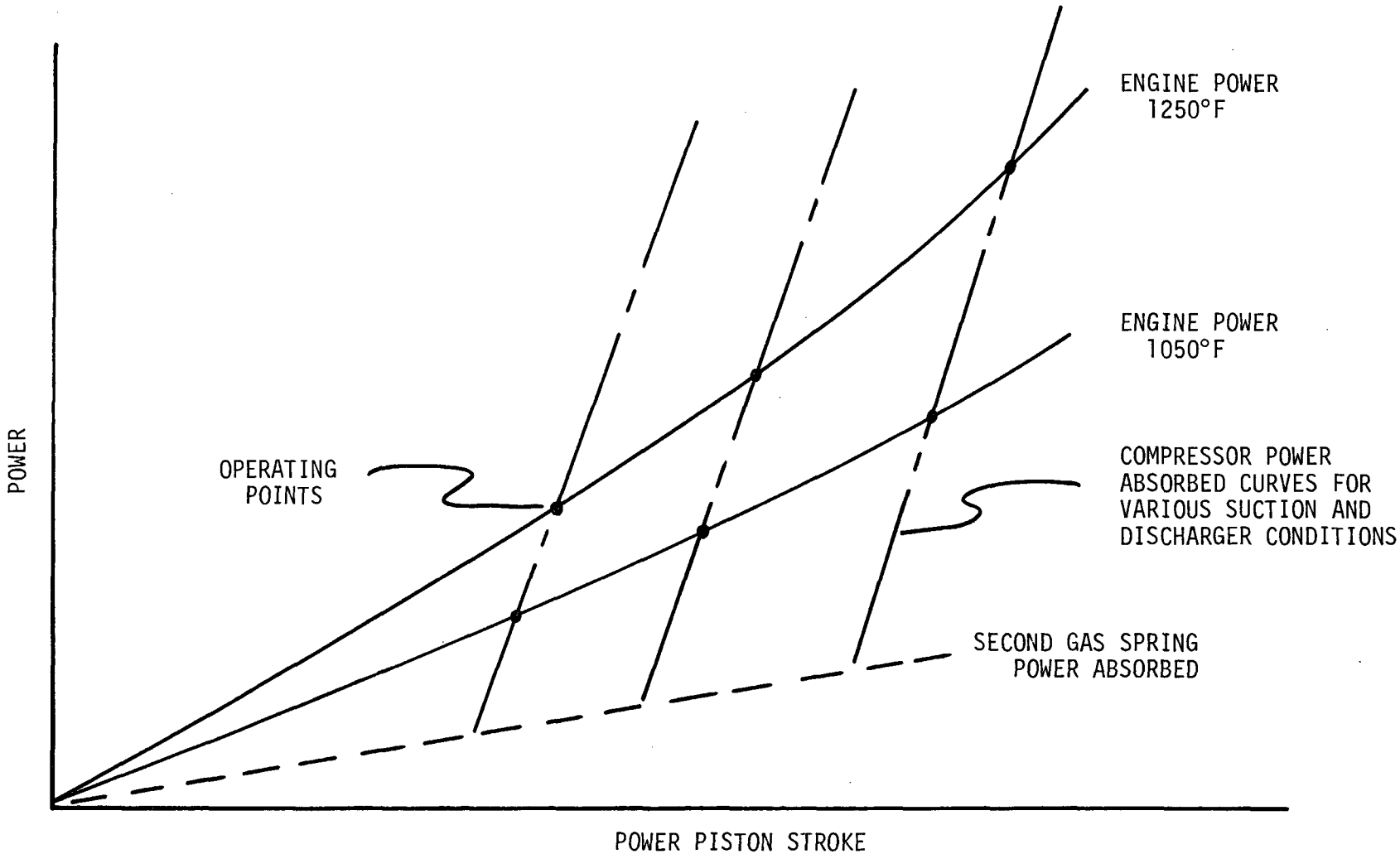

Figure 5-2. ENGINE-COMPRESSOR MATCHING CHARACTERISTICS

For given compressor suction and discharge conditions and driving frequency, the compressor and second gas spring absorb power along a single power versus stroke curve. The operating point of the engine will be where these curves intersect. As frequency or compressor conditions change, the compressor curve will shift and a new operating point will occur. If firing rate is controlled to insure a constant heater head temperature, the new operating point will remain essentially on the same engine curve (frequency has a much smaller effect on the engine curve than it does on the compressor curve). If firing rate is held constant, the heater head temperature will change until the engine curve (at the new temperature) intersects the new compressor curve at the original firing rate.

To evaluate this technique for engine/compressor matching, and to quantify its predictive usefulness, the test matrix shown in Table 5-3 was to be conducted. This matrix was designed to move the operating point to the six locations shown in Figure 5-2. After this series of tests, the compressor conditions were to be changed while maintaining a constant firing rate. It was expected that the engine would operate at a lower heater head temperature. Based on the quantitive understanding of matching at the time, a change to the compressor configuration would then be made to raise the heater head temperature to the original level. This test is defined in Table 5-4 and described graphically in Figure 5-3.

Maximum Engine Performance

Following the compressor performance verification and engine matching tests, the engine was to be run for maximum power output. It was expected that this would occur at the highest allowable stroke and heater head temperature. Based on the engine/compressor matching results, a compressor configuration was to be chosen which would permit the engine to operate in this range. This test point is shown in Table 5-5.

Component Level Performance

For the entire series of integrated tests described above, component level instrumentation installed on the engine would measure hot side gas temperature, pressure and temperature drops across the regenerator, displacer gas spring heat flux, combustor heat loss, and compressor piston stroke.

TABLE 5-3

ENGINE/COMPRESSOR MATCHING TEST POINTS

BUILD CONFIGURATION	HEATER HEAD TEMPERATURE	SUCTION PRESSURE	DISCHARGE PRESSURE	REGULATOR PRESSURE
1-64	1250°F	80	160	NONE
1-64	1250°F	80	200	NONE
1-64	1250°F	96	288	NONE
1-64	1050°F	80	160	NONE
1-64	1050°F	80	200	NONE
1-64	1050°F	96	288	NONE

FIRING RATE AS REQUIRED

COOLANT TEMPERATURE - 70°F

TABLE 5-4

CONSTANT FIRING RATE ENGINE/COMPRESSOR MATCHING TEST POINTS

BUILD CONFIGURATION	HEATER HEAD TEMPERATURE	FIRING RATE	SUCTION PRESSURE	DISCHARGE PRESSURE	REGULATOR PRESSURE
1-64	1250°F	AS REQ'D	80	200	NONE
1-64	TBD	UNCHANGED	96	288	NONE
TBD	1250°F	UNCHANGED	96	288	TBD

COOLANT TEMPERATURE - 70°F

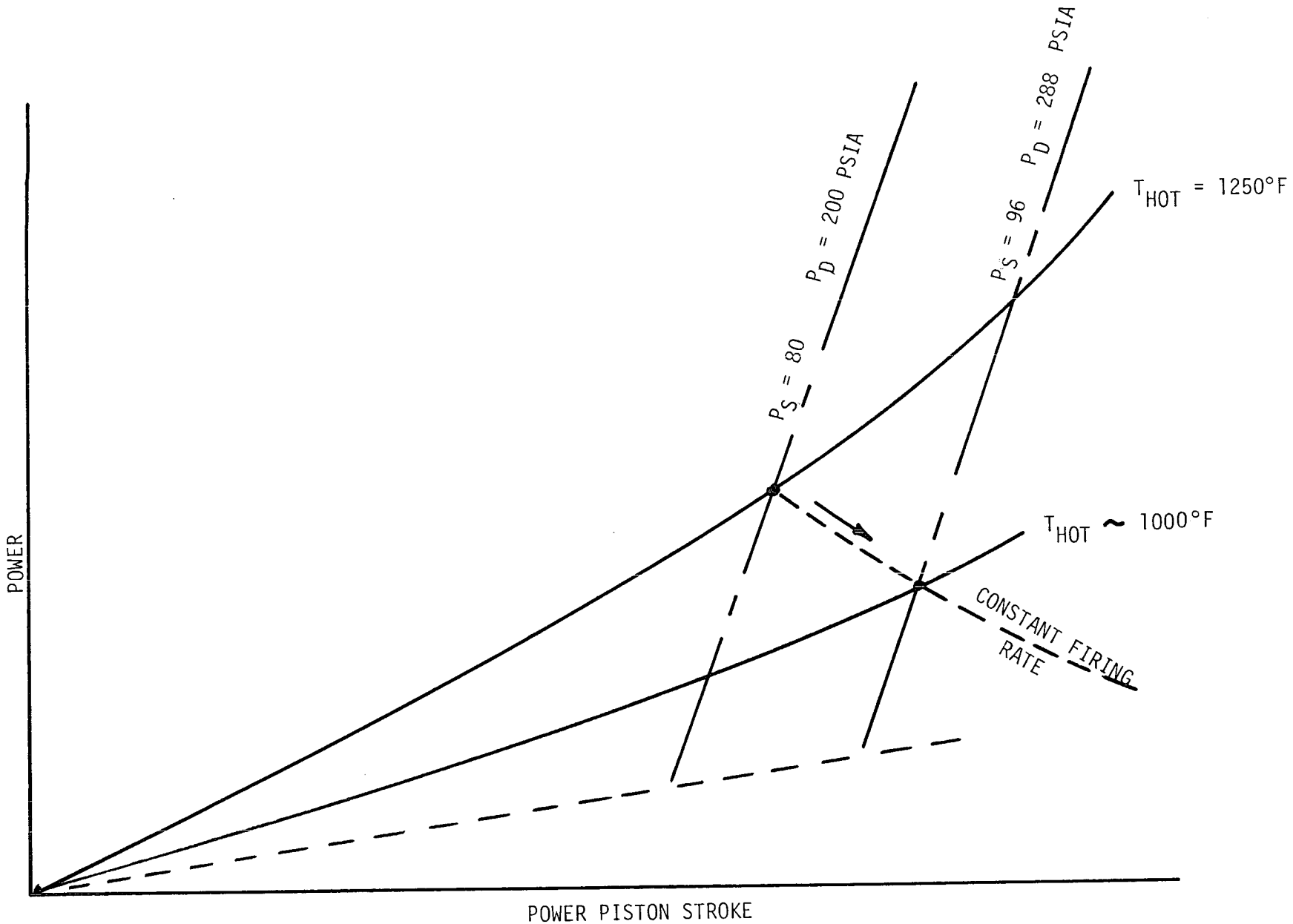

Figure 5-3. ENGINE-COMPRESSOR MATCHING WITH CONST. FIRING RATE

TABLE 5-5

MAXIMUM ENGINE POWER TEST POINT

BUILD CONFIGURATION	HEATER HEAD TEMPERATURE	ENGINE STROKE RELATIVE TO HSG.	SUCTION PRESSURE	DISCHARGE PRESSURE	REGULATOR PRESSURE
TBD	1250°F	~1.3 IN.	TBD	TBD	TBD

COOLANT TEMPERATURE - 70°F

FIRING RATE AS REQUIRED

These were to be monitored during the testing described above and would allow estimates of regenerator effectiveness, flow work, heater head conductance, displacer gas spring losses, and combustor efficiency. The equations used in making these estimates are shown in Table 5-6. The component level data taken during the previous tests were then to be reviewed when these tests were completed. Those data which appear to be most fruitful in evaluating the underlying physical mechanisms of the real Stirling cycle would then be supplemented by a final series of tests. A separate plan was planned to be issued at this time. (Due to rescoping of the program, these supplemental tests were not run. However, the component test data obtained during the preceding tests were used to address this test objective.)

5.2 TEST DATA AND MAJOR RESULTS

Tests were run to meet the requirements of the approved Test Plan after the check-out tests were completed. Each test has a complete DAS output data set, such as the example given in Section 4.2.3, where available (in some tests, complete output data sets could not be obtained due to instrument failures, data logger failure, etc.). The data sets are presented in Appendix B.

The objectives and general results of the tests are summarized in Table 5-7. Table 5-8 presents a summary of test results, highlighting the major test parameters and adding several calculated values to the results, including the Beale number. Table 5-9 gives the definitions for the terms used in Table 5-8.

As noted in Table 5-7, tests 1 through 6 have some questionable results due to minor signal conditioning and algorithm errors. These data have been used only to supplement the data obtained in Test 7 through Test 33. Tests 7 through 13 were run according to the test matrix at design charge pressure with no compressor pressure regulator (compressor gas springs fed by compressor suction gas). Tests 14 through 21 were run at similar conditions but with the compressor regulator installed and set at various levels. From these tests a compressor regulator pressure of 95 psia was determined to be near-optimum for most test conditions. Tests at higher engine charge pressures were then run (Tests 22-30). These tests achieved the highest

Table 5-6. TEST MEASUREMENTS AND DATA REDUCTION MODELS

		PRIME TRANSDUCERS	EQUATIONS OR MODELS	PRIME INDEPENDENT VARIABLES
COMPONENT LEVEL	REGENERATOR EFFECTIVENESS	$T_H(t)$, $T_c(t)$	$E \approx \frac{T_{HAVG} - T_{cMIN}}{T_{HMAX} - T_{cMIN}}$ (a)	T_H, FREQ, POROSITY, Pch
	FLOW WORK	$\Delta P_H(t)$, $\Delta P_c(t)$, $\Delta P_R(t)$ $X_D(t)$	$\dot{W}_{AVG} \approx \frac{(\Delta P_{RMS})(\dot{m}_{AVG})}{\rho_{AVG}}$; WHERE $\Delta P_{RMS} = \frac{\Delta P_{MAX}}{\sqrt{2}}$	POROSITY, FREQ, T_H, Pch
	HEATER HEAD U	T_W, T_H	$U_H = \dot{Q}_{IN}/[(T_W - T_H)(A)]$ (b)	FREQ, T_H
	COOLER U	T_W, T_C	$U_c = \dot{Q}_{OUT}/[(T_c - T_W)(A)]$ (c)	FREQ, T_c
	COMPRESSOR STROKE	$X_c(t)$	$\dot{W}_{COMP} = [\phi P_c(t)\, dX_{c/G}](FREQ)(A)$	
	DISPLACER GAS SPRING LOSSES	P_{GS}, T_{GS}, T_W	$\dot{W}_{LEAKAGE} = [\phi P_{GS}(t)\, dX_{D/P}](FREQ)(A) - UA\,(T_W - T_{GS})$	P_{GS}, $\dot{Q}_{GS}$ (= UA $(T_W - T_{GS})$)
	COMBUSTOR	$\dot{m}_{FUEL}$, $\dot{m}_{AIR}$, T_{AIR}	$\eta = \frac{(\dot{m}_{FUEL})(HHV) - LOSSES}{(\dot{m}_{FUEL})(HHV)}$ (b)	$\dot{m}_{FUEL}$
ENGINE LEVEL	$\dot{Q}_{IN}$	$\dot{m}_{FUEL}$, $\dot{m}_{AIR}$, T_{AIR}	$\dot{Q}_{IN} = (\eta_{COMB})(\dot{m}_{FUEL})(HHV) - KA\Delta T$ (b, d)	$\dot{m}_{FUEL}$
	POWER VS. STROKE @ CONST. TEMP.	$P_{c1, 2, 3, 4}(t)$, $P_{2GS}(t)$, $X_p(t)$, $X_H(t)$ T_W	$\dot{W} = [\phi P(t)\, dX_{P/G}](FREQ)(A)$	FREQ, Pch
	EFF. VS. STROKE @ CONST. TEMP.	AS ABOVE	$\eta = \frac{\Sigma \dot{W}}{\dot{Q}_{IN}}$	FREQ, Pch
	POWER VS. STROKE @ CONST. FIRING RATE	AS ABOVE	SAME	FREQ, Pch
SYSTEM LEVEL	COMP. POWER VS. T_{AMB} @ FIXED FIRING RATES	$\dot{m}_{FREON}$, T_{SUC}, T_{DIS}, P_{SUC}, P_{DIS}	$\dot{W} = \dot{m}_{FREON}\, \Delta h$ (ASSUMES ST. ST. OPERATION)	PRESSURE RATIO = P_{DIS}/P_{SUC}
	COMP. POWER VS. T_{AMB} @ CONST. HEATER HEAD TEMPS.	AS ABOVE	SAME	SAME

TABLE 5-6
(CONT.)

NOTES

(a) T_{HMAX} = MAXIMUM FLUID TEMPERATURE @ HEATER END OF REGENERATOR

T_{cMIN} = MINIMUM FLUID TEMPERATURE @ COOLER END OF REGENERATOR

T_{HMIN} = MINIMUM FLUID TEMPERATURE @ HEATER END OF REGENERATOR

$$T_{AVG} \simeq \frac{(T_{HMAX} + T_{HMIN})}{2}$$

THERMODYNAMIC EFFECTS (I.E., HEATING/COOLING FROM FLUID COMPRESSION/EXPANSION) ARE IGNORED; THE ERROR SHOULD BE SMALL (SEE A. SCHOCK "STIRLING ENGINE NODAL ANALYSIS", J. ENERGY 2, 354 (1978))

(b) $\dot{Q}_{IN}$ CAN BE COMPUTED, IF THE COMBUSTOR η AND CONDUCTION LOSSES ARE KNOWN, THUS:

$$\eta_{COMB} = \frac{(\dot{m}_{FUEL})(HHV) - \text{COMBUSTOR LOSSES}}{(\dot{m}_{FUEL})(HHV)}$$

AND CONDUCTION LOSSES ALONG ENGINE $\simeq (K)(A)(\Delta T)$. ALSO, THE FLUID TEMPERATURE T_H IS A TIME-AND-POSITION AVERAGE ONE.

(c) $\dot{Q}_{OUT} = \dot{m}C_p\ \Delta T$ OF COOLING WATER.

(d) ALTERNATELY, FROM AN ENERGY BALANCE ON THE HEATER CONTROL VOLUME, ASSUMING WORK ~ 0, KINETIC ENERGY ~ 0, AND IDEAL GAS BEHAVIOR (He IN THE PRESSURE/TEMPERATURE RANGE OF INTEREST HAS COMPRESSIBILITY ~ 1; ALSO, ITS ENTHALPY $\neq$ f (PRESS), AS FOR AN IDEAL GAS, THEREFORE IDEAL GAS ASSUMPTION VALID):

$$dQ + h\ dm_{IN} - h\ dm_{OUT} = dU$$

WHERE $dU = C_V\ (T_{IN} - T_{OUT})$, AS FOR AN IDEAL GAS AND THE MASS FLOWS CAN BE (APPROXIMATELY) DETERMINED FROM THE DISPLACER AND PISTON MOTIONS. THE ENTHALPIES, h, CAN BE DETERMINED (AS FOR IDEAL GAS) SINCE TIME - VARYING INLET AND OUTLET GAS TEMPERATURES WILL BE MEASURED.

TABLE 5-6

(CONT.)

NOMENCLATURE

T = TEMPERATURE

P = PRESSURE

X = STROKE

W = WORK

t = TIME

A = AREA

FREQ = OPERATING FREQUENCY

U, K = HEAT TRANSFER COEFFICIENTS

Q = HEAT

m = MASS

h = ENTHALPY

NOTE: A PERIOD ABOVE A PARAMETER DENOTES A DERIVATIVE WITH RESPECT TO TIME

SUBSCRIPTS

H = HEATER; HOT FLUID; HOUSING

C = COOLER; COLD FLUID; COMPRESSOR

D = DISPLACER

P = PISTON (POWER)

/G = WITH RESPECT TO GROUND (I.E., ABSOLUTE)

W = WALL

GS = GAS SPRING

CH = CHARGE (I.E., AVERAGE)

Table 5-7. PHASE IIIB TEST HISTORY

TEST NO.	OBJECTIVES	RESULTS
PRIOR TO 11/5/82	Check-Out Runs	• Corrected Signal Conditioner Errors • Corrected Algorithm Errors
1 - 6	Test Matrix Points (Incomplete & Used Only as Supplemental)	• Corrected Remaining Signal Conditioning Errors • Corrected Remaining Algorithm Errors • Engine Overstroking Due to Compressor Mis-Match • Ran Low Compressor Suction Pressure Cases
7 - 13	Test Matrix Points	• Data With No Gas Spring Regulator • Established Compressor Stall Limit
14 - 21	Test Matrix Points	• Data w/Gas Spring Regulator @ Various Settings • Optimized Gas Spring Regulator Setting • Established Part of Compressor Map
22 - 30	Test Matrix Points	• Data with Engine at Various Charge Pressures • Achieved Maximum Power Points • Establish Rest of Compressor Map • Established Engine Map
31 - 33	Test Matrix Points & Dynamic T/C Test Attempt	• Repeated Maximum Power Point • Ran Constant Firing Rate Tests • Dynamic T/Cs Installed - Inconclusive Tests

Table 5-8. TEST RESULTS SUMMARY

TEST#	1	2	3	4	5	6	7	8	9	10	11	12
BUILD#	1-65	1-65	1-65	1-65	1-65	1-65	1-65	1-65	1-65	1-65	1-65	1-65
DATE	11/5/82	11/5/82	11/11/82	11/16/82	11/16/82	11/16/82	11/19/82	11/19/82	11/22/82	11/22/82	11/22/82	11/22/82
TIME	14:19	15:21	11:22	10:59	11:57	13:00	9:01	10:26	10:50	11:41	13:17	13:54
PCHARGE, PSIA	885.00	885.00	885.00	885.00	885.00	925.00	885.00	885.00	885.00	885.00	885.00	885.00
Q FIR. RATE,KBTU/H	49.81	60.41	49.67	53.13	64.09	66.66	38.56	47.56	52.22	65.38	65.60	68.22
Q COOLER,KBTU/H	23.92	31.21	24.82	23.69	26.38	32.48	19.69	23.85	23.65	27.92	29.19	27.53
COMBUST ETA(HHV),%	59.90	59.95	56.88	53.40	53.51	56.80	57.09	60.21	61.00	55.86	54.90	57.81
T HOT,DEG F	1045.00	1056.00	1063.00	1221.00	1245.00	1142.00	1063.00	1037.00	1042.00	1237.00	1236.00	1242.00
COMP DISCH P,PSIA	201.00	269.00	176.00	167.00	203.00	255.00	163.00	197.00	237.00	201.00	220.00	207.00
COMP SUCT P,PSIA	95.00	103.00	82.00	77.00	82.00	85.00	81.00	81.00	82.00	95.00	90.00	79.00
PRESS RATIO	2.12	2.61	2.15	2.17	2.48	3.00	2.01	2.43	2.89	2.12	2.44	2.62
R-22 FLOW,LBM/H	231.00	198.00	217.00	368.00	417.00	686.00	254.00	190.00	183.00	419.00	353.00	301.00
GAS SPRG REG,PSIA	108.00	108.00	108.00	-	-	-	-	-	-	-	-	-
FREQ,HZ	26.81	28.41	26.47	25.25	26.29	28.16	25.17	26.01	27.36	26.67	27.00	26.25
X P/G,IN	0.93	1.11	0.94	0.89	1.02	1.05	0.80	0.89	0.94	1.03	1.06	1.00
X P/H,IN	1.12	1.32	1.11	1.05	1.19	1.24	0.94	1.05	1.11	1.22	1.25	1.18
X D/H,IN	1.53	1.63	1.67	1.77	1.85	1.74	1.54	1.62	1.44	1.87	1.88	1.87
DISPL/PIST,DEG	72.00	70.00	66.00	54.00	54.00	58.00	63.00	66.00	72.00	54.00	55.00	56.00
X C/P,IN	1.24	1.27	1.39	1.51	1.52	1.35	1.33	1.36	1.45	1.47	1.51	1.57
COMP/PIST,DEG	-	-	-	-	-	-	-	-	-	-	-	-
HTR DELP,PSI	13.60	16.06	13.54	13.13	15.17	17.05	10.84	13.07	13.42	15.88	16.70	15.41
REG DELP,PSI	16.93	23.26	16.76	14.00	16.82	21.68	12.83	16.12	17.63	17.46	18.40	16.82
CLR DELP,PSI	28.77	34.28	28.42	22.50	27.13	33.87	21.33	27.83	28.65	27.48	29.47	27.83
COMP SP DELP,PSI	318.00	387.00	303.00	262.00	299.00	352.00	244.00	288.00	322.00	313.00	329.00	308.00
SECOND GS DELP,PSI	155.00	239.00	160.00	147.00	188.00	214.00	117.00	145.00	172.00	187.00	197.00	177.00
COMP SP POWER,KW	-	-	-	1.36	1.65	1.57	0.92	1.05	1.04	1.62	1.67	1.61
DISPL GS POWER,KW	-	-	-	0.66	0.82	0.94	0.54	0.67	0.72	0.83	0.87	0.80
INDICATED POWER,KW	-	-	-	2.01	2.47	2.51	1.46	1.72	1.77	2.45	2.53	2.41
INDICATED EFFIC,%	-	-	-	24.20	24.61	22.58	22.63	20.48	18.93	22.87	23.99	20.88
COMP CYL POWER,KW	0.88	0.79	1.12	1.39	1.62	1.45	0.99	1.00	1.10	1.67	1.67	1.58
COMP GS POWER,KW	0.17	0.19	0.28	0.22	0.25	0.27	0.16	0.18	0.23	0.25	0.28	0.28
COMP TOTAL PWR,KW	1.05	0.98	1.40	1.61	1.87	1.72	1.15	1.18	1.32	1.92	1.95	1.85
SECOND GS POWER,KW	-	-	0.20	0.18	0.21	0.23	0.15	0.26	0.13	0.25	0.22	0.26
OTHER DISSIP,KW	-	-	-	0.22	0.39	0.56	0.16	0.28	0.32	0.28	0.36	0.30
BEALE NUMBER	-	-	-	.0151297	.0157560	.0137248	.0123148	.0125685	.0116311	.0150269	.0149600	.0155271
2GS VOL MODUL,(-)	-	-	.0794815	.0751852	.0852099	.0887901	.0673086	.0751852	.0794815	.0873580	.0895062	.0844938
2GS DISSIP,KJ/HZ	-	-	.0075557	.0071287	.0079878	.0081676	.0059595	.0099962	.0047515	.0093738	.0081481	.0099048

Table 5-8. Continued

TEST#	13	14	15	16	17	18	19	20	21	22	23	24
BUILD#	1-65	1-65	1-65	1-65	1-65	1-65	1-65	1-65	1-65	1-65	1-65	1-65
DATE	11/22/82	11/30/82	11/30/82	12/02/82	12/10/82	12/10/82	12/10/82	12/10/82	12/10/82	12/13/82	12/13/82	12/14/82
TIME	14:34	10:27	11:09	13:35	8:54	9:51	10:39	11:39	12:36	11:20	11:58	9:56
PCHARGE, PSIA	885.00	890.00	885.00	885.00	885.00	890.00	890.00	885.00	885.00	985.00	1085.00	1185.00
Q FIR. RATE,KBTU/H	61.64	66.47	73.93	54.42	42.39	51.05	55.21	59.20	66.96	58.99	59.97	39.38
Q COOLER,KBTU/H	26.64	27.65	32.66	23.29	21.13	25.44	29.31	25.28	30.08	25.16	26.07	19.12
COMBUST ETA(HHV),%	56.73	54.97	57.54	53.27	55.03	60.29	58.94	54.43	56.25	54.09	55.07	59.54
T HOT,DEG F	1225.00	1232.00	1210.00	1243.00	1049.00	1040.00	1056.00	1260.00	1218.00	1251.00	1247.00	996.00
COMP DISCH P,PSIA	211.00	197.00	233.00	163.00	159.00	195.00	229.00	160.00	200.00	163.00	162.00	160.00
COMP SUCT P,PSIA	65.00	80.00	59.00	77.00	80.00	82.00	82.00	80.00	80.00	80.00	81.00	82.00
PRESS RATIO	3.25	2.46	3.95	2.12	1.99	2.38	2.79	2.00	2.50	2.04	2.00	1.95
R-22 FLOW,LBM/H	200.00	330.00	179.00	327.00	243.00	186.00	140.00	-	279.00	318.00	318.00	178.00
GAS SPRG REG,PSIA	-	80.00	80.00	80.00	95.00	95.00	95.00	95.00	95.00	95.00	95.00	95.00
FREQ,HZ	26.04	26.56	27.00	25.46	25.75	26.50	27.54	26.00	27.00	26.56	26.85	26.81
X P/G,IN	0.99	0.99	1.08	0.94	0.88	0.98	1.03	0.98	1.07	0.91	0.84	0.62
X P/H,IN	1.15	1.18	1.28	1.10	1.04	1.13	1.23	1.15	1.25	1.07	0.98	0.73
X D/H,IN	1.81	1.79	1.90	1.79	1.62	1.67	1.74	1.85	1.90	1.72	1.62	1.18
DISPL/PIST,DEG	59.00	59.00	61.00	53.00	61.00	66.00	66.00	54.00	58.00	53.00	60.00	77.00
X C/P,IN	1.63	1.56	1.68	1.54	1.31	1.32	1.36	1.50	1.47	1.49	1.43	1.10
COMP/PIST,DEG	-	28.00	20.00	32.00	26.00	19.00	16.00	29.00	24.00	27.00	33.00	25.00
HTR DELP,PSI	14.59	15.12	17.35	13.36	12.48	14.06	16.00	14.65	16.76	14.24	15.53	10.66
REG DELP,PSI	16.12	17.05	18.40	14.41	15.12	17.63	20.04	15.59	19.28	16.46	17.75	14.59
CLR DELP,PSI	26.84	28.24	33.11	21.74	23.56	29.53	33.22	24.79	31.23	24.20	27.25	22.33
COMP SP DELP,PSI	307.00	319.00	355.00	274.00	277.00	323.00	363.00	297.00	352.00	288.00	309.00	282.00
SECOND GS DELP,PSI	160.00	182.00	207.00	166.00	142.00	167.00	193.00	173.00	187.00	173.00	152.00	92.00
COMP SP POWER,KW	1.51	1.65	1.83	1.44	1.05	1.15	1.25	1.56	1.67	1.50	1.49	0.72
DISPL GS POWER,KW	0.77	0.83	0.98	0.67	0.61	0.76	0.86	0.75	0.89	0.72	0.74	0.47
INDICATED POWER,KW	2.28	2.49	2.81	2.11	1.65	1.92	2.11	2.31	2.56	2.22	2.23	1.19
INDICATED EFFIC,%	22.20	23.22	22.53	24.84	24.16	21.24	22.09	24.45	23.18	23.79	23.05	17.31
COMP CYL POWER,KW	1.35	1.69	1.43	1.44	1.01	0.98	0.97	1.45	1.48	1.49	1.36	0.72
COMP GS POWER,KW	0.33	0.30	0.40	0.27	0.20	0.21	0.21	0.18	0.28	0.28	0.25	0.16
COMP TOTAL PWR,KW	1.68	1.99	1.83	1.71	1.21	1.19	1.18	1.63	1.76	1.78	1.61	0.88
SECOND GS POWER,KW	0.35	0.13	0.13	0.14	0.14	0.32	0.29	0.20	0.35	0.17	0.40	0.12
OTHER DISSIP,KW	0.25	0.37	0.85	0.26	0.30	0.41	0.64	0.48	0.45	0.27	0.22	0.19
BEALE NUMBER	.0151943	.0157662	.0162263	.0150355	.0122959	.0127238	.0123610	.0154180	.0151374	.0140066	.0137954	.0090623
2GS VOL MODUL,(-)	.0823457	.0844938	.0916543	.0787654	.0744691	.0809136	.0880741	.0823457	.0895062	.0766173	.0701728	.0522716
2GS DISSIP,KJ/HZ	.0134409	.0048946	.0048148	.0054988	.0054369	.0120755	.0105301	.0076923	.0129630	.0064006	.0148976	.0044759

Table 5-8. Continued

TEST#	25	26	27	28	29	30	31	32	33
BUILD#	1-65	1-65	1-65	1-65	1-65	1-65	1-65	1-65	1-65
DATE	12/14/82	12/14/82	12/14/82	12/14/82	12/14/82	12/14/82	1/6/83	1/6/83	1/6/83
TIME	10:37	11:16	11:59	12:41	13:41	14:24	9:56	10:37	11:38
PCHARGE, PSIA	1185.00	1185.00	1185.00	1185.00	1185.00	1185.00	880.00	885.00	1185.00
Q FIR. RATE,KBTU/H	52.35	61.15	68.98	79.05	74.98	76.12	61.20	61.20	81.60
Q COOLER,KBTU/H	24.84	25.54	29.46	33.06	34.16	35.28	-	-	-
COMBUST ETA(HHV),%	61.82	55.06	56.00	59.44	55.31	56.56	-	-	-
T HOT,DEG F	1042.00	1257.00	1251.00	1239.00	1254.00	1213.00	1258.00	1180.00	1202.00
COMP DISCH P,PSIA	205.00	164.00	198.00	240.00	232.00	281.00	164.00	198.00	281.00
COMP SUCT P,PSIA	82.00	80.00	80.00	79.00	64.00	95.00	78.00	80.00	88.00
PRESS RATIO	2.50	2.05	2.48	3.04	3.63	2.96	2.10	2.48	3.19
R-22 FLOW,LBM/H	171.00	292.00	267.00	226.00	141.00	239.00	-	-	-
GAS SPRG REG,PSIA	95.00	95.00	95.00	95.00	95.00	95.00	95.00	95.00	95.00
FREQ,HZ	28.47	27.73	28.26	29.45	29.09	30.21	25.90	26.80	30.20
X P/G,IN	0.75	0.75	0.85	0.90	0.88	0.98	1.00	1.03	0.96
X P/H,IN	0.90	0.89	0.99	1.07	1.06	1.16	1.18	1.20	1.13
X D/H,IN	1.35	1.50	1.59	1.62	1.65	1.66	1.87	1.77	1.60
DISPL/PIST,DEG	75.00	60.00	63.00	63.00	64.00	64.00	52.00	60.00	64.00
X C/P,IN	1.30	1.43	1.49	1.52	1.54	1.42	1.51	1.48	1.44
COMP/PIST,DEG	21.00	37.00	29.00	23.00	23.00	18.00	28.00	22.00	17.00
HTR DELP,PSI	15.06	15.12	18.16	20.10	20.45	21.27	14.24	14.88	19.87
REG DELP,PSI	19.57	17.05	20.86	23.20	22.79	26.42	15.88	17.58	25.84
CLR DELP,PSI	32.75	26.89	34.16	38.62	39.32	42.95	23.50	28.30	41.89
COMP SP DELP,PSI	349.00	313.00	355.00	399.00	408.00	452.00	306.00	342.00	446.00
SECOND GS DELP,PSI	146.00	146.00	173.00	204.00	196.00	229.00	180.00	190.00	224.00
COMP SP POWER,KW	1.05	1.51	1.81	1.83	1.90	1.96	1.65	1.59	1.89
DISPL GS POWER,KW	0.72	0.72	0.91	0.96	0.95	1.07	0.74	0.84	1.10
INDICATED POWER,KW	1.77	2.23	2.72	2.78	2.85	3.03	2.39	2.43	2.99
INDICATED EFFIC,%	18.68	22.64	24.03	20.22	23.49	23.99	-	-	-
COMP CYL POWER,KW	0.95	1.41	1.54	1.49	1.36	1.43	1.50	1.41	1.46
COMP GS POWER,KW	0.22	0.27	0.30	0.35	0.36	0.32	0.27	0.28	0.34
COMP TOTAL PWR,KW	1.17	1.69	1.84	1.85	1.72	1.75	1.77	1.69	1.81
SECOND GS POWER,KW	0.19	0.18	0.50	0.23	0.23	0.28	0.28	0.29	0.42
OTHER DISSIP,KW	0.41	0.36	0.38	0.70	0.90	1.00	0.34	0.45	0.76
BEALE NUMBER	.0102957	.0134672	.0144901	.0131488	.0137755	.0128868	.0156950	.0150791	.0130586
2GS VOL MODUL,(-)	.0644444	.0637284	.0708889	.0766173	.0759012	.0830617	.0844938	.0859259	.0809136
2GS DISSIP,KJ/HZ	.0066737	.0064912	.0176929	.0078098	.0079065	.0092685	.0108108	.0108209	.0139073

Table 5-9. NOMENCLATURE FOR TABLE 5-8

TEST#	# in present test series
BUILD#	Defines HAHP parameters (geometry)
DATE	Of test
TIME	Of test
PCHARGE, PSIA	FPSE working fluid (He) average pressure, @ TH
Q FIR. RATE,KBTU/H	Combustor firing rate (HHV)
Q COOLER,KBTU/H	Heat rejected by FPSE cooler
COMBUST ETA(HHV),%	Combustor efficiency (HHV)
T HOT,DEG F	FPSE hot side metal (i.e., heater head tube) temperature
COMP DISCH P,PSIA	R-22 pressure at compressor discharge
COMP SUCT P,PSIA	R-22 pressure at compressor inlet
PRESS RATIO	Compressor discharge/suction
R-22 FLOW,LBM/H	Refrigerant mass flowrate
GAS SPRG REG,PSIA	Setting of compressor gas spring regulator
FREQ,HZ	Operating frequency
X P/G,IN	Absolute power piston stroke (i.e., relative to ground)
X P/H,IN	Relative power piston stroke (i.e. relative to FPSE housing)
X D/H,IN	Displacer stroke relative to FPSE housing
DISPL/PIST,DEG	Displacer/power piston phase angle
X C/P,IN	Compressor piston stroke relative to FPSE power piston
COMP/PIST,DEG	Compressor piston/power piston phase angle
HTR DELP,PSI	Δ P across FPSE heater head tube
REG DELP,PSI	Δ P across FPSE regenerators
CLR DELP,PSI	Δ P across FPSE cooler tubes
COMP SP DELP,PSI	FPSE compression space Δ P
SECOND GS DELP,PSI	FPSE second gas spring Δ P
COMP SP POWER,KW	Power developed in FPSE compression space
DISPL GS POWER,KW	Power developed by FPSE displacer gas spring
INDICATED POWER,KW	Power available at FPSE power piston
INDICATED EFFIC,%	Indicated Power/Q into Engine Heater Head
COMP CYL POWER,KW	Sum of power developed in both compressor cylinders
COMP GS POWER,KW	Sum of power dissipated by both compressor gas springs
COMP TOTAL PWR,KW	Sum of COMP CYL POWER & COMP GS POWER
SECOND GS POWER,KW	Power dissipated by second gas spring
OTHER DISSIP,KW	Indicated Power - Second GS Power - Comp Total Power
BEALE NUMBER	(Indicated Power,W)/(PCharge,Bar)(Freq, HZ) ($X_{P/H}$*Bore^2,cm^3)
2GS VOL MODUL,(-)	Second GS Volume Modulation = ($X_{P/H}$)(GS Area)(2*GS Volume)
2GS DISSIP,KJ/HZ	Work done (dissipated) by second gas spring per cycle

operating frequencies and power levels of the test series. Finally, tests 31-33 were run to verify the maximum power point (3 Kw) and to operating the engine at a fixed firing rate while varying the compressor load. These last tests incorporated the fast response thermocouples which had been returned to the vendor because they did not meet the size specifications. The reworked thermocouples unfortunately did not yield useable data and there was insufficient test time available to conduct further checkout of the thermocouples or their installation.

Significant results of the tests are highlighted below. Subsequent sections discuss these results in greater detail.

1) Engine performance was repeatable and closely followed basic Stirling engine trends. Power increased with stroke, heater head temperature, and charge pressure.
2) Peak engine power was 3KW.
3) Engine heat exchanger flow losses were considerably larger than predictive models indicate.
4) Compressor power was significantly less than predicted for a given set of conditions.
5) Trends of engine/compressor matching were as expected and could be predicted with basic dynamic models.

5.3 COMPRESSOR VERIFICATION

5.3.1 COMPRESSOR TEST DATA

Compressor testing on the integrated test stand was performed over a range of suction and discharge pressures representing HAHP operating conditions. The compressor natural frequency was also varied by means of the compressor gas spring pressure regulator. Two operating characteristics somewhat restricted the possible test range:

1) At high compressor pressure ratios and low engine power levels, the compressor piston tended to stall.
2) Simultaneous high compressor pressure ratio and high (108 psia) compressor gas spring regulator conditions caused the engine to stroke to its physical limits at low engine heater head temperatures.

Compressor test data is summarized in Table 5-8. Raw test data is contained in Appendix B. Figures 5-4 and 5-5 show plots of this data in terms of compressor power versus power piston (compressor housing) absolute stroke. Compressor power is taken to be the PdV diagram of all four compressor gas volumes (two working spaces, two gas springs). Trend lines are drawn through points with approximately the same discharge pressure, suction and excitation frequency. These lines give the power versus stroke characteristics for given operating conditions. Figure 5-6 shows the same data for specific compressor suction/discharge conditions.

5.3.2 COMPARISON OF TEST RESULTS TO PREDICTIONS & COMPRESSOR COMPONENT TESTS

A second order compressor code was developed in Phase II of this project (Reference 1). It correlated quite well against compressor component test data, as shown in Figure 5-7. However, it was observed in the Phase II engine/compressor integrated tests that this code overpredicted compressor performance on the integrated test stand. Several possible explanations for this were examined. The effects of excessive suction superheat, and of non-sinusoidal motion during integrated tests (compared to component tests) were examined and found to be small (see Reference 1). Other explantions were also considered, but the lack of a compressor piston LVDT to trace piston motion restricted interpretation of integrated test data. This deficiency led to the modification of the compressor and housing for installation of a compressor LVDT in Build #1-65.

The compressor code (which represents compressor component performance) was run for the present Phase IIIB compressor test conditions, and a performance map was generated as shown in Figure 5-8. A comparison of the test data of Figures 5-4 and 5-5 versus the prediction of Figure 5-8 discloses significant differences. In general, the code predicts about twice the R-22 flow and compressor power observed. The compressor piston stroke is overpredicted by about 30%.

The short compressor piston strokes measured suggested that friction within the compressor could be higher than anticipated. The code was run again, with much higher (viscous) friction forces assumed. As shown on Figure 5-9 for Test No. 17, if the assumed friction level is increased to approximately 10 times the estimated value, the predicted and tested compressor results match closely.

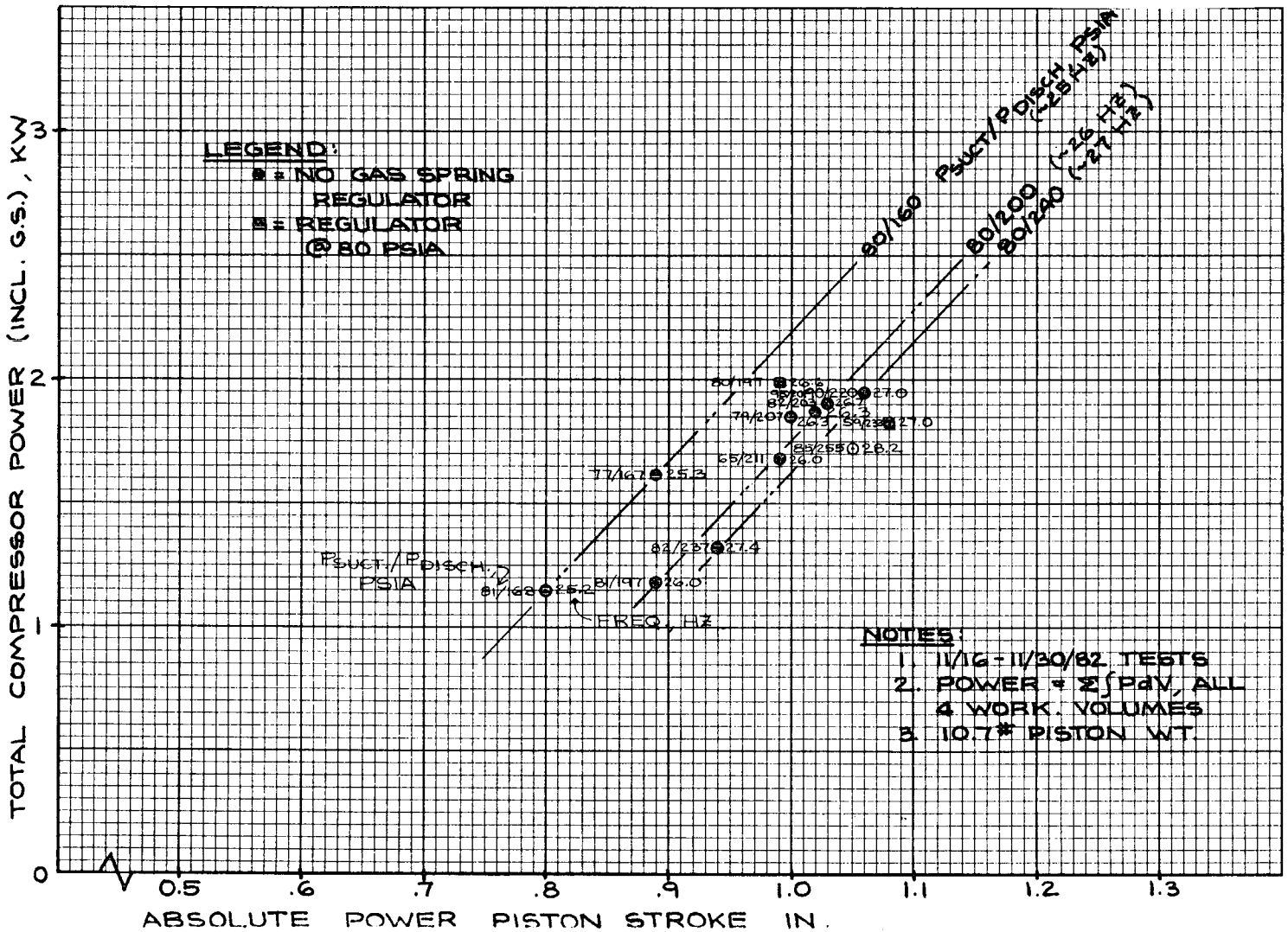

Figure 5-4. COMPRESSOR TEST DATA - NO REGULATOR AND 80 PSIA REGULATOR

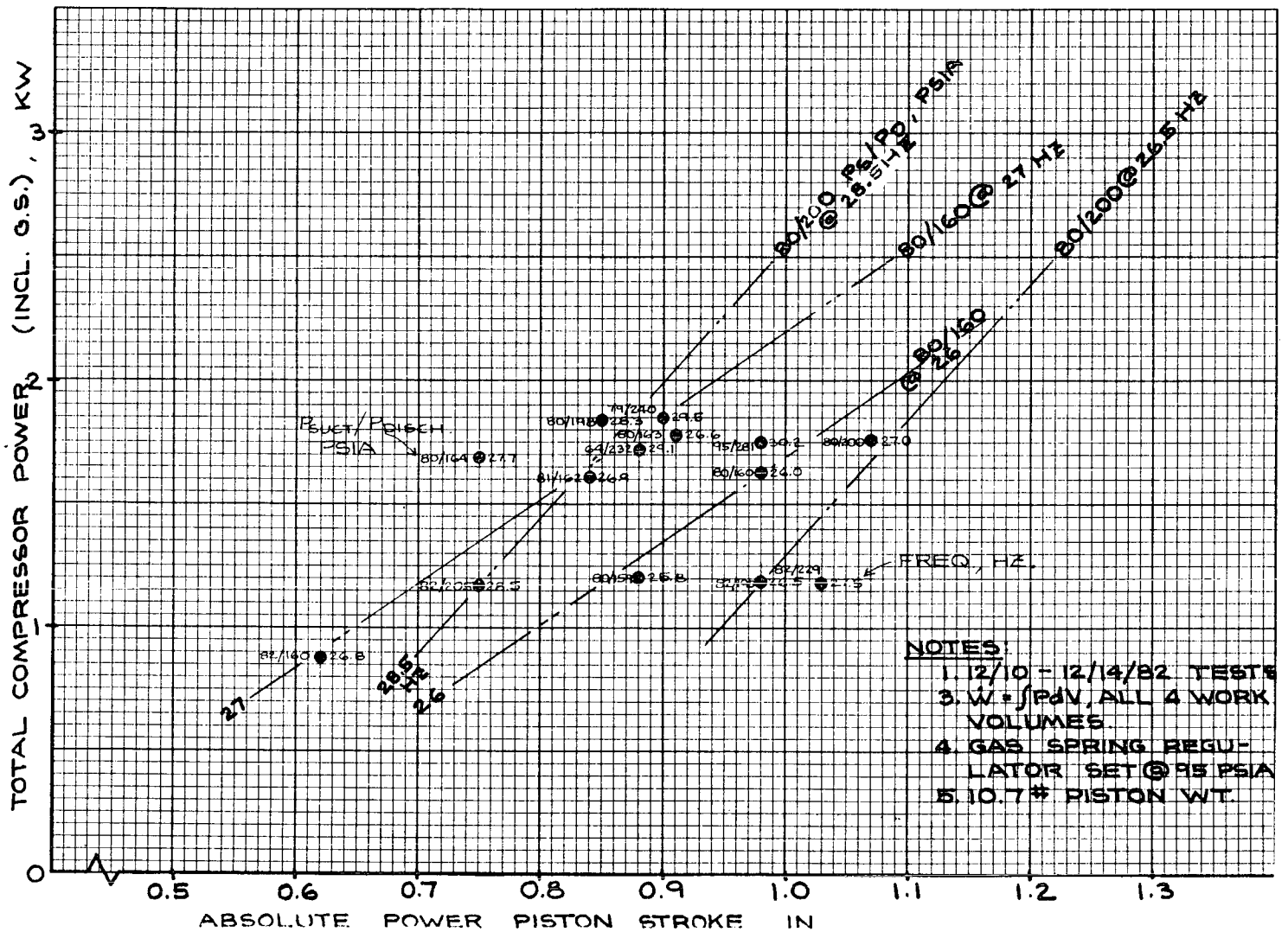

Figure 5-5. COMPRESSOR TEST DATA - REGULATOR AT 95 PSIA

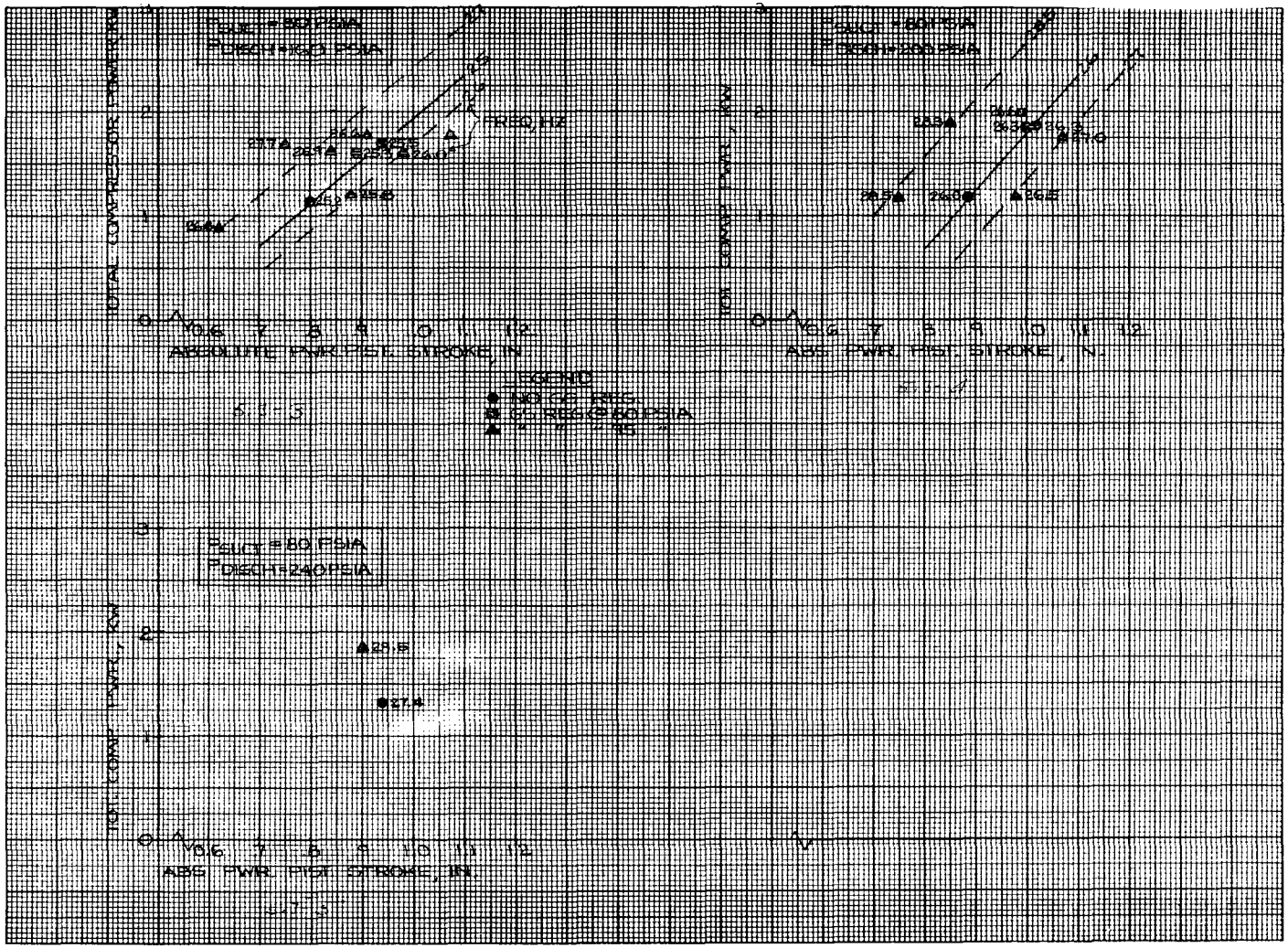

Figure 5-6. COMPRESSOR TEST DATA FOR VARIOUS SUCTION/DISCHARGE CONDITION

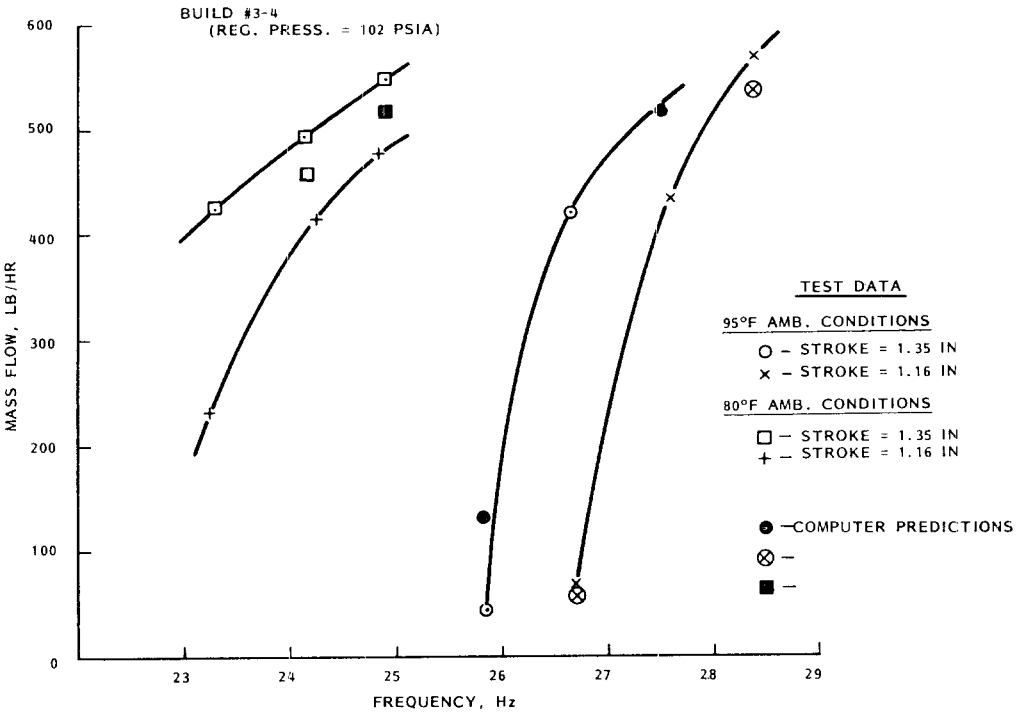

Compressor Model/Test Data Correlation for Flow Rate

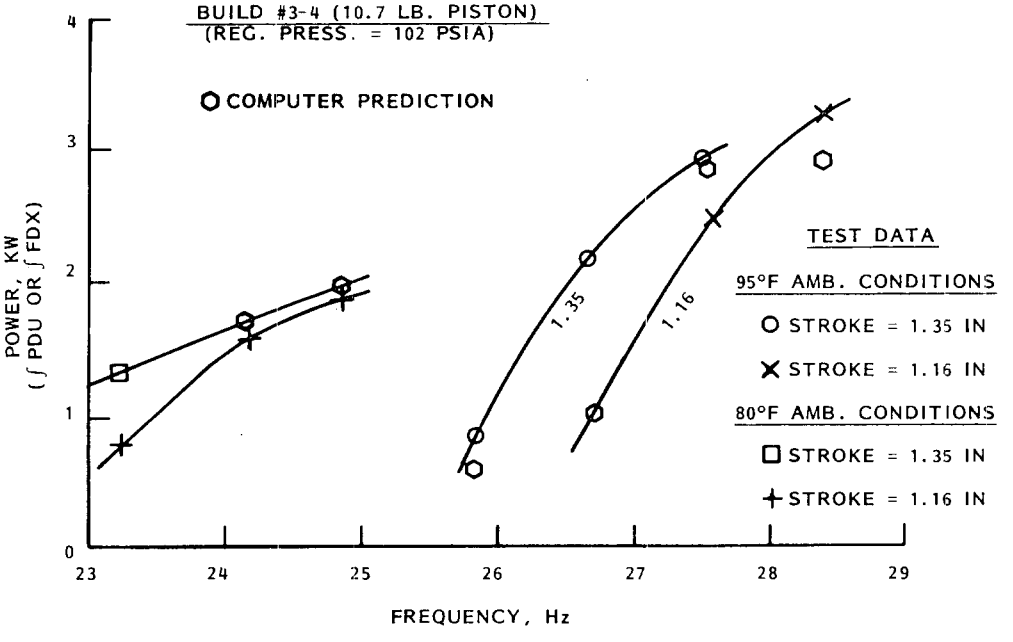

Compressor Model/Test Data Correlation for Power

Figure 5-7. COMPRESSOR CODE/COMPONENT TEST CORRELATION

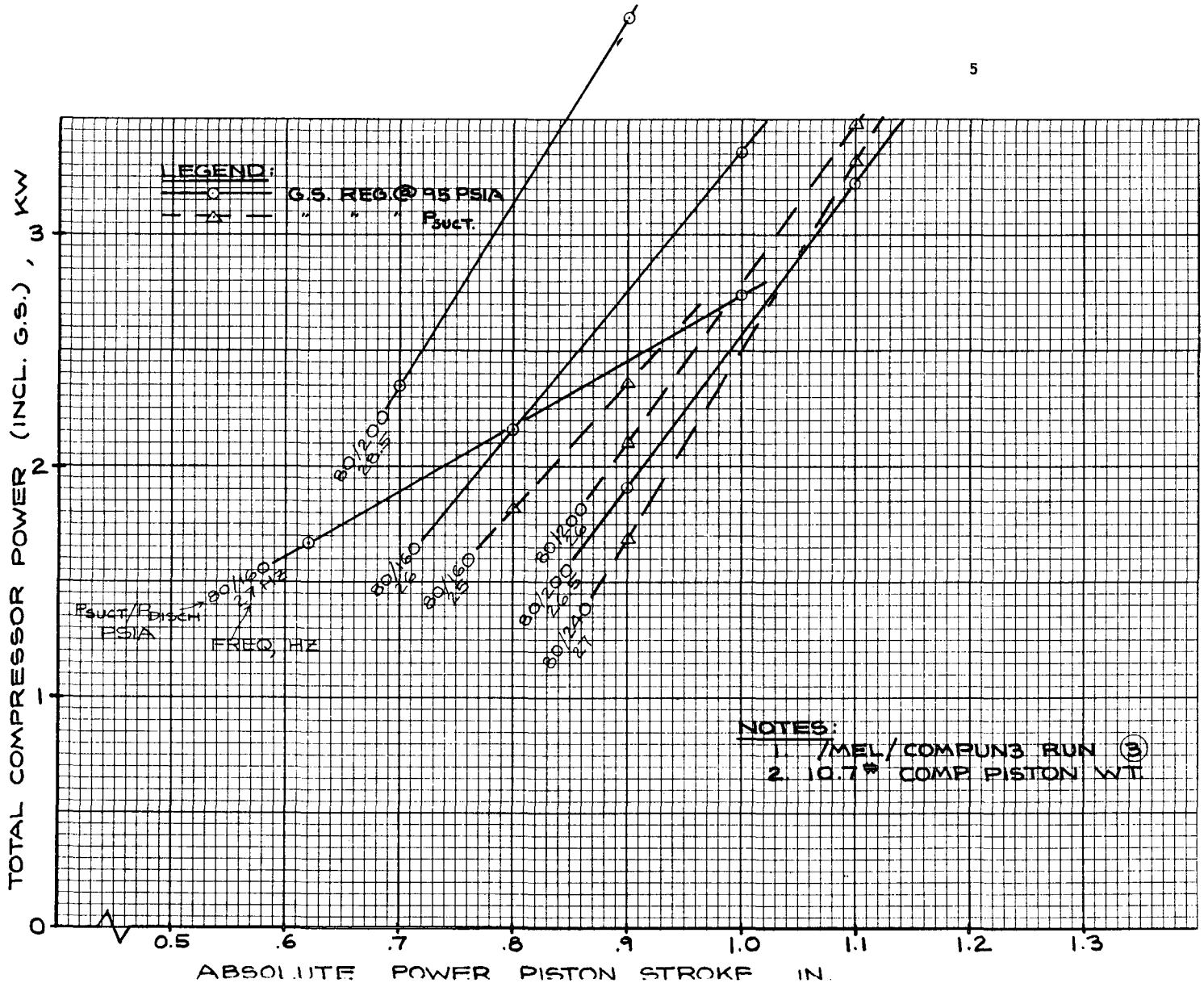

Figure 5-8. PREDICTED COMPRESSOR PERFORMANCE

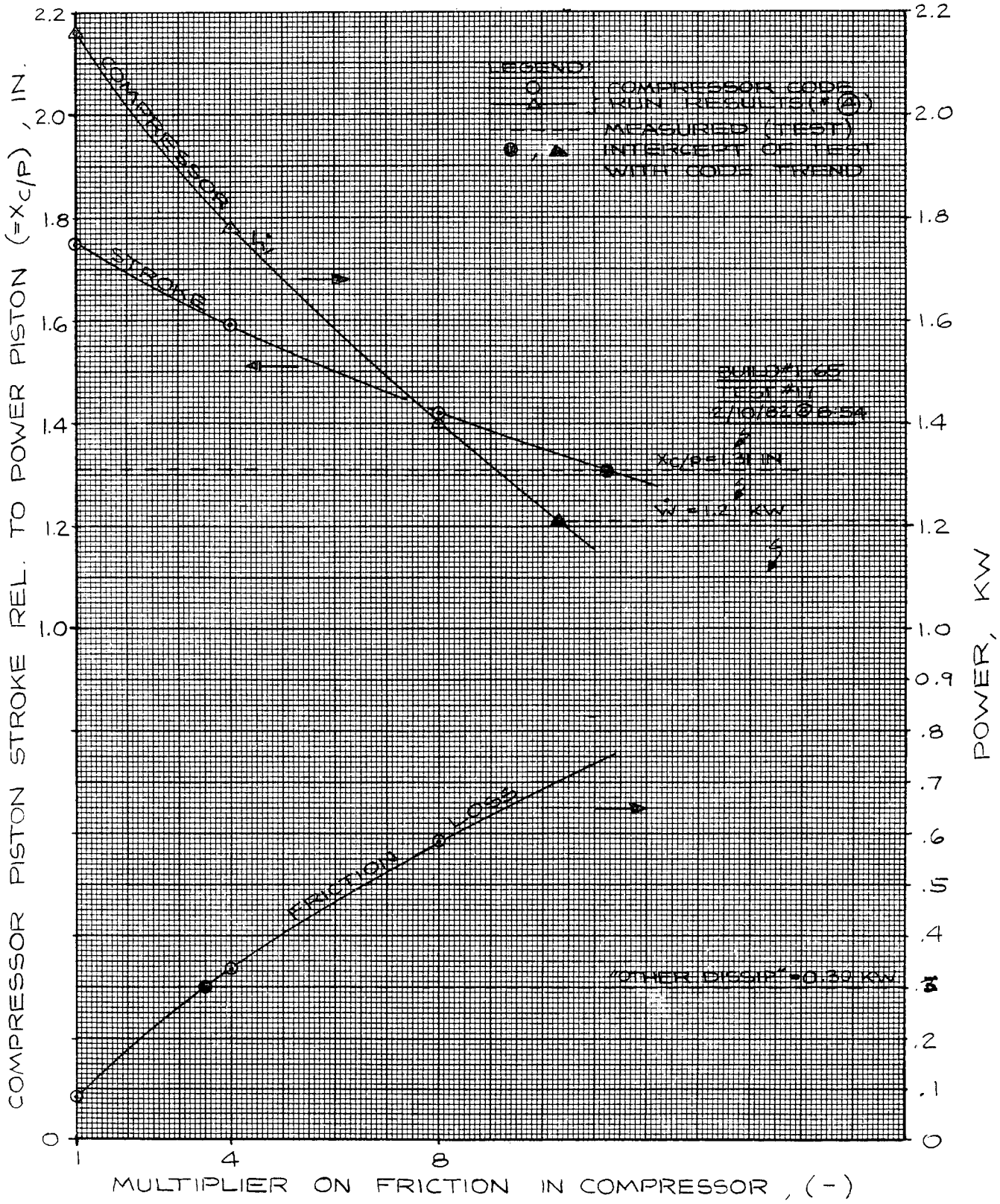

Figure 5-9. INFLUENCE OF FRICTION ON PREDICTED COMPRESSOR OPERATING CONDITIONS

However, the friction power dissipated at this level is approximately 0.75 kw, much higher than the "Other Dissipation" value of 0.3 KW given in Table 5-8. (See Section 5.4.3) Another test (#27) was similarly modelled, with the same large frictional power. Therefore, friction (or purely viscous dissipation) was ruled out as the sole contributor to the discrepancy between predicted and measured compressor power. Another possibility considered was the effect of the compressor piston operating somewhat off-center, the more so at high pressure ratios. It was difficult to measure the precise shift in compressor piston centering by means of the LVDT; the LVDT installation and tolerance stack-up prevented a precise determination of electrical versus geometrical zero. The pressure transducers were also somewhat inadequate to this task. Differential pressure readings are precise, but the absolute value of pressure is less certain, as the temperature-compensation circuitry at the transducers does not fully compensate for operating temperatures. Therefore, to examine this possibility, the power measurements from the upper and lower cylinders were used for this task. Figure 5-10 illustrates the imbalance in power measured, versus total power and versus pressure ratio. Although some imbalance is evident, it is not enough to invalidate code predictions (the code is correlated against a compressor operating in a centered mode but code cases run with the piston off center show low sensitivity to this mode of operation).

5.3.3 INTERPRETATION AND EVALUATION

The Phase IIIB integrated engine/compressor tests confirmed the comparable Phase II tests: The compressor output R-22 mass flow and power absorbed from the engine are below that observed in compressor component tests. Installation of the LVDT for the Phase IIIB tests confirmed that the compressor piston stroke was less in the engine/compressor integrated tests than that measured in the compressor component tests, thereby accounting for the reduced flow and power absorbed. Off center compressor piston operation and simple high friction causes were ruled out as single acting causes of the reduced piston motion.

The principal factors that could affect the reduced motion of the compressor piston are listed in Table 5-10. Aside from the possible acoustic effects of the coil spring R-22 tubes on mass flow, the most likely factor that may

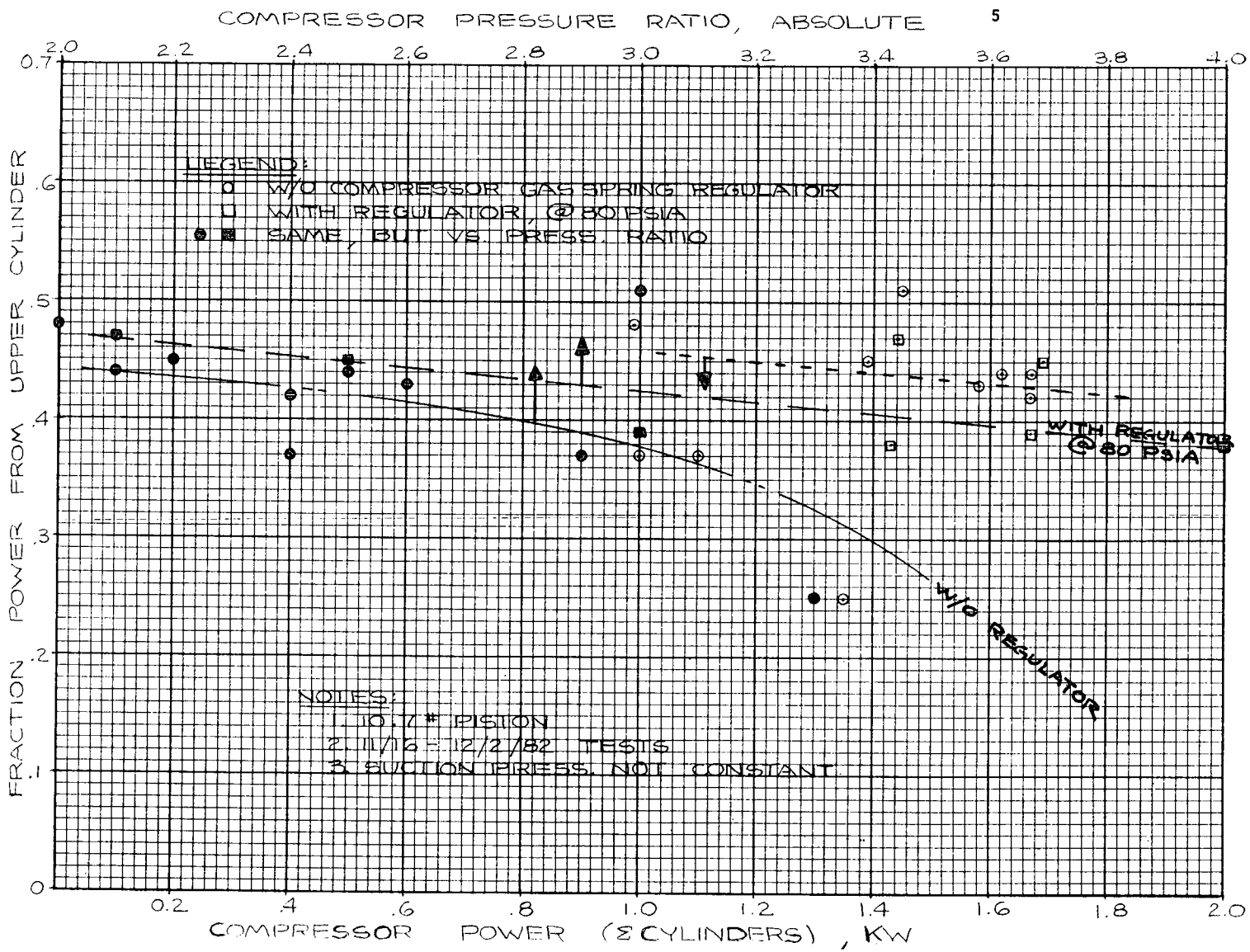

FIGURE 5-10. CYLINDER POWER BALANCE IN COMPRESSOR

Table 5-10. PRINCIPAL DIFFERENCES BETWEEN COMPRESSOR COMPONENT TESTS AND ENGINE COMPRESOR INTEGRATED TESTS

FACTOR OR FEATURE	COMPONENT TEST	ENGINE/COMP. INTEGRATED TEST
ENVIRONMENT	AMBIENT PRESSURE & TEMPERATURE	SUBJECT TO CHARGE PRESSURE & BOUNCE SPACE TEMPERATURE CONDITIONS
STEEL SPRING COIL TUBES	NONE	3 ON SUCTION, 1 ON DISCHARGE POTENTIAL TUNING EFFECT ON R-22 MASS FLOW
3-RING, 10.7 LB PISTON	YES	YES
GAS SPRING REGULATOR	YES	YES
OIL LUBRICATION	YES	YES, BUT MAY BE DIFFERENT
LVDT ROD	YES	YES, BUT MAY HAVE MORE FRICTION

affect compressor piston motion would be the high pressure on the compressor housing in the integrated tests. The component tests in ambient air resulted in a net pressure differential between the R-22 inside of the compressor and the medium surrounding the compressor of between 50 psi (suction to ambient) and 250 (discharge to ambient). When in the integrated test stand, the pressure differential is reversed to about 800-900 psi (helium to freon). Thus, it is possible that distortion of the compressor housing would cause leakage of freon past seals and/or excessive mechanical friction on sliding parts, thereby reducing delivered flow and (hence) measured power absorbed by the compressor. However, the "loss" would not be great enough to explain the complete difference between compressor/component test data and engine/compressor integrated test data. This leaves open the possibility that additional factors may be causing (or contributing) to the deficiencies. This could include value distortion, thermal choking in the R-22 flow passages, thermal effects on regulator operation and others.

Additional diagnostic testing on the compressor would be required to determine the performance (low stroke) deficiency. The existing compressor would have additional thermocouples added to several housing locations and a few selected pressure transducers would also be added. These would be used to pinpoint high loss areas or operating anomolies in the compressor when operated with the engine in the integrated test configuration. Some selected hardware changes to the compressor would also be made for diagnostic purposes. Other pressure regulators (developed in Phase II) would also be tested and different piston ring configurations (also developed in Phase II) would be tested to alter the configuration and provide additional diagnostic data. Tests might also be run on the compressor component test stand to determine the effects of the external environment.

5.4 FPSE PERFORMANCE TESTS

5.4.1 ENGINE TEST DATA

For a given build (geometry), FPSE hot and cold side temperatures, charge pressure, and compressor conditions fully determine FPSE operation and dynamics. These parameters were varied in order to characterize FPSE performance over the entire regime of potential operating conditions. The resulting test data was presented in Table 5-8 in summary format. The detailed test data is given in Appendix B.

Figure 5-11 shows the resulting FPSE map. The engine side parameters determine the specific curve along which the FPSE can operate. Compressor conditions set the exact operating dynamics (frequency and stroke). Stable operation occurs at the intercept of the FPSE and compressor operating curves.

5.4.2 COMPARISON TO PHASE II DATA

A comparison of build #1-65 engine performance with earlier Phase II builds is shown in Figure 5-12. This figure shows the Phase II and the present Phase IIIB test high power points. Differences in performance between the Phase II "Baseline Engine" and the "Modified Engine" are primarily due to differences in heat exchanger designs. This is explained in detail in Reference 1.

For the Phase IIIB tests, the heat exchanger designs are identidal to the "Baseline Engine". The Phase IIIB tests were conducted on Build #1-65, which was configured to be nearly identical to Build #1-52 of Phase II. Build #1-65 is also very similar to Builds #1-50, 1-51, 1-53 and 1-54. The differences in performance between Build #1-65 and Builds #1-50 through 1-54 are due to:

1) Build #1-65 test data was acquired and processed by a digital DAS. Earlier Phase II test data acquisition was partly manual and data reduction was also manual.
2) Engine power computations for Build 1-65 are direct, obtained by numerical integration of digitized Fdx diagrams for the engine working space and displacer gas spring. For Builds 1-50 through 1-54, engine power was taken as the sum of the power absorbed by the compressor and the engine second gas spring.
3) Power dissipated by the engine second gas spring was measured 40 to 50 percent lower on Build 1-65 than on previous builds. This was not due to hardware changes but rather careful matching of pressure and position signal shifts to improve calculation accuracy (see Section 4.3.2).
4) Engine efficiency calculations in Phase II utilized an estimated heat loss from the combustor outer surface in calculating engine efficiency. Tests on Build 1-65 accurately measured this heat loss, leading to a more accurate engine efficiency estimate.

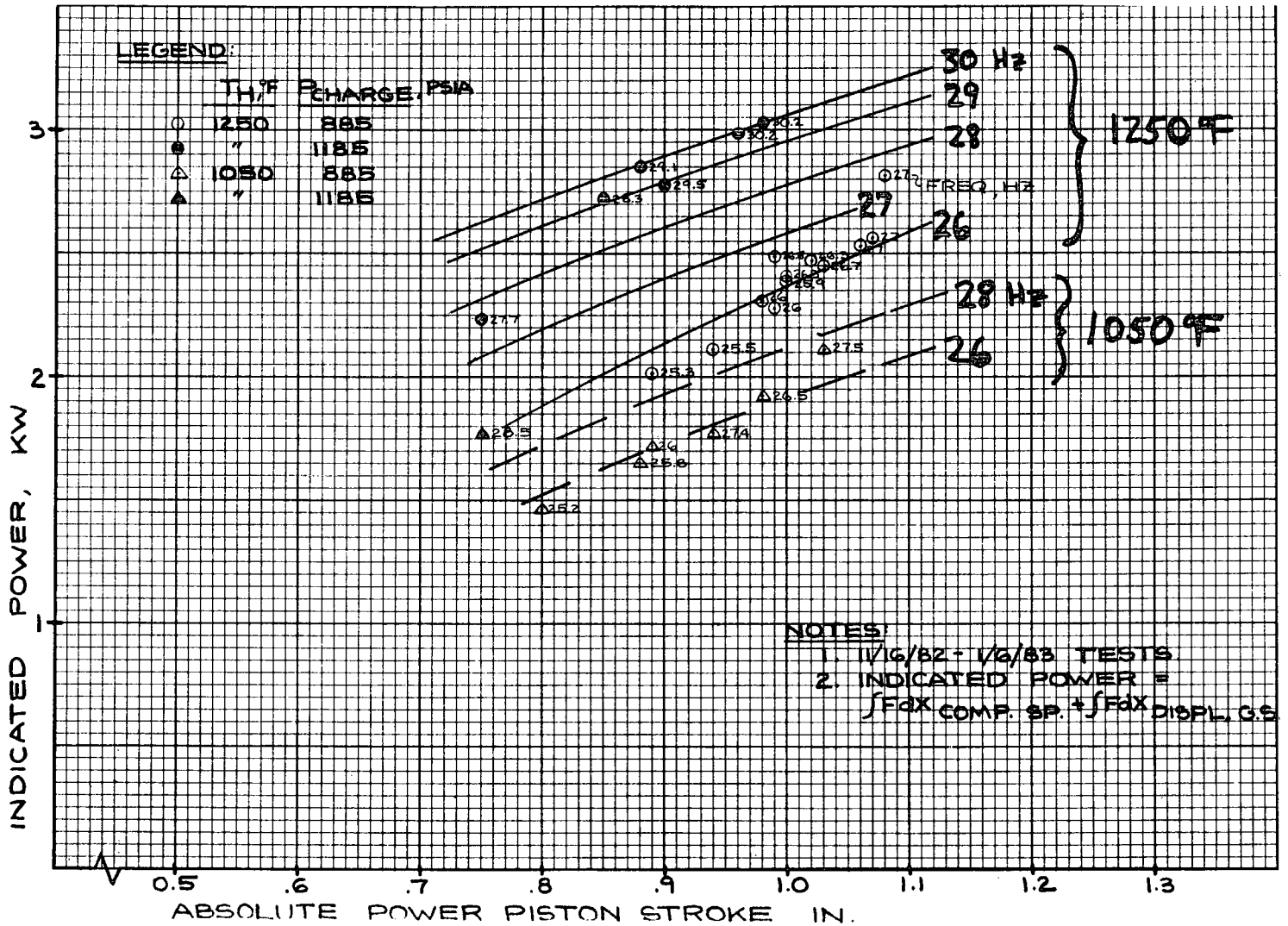

Figure 5-11. FPSE PERFORMANCE MAP

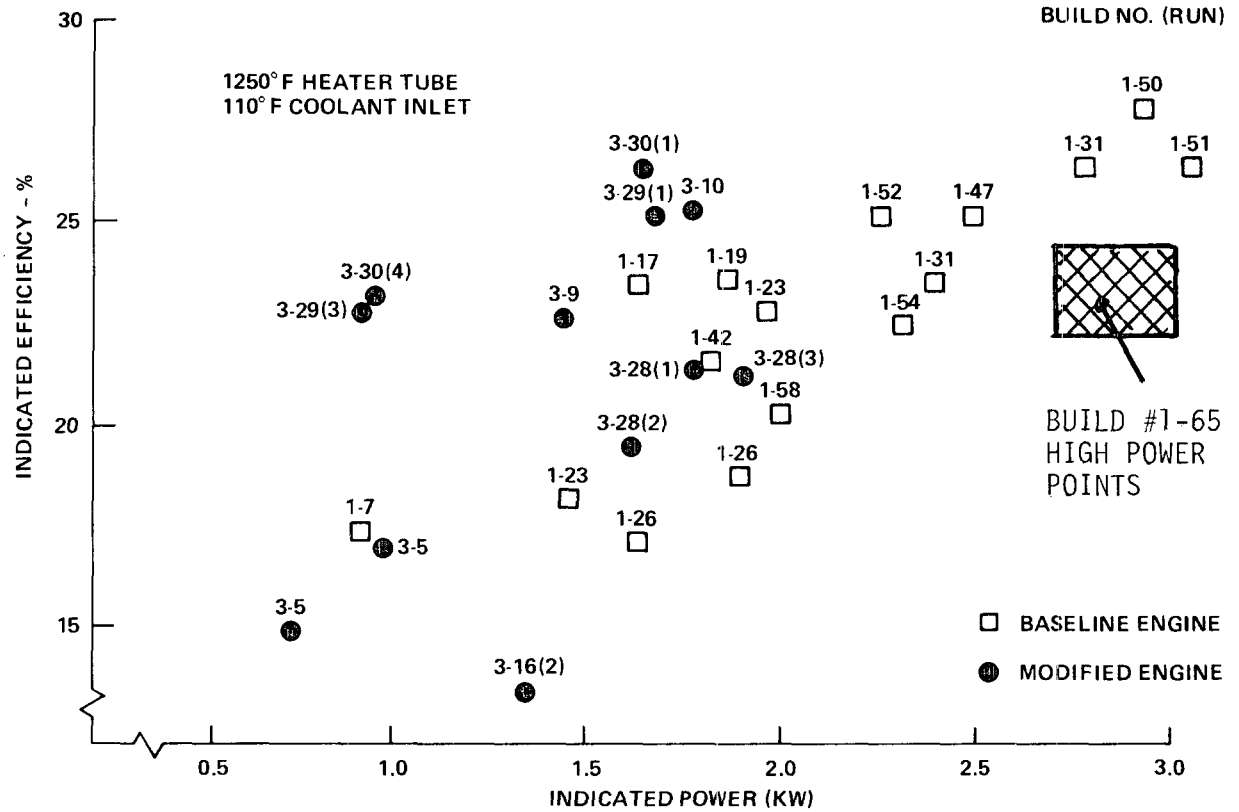

Figure 5-12. POWER/EFFICIENCY RELATION FOR PROTO 2 ENGINE

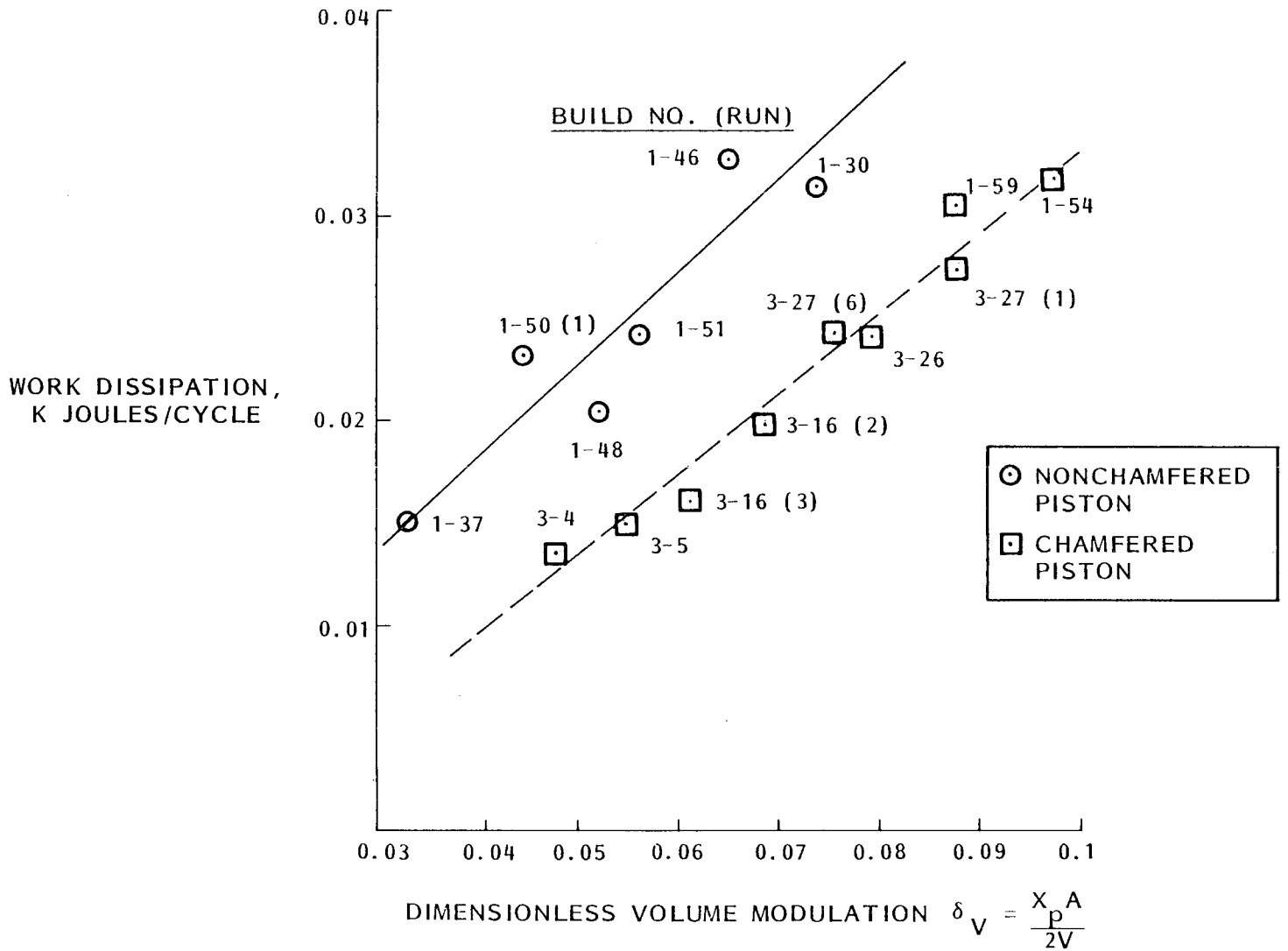

Figure 5-14. SECOND GAS SPRING WORK DISSIPATION

consumption for various frequencies, strokes, second gas spring volumes and second gas spring piston areas.

The second gas spring geometry of Build 1-65 is identical to that of the "chamfered piston" used in the Phase II tests (the lower curve of Figure 5-14). Comparing the Phase IIIB test results of Figure 5-13 with the previous Phase II tests of Figure 5-14 shows that the recent tests exhibit a significantly lower energy dissipation and more scatter. Due to the sensitivity of the second gas spring P-V integration to signal phase matching (see Section 4.3.2), the scatter is to be expected. A curve fit of the Phase IIIB data is plotted in Figure 5-15 with the results of Phase II. As shown, there is a significant difference, showing lower work dissipation for the Phase IIIB tests.

Due to the care taken in properly matching the second gas spring pressure and displacement signals, and the digital acquisition and integration of the signals, it is believed that the Phase IIIB tests are more representative of the actual second gas spring dissipation than the Phase II tests. It is also suspected that a faulty signal conditioning module may have introduced additional phase shift errors during the earlier Phase II tests.

The power loss due to the second gas spring is still above the design goal of 150 watts and additional refinement in the second gas spring design would be required to reduce the losses. However, the option of eliminating the second gas spring and, hence, the losses, is also an attractive approach. This could be accomplished by significantly reducing the compressor housing weight, resizing the displacer/piston bores, or by combinations of several options aimed at increasing the operating frequency of the engine/compressor. These options would be examined as part of a redesign of the FPSE/linear compressor unit.

Indicated Power Versus Brake Power

An examination of the test data shows a substantial difference between engine indicated power and the power actually available to drive compressor. Part of the engine power is required to drive the second gas spring where, through throttling, between 100 and 500 watts are dissipated (see Table 5-8 and the discussion in the previous section). Losses in the

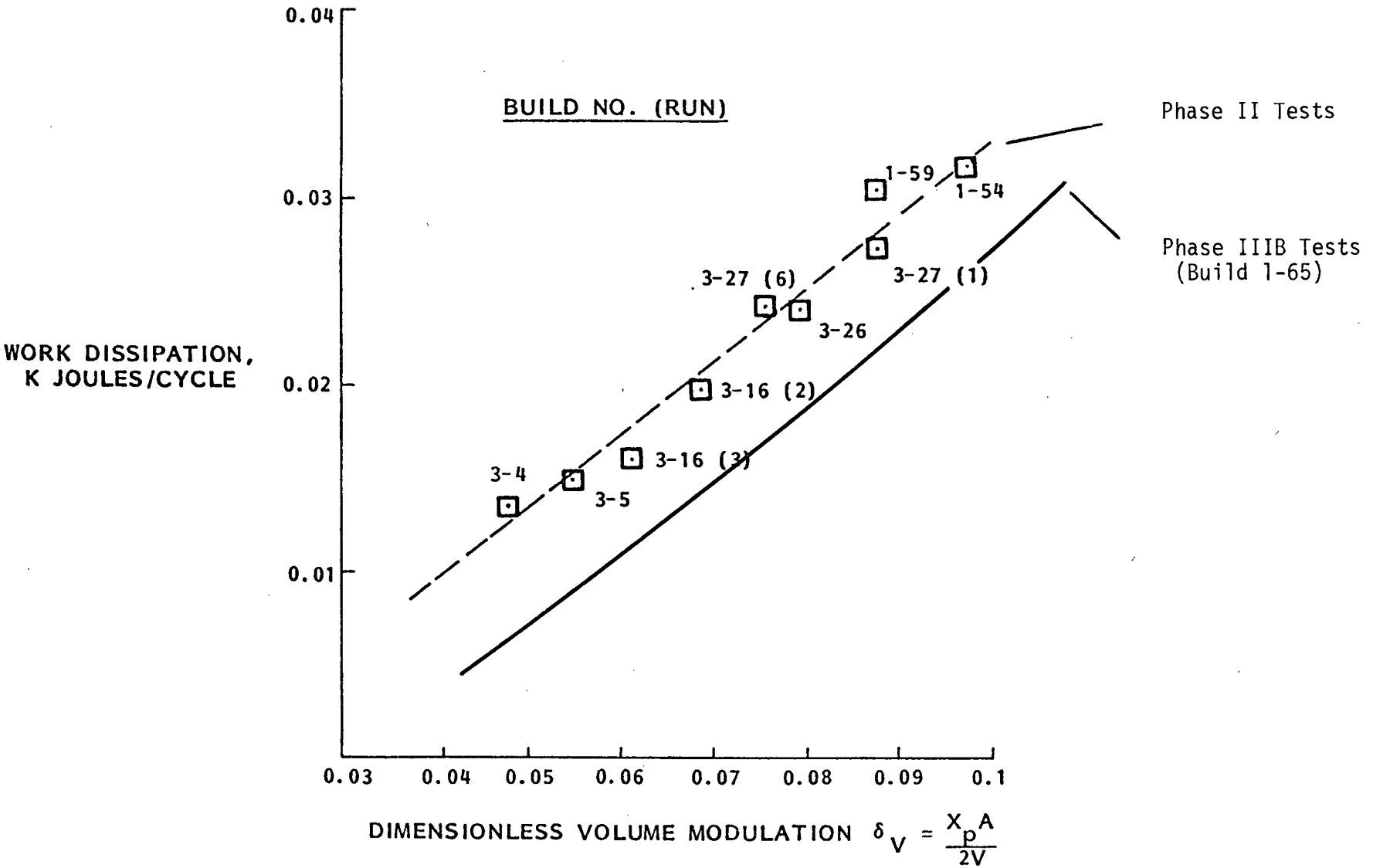

Figure 5-15. COMPARISON OF PHASE II AND PHASE IIIB SECOND GAS SPRING WORK DISSIPATION

second gas spring are much higher than originally designed for, thereby reducing the power available to drive the compressor.

If the power dissipated by the second gas spring and the compressor are subtracted from the engine indicated power, the difference should be the frictional losses of the power piston, second gas spring piston, compressor piston, the support bearing at the upper end of the pressure vessel, the LVDT rods and miscellaneous mechanical parts. These have been previously estimated at less than 300 watts at design stroke and frequency. The actual difference, labeled as "Other Dissipation" in Table 5-8, is considerably higher, particularly at higher frequencies and strokes.

One possible explanation for the high "Other Dissipation" value is excessive friction in the compressor, which also would help to explain the low stroke/flow/power of the compressor. However, as noted in Section 5.3.2, simple friction on the compressor piston is not enough to explain the compressor performance differences between component tests and integrated engine/compressor tests. A more complex set of factors are contributing to the compressor performance anomolies.

These results do indicate a probable link between the large "Other Dissipation" values and the compressor performance deficiencies in integrated engine/compressor testing. The diagnostic testing for the compressor issues described in Section 5.3.3 would be used to address the "Other Dissipation" question as well through thermocouple measurements of suspected high friction areas. Additional interpretive analyses would also be conducted to determine the feasibility of other explanations and to interpret test data from the diagnostic tests.

Test Versus Predicted Indicated Power

A second order thermodynamic code, described in Reference 1, was used to predict the Build #1-65 performance obtained in the Phase IIIB tests. The results are shown in Figure 5-16 superimposed on test results. As in the Phase II tests (see Figure 5-17) the code overpredicts indicated power. Previous interpretations of Phase II test data had identified the principal reason for this being that the code overestimates heat exchanger effectiveness. However, the Phase IIIB tests also showed that the code significantly underestimated heat exchanger flow losses (see Section 5.6).

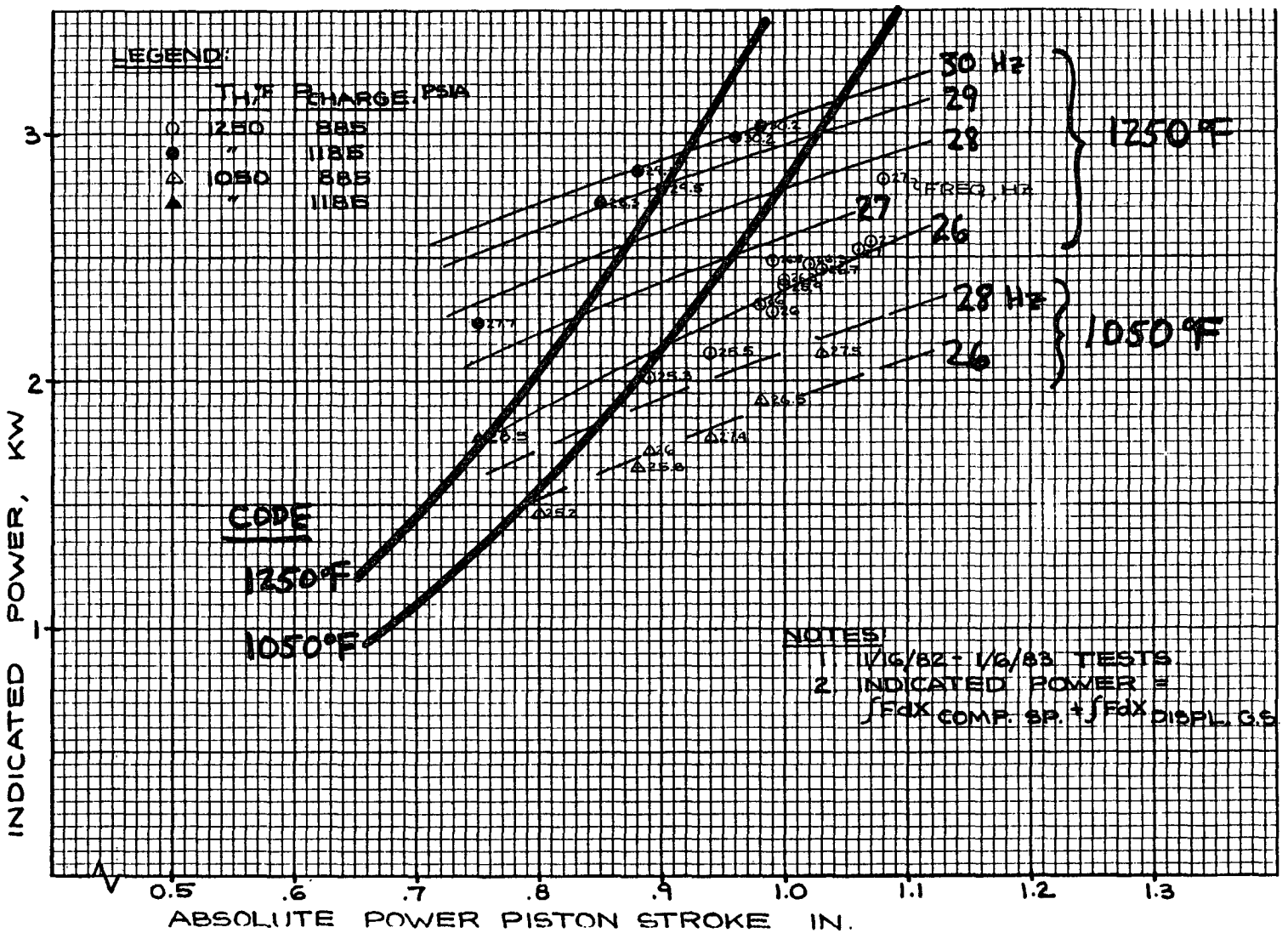

Figure 5-16. FPSE TEST PERFORMANCE VERSUS PREDICTION

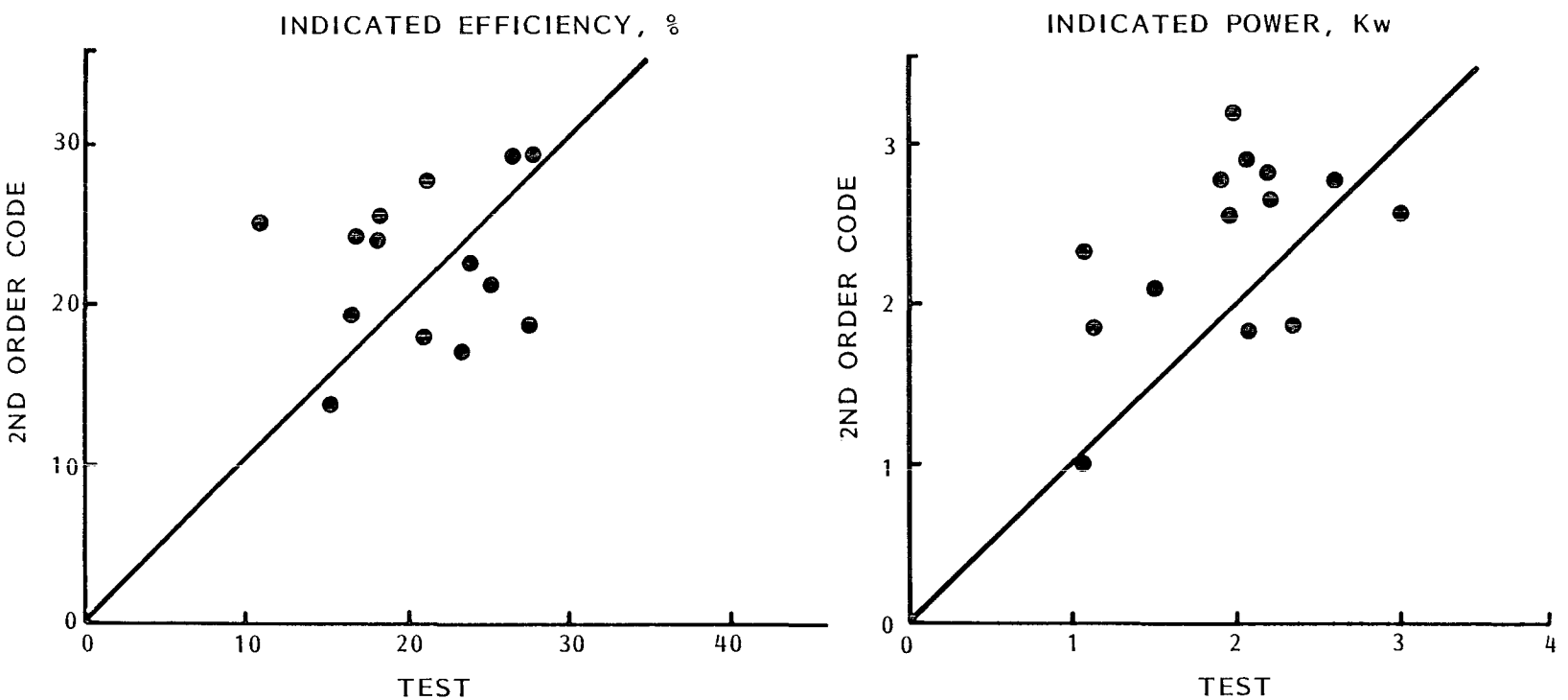

Figure 5-17. 2ND ORDER CODE CORRELATION WITH PHASE II TEST DATA

The detailed heat exchanger loss data given in Section 5.6 can be used to modify the second order code to obtain better test correlation. However, these heat exchanger data only represent a single configuration and it is known that the cooler losses are exceptionally high due to the use of a spiral spring insert in the cooler tubes. A far more comprehensive approach would be to conduct additional tests on the Build 1-65 unit by varying the engine dynamic part geometries (with existing hardware) to generate heat exchanger data over a wider range of conditions. This data could then be used to establish a more general heat exchanger model for the code. A further step would be to instrument the Phase II "Modified Proto 2" engine housing with the same sensors used in Build #1-65. This would provide heat exchanger test data on a significantly different set of heat exchangers. The modified Proto 2 unit has double heater head tubes, a larger, higher effectiveness regenerator, and shell and tube cooler assemblies with no spiral spring inserts. The modified Proto 2 unit has lower heat exchanger flow losses and higher effectiveness components: test data on this unit would provide a significantly broader data base for the code heat exchanger models.

5.5 MATCHING ANALYSIS VERIFICATION

The basic engine/compressor matching procedure was described in Section 2.3. The principals of the technique were validated using the Phase IIIB test data, as described below. This provides a method for both predicting the coupled operation of a FPSE and a linear free-piston compressor (a four-body dynamic system) and for evaluating and designing control systems and components.

5.5.1 ENGINE/COMPRESSOR MATCHING TEST DATA

The Phase IIIB test data taken on the Proto 2 engine follows the trends predicted by the matching analysis of Section 2.3. Figure 5-18 shows engine indicated power versus power piston stroke for two charge pressures and two heater head temperatures. For a given charge pressure, the engine power levels are higher at higher heater temperatures (for the same stroke). Also, for a given heater head temperature, engine power levels increase with charge pressure. For a fixed heater head temperature and change pressure, engine/compressor match points occur at longer or shorter strokes depending on the location of the compressor power (absorbed) curve. This behavior is

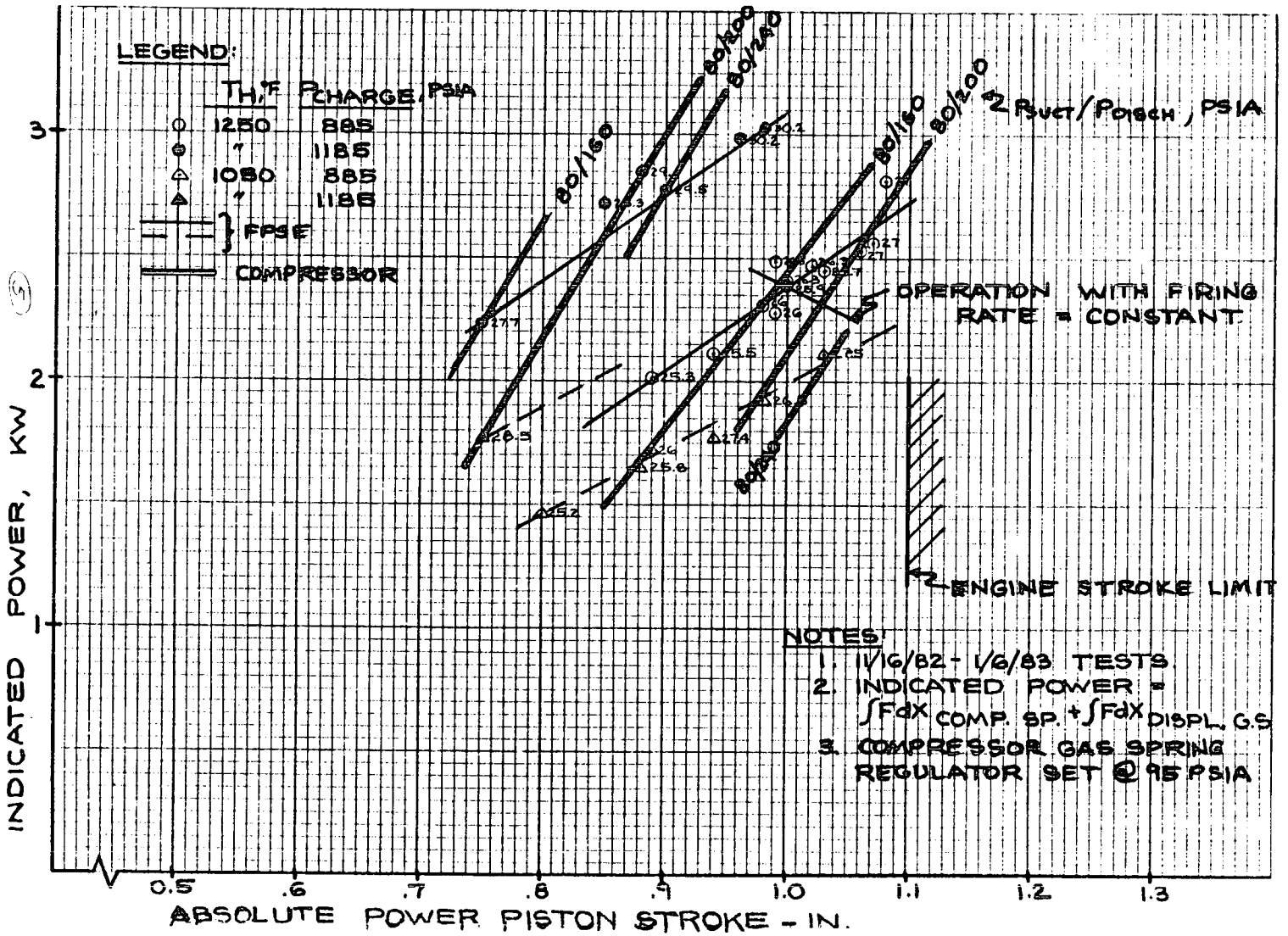

Figure 5-18. FPSE/COMPRESSOR PERFORMANCE MAP (TEST)

best illustrated in those cases where the compressor operates at the same suction pressure, discharge pressure and frequency but at two different strokes.

Figures 5-19 and 5-20 present simplified engine/compressor matching curves from the Phase IIIB tests. Figure 5-19 shows operation with no gas spring regulator on the compressor. Figure 5-20 shows operation with the compressor gas spring regulator set to 95 psia. In Figure 5-19, with the engine operated at either a 1250°F or a 1050°F heater heat temperature, matched operation with the compressor occurs at longer strokes as the discharge pressure on the compressor is increased (suction pressure held constant in these tests). As discharge pressure is increased, the compressor natural frequency increases, causing an increase in operating frequency and stroke of the engine/compressor unit. Power output of the engine increases along with the power demand of the compressor until a new stable operating point is reached. With the compressor gas spring regulator, the compressor natural frequency is increased (for the 95 psia regulator setting), thereby shifting the match points to the right (Figure 5-20). Since this results in longer strokes, the engine power developed is higher and compressor output increases accordingly. Figures 5-19 and 5-20 illustrate the effects heater head temperature (controlled by combustor firing rate) and compressor gas spring regulator pressure (controlled directly) have on engine/compressor operating points and highlights the control options available for the unit.

5.5.2 MATCHING FLEXIBILITY AND HAHP CONTROL

Matching analyses are especially important in designing overall control approaches for the HAHP. The basic control approach for the Proto 2 HAHP consists of two combustor firing rates (same heater head temperature). The high firing rate is used for the hot and cold extremes of ambient temperature where maximum engine power is required. The low firing rate is used for the mid range of ambient temperature where the unit is run at low capacity. This control system requires that the compressor power absorbed curves cluster near the full stroke and full power areas of the engine map for the extreme ambient temperature day cases and near the half power area of the engine map for the mid-range ambient temperature day cases. The compressor gas spring pressure regulator could then be used to fine tune the compressor dynamic characteristics to achieve the required match point.

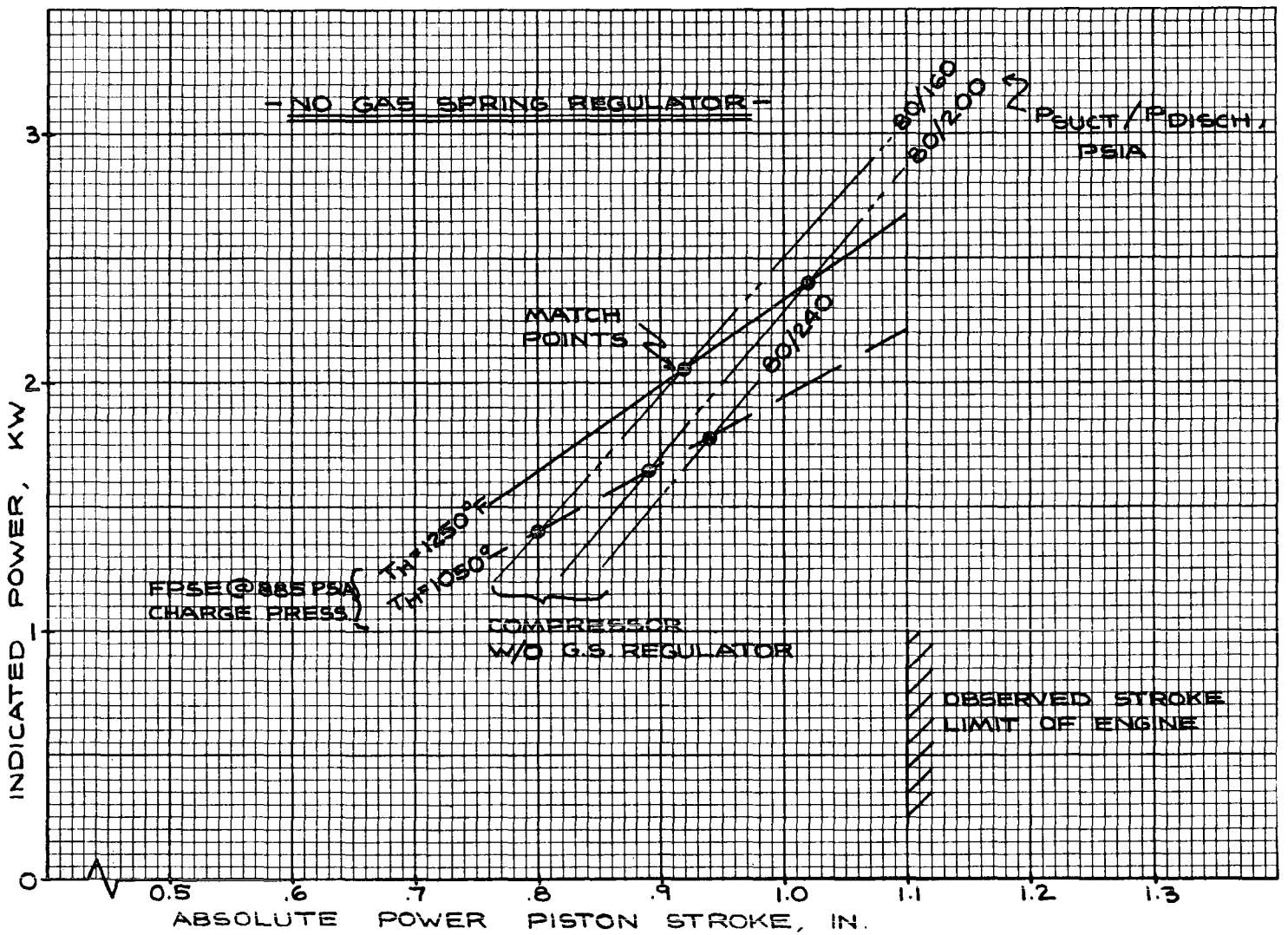

Figure 5-19. FPSE/COMPRESSOR MATCH - NO COMPRESSOR GAS SPRING REGULATOR

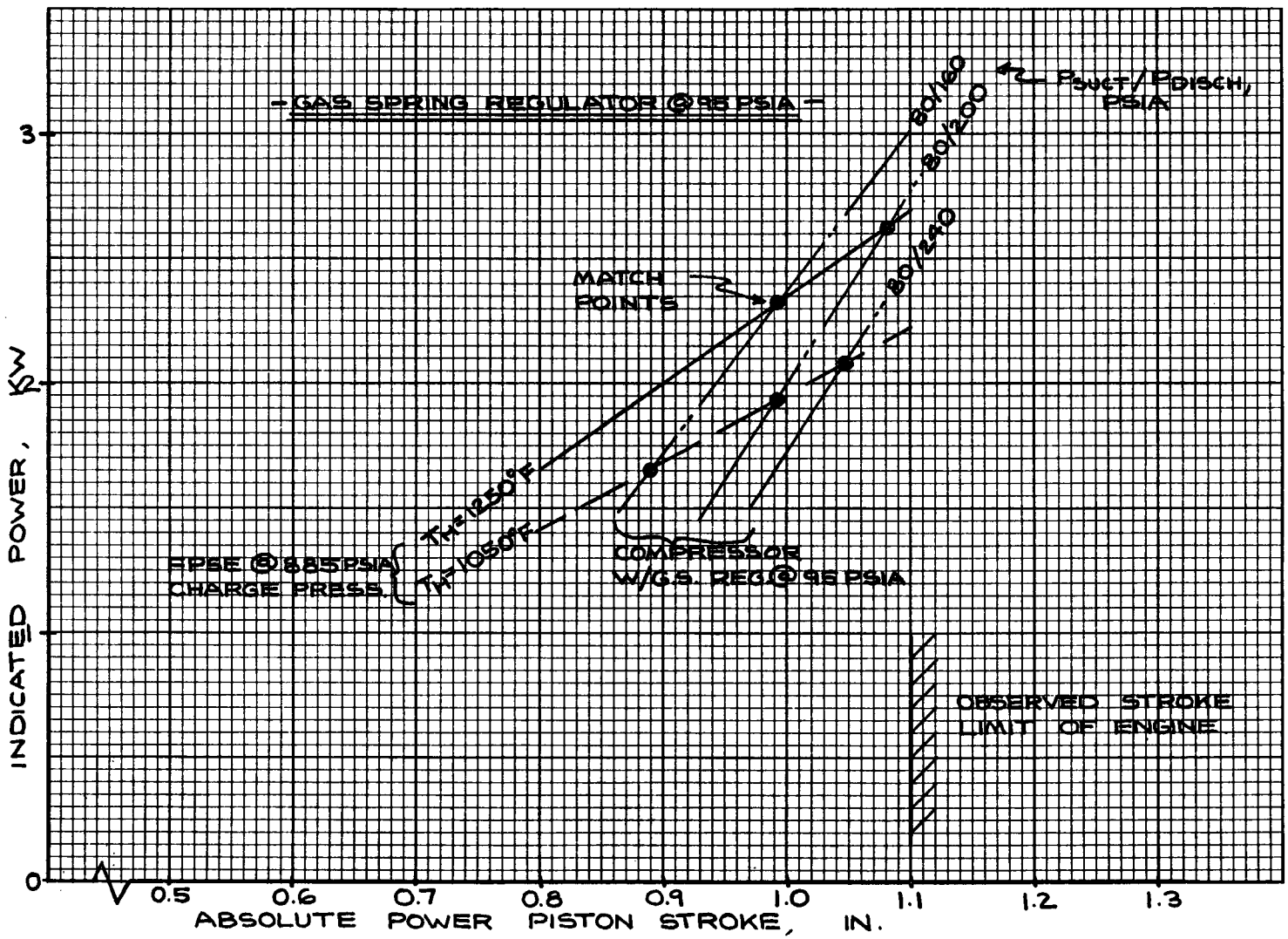

Figure 5-20. FPSE/COMPRESSOR MATCH - COMPRESSOR GAS SPRING REGULATOR AT 95 PSIA

The Phase IIIB tests verified the feasibility of this control system concept. The data of Figures 5-19 and 5-20 showed that without compressor gas spring pressure regulation, the engine firing rate would have to be modulated to maintain full stroke/power conditions as ambient temperature changes caused changes in compressor suction and discharge conditions. With regulation, the position of the compressor load curve can be controlled to minimize the shift in engine/compressor operating stroke or to effect a change in operation. This is illustrated in Figure 5-21. If ambient temperature changes cause a shift in compressor/discharge pressure from 160 psia to 200 psia, the match point shift can be minimized by decreasing regulator pressure setting from 95 psia to 80 psia. If, however, a higher power output is required, regulator pressure setting can be held constant (as illustrated in Figure 5-21), reduced only slightly (to say 90 psia) or increased further (to say 100 psia).

5.5.3 EVALUATION OF MATCHING AND CONTROL TECHNIQUE

Whether or not an active compressor gas spring regulator control is required or not depends on the specific operating characteristics of the FPSE/linear compressor unit. An active control system would consist of a regulator physically similar to the units tested, but instead of being set to a fixed pressure, the regulator pressure would be varied with ambient conditions according to a preset schedule. Compressor discharge pressure could be used as both the feed pressure for the regulator and as the control signal. Or, ambient temperature might be used directly as the control input signal. Whatever the specific design, it appears that the basic HAHP control concept can meet the product operating requirements with, at most, the addition of an active control on compressor gas spring pressure.

The basic engine/compressor matching technique developed for analyzing unit operation was verified by the Phase IIIB tests and would appear to have potential for use in other FPSE/load units. If the engine and load are well characterized, the preparation of the matching maps would be straightforward. Since the linear free-piston compressor represents the most dynamically complex load for the FPSE, other types of loads may prove to be easier to characterize, leading to simplified engine/load matching and control systems.

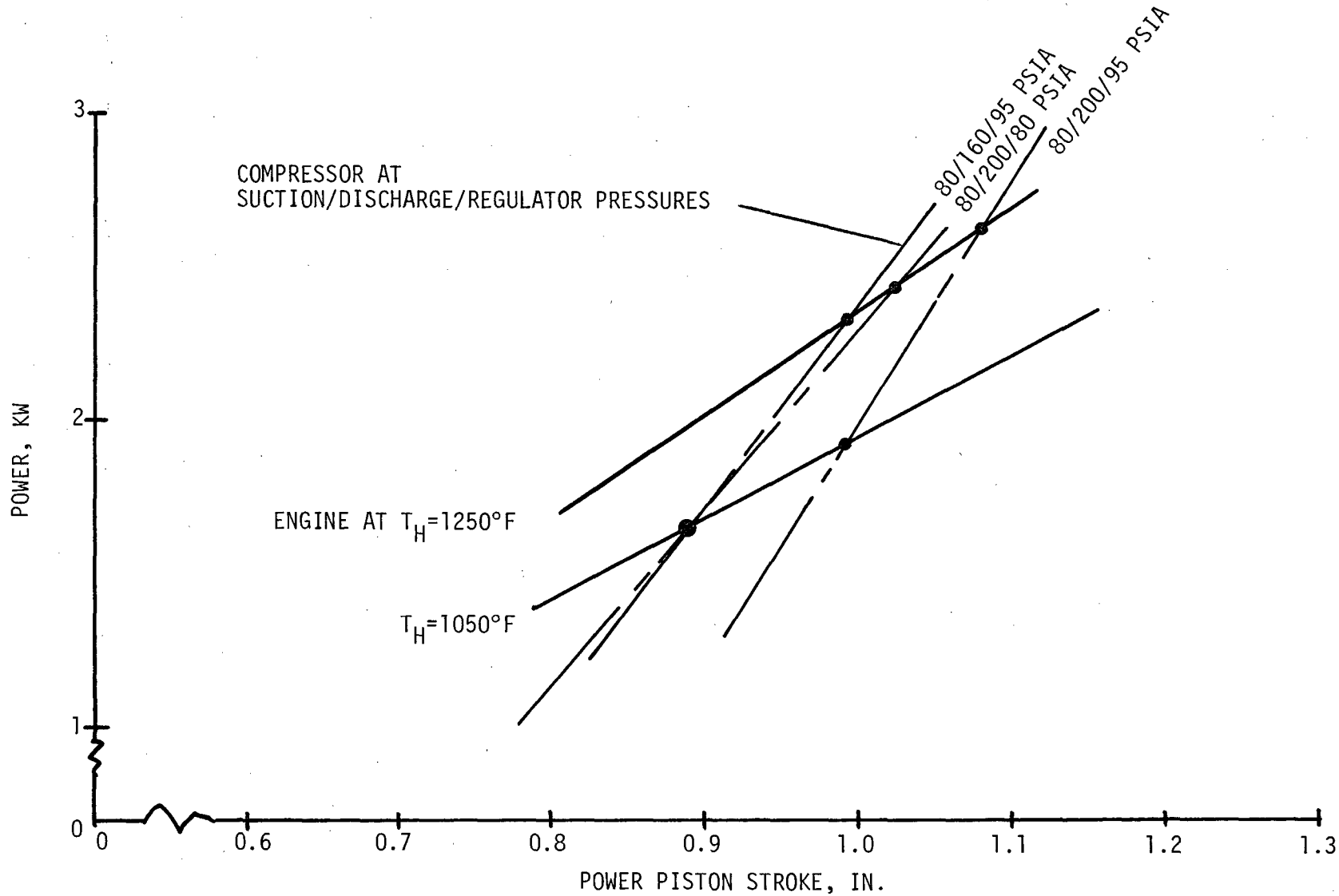

Figure 5-21. GAS SPRING CONTROL OF ENGINE/COMPRESSOR MATCH POINT

5.6 HEAT EXCHANGER LOSSES

One of the principal goals of the Phase IIIB test program was to generate engine heater head, regenerator and cooler performance data. These data could then be used to upgrade engine performance predictions and design tools for both evaluating the potential performance of the FPSE and for redesigning the engine.

Unfortunately, the fast response thermocouples which were to be used to directly measure heat exchanger and regenerator thermal performance were not fabricated to specification by the vendor and were not reworked satisfactorily until the tests were completed. However, pressure loss data was obtained over a broad range of test conditions and were analyzed as described below.

5.6.1 MEASURED LOSS DATA

One of the major losses affecting the Proto 2 engine efficiency is the flow friction losses through the heater head, regenerator and cooler. Contrary to predictions, the pressure drop across the cooler constitutes the major pressure loss among the three sections (See Table 5-8). The power loss across the cooler is almost 50% of the total loss while the heater and the regenerator split the remaining losses almost equally. The total flow friction losses, as percentage of the indicated power, are between 30 to 40%, which is significantly higher than the 10% range for optimized engine designs.

Figure 5-22 is a compilation of all Phase IIIB test data on the total flow friction losses, plotted against the parameter $(f_{op})^2(X_p)^2(P_{CH})$. For a given set of hardware, the pressure drop and the flow friction loss will vary in the following relationships depending on the types of flow:

$\text{Loss} \sim (\rho v)^2$: Laminar

$\rho^{1.2} v^{1.8}$: Turbulent

ρv^3 : Entrance and exit losses

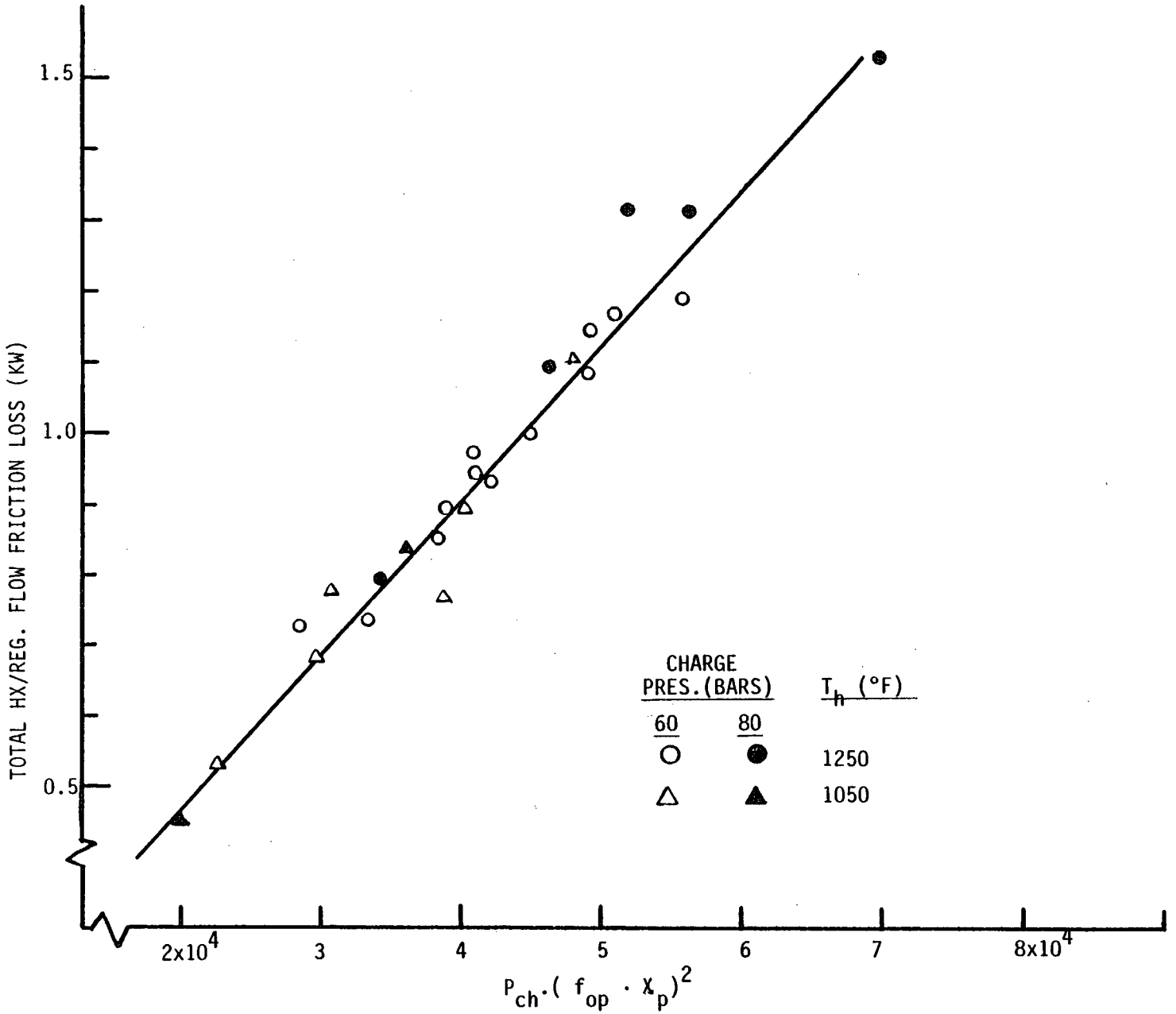

Figure 5-22. HEAT EXCHANGERS AND REGENERATOR FRICTION LOSS

The test results for total friction loss, as indicated in Figure 5-22, correlates closest to the turbulent flow relationship. This reinforces the observation that the dominant losses are attributable to the turbulent skin friction along the cooler and the heater tube walls.

5.6.2 COMPARISON TO PREDICTIONS

The analytical predictions of the pressure drops across the heat exchangers and the regenerator, using quasi-steady state equations, often under-predict the true values as illustrated in the examples shown in Table 5-11.

In this table, test cases are compared to previous calculations made for similar frequency, piston stroke, and displacer stroke conditions. Calculation technique 1 is a GE code which uses a stepwise calculation technique through time in which steady state equations for pressure drop are applied at each time interval. Calculation technique 2 is a steady state pressure drop calculation based on average flow rate and mean gas properties prepared by Sunpower, Inc. for the Proto 2 engine. As can be seen, considerable improvement is required in the models to improve accuracy. For the cooler, the presence of the spiral spring insert, added to promote heat transfer, is suspected to be a large contributor to the high losses and to the large discrepancy between test and prediction. However, the regenerator losses are substantially underpredicted and additional analyses are required to determine how much of the higher losses are due to the specific design and how much is due to model deficiencies.

5.6.3 INTERPRETATION OF RESULTS

The heat exchanger loss data provided insight into the performance deficiencies of the Proto 2 FPSE and the models used to design the engine. The data confirmed the conclusions of the Phase II program (Reference 1):

1) The flow losses in the engine heat exchangers must be reduced substantially to realize the engine efficiency goals.
2) The effectiveness of the regenerators must be increased to meet thermal performance requirements, even at the expense of some additional pressure loss.

Table 5-11. Comparison of Measured Versus Predicted Heat Exchanger Flow Losses

CODE	f (HZ)	X_D (IN)	X_p (IN)	PUMPING POWER LOSS (KW)			
				HEATER	REGEN.	COOLER	TOTAL
TEST (#4)	25.25	1.77	1.05	0.19	0.21	0.33	0.73
CALC. 1	24.7	1.65	1.06	0.279	0.059	0.06	0.398
CALC. 2	24.7	1.65	1.06	0.171	0.041	0.06	0.272
TEST (#11)	27.0	1.88	1.25	0.28	0.31	0.49	1.08
CALC. 1	27.2	1.75	1.26	0.496	0.081	0.089	0.666
CALC. 2	27.2	1.75	1.26	0.199	0.041	0.045	0.285

Calculation 1: Step-wise integration of steady-state equations. (GE-TDP)

Calculation 2: Steady-state equation using average flow rate and mean gas properties. (SUNPOWER)

However, the Phase IIIB test also pinpointed the cooler as the major contributor to the heat exchanger losses and provided guidance on which component models needed revisions to improve predictive accuracy.

Use of the Proto 2 heat exchanger test data for revising the design models and, subsequently, the engine design, must be tempered by the deficiencies of the design itself. Since a new engine design would be significantly different than the existing design, models correlated to the Phase IIIB test data might be too far from an "optimum" design to achieve the predictive accuracy required. In addition, the lack of direct measurements of engine heat exchanger dynamic temperatures limits better thermal modelling of these components.

The next logical step in improving the engine models and increasing engine performance would be to broaden the test data base. This would be accomplished by:

1) Limited testing of the Phase IIIB instrumented Proto 2 engine with the fast-response thermocouples installed.
2) Installation of the same dynamic pressure and temperature instrumentation and DAS in the existing "Modified" Proto 2 engine housing (Reference 1 describes this design and its performance).

The first tests would simply be an extension of the Phase IIIB tests with use of the originally planned dynamic thermocouples. The second test would be a program similar to the Phase IIIB tests, although on a smaller scale. The Modified Proto 2 engine had a double tube heater head design, larger, more effective regenerators and shell and tube type cooler sections without spiral spring inserts. Steady state flow tests indicated that the heat exchanger pressure losses were substantially lower than for the original or "Baseline" Proto 2 engine, and performance tests showed high heat exchanger thermal performance. Engine efficiency was higher, but power output was lower due to the significant increase in void volume. Tests on this engine would provide data on a significantly different set of heat exchanger models. These tests would also be combined with the diagnostic compressor tests discussed in Section 5.3.3 to accomplish both objectives within a single test series.

SECTION 6

CONCLUSIONS AND RECOMMENDATIONS

SECTION 6
CONCLUSIONS AND RECOMMENDATIONS

The conclusions and recommendations reached through the Phase III test and analysis program are summarized below. Included is an estimate of the performance potential of the existing FPSE hardware without a major redesign/rebuild.

6.1 RESULTS AND CONCLUSIONS

6.1.1 FPSE INDICATED POWER

The maximum FSPE indicated power obtained from the test was over 3 KW at a 1250°F heater heat temperature and 80 Bars charge pressure, as shown in Figure 6-1. At lower charge pressures and heater head temperatures, the power output is reduced accordingly. At 60 Bars charge pressure, the maximum indicated power is about 2.9 KW at 1.08" power piston stroke. It is believed that higher power levels could be achieved at longer strokes but attempts to operate at a longer stroke resulted in mechanical collision of the dynamic components on their stops.

The effect of expansion to compression space phase angle and their swept volume ratio is shown in Figure 6-2. It is seen that the power output is strongly influenced by the volume phase angle and the swept volume ratio. The volume phase angles of the Proto 2 appear to far exceed the optimum value, which lies between 100 to 120°. The swept volume ratio is too low and should be brought up to a ratio of about 1.0. Changes in the engine dynamic components thus appear to be capable of significantly improving indicated power.

6.1.2 ENGINE INDICATED EFFICIENCY

The maximum engine indicated efficiency achieved was 25%, as indicated in Figure 6-3 which shows indicated efficiency plotted against the power piston stroke of various test points. The scattering of efficiency data when correlated with the piston stroke appears wider than that of other performance parameters, such as the indicated power. Part of the scatter occurs because the calculation of efficiency is an end result of all other measurements, including the fuel input, combustion efficiency and the engine indicated power. Nevertheless, Figure 6-3 does illustrate the trend of engine efficiency, indicating an efficiency plateau of 25% for the existing Proto 2 hardware.

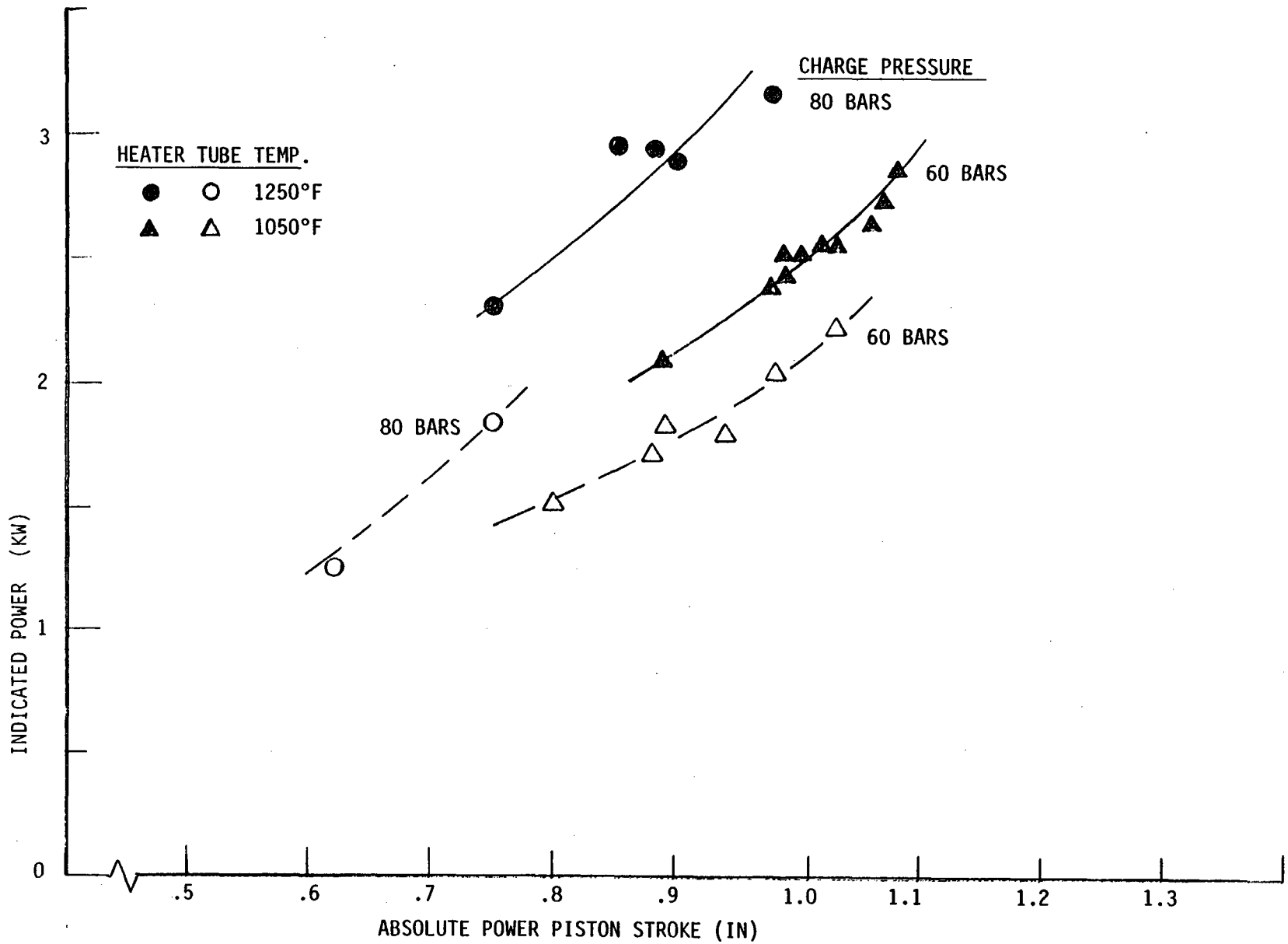

Figure 6-1. FPSE INDICATED POWER TREND

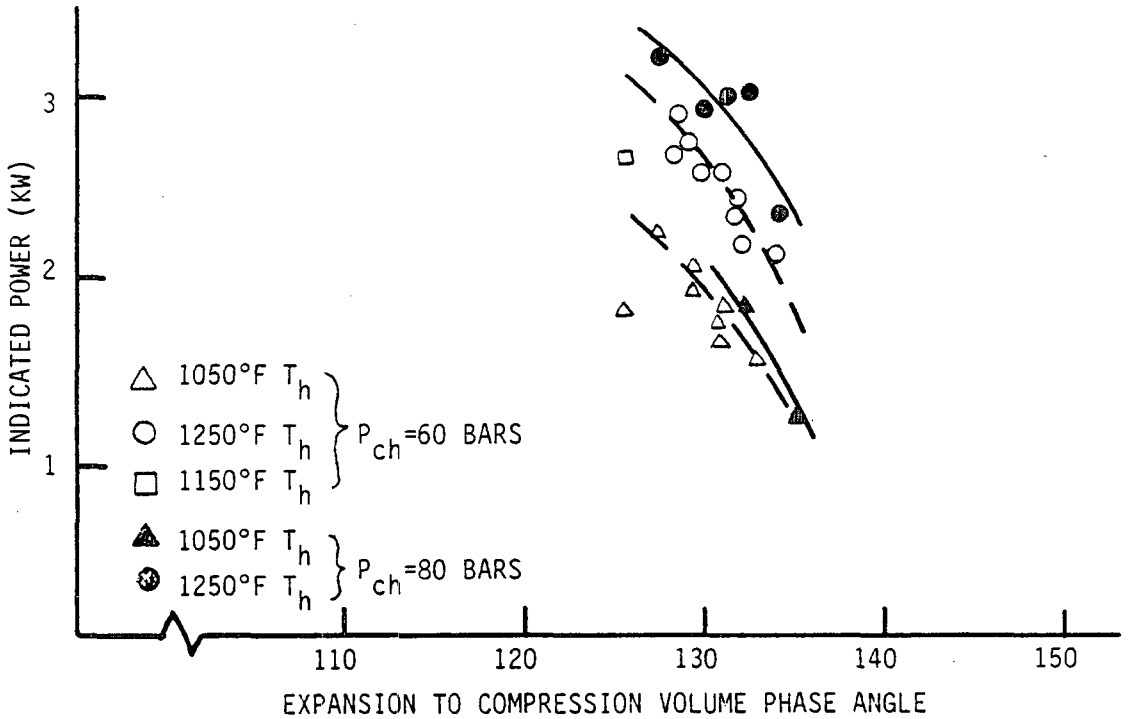

(A)

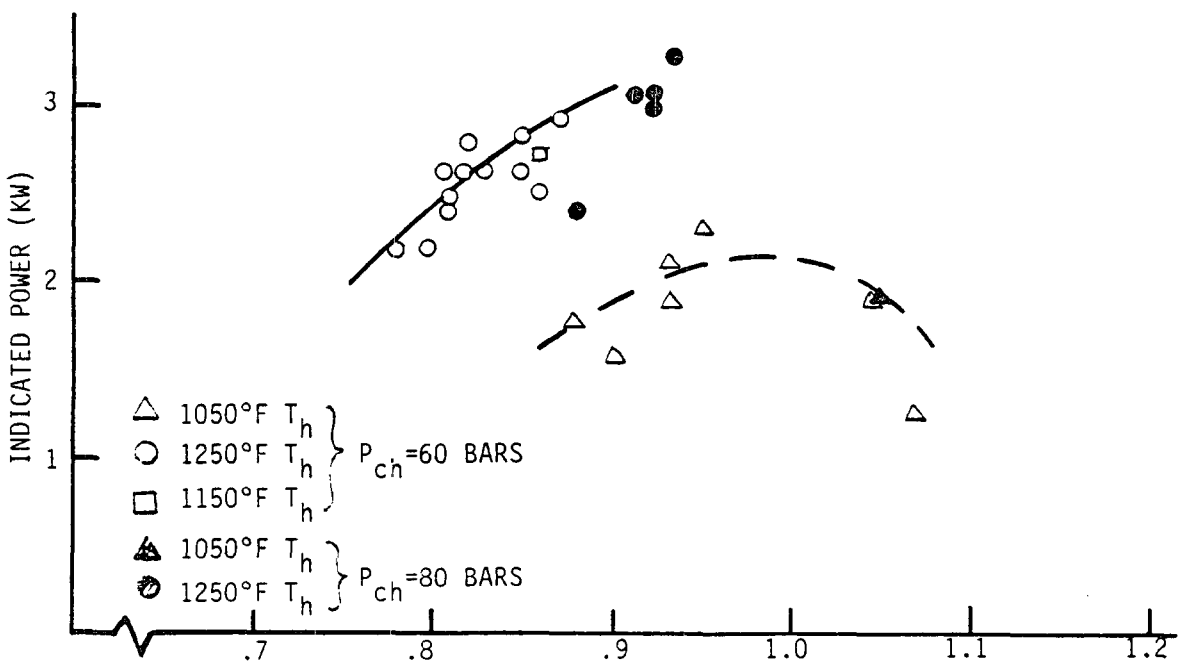

(B)

Figure 6-2. EFFECT OF PHASE ANGLE AND SWEPT VOLUME RATIO ON ENGINE POWER

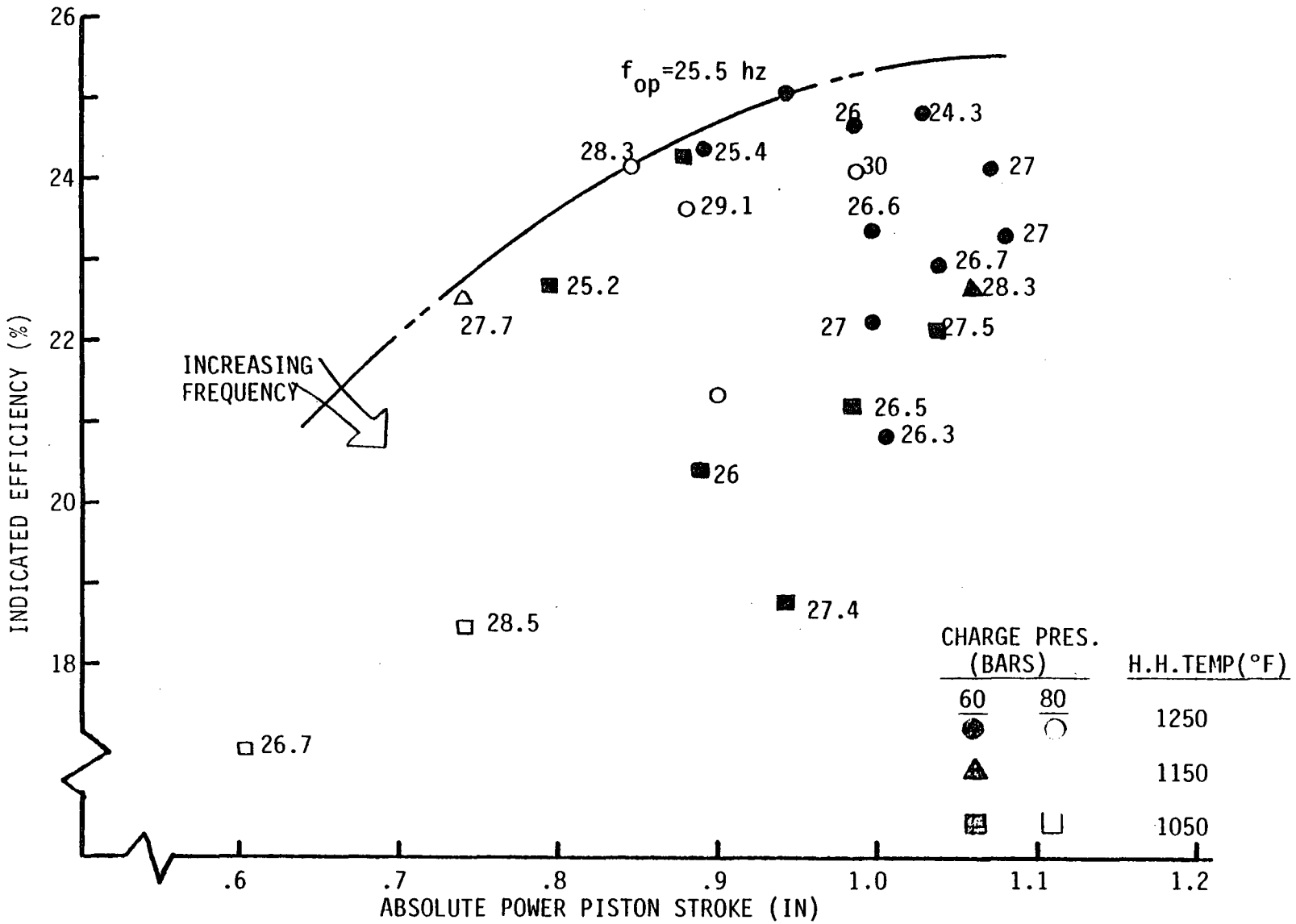

Figure 6-3. EFFECT OF PISTON STROKE AND FREQUENCY ON ENGINE EFFICIENCY

Another reason for the scatter shown in Figure 6-3 is that operating frequency has a significant effect on engine efficiency. As the frequency is increased, the engine efficiency descreases rapidly. It appears that the increase of heat and power losses within the engine exceeds the rate of power gain as the operating frequency is increased. This is due to the high loss levels in the engine heat exchangers. If the heat exchanger were redesigned for lower losses, the indicated efficiency would be higher and less sensitive to frequency.

6.1.3 ENGINE HEAT EXCHANGER FLOW FRICTION LOSSES

One of the major losses affecting efficiency is the flow friction loss through the heater head, regenerator and cooler. Contrary to early predictions, the pressure drop across the cooler constitutes the major loss among the three components. The power loss across the cooler is almost 50% of the total loss while the heater and the regenerator split the remaining losses almost equally. Total flow friction losses, as a percentage of indicated power, are between 30-40%, significantly higher than the 10% range for optimized engine designs.

The tested total friction loss correlates closest to a turbulent flow relationship. This reaffirms the observation that the dominant losses are attributable to the turbulent skin friction along the cooler and the heater tube walls. The high cooler loss appears largely due to the use of spiral spring inserts in the cooler tubes, originally added to enhance heat transfer. Redesign of the engine heat exchangers to improve performance would concentrate on reducing flow losses in the cooler and heater. Flow losses in the regenerator would be increased due to a higher effectiveness matrix, but total flow losses for the heater head, regenerator and cooler would be reduced significantly.

6.1.4 OTHER POWER LOSSES

The engine second gas spring, installed on the power piston to boost operating frequency, caused a significant penalty in output power. Energy dissipation by the second gas spring ranged from 200 to 500 watts, depending on stroke and frequency. Other losses (seal and bearing friction) are estimated to be in the range of 150 to 200 watts.

Significant reduction in second gas spring power dissipation will be required to achieve higher engine brake efficiencies. This can be accomplished by redesign of the second gas spring, but a more productive approach may be to alter the compressor housing design (lighter) or to change the displacer/power piston geometry so that the secong gas spring could be eliminated.

6.1.5 COMPRESSOR PERFORMANCE

The Proto 2 compressor performed with shorter compressor piston strokes when driven by the FPSE than when tested on its own test stand. This resulted in reduced output refrigerant flow and somewhat lower efficiency. The prime candidate explanation is the different test environments between the tests with the engine and those on the test stand. When tested with the engine, the compressor housing is subjected to a high external pressure which may distort portions of the housing and cause excessive piston friction. Analyses indicate this would be only one factor, however, and additional diagnostic testing is required to determine the source(s) restricting piston motion.

The compressor met its performance goals on its own test stand. Therefore, if the cause of restricted compressor piston motion can be corrected, it is expected that compressor performance goals can be met when driven by the engine. However, in addition to the two freon compression spaces, the compressor also contains two gas springs to ensure centering of the compressor piston and boost compressor natural frequency to the required level. The two gas springs are connected to each other and to other fluid compartments through clearance or vent holes. These small flow passages contribute to throttling losses in addition to the heat transfer loss associated with the gas springs. These losses represent about 20% of the brake input power for the compressor. Design refinements in the compressor gas springs and flow passages could improve overall compressor efficiency 5 to 10 points (up to 80%).

6.1.6 ENGINE/COMPRESSOR MATCHING AND CONTROL

The Phase IIIB tests confirmed both the engine/compressor matching analysis and the control concept for the HAHP. Figure 6-4 shows the engine and compressor map derived from some of the Phase IIIB tests. The engine power

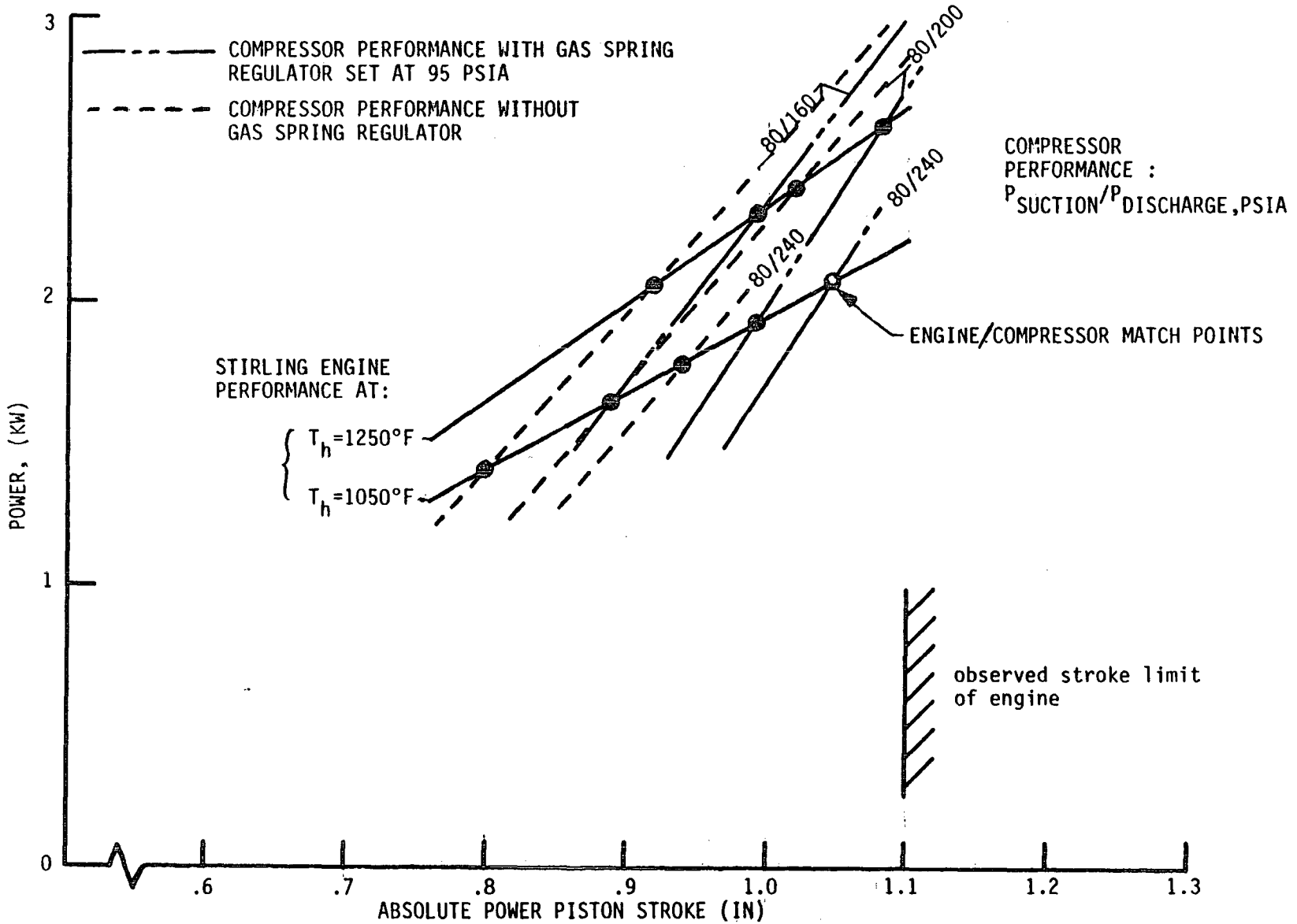

Figure 6-4. ENGINE/COMPRESSOR MATCHING AND CONTROL MAP

output as a function of piston stroke and heater head temperature is shown superimposed on the compressor power requirement for various compressor suction/discharge conditions and two different compressor gas spring pressure regulator schedules. (The compressor power curves include the engine second gas spring dissipation.)

As shown in Figure 6-4, stable operating points were achieved as predicted. Also shown is the ability of compressor gas spring regulator pressure to shift the match point of the engine and compressor to longer strokes and higher power. This confirms the use of a simple 2 step engine combustor firing rate control with a compressor regulator to control operation of the HAHP system over the heat pump ambient temperature range, throttling the system at intermediate temperatures to maximize COP at low load conditions.

6.1.7 PREDICTIVE DESIGN TOOLS

The individual heater head, regenerator and cooler loss data from the Phase IIIB tests significantly differed from the values predicted by models from a variety of sources. Table 6-1 shows a comparison of these losses for two test points to predictions from the GE model used to design the engine and an independent analysis conducted by Sunpower, Inc. As shown, the models seriusly underpredict the losses for both the regenerator and cooler.

The high levels of losses in the engine heat exchangers probably contributes to the predictive discrepancies, since most Stirling engine models are correlated to more optimized engines. However, more fundamental experimental data on FPSE heat exchangers is required to improve the test/analysis correlation. This step will be necessary to establish sufficient confidence in the model to permit an engine redesign.

6.2 PERFORMANCE POTENTIAL

Based on the performance trends obtained from the Phase IIIB test data, it is possible to estimate the system performance potential with design changes to the engine. If an absolute piston stroke of 1.2" can be obtained (without mechanical collision) at a 28 Hz operating frequency and a 60 Bars charge pressure, the estimated power breakdown of this operating point is shown in Table 6-2, compared with two typical test data points. As shown, it is estimated that with a slight increase in stroke (and the attendant

Table 6-1. Comparison of Measured Versus Predicted Heat Exchanger Flow Losses

CODE	f (HZ)	X_D (IN)	X_p (IN)	PUMPING POWER LOSS (KW)			
				HEATER	REGEN.	COOLER	TOTAL
TEST (#4)	25.25	1.77	1.05	0.19	0.21	0.33	0.73
CALC. 1	24.7	1.65	1.06	0.279	0.059	0.06	0.398
CALC. 2	24.7	1.65	1.06	0.171	0.041	0.06	0.272
TEST (#11)	27.0	1.88	1.25	0.28	0.31	0.49	1.08
CALC. 1	27.2	1.75	1.26	0.496	0.081	0.089	0.666
CALC. 2	27.2	1.75	1.26	0.199	0.041	0.045	0.285

Calculation 1: Step-wise integration of steady-state equations. (GE-TDP)

Calculation 2: Steady-state equation using average flow rate and mean gas properties. (SUNPOWER)

Table 6-2. POWER AND LOSS BREAKDOWN FOR PHASE IIIB TEST & POTENTIAL ENGINE PERFORMANCE

	TYPICAL TEST DATA TO DATE		EXISTING HARDWARE	POTENTIAL WITH HARDWARE MODIFICATION*
Charge Pressure, Bars	60	80	60	60
Frequency, Hz	26.3	30.2	28	27
Piston Stroke, In	1.02	0.98	1.2	1.1
Heat Input, KW	10.0	12.62	16.5	10.0
Basic Power, KW	3.51	4.67	5.8	3.9
HX/Reg. Flow Friction, KW	.94	1.50	1.4	0.4
Ind. Power, KW	2.57	3.17	4.4	3.5
2nd G.S. Loss, KW	0.55	1.22	0.8	0.4
Other Losses, KW	0.15	0.20	0.2	0.2
Work to Compressor, KW	1.87	1.75	3.2	2.9
Ind. Eff. (%)	25.7	25.1	26.6	35.0
Brake Eff. (%)	18.7	13.9	16.4	29.0

*98% Regenerator Effectiveness; HX Flow Work = 10% (Basic Power)

frequency), a significant increase in the engine power could be realized. However, both indicated and brake efficiencies would still be low, due to high heat exchanger flow losses, low regenerator effectiveness and high second gas spring dissipation.

Additional, more substantial hardware modifications to the engine would be required to achieve a significant improvement in engine efficiency. A reduction of heat exchanger flow losses from 30 to 40% of indicated power to approximately 10% should be possible, based on existing optimized engine designs. In addition, the regenerator effectiveness would be increased from the present 92-93% to 97-98% by increasing its size and using a finer wire matrix (at some increase in regenerator flow losses). This could result in the indicated efficiency improvement shown in Figure 6-5.

To improve engine brake efficiency, it will be necessary to reduce the power dissipated in the second gas spring (or eliminate the gas spring entirely). A detailed discussion on the second gas spring and its potential improvements is given in Reference 1. If the second gas spring loss can be reduced to its original design value (less than 200 watts), then a brake efficiency of 29% or better could be realized. A breakdown of the "improved" design is also given in Table 6-2.

The improved Proto 2 engine design projected in Table 6-2 is for the basic Proto 2 configuration, with changes to the externally mounted heater head, regenerator and cooler, and some modifications to the internal dynamic components. The basic engine concept and housing design would be the same and could be accomplished with existing hardware. More extensive changes to the engine design would require a complete engine rebuild, but would have the potential for higher performance (elimination of the second gas spring, for example). However, this step would only follow improvement of the engine design tools and use of the existing hardware to validate the projected improvements shown in Table 6-2.

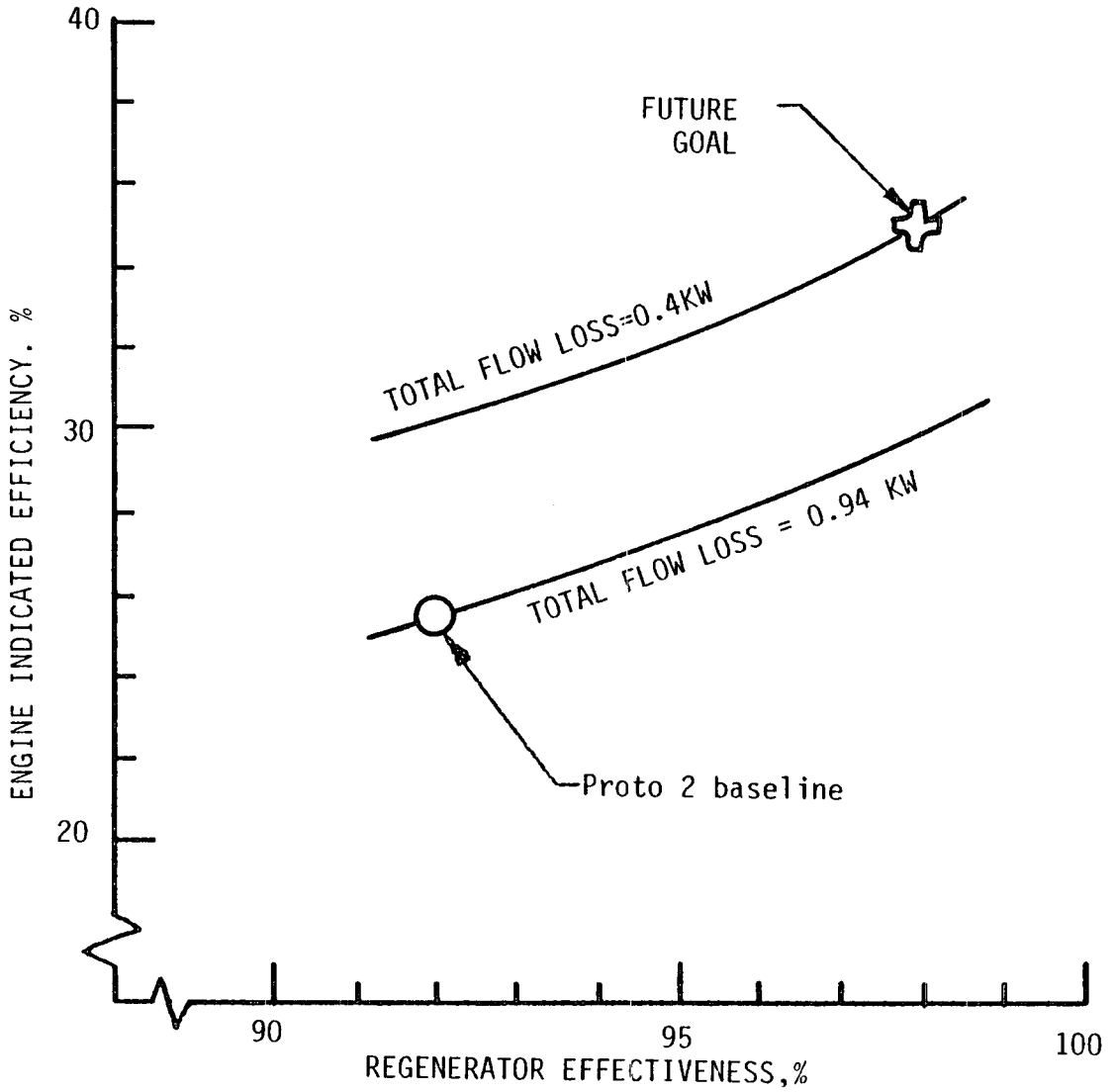

Figure 6-5. EFFECT OF REGENERATOR EFFECTIVENESS AND TOTAL ENGINE FLOW LOSSES ON ENGINE EFFICIENCY

6.3 RECOMMENDATIONS

6.3.1 GENERAL RECOMMENDATIONS

Based on the results of the Phase II, Phase IIIA and Phase IIIB HAHP programs, the following general recommendations have been formulated.

1) Development of the FPSE/Linear Inertia Compressor Heat Activated Heat Pump Concept should be continued. This concept offers:
   - High potential performance
   - Low production cost
   - Mechanical simplicity (high potential reliability and low maintenance costs)
   - Hermetically sealed engine/compressor unit (the standard for residential and light commercial heat pumps)

   The concept is technically reasonable and capable of successful development, as verified by the NASA Lewis Research Center. Additional technology development work is required, not only to achieve target performance levels but also to develop long life seals and bearings.

2) The dynamic complexity issue facing the FPSE/Linear Inertia Compressor concept should be solved directly. Resorting to additional mechanical or electrical complexity to reduce the dynamic complexity of the FPSE/linear compressor unit increases production costs and degrades reliability in the final product. Tests in the Phase IIIB program validated the technique for matching the existing engine/compressor unit over the range of operating conditions and permitted evaluation of the simple HAHP control system. This effort should be continued in parallel with further engine/compressor development.

3) Engine/compressor performance must be increased to competitive levels. "Competitive" performance goals for the engine and compressor will vary depending on the performance of competing products, the cost of gas, oil and electricity, and the climate where the HAHP competes. For the engine, a short term goal of 32% efficiency, evolving to 37-38% is generally required. These goals are modest compared to other Stirling projects and the HAHP program would benefit from these other, more demanding projects. For the compressor, the current goal of 70% efficiency has been achieved. The longer range goal of 80% appears to be achievable with normal evolutionary improvements in compressor design.

To improve engine performance, the engine heat exchanger designs must be improved:

- Regenerator effectiveness must be increased from the 92 to 95% range of the Proto 2 units to 98%.
- Heater head and particularly cooler flow losses must be reduced.

In addition, power dissipation of the second gas spring must be reduced from 500 watts to less than 200 watts.

4) FPSE simulation model accuracies must be significantly improved. Current models can overpredict FPSE efficiencies by as much as a factor of 60%. Better models of the engine heat exchangers are required, and should be developed using component test data generated over a wide range of engine operating conditions. Thermal loss models for internal components of the engine must also be improved.

6.3.2 SHORT TERM PROGRAM RECOMMENDATION

Several short term tasks have been identified to address the next step in the development of FPSE/Linear Inertia Compressor concept. In these tasks, emphasis has been placed on utilization of existing hardware and test facilities to the extent possible. The scope and approach of these tasks are summarized in Figure 6-6 and a realistic schedule is shown in Figure 6-7.

Task 1: Extended Compressor Testing. The objective of this task is to isolate and identify the causes of restricted compressor piston motion when driven by the FPSE. This would require additional thermocouples on the compressor housing and, perhaps, some additional pressure transducers to aid in diagnostic testing. Testing on the compressor test stand alone may also be utilized to provide a set of reference data on the compressor hardware tested in Phase IIIB with the engine. Additional testing of the compressor under variations in suction/discharge pressures and compressor regulator settings would also be conducted.

Task 2: Modified Proto 2 Housing Testing. The objective of these tests would be to generate engine/compressor performance data and individual engine heat exchanger performance data on the Modified Proto 2 engine last tested in the Phase II program. This engine

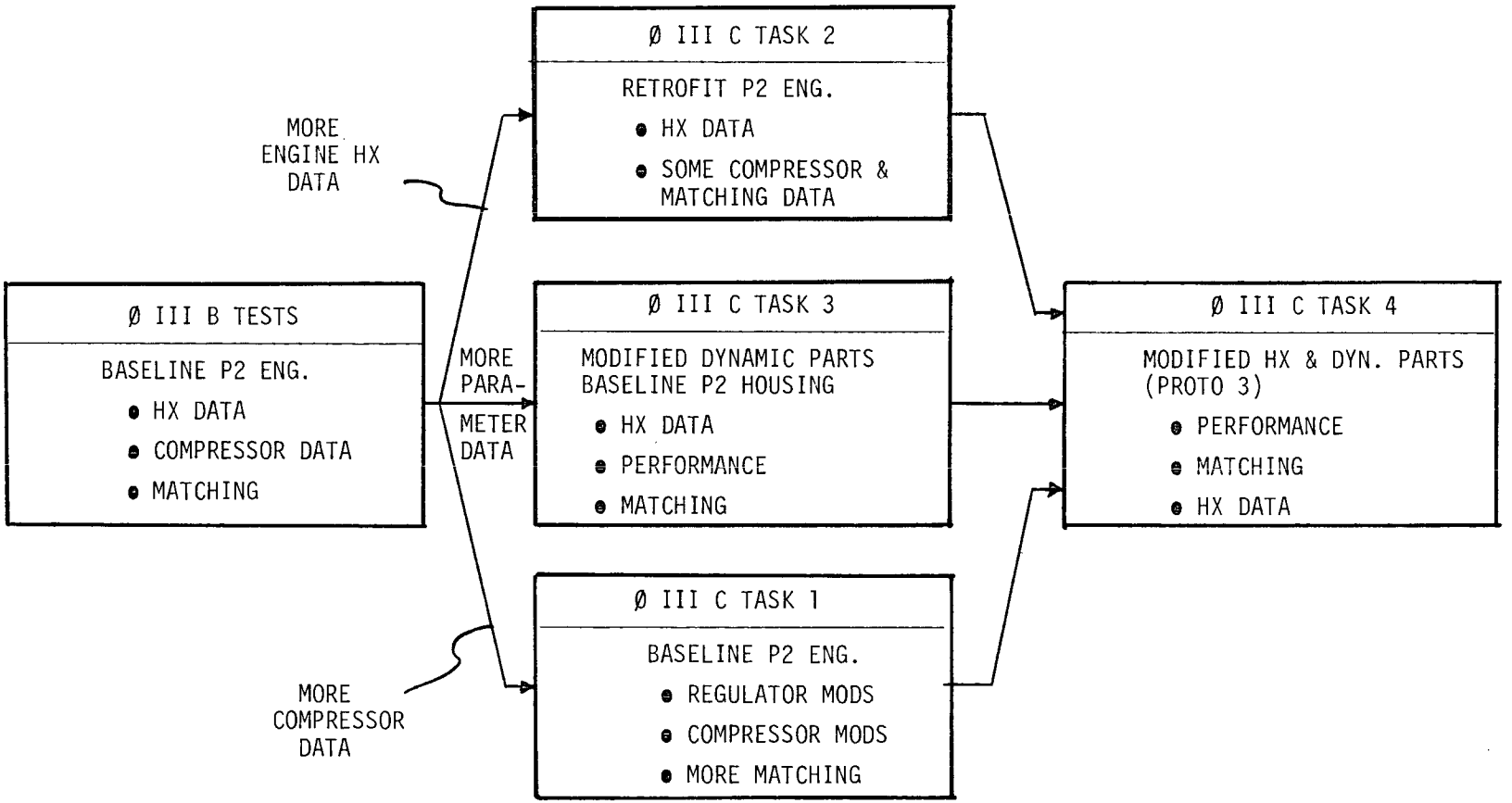

Figure 6-6. ØIIIC Program Candidate Tasks

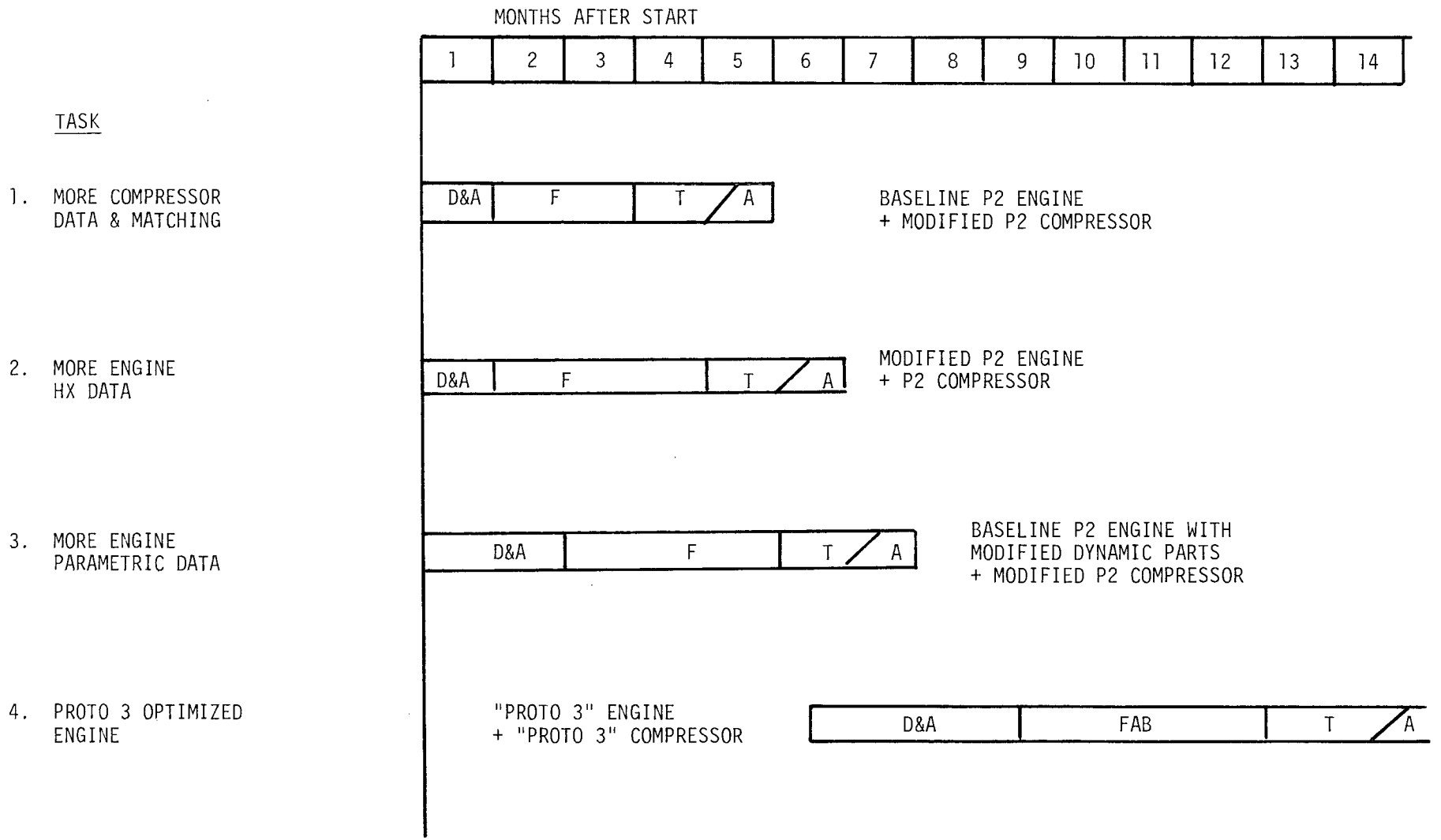

Figure 6-7. CANDIDATE TASK SCHEDULE

utilizes larger, more effective regenerators, double tube heater head units, and individual shell and tube cooler units. Phase II tests indicated higher thermal performance and lower pressure losses for the Modified Proto 2 engine than for the Baseline Proto 2 engine. The tests performed in Phase IIIB on the Baseline Proto 2 engine would be repeated for the Modified Proto 2 engine, thereby significantly broadening the data base for correlating the engine design tools.

Preceding these tests, the existing instrumented baseline Proto 2 engine would be tested with the dynamic thermocouples to verify their capabilities. If the dynamic thermocouples are validated, selected repeat tests of the Phase IIIB program would be run to provide direct engine heat exchanger performance data for these cases.

Task 3: Parametric Engine Data Tests. The objective of this task would be to provide engine performance and engine heat exchanger performance data over as broad a range of thermal and flow conditions as possible. For these tests, the existing instrumented baseline Proto 2 engine housing would be used. Selective changes to the engine dynamic components would be made to force the engine to run over a wide range of volume ratios, strokes, phase angles, etc. The data would then be available for correlating the engine design tools. Additional tests would also be conducted on configurations with modified compressor pistons. This would enlarge the matching analysis base for future work and provide load/match variations for the engine tests.

Task 4: Proto 3 Engine/Compressor Tests. The objective of this task would be to maximize engine/compressor performance within the current envelope of the Proto 2 engine housing and compressor hardware. In this task, results of Tasks 1, 2 and 3 would be used to upgrade the engine and compressor design simulation models and the engine/compressor matching analysis. Using the upgraded models, feasible changes would be made to the engine heat exchangers and dynamic components. The rebuilt engine/compressor would then be

tested with the same instrumentation and DAS used in previous tests to confirm the predictive accuracy of the design simulation models.

If successful, the Task 4 effort would permit a redesign of the basic FPSE/Linear Inertia Compressor unit to meet or exceed the performance goals shown in Table 6-2. The program of Tasks 1 through 4, including analytical model improvements, would maximize the technology development on the FPSE/linear compressor concept using existing hardware and low cost test programs.

REFERENCES

REFERENCES

1) Development and Demonstration of a Stirling/Rankine Heat Activated Heat Pump, Phase II Final Report, GE Document No. 82 AEP-001.

2) Stirling/Rankine Gas Fired Heat Pump Program: Phase IIIA - Technology Development. First Semi-Annual Report, GE Document No. 82-AEP-004.

3) Documentation of ISM. FOR. and Its Application to the General Electric Free-Piston Stirling Engine. Martini Engineering Report dated December 14, 1982.

APPENDIX A

NOMENCLATURE AND ABBREVIATIONS

APPENDIX A
NOMENCLATURE AND ABBREVIATIONS

This appendix lists the frequently used symbols and abbreviations used in this report. For equation symbols, the units used in the text are noted. Special symbols and abbreviations used in only one table or figure are defined in the table or figure.

TERMS

Cv	specific heat at constant volume, BTU/lb^{o}R
Cp	specific heat at constant pressure, BTU/lb^{o}R
CRT	Cathode Ray Tube (DAS display screen)
DAS	Data Acquisition System
F	Force, lbf
F.S.	Full Scale (of instrumentation)
f	frequency, Hz
f_{op}	operating frequency, Hz
FPSE	Free Piston Stirling Engine
g	gravitational constant, 32.174 ft/sec^2
2G.S.	second gas spring of engine (also G.S.)
GPM	gallons per minute (engine coolant flow)
h	enthalpy, BTU/lb
HHV	higher heating value (of fuel)
HX	heat exchanger
k	spring constant, lb/in (also K)
LVDT	Linear Variable Differential Transformer
m	mass, lb
p	pressure, psi, psia
P-P	peak to peak (instrumentation)
PR	compressor pressure ratio (p_{DISCH}/p_{SUCT})
p_{CH}	engine charge pressure, psia, Bars
Q	thermal energy, BTU or kw
RAM	Random Access Memory (for DAS)
ROM	Read Only Memory (for DAS)
REG	engine regenerator or compressor gas spring pressure regulator
SCFM	standard cubic feet per minute
S	entropy, BTU/^{o}R
s	displacement (used with Fds to denote force integration)
T	temperature, ^{o}F, ^{o}R, ^{o}K
T_H	engine heater tube temperature, ^{o}F
t	time, sec., min., hrs.
T/C	thermocouple
U	fluid internal energy, BTU
u	one dimensional gas velocity, ft/sec.

V	volume, ft^3, in^3
V	gas velocity, ft/sec (used in Sections 2.2.2 and 5.6 to be consistant with fluid flow terminology)
W	work, ft-lb
WFM	waveform (DAS processing)
x	displacement, in.
X	body force, lb.
z	distance from gravitational datum, in.
ε	effectiveness, dimensionless
θ	thermocouple time constant, sec.
ρ	gas density, lb/ft^3
τ	period, sec.
ω	temperature excursion frequency, sec^{-1}

SUPERSCRIPTS

• time rate of change (as in $\dot{m} = dm/dt$)

— averaged value of quantity (as in $\overline{\dot{m}} = \int (dm/dt)dt$

SUBSCRIPTS

amb	ambient
avg	average
C	cold (engine cold side)
c	compressor piston
d	displacer
D,DISCH	compressor discharge
f	force
H	hot (engine hot side)
m	mass
N	natural (natural frequency)
p	engine power piston
REG	compressor gas spring pressure regulator setting
rms	root mean square
S,SUCT	compressor suction

ORNL/Sub/82-17485/1
Dist. Category UC-95d

INTERNAL DISTRIBUTION

1. R. S. Carlsmith
2. F. C. Chen
3. J. E. Christian
4. J. A. Conlin
5. J. L. Crowley
6. N. Domingo
7. S. K. Fischer
8. W. Fulkerson
9. S. M. Gillis, Consultant
10. V. O. Haynes
11. F. R. Kalhammer, Consultant
12. T. R. LaPorte, Consultant
13. M. Lessen, Consultant
14. W. P. Levins
15. J. F. Martin
16. H. A. McLain
17. V. C. Mei
18. J. W. Michel
19. R. E. Minturn
20. G. Samuels
21. A. C. Schaffhauser
22. R. A. Stevens
23. M. P. Stulberg
24. C. D. West
25. W. H. Williams, Consultant
26. K. H. Zimmerman

27-28. Central Reseach Library
29. Document Reference Section
30. Laboratory Records - RC
31-32. Laboratory Records
33. ORNL Patent Section

EXTERNAL DISTRIBUTION

34. William Beale, Sunpower, Inc., 6 Byard Road, Athens, OH 45701
35. Glendon M. Benson, Energy Research and Generation, Inc., Lowell & 57th Street, Oakland, CA 94608
36. Don Beremand, NASA-Lewis Research Center, Mail Stop 500-215, 21000 Brookpark Rd. Cleveland, OH 44135
37. James M. Calm, Project Manager, Heat Pump Development, Electric Power Res. Inst., 3412 Hillview Avenue, Palo Alto, CA 94303
38. Stig C. Carlqvist, Societe ECA, 17, avenue du Chateau, 92190 Meudon-Bellevue, France
39. W. S. Chiu, Systems Engineering, General Electric Company, P.O. Box 527, King of Prussia, PA 19406
40. M. Clinch, Gas Research Institute, 8600 W. Bryn Mawr Avenue, Chicago, IL 60631
41. J. G. Daley, Argonne National Laboratory, 9700 South Cass Avenue, Argonne, IL 60439
42. G. Dochat, Mechanical Technology, Inc., 968 Albany-Shaker Rd., Latham, NY 12110
43. T. Finkelstein, TCA, P.O. Box 643, Beverly Hills, CA 90213
44. R. J. Fiskum, Energy Conversion Equipment Branch, CE-113.2, Department of Energy, 1000 Independence Avenue S.W., Washington, DC 20585
45. M. Fukiwake, Agency of Industrial Science and Technology, Ministry of International Trade and Industry, 1-3-1 Kasumigaseki, Chiyoda-Ku, Tokyo, Japan
46. D. R. Gedeon, Sunpower, Inc., 6 Byard St., Athens OH 45701

47. L. Goldberg, University of Minnesota, The Underground Space Center, 11 Mines and Metallurgy, 221 Church Street, SE, Minneapolis, MN 55455
48. T. J. Heames, Argonne National Laboratory, 9700 South Cass Avenue, Argonne, IL 60439
49. F. W. Hoehn, Rockwell International Corp., 6633 Canoga Avenue, Canoga Park, CA 91304
50. J. Hogan, General Electric Co., P.O. Box 8666, Philadelphia, PA 19101
51. Bob Holtz, Argonne National Laboratory, 9700 South Cass Avenue, Argonne, IL 60439
52. Y. Ishizaki, Cryogenic Systems, 253-5 Yamanouchi, Kamakura 247, Japan
53. Naotsugu Isshiki, 2-29-6 Kyodo Setagayaku, Tokyo 156, Japan
54. T. Kapus, Building Equipment Division, Department of Energy, CE-113, 1000 Independence Avenue, S.W., Washington, DC 20585
55. Prof. Nobuhide Kasagi, University of Tokyo, Dept. of Mechanical Engineering, Bunkyo-Ku, Tokyo 113, Japan
56. V. H. Larson, Cleveland State University, 1983 East 24th St., Cleveland, OH 44115
57. K. P. Lee, Manager, Facility and Manufacturing Automation, P.O. Box 809, Sudbery, MA 01776
58. A. Maret, Gas Research Institute, 8600 W. Bryn Mawr Avenue, Chicago, IL 60631
59. W. Martin, Martini Engineering, 2303 Harris, Richland, WA 99352
60. G. McLennan, Argonne National Laboratory, 9700 South Cass Avenue, Argonne, IL 60439
61. R. C. Meijer, Advanced Energy Programs Dept., General Electric Company, P.O. Box 527, King of Prussia, PA 19406
62. N. P. Nightingale, Stirling Engine Systems Division, Mechanical Technology, Inc., 968 Albany-Shaker Rd., Latham, NY 12110
63. Herbert Nilsson, United Stirling AB, Box 856, S-201 80 Malmo, Sweden
64. W. Perceval, United Stirling, Inc., 211 Strand, Alexandria, VA 22314
65. C. J. Rallis, University of Witwatersrand, School of Mechanical Engineering, 1 Jan Smuts Avenue, Johannesburg 2001, South Africa
66. G. Rice, Department of Engineering, The University of Reading, Reading, Berkshire, England
67. A. Ross, Ross Enterprises, 37 West Broad Street, Suite 360, Columbus, OH 43215
68. J. D. Ryan, Energy Conversion Equipment Branch, CE-113.2, Department of Energy, 1000 Independence Avenue S.W., Washington, DC 20585
69. A. Schock, Fairchild Industries, Germantown, MD 20874
70. J. Schuster, Gas Research Institute, 8600 W. Bryn Mawr Ave., Chicago, IL 60631
71. D. J. R. Senft, Department of Mathematics/Computer Science, University of Wisconsin, River Falls, WI 54022
72. R. Shoureshi, Dept. of Mechanical Engineering, College of Engineering, Wayne State University, Detroit, MI 48202
73. J. L. Smith, Jr., Mechanical Engineering Department, Massachusetts Institute of Technology, Cambridge, MA 02139

74. J. G. Slaby, National Aeronautics and Space Administration, Lewis Research Center, Cleveland, OH 44135
75. D. R. Taylor, Royal Naval Engineering College, Manadon Plymouth, Devon PL5 3AQ, England
76. W. P. Teagan, Arthur D. Little, Inc., Cambridge, MA 02140
77. R. C. Tew, NASA-Lewis Research Center, 21000 Brookpark Rd., Cleveland, OH 44135
78. L. G. Thieme, NASA-Lewis Research Center, 21000 Brookpark Rd., Cleveland, OH 44135
79. I. Urieli, Sunpower, Inc., 6 Byard St., Athens, OH 45701
80. Valerie J. Van Griethuysen, Energy Conversion Branch, Aerospace Power Division - Aero Propulsion Laboratory, Dept. of the Air Force, Wright-Patterson AFB, OH 45433
81. G. Walker, University of Calgary, Dept. of Mechanical Engineering, 2920 24th Ave., NW, Calgary, Canada T2N1N4
82. B. P. Wang, Mechanical Engineering Department, University of Texas at Arlington, P.O. Box 19023, Arlington, TX 76019
83. M. A. White, University of Washington, Joint Center for Graduate Study, 100 Sprout Road, Richland, WA 99352
84. L. Williams, Logan Lewis Library, Research Division, Carrier Corporation, Carrier Parkway, Syracuse, NY 13221
85. L. Wright, Gas Research Institute, 8600 Bryn Mawr Avenue, Chicago, IL 60631
86. H. Yeh, School of Engineering, University of Pennsylvania, Philadelphia, PA 1904
87. Institute for Energy Analysis, ORAU-Library
88. Office of the Assistant Manager for Energy R&D, U.S. Department of Energy, Oak Ridge Operations, Oak Ridge, TN 37831
89. Energy Conservation Distribution, Oak Ridge National Laboratory, Building 9102-2, Rm. 112, Oak Ridge, TN 37831

90-340. Distribution for Category UC-95d.